Norwegian University of Life Sciences

Master's Thesis 2024 60 ECTS
Faculty of Veterinary Medicine

Optimization of siRNA and mRNA transfection in Atlantic salmon erythrocytes as an approach for studying antiviral responses

Jeremiah Paul Joseph
Chemistry and Biotechnology (Siv.ing) – Molecular Biology

Acknowledgements

The thesis was done in the period of August 2023 – May 2024, and is a part of a master's degree in Chemistry and Biotechnology (Siv.ing) at the Norwegian University of Life Sciences (NMBU). The master thesis was funded by the Research Council of Norway (NFR) through the RED FLAG project (project # 302551) and was performed at the Norwegian Veterinary Institute (NVI), in collaboration with NMBU. Other project partners in RED FLAG include the Arctic university of Norway (UiT), the University of British Columbia (UBC)-Canada and Universidad Miguel Hernández de Elche (UMH)-Spain.

First and foremost I would love to thank my supervisor Maria Krudtå Dahle for letting me be a part of the Red Flag project. The knowledge, experience, and skills I have gained throughout this thesis is priceless, and I will forever be grateful to you. This journey has led me to meet some incredible people like Frieda Betty Ploss, Thomais Tsoulia and Laura Vanessa Solarte Murillo who has guided me in the laboratory, but also mentally. And to Laura, may you never change. I would love to thank Marit Aamudsen, Leo Gunasekaren, Haitham Tartor, Saima Mohammed, Inger Heffernan, Brit Tørud, Simon Weli and Adriana Andresen for nice conversations and help when needed. Also, I would like to thank the section of fish health at NVI for always greeting me with a friendly smile.

To my supervisor Espen Rimstad, thank you so much for the counseling meetings which was thought-provoking, but always made me think, reflect and learn so much. To Espen's group, Ingvild Berg Nyman, Lars Ole Sti Dahl and Stine Braaen, thank you for the help in the laboratory at NMBU, and a huge thanks to Stine Braaen for answering all the questions I had.

To partners in Spain, thank you for hosting when we visited UMH-Spain, and to Maria del Mar Ortega-Villaizán and Veronica Chico Gras, thank you for answering questions I sent by mail.

Lastly, thank you family and friends for support, I love you all.

Jeremiah Paul Joseph

Ås, May 2024

Abstract

Atlantic salmon have nucleated erythrocytes (Red blood cells, RBCs), possessing not only respiratory function, but also some immune functions. Piscine orthoreovirus-1 (PRV-1) is a dsRNA virus that infects A. salmon RBCs and the heart, resulting in Heart and skeletal muscle inflammation (HSMI). PRV induces an innate antiviral response in RBCs, a response also mimicked by poly(I:C). The pattern recognition receptors (PRR) that activate the innate antiviral response against dsRNA in RBC have not been determined, and functional gene studies can increase that knowledge. Transfection of small interfering RNA (siRNA) can result in silencing of a gene, and this mechanism is termed RNA interference (RNAi). RNAi could potentially be used for functional gene-studies in A. salmon RBCs.

This thesis aims to characterize the expression of the siRNA system in A. salmon RBCs and optimize transfection of siRNA. The aim is to ultimately silence the dsRNA receptors TLR3, RIG-I, RLR3, and the RIG-I mediator MAVS in A. salmon RBCs and study the antiviral response.

It was first determined that genes involved in the siRNA system was expressed in RBCs, and siRNA transfection in A. salmon RBCs was successfully established using electroporation.

To control the function of the siRNA system in RBCs, mRNA-GFP was synthesized by in vitro transcription, and mRNA transfection was also optimized, aiming for a co-transfection with anti-GFP siRNA. The experiment was also set up in Chinook Salmon Embryo – 214 (CHSE-214) cells. Silencing was not observed for either A. salmon RBCs or CHSE-214. Despite the failed control experiment, siRNAs were designed against the target genes as planned. For each target gene, three 21 nt siRNA was designed, ordered, pooled together for each target, and transfected in A. salmon RBCs. Additionally, three longer siRNAs (27 nt) were ordered for MAVS to test the hypothesis that longer siRNAs could be more efficient. No silencing could be shown at the mRNA level or functional level (i.e. effects of poly(I:C) stimulation). Transfection of all siRNAs induced a high antiviral response measured by increased Mx and ISG15 gene expression, in particular day 1. The longer 27 nt siRNAs led to an even higher antiviral response. All dsRNA receptor target genes, but not the MAVS gene, were induced by siRNA transfection at Day 3 and Day 6, making it hard to evaluate any silencing effects. In summary, no silencing could be reported in A. salmon RBCs.

Sammendrag

Atlantisk laks har erytrocytter (Røde blodceller, RBCs) med cellekjerne, som ikke bare har respiratorisk funksjon, men også noe immunfunksjon. Piscine orthorevirus-1 (PRV-1) er et dsRNA virus som angriper laksens RBC og hjerte. Dette kan resulterer i Hjerte- og skjelettmuskelbetennelse (HSMB). PRV induserer en medfødt antiviral respons i RBC, en respons mimikert av poly(I:C). Reseptoren(e) som aktiverer en medfødt antiviral respons mot dsRNA i RBC har ikke blitt bestemt, men funksjonelle genstudier kan utvide denne kunnskapen. Transfeksjon av små inhiberende RNA (siRNA) kan resultere i at mål-mRNA ikke kan uttrykke protein, en mekanisme som kalles RNA interferens (RNAi). RNAi kan potensielt brukes for funksjonelle genstudier i laksens RBCs.

Denne oppgaven har som mål å karakterisere ekspresjon av siRNA systemet i laksens RBCs, og optimalisere siRNA transfeksjon. Målet er å for å undertrykke ekspresjonen av dsRNA reseptorene TLR3, RIG-I, RLR3 og RIG-I mediatoren MAVS i lakse-RBC, og studere effekten på antiviral respons mot dsRNA

Det ble først bestemt at genene som er involvert i siRNA systemet var utrykket i RBCs, og siRNA tranfeksjon i laksens RBCs var etablert ved elektroporering.

Som kontroll på et funksjonelt siRNA system i RBCs, ble mRNA-GFP syntetisert ved in vitro transkripsjon, og mRNA transfeksjon ble optimalisert, med hensikt å utføre et ko-transfeksjons eksperiment med anti-GFP siRNA. Co-transfeksjons eksperimenetet ble også utført på celler fra kongelaks (CHSE-214). Ingen ekspresjons-endringer ble observert i laksens RBCs og CHSE-214. Selv om ingen endringer var observert ble siRNA designet mot målgener som planlagt. For hvert målgen ble tre 21 nt siRNA designet, bestilt, samlet sammen, og transfektert i laksens RBCs. I tillegg ble tre lenger siRNAer (27 nt) bestilt mot MAVS fordi å teste hypotesen angående at lengre siRNA kan være mer effektiv. Ingen ekspresjons-endring ble vist ved mRNA nivå eller funksjonell nivå (det vil si poly(I:C) stimulering). Transfeksjon av alle siRNAene induserte en høy antiviral respons målt ved økning av Mx og ISG15 gen ekspresjon, i hvert fall ved dag 1. Lenger 27 nt siRNA viste til høyere antiviral respons. Alle dsRNA reseptorene mål-gener, men ikke MAVS genet, var indusert av siRNA transfeksjon ved Dag 3 og Dag 6, som gjør det vanskelig å evaluere noe undertrykkings effekt. Oppsummert, ingen undertrykking i laksens RBCs kan bli rapportert.

Table of Contents

List of Abbreviations

Abbreviation	Full description
A. salmon	Atlantic Salmon
Ago2	Argonaute 2 protein
APC	Antigen-presenting cell
cDNA	Complimentary DNA
CHS	Chalcone synthase
CHSE-214	Chinook salmon embryonic cell line 214
CLRs	C-type lectin receptors
CMS	Cardiomyopathy syndrome
CPE	Cytopathic effect
CTL	Cytotoxic T-cells
DMSO	Dimethyl sulfoxide
DPBS	Dulbecco phosphate-buffered saline
DsiRNA	Dicer substrate siRNA (25-27 bp)
EDTA	Ethylenediaminietatraacetic acid
EF1α	Elongation Factor 1α
EIBS	erythrocyte inclusion body syndrome
EPC	Epithelioma papulosum Cyprini
FCS	Fetal calf serum
FITC	Fluorescein isothiocyanate
PE	Phycoerythrin

FSC	Forward Scatter
GFP	Green fluorescent Protein
HSMI	Heart- and skeletal muscle inflammation
HEK293-A	Human Embryonic Kidney 293-A
IFN	Interferon
IPN	Infectious pancreatic necrosis
IPNV	Infectious pancreatic necrosis virus
IRF	Interferon-regulating factors
ISA	Infectious salmon anemia
ISAV	Infectious salmon anemia virus
ISG	Interferon stimulated genes
ISVP	Infectious subviral particles
IVT	In vitro transcription
LGP2/RLR3	Laboratory of genetics and physiology 2/ Rig-Like receptor 3
L-MAVS	27 bp ds-siRNA MAVS
L-siMAVS	Pooled 27bp MAVS siRNA
luc	Luciferase
lyric	LYRIC protein (AEG-1)
MAVS	Mitochindrial antiviral signaling protein
MDA5	Melanoma differentiation-associated protein 5
MHC class 1	Major histocompatibility complex class 1
miRNAs	microRNAs
MRV	Mammalian Orthoreovirus

mtdha	protein LYRIC-like
Mx	Myxovirus resistence interferon-induced protein
NCBI	National library for biotechnology information
NCT	No template control
NETs	Nuclear extracellular traps
NK-cells	Natural Killer cells
NLRs	NOD-like receptors
PAMP	Pathogen-associated molecular patterns
PD	Pancreatic disease
PI	Propidium iodine
piRNAs	Piwi-interacting RNAs
PKR	protein kinase R
PKR	Protein kinase
PMCV	Piscine myocarditis virus
poly(I:C)	Polyriboinosinic:polyribocytidylic acid
PRRs	Pattern recognition receptors
PRV	Piscine orthoreovirus
PVP	Polyvinylpyrrolidone
qPCR	Quantitative polymerase-chain-reaction
RBCs	Red blood cells/erythrocytes
RIG-I	Retinoic acid-inducible gene I
RIN	RNA integrity number
RISC	RNA-induced silencing complex

RLRs	RIG-I-like receptors
RNAi	RNA interference
RNase 3/Dicer	Ribonuclease III
RT	Reverse transcriptase
RTC	No reverse transcriptase control
RTG-2	Rainbow trout gonadal fibroblast-like cell line
RT-qPCR	Reverse transcription qPCR
SAM	S-adenoyl-methionine
SD	Standard deviation
SGPV	Salmon Gill Poxvirus
SHK-1	Salmon Head Kidney 1
shRNA	Short hairpin RNA
siMAVS	Pooled 21bp MAVS siRNA
siRIG-I	Pooled 21bp RIG-I siRNA
siRLR3	Pooled 21bp RLR3 siRNA
siRNA	small-interfering RNA
siRNA-AF488	Allstars Neg. siRNA AF488
siTLR3	Pooled 21bp TLR3 siRNA
snd1	staphylococcal nuclease and tudor domain containing 1
SSC	Side scatter
SR-as	class-A scavenger receptors
taf11	TATA-box binding protein associated factor 11
tarbp2	TARBP2 subunit of RISC loading complex

TCR	T-cell receptors
TLRs	Toll-like receptors
VHSV	Viral hemorrhagic septicemia virus
VSR	Viral suppressors of RNAi

1. Introduction

1.1 The life cycle of wild and farmed Atlantic salmon

1.1.1 Wild Atlantic salmon

Atlantic salmon (*Salmo salar*) belongs to the Salmonidae family and is an anadromous species, meaning that its life commences in freshwater while growth to adult salmon takes place in the ocean. There are, however, a few landlocked variants as well (1, p.1, p.306). The Atlantic salmon resides in the North Atlantic Ocean, arriving from waterways on the west coast of Europe and east coast of North America (1, p. 7).

Figure 1: Distribution of the Atlantic salmon in the North Atlantic Ocean (1, p.7). Made in BioRender.com.

A. salmon spawn in rivers from September until February. The eggs hatch the coming spring, and the newly hatched salmons are called yolk sac fry. They will feed on their yolk sac for nutrition, and when they are ready to start feeding on external feed, they are called fry, and develop into parr after 3-8 weeks (1, p.5). A. salmon stay in the river for some years, and the number of years vary between rivers. Before migrating into the ocean, the A. salmon must have smoltified, a process with morphological, biochemical, physiological and behavioral transformations. For example, the body becomes slender and silvery, growth hormone levels increase, appetite and schooling behavior increases, and osmoregulatory capacity is changed from being in a low-salt (i.e. below physiological salt concentration) environment in fresh water to cope with the high salt concentration in sea water (2, p. 82-84). The smolt is

adapted to life in the ocean (1, p.8). However, the smoltification process is reversible (3). A fully smoltified salmon can revert its osmoregulatory capacity to high-salt environment if it is retained in fresh water (2, p.84, 3).

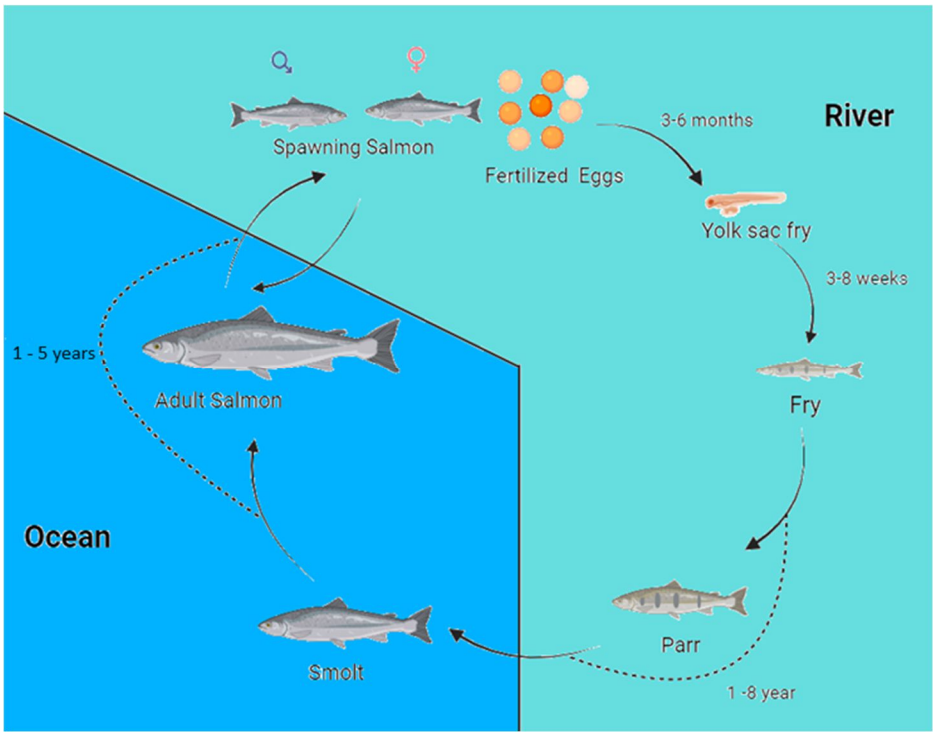

Figure 2. Atlantic salmon life cycle in the wild. Made in BioRender.com (2, p. 5, 4).

When the smolt reaches the ocean, the fish has developed into post-smolt. Post-smolts are active swimmers, using nighttime for migration and daytime for prey detection and predator avoidance (1, p.11). In the ocean, the post-smolts evolves into adult salmon. The adult salmon can return to their river of origin and migrate upstream when they become sexually mature (1, p. 12). The great majority of adult A. salmon die after the first spawning, but a few individuals may reenter the ocean, and return to the river for an additional spawning (1, p. 6, 5). Depending on the number of years in the ocean, and how long they live, an A. salmon can weigh 1 -25 kg (or larger) and live around 13 years (1, p. 5-6).

1.1.2 A. salmon in aquaculture

The A. salmon in aquaculture are kept in a «human-created-environment». Eggs are obtained from female broodfish, fertilized, and then disinfected with iodine before taken into an egg incubation facility (2, p.51, p.397). The eggs develop from “green eggs” to “eyed-

eggs" and are kept in egg trays to hatch into yolk sac fry (2, p.57-58). The yolk sac fry will start swimming up to the surface when they are ready to be fed, which is when less than 10% of the yolk sac remains. (2, p. 60, p.73). The yolk sac fry then develops into parr, and is vaccinated before smolt-stage is achieved (2, p. 64). The smoltification process is impacted by environmental factors photoperiod and temperature regulated by the fish farm depending on desired time of smoltification (2, p. 86). When efficient hypo-osmoregulation is achieved, the smolts are transported to sea water (2, p. 38-39, p. 91- 92). The salmon is slaughtered prior to sexual maturity at a weight of 4-6 kilos (6).

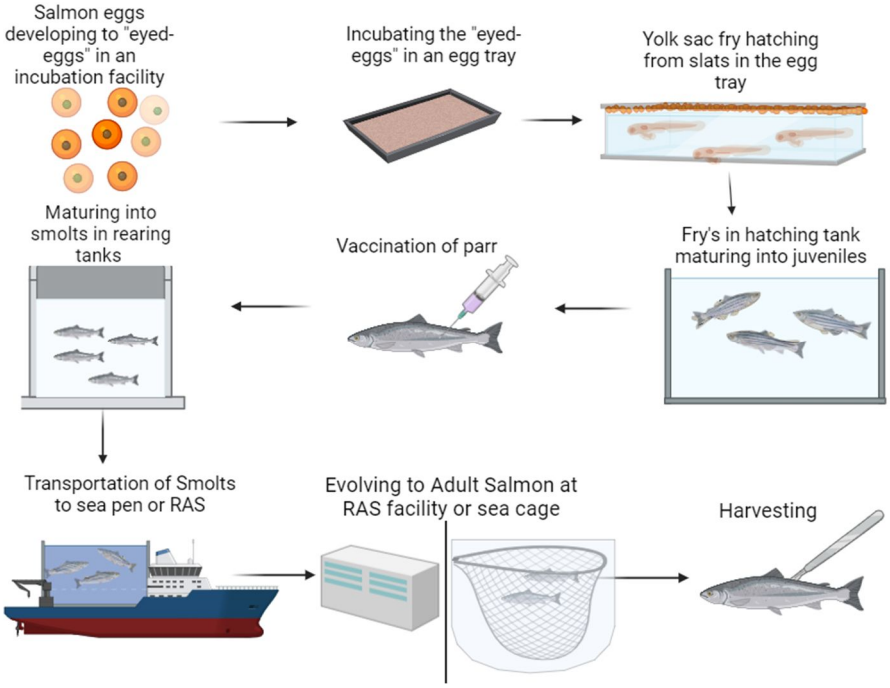

Figure 3. A simple outline of salmon life in aquaculture. Made in BioRender.com (2, p. 40-41, p. 64, p. 86, 6)).

1.1.3 Impact of salmon farming procedures on fish health.

All handling of fish are stressors (7). In A. salmon farming, handling include sorting, moving, vaccination, transportation, pumping, crowding and treatments against parasites like salmon louse. Everything from oxygen-content, water-flow, temperature, feeding, disease control, transportation and harvesting must be controlled to reduce stress. Sea pens used in A. salmon farming has many advantages such as continuous water stream that brings fresh oxygenated water, enables large cage sizes, but stress still occurs due to oxygen-level, density, feeding and disease control, i.e. mostly sea lice control (2, p.100, 7). Stress is

undesirable since it increases the susceptibility for diseases (7). The mortality rate of farmed salmon in the period after transfer to sea water until slaughter was 16.7% in 2023 (7). Detailed information about the cause of death from the fish farms is partly unavailable, but a questionnaire to fish health professionals reveals that a combination of mechanical handling procedures and infectious diseases are major causes (7). However, the cause of death may not be identical to the initial cause of disease. There is a need to improve the health and welfare of farmed salmon in Norway.

1.2 Fish Red Blood Cells

1.2.1 Gas exchange in Atlantic salmon

The primary organ for gaseous exchange is the gills. The gills has respiratory function, but are also involved in salt-water exchange and excretion of nitrogenous waste (8, p.24).

A. salmon have four gill arches on each side with two rows of filament each and the gills are supplied with blood through the filaments. From short afferent lamellae arteries, deoxygenated blood flows in the second lamellae located above and below each filament (2, p. 18-19, 8, p.25-26). The blood flows in the opposite direction, from which water flow through the gills when swimming, resulting in a counter-current exchange, where the oxygen in the water is transferred to the blood (8, p.26). The blood cell in charge of oxygen transportation is the erythrocyte (RBC). Oxygen is transported through the blood circulation to other cells to support energy-requiring processes such as metabolism and growth (9).

1.2.2 Erythrocytes

RBCs occupy ≈40% of the total blood-volume in A. salmon and are the most abundant cell in teleost fish, with some fish species in the Antarctic being an exception as they lack RBCs (10, p.73, 11, 12). The blood takes up about 2 – 5% of the body volume, which is lower compared to terrestrial animals (8%) (10, p.73). The biggest attribute of RBCs is their ability to bind oxygen from water utilizing the tetrameric protein hemoglobin (11).

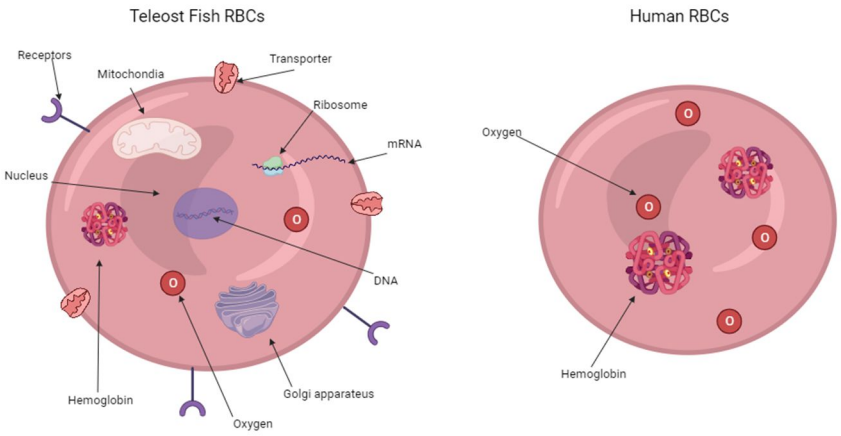

Figure 4. Rough outline of some cellular and molecular components in teleost erythrocytes versus human erythrocytes. Made in BioRender.com

A. salmon RBCs are shaped by microtubilin to an elliptical-shape ≈17 µm in length, which is larger and different in shape compared to human RBCs (≈8 µm, biconcave disc) (13, 14). The biconcave disc shape has been hypothesized to optimize flow properties, an elliptical shape, however, does have advantages like higher laminar flow in major blood vessels (14). Salmonid RBCs have a nucleus with DNA and other organelles like mitochondria and golgi complex (15). The presence of DNA enables teleost fish RBCs to produce proteins. In contrast, mature human RBCs lack most organelles, ribosomes and cell nuclei and thus do not produce proteins. Teleost fish RBCs are also equipped with some additional immune functions, lacking in human RBCs (15). The ability to undergo functional changes in response to external signals that fish RBCs inhabit could potentially spark a discussion on whether RBCs should be divided into different groups, depending on differences in functions, which may be compared to the polarization seen in human monocytes and macrophages (16, 17).

1.3 The immune system

The immune system defends the host against foreign pathogenic microbes. It is roughly divided into two systems: the innate immune system and the adaptive immune system.

1.3.1 The innate immune system

When a pathogen invades a host, the innate immune system is activated (8, p. 144 – 147). It is well conserved between many different animal species, giving a non-specific response, which lacks "memory". The innate immune system includes 1) a surface barrier, 2) a humoral barrier, and 3) a cellular barrier.

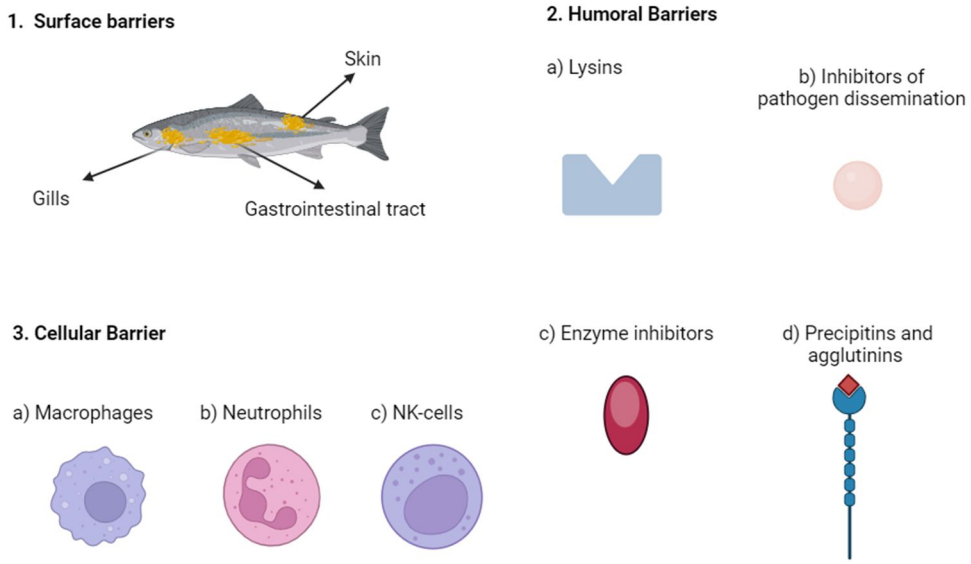

Figure 5. Rough illustration of different components involved in the surface barrier, humoral barrier, and cellular barrier. 1) Surface barrier. Mucus on gills, skin, and gastrointestinal tract. 2) Humoral barrier. a) Lysins: Proteins that destroy pathogen cell walls/membranes. Examples are complement proteins, antimicrobial peptides and lysozymes. b) Inhibitors of pathogen dissemination. Examples are interferons (IFN) or transferrin. c) Enzyme inhibitors, acting by to neutralize pathogen enzymes needed to e.g. spread in tissues. An example is antiproteases. d) Precipitins and agglutinins; Proteins involved in pattern recognition of pathogens leading to inhibition by cross-binding, clustering and/or triggering phagocytosis. Examples of these proteins are pentraxins and lectins. 3) Cellular barrier. Cells that kill and eliminate pathogens by phagocytosis, cytotoxicity, or nuclear extracellular traps (NETs), and/or present antigens to the adaptive immune system. a) Macrophages, b) Neutrophils, c) Natural killer cells (NK-cells). (8, p. 144 – 150). Made in BioRender.com.

The surface barrier consists of mucus that traps and kills microorganisms with the assistance of the humoral barrier (8, p. 145 – 150, 18). If a pathogen evades the surface barrier, it will be confronted with the humoral and cellular barrier (18). The pathogen can be recognized (*in vivo*) by molecular motifs foreign to the host, referred to as pathogen-associated molecular patterns (PAMPs) (19, p. 55). The host is equipped with antigen-presenting cells (APC) that have pattern recognition receptors (PRRs) for PAMPs. Different PRRs exist - like Toll-like receptors (TLRs), C-type lectin receptors (CLRs), NOD-like receptors (NLRs), and RIG-I-like

receptors (RLRs) (19, p.62). The PRRs initiate a signaling pathway which leads to gene expression and secretion of cytokines. Cytokines are proteins active in cell-cell communication and recruit the cellular barrier for elimination of the pathogens or infected cells (19, p.65). The complement system assists the cellular barrier by inducing lysis of foreign pathogenic cells like bacteria and parasites (19, p.54-55).

1.3.2 Stimulation of the adaptive immune system

Activation of the innate immune system stimulates the adaptive system (20, p.3 – 14). The adaptive immune system is specific and has a "memory" for recognizing past infections. APCs present "processed pathogenic molecules" through MHC-receptors to T-cell receptors (TCR) on T-cells to activate them. Two important types of T-cells are CD4+ T-cells and CD8+ T-cells. CD4+ T-cells support the humoral and cellular immunity of the adaptive immune system. The humoral immune system consists of pathogen-specific antibodies secreted from B-lymphocytes. The CD4+ T-cells support the B-lymphocytes, but also assist macrophages and neutrophils in engulfing cells. CD8+ T-cells are cytotoxic T-cells (CTL) that can specifically lyse infected cells. Cytokines secreted from the APC also assist with the recruitment of the cell-mediated adaptive immune system.

1.4 Viral diseases in aquaculture of A. salmon

One of the most common problems in salmon aquaculture is viral infections (21). Major viral diseases in Norwegian A. salmon aquaculture include pancreatic disease (PD), infectious salmon anemia (ISA), infectious pancreatic necrosis (IPN), cardiomyopathy syndrome (CMS) and heart- and skeletal muscle inflammation (HSMI) (7).

Table 1. Numbers of farms reporting disease outbreaks of ISA, PD, CMS, HSMI and IPN from year 2013 to 2023. Numbers with "*" also include results from private laboratories (7).

Viruses	2014	2015	2016	2017	2018	2019	2020	2021	2022	2023
ISA	10	15	12	14	13	10	23	25	15	18
PD	142	137	138	176	163	152	158	100	98	58
CMS	107	105	90	100	101	82	154*	155*	131*	129*
HSMI	181	135	101	93	104	79	161*	188*	147*	184*
IPN	48	30	27	23	19	23	22*	20*	12	12

1.4.1 Viruses in salmon aquaculture

Viruses are infectious agents dependent on a host-cell for replication (8, p. 186 – 188). When extracellular the viruses shield their genome inside a protein coat (capsid), and some viruses have an additional membrane envelope. The genome is either DNA or RNA, which can be double stranded (ds) or single stranded (ss); linear or circular; continuous or segmented. A ssRNA genome can be either negative or positive sense, where a positive sense strand encodes proteins (8, p. 186 – 188). The Baltimore classification lists seven major classes of viral genomes, but only six of these classes have been found in fish.

Table 2. Virus, family, genome, and viral disease that is mentioned in Fish health report 2023. (7)

Virus	Family	Genome	Disease in Salmon
Salmonid alphavirus	*Togaviridae*	+ssRNA	Pancreatic disease (PD)
Infectious salmon anemia virus (ISAV)	*Orhomyxoviridae*	-ssRNA	Infectious Salmon Anemia (ISA)
Infectious pancreatic necrosis virus (IPNV)	*Birnaviridae*	dsRNA	Infectious Pancreatic necrosis (IPN)
Salmon gill poxvirus (SGPV)	*Chordopoxvirus*	dsDNA	Salmon Gill Poxvirus Disease (SGPVD)
Piscine orthoreovirus (PRV)	*Reoviridae*	dsRNA	Heart and skeletal muscle inflammation (HSMI)
Piscine myocarditis virus (PMCV)	*Totiviridae*	dsRNA	Cardiomyopathy syndrome

Various effects of a virus infection on the host cell are illustrated in Figure 6.

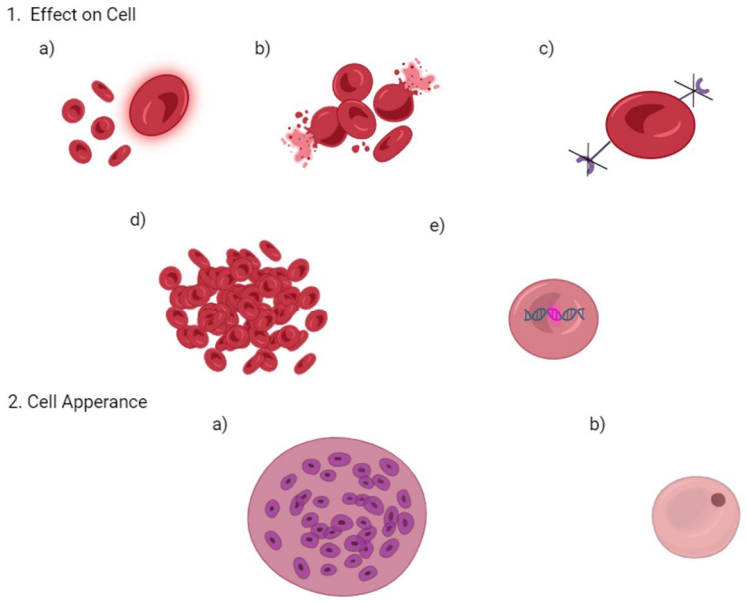

Figure 6. 1. Effects on the cell. a) Cloudy swelling, b) Irreversible changes resulting to cell death, cytopathic effect (CPE), c) Loss/damage to cell-function, d) Transformation to a neoplastic state, e) Persistent infection. 2. Cell appearance changes. a) Formation of a multinucleate giant cell or syncytium or b) Inclusion bodies (8, p. 195). Made in BioRender.com.

1.4.2 Heart and skeletal muscle inflammation (HSMI)

One of the most prevalent viral diseases affecting Norwegian fish farms, according to the annual fish health report from NVI (7), is HSMI that is caused by PRV.

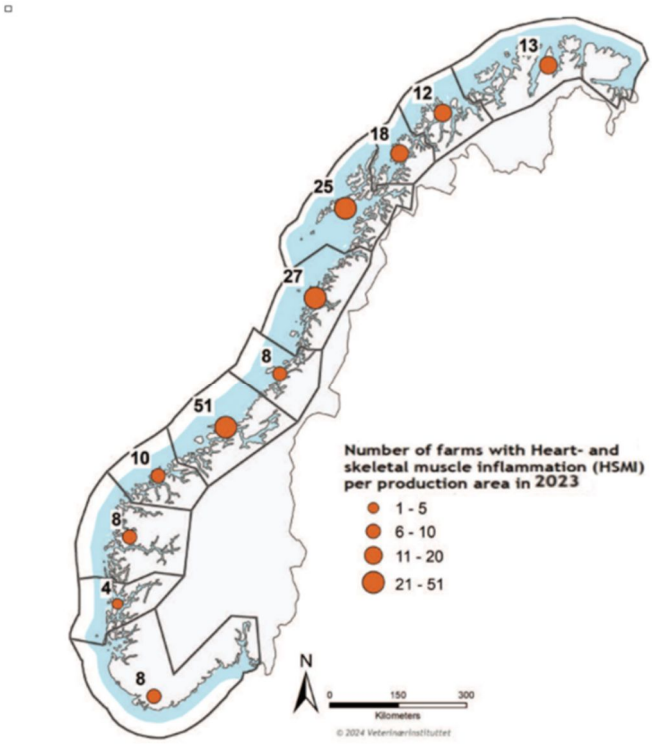

Figure 7. Outbreaks of HSMI in different regions of Norwegian fish farms. (7)

HSMI was first discovered in 1999, but the virus itself was identified 11 years later in 2010 (22). As the name of the disease imply, the heart and skeletal muscle are infected and inflamed, and the disease can lead to a mortality rate up to 20%. In 2023, there were 184 registered cases of HSMI, but the viral infection is much more prevalent, and many PRV infections are not associated with clinical disease (7). Vulnerability to stress and sensitivity to hypoxic environments is associated with PRV infection and HSMI (23). No commercial vaccines exist against the virus, but experimental vaccines have shown effect (21, 24, 25). There are three known subtypes of PRV; PRV 1-3 (22). PRV-1 is the causative agent of HSMI in Atlantic salmon. PRV-2 is the causative agent of erythrocyte inclusion body syndrome (EIBS) in Coho salmon (*Oncorhynchus kisutch*) and PRV-3 causes HSMI-like disease with anemia in Rainbow trout (*Oncorhynchus mykiss*) (26) and in Coho salmon (27).

1.4.2.1 PRV infection

PRV has a segmented dsRNA genome packed in a double protein capsid. There is no envelope. The genome encodes at least eleven proteins important for viral replication and capsid structure (21, 28).

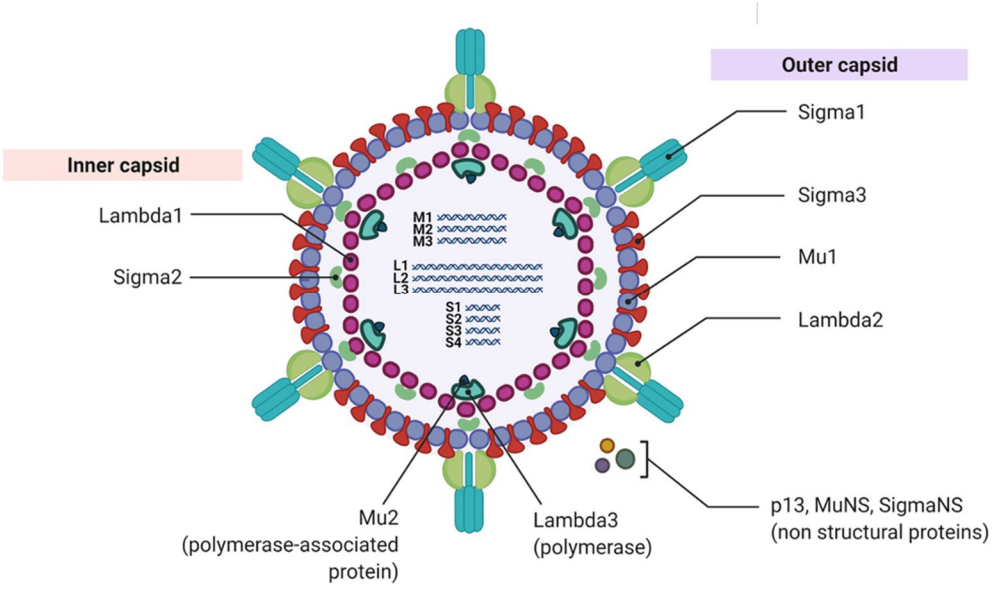

Figure 8. PRV virus structure (28).

The cells that PRV are known to infect are erythrocytes, myocytes and macrophages (21). Limited information is available on how PRV enters the cells, but a suggested infection mechanism is based on research performed on the mammalian counterpart: Mammalian orthoreovirus (MRV) (22). Orthoreoviruses can bind to cell surface receptors glycans and receptors, utilizing protruding surface proteins. Penetration is achieved by endocytosis resulting in a stripped virus core containing dsRNA genome in the cytoplasm. The dsRNA genome is transcribed into mRNA by its own RNA polymerase inside the virus core, and transcripts exit into the cytoplasm, and are translated by the cellular machinery. µNS is a central protein in the replication process (29). It brings viral proteins together, constructing a "viral factory". This clustering can be observed in PRV infected erythrocytes as "spots" seen in a light microscope, referred to as "inclusion bodies" (30). How the virus is released is unknown, but hemolysis of blood cells has been observed in spleen and head kidney, indicating cell lysis (31).

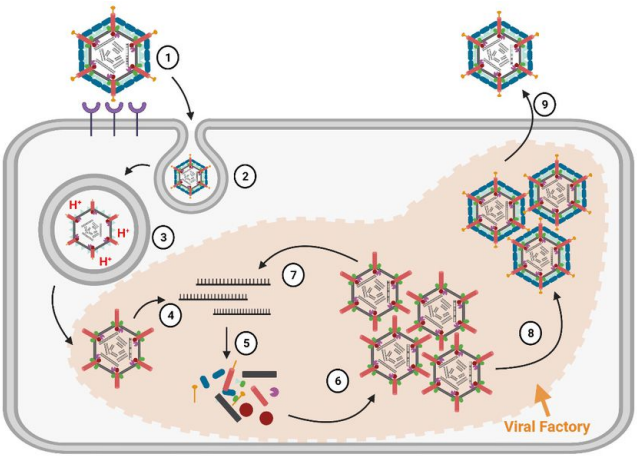

Figure 9. Mammalian ortherovirus cell infection (32).

In the acute phase of a PRV infection, 50% of RBCs contain dark inclusions filled with virus progeny and PRV is released at high levels to blood plasma (21). The heart infection and inflammation, forming the characteristic pathology of HSMI, appears a few weeks after the acute phase. Regeneration of the heart usually follows this phase. The virus can then persist possibly throughout the salmon's life, primarily in macrophages and RBCs. Persistent virus is also associated with black spots observed in the salmon filet (33). Wild salmon have a prevalence of 10-20% of the PRV virus and can possibly eradicate a PRV infection (34). Farmed salmon has not shown the ability to eradicate PRV, and since it appears to be life-long persistent-phase, more than 90% are still infected at slaughter (7, 21).

1.4.2.2 RBC innate antiviral responses to PRV

PRV-1 induces an immune response when infecting A. salmon.

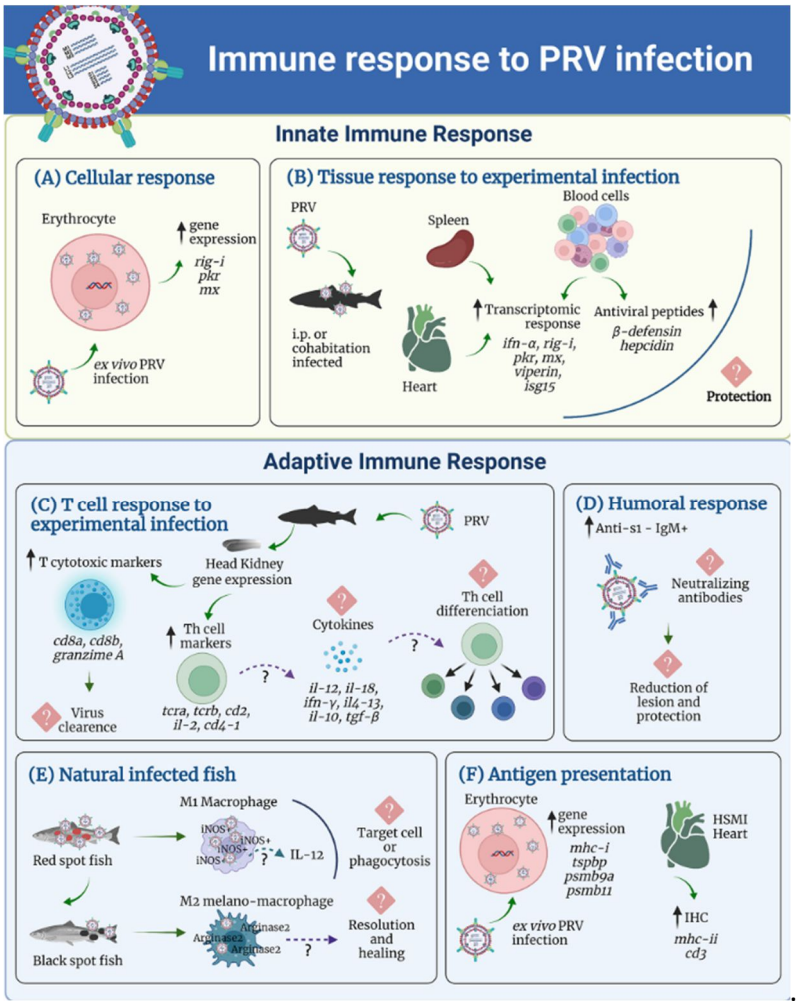

Figure 10. Immune response by the immune system of salmon when infected by PRV-1. (28)

RBCs possess PRRs that interact with dsRNA or an agonists of dsRNA such as polyriboinosinic:polyribocytidylic acid (poly(I:C)) (22). These receptors include transmembrane TLR3 in endosomes and cytoplasmic retinoic acid-inducible gene I (RIG-I) which have been identified in Rainbow trout RBCs and A. salmon RBCs (35, 36). In addition to RIG-I, the RLR receptors melanoma differentiation-associated protein 5 (MDA5) and RIG-like receptor 3 (RLR3, also referred to as LGP2) has also been identified in A. salmon RBCs (36). The interaction with the PRRs initiates a signaling pathway that stimulates interferon-regulating factors (IRFs) (37). IRF7 is highly expressed in A. salmon during high PRV infection-levels (38). The IRFs stimulate the secretion of IFN, contributing to cell-cell communication by upregulating interferon stimulated genes (ISG) through the JAK-STAT pathway (37). IFNa and IFN2 are secreted from activation of the RIG-I pathway, while IFN-β is secreted through activation of the TLR3 pathway. IFNa is secreted at higher levels compared to the other IFNs during PRV-infection, indicating dsRNA sensing by the RIG-I pathway (38). ISGs are antiviral

genes, functioning by inhibiting virus replication. From *ex vivo* studies, ISGs such as interferon-induced GFP-binding proteins (Mx protein) and protein kinase R (PKR) are highly expressed during PRV-infection (28). Mx proteins trap nucleocapsids and PKR can inhibit viral translation (39). The expression of ISGs decreases PRV protein production, but not the PRV RNA level (21). This is probably linked to blocking of translation and virus release. Antigen presenting genes, such as major histocompatibility complex class 1 (MHC class 1 antigen), tapasin and proteasome subunits, are expressed at high levels (38), indicating that RBCs play a role in stimulating the adaptive immune system (22).

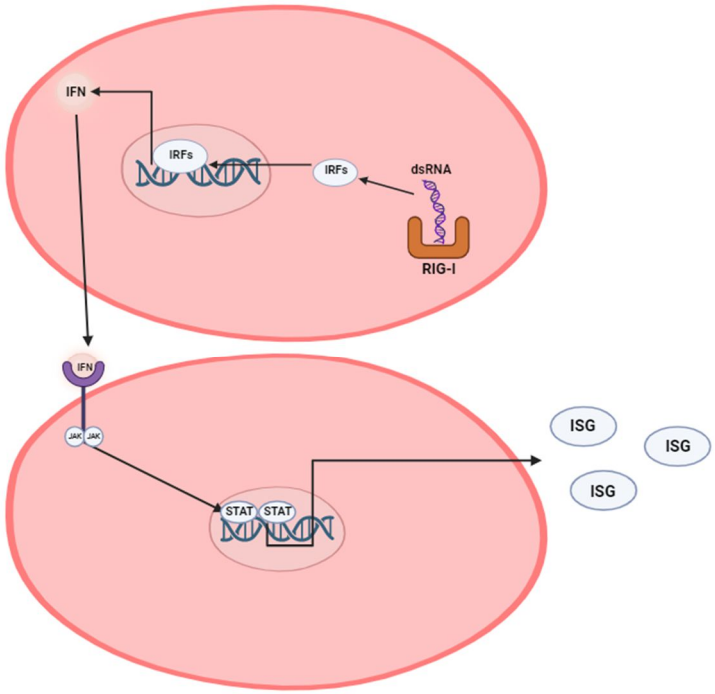

Figure 11. Simple illustration of the red blood cell immune response when infected by dsRNA-virus. Made in BioRender.com.

In vivo infection with PRV induces a strong immune response. Increased expression of ifn-a, rig-I, pkr, mx-α, viperin and isg15 is observed in blood, heart and spleen (23). Additionally, the expression of β-defensin and hepcidin is observed in blood cells. However, this immune response does not lead to eradication of the virus, as viruses have demonstrated the ability to evade the immune system. Notably, IPNV and ISAV have portrayed pathways to evade the IFN type 1 response. Considering that PRV can infect macrophages, it is hypothesized that macrophages are utilized for evading the immune system (21).

1.5 RNAi

For gene studies in a cell, RNA interference (RNAi) has been a revolution (40). RNAi works by diminishing the amount of mRNAs in the cytoplasm, thereby suppressing the translation of a gene into protein. The depletion of mRNA is achieved by a dsRNA molecule homologous to the target mRNA, resulting in the cleavage of the mRNA.

1.5.1 The discovery of RNAi

RNAi was discovered by Napoli and Jorgensen who hypothesized that introduction of a transgene can cause "co-suppressesion" of a gene in 1990, after a failed attempt to overexpress chalcone synthase (CHS) in *Petunias* (41, 42). Romano and Macino reported similar observations in *Neurospora crassa* in 1992 and hypothesized that homologous RNA caused suppression of an endogenous gene (42). RNAi was first documented in 1995 after Guo and Kemphues achieved degradation of par-1 mRNA in *Caenorhabditis elegans* by introducing dsRNA (43). Through experiments on *C.elegans* by Fire *et al*. in 1998, dsRNA was identified as important for silencing, as opposed to ssRNA (44). Two teams of biochemists, on the other hand, suggested that dsRNA is processed into smaller intermediates of 21-23 nt RNA, termed small-interfering RNA (siRNA), which are the true effector molecules (45, 46). The 21-23 RNA suggestion was later confirmed by Elbashir *et al*. (47) in *Drosophila* cells.

1.5.2 The mechanism of RNAi

RNAi operates in a two-step mechanism: 1) Slicing of dsRNA into siRNA, and 2) mRNA cleavage activity mediated by the RNA-induced silencing complex (RISC) (40). The enzyme that facilitates the first process is a ribonuclease III (RNase 3) enzyme termed Dicer, discovered by Bernstein *et al*. in 2001 (48). Dicer cleaves the dsRNA into a ds-siRNA with a 3'-hydroxyl and 5'-phosphate groups, and a 3' overhang of two unpaired nucleotides on each strand (49). The cleavage starts at the termini of the dsRNA and proceeds along the dsRNA using ATP-dependent translocation. The protein responsible for RISC activity is Argonaute 2 (Ago2) (40). The Argonaut protein family possesses two characteristic domains: PAZ and PIWI. The PIWI-domain exhibits a conserved secondary structure similar to RNase H enzyme, inhabiting nuclease activity. The PAZ-domain is responsible for binding of the siRNA. Ago2

has RISC-activity, but is also responsible for unwinding of ds-siRNA, by cleaving the non-incorporated strand and binding to incorporated strain.

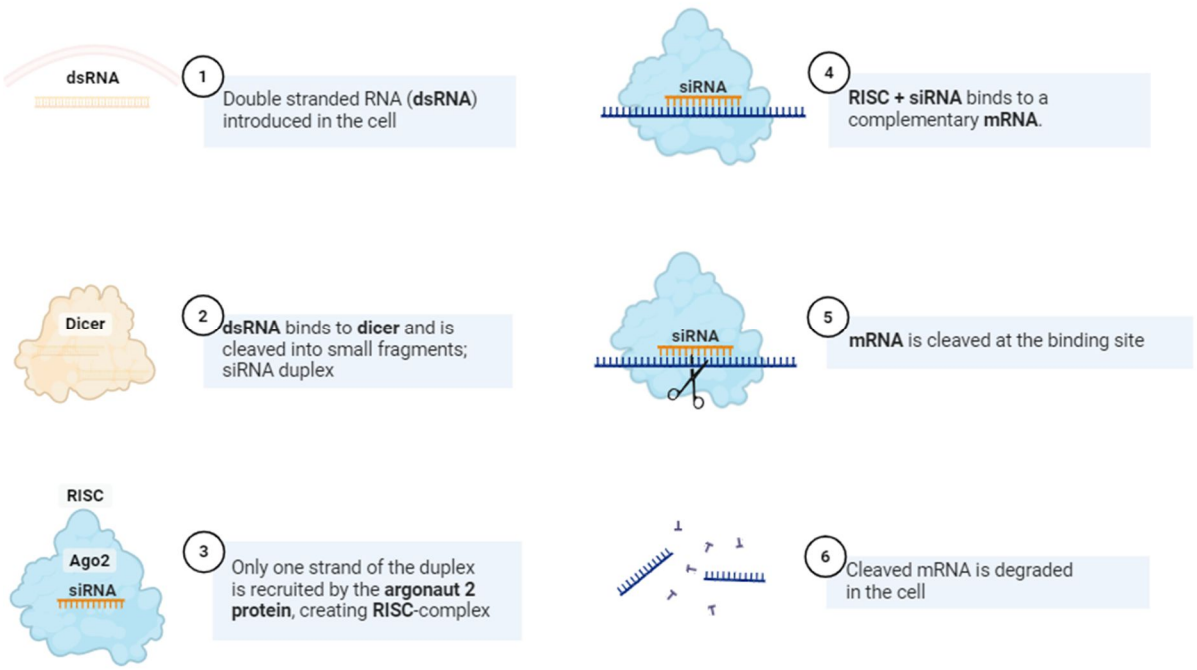

Figure 12. siRNA mechanism for silencing of a gene in a cell. Made in BioRender.com.

Other types of small RNA with regulatory mechanisms are piwi-interacting RNAs (piRNAs) and microRNAs (miRNAs) (50). The miRNAs inhibit gene expression in a post-transcriptional matter as siRNA, but piRNA; however, is associated with protection from mobile genetic element in animal germline (50, 51). miRNA differs in terms of mechanism. The miRNA is transcribed from RNA polymerase II to a primary miRNA (pri-miRNA) with a 5'cap, 3' polyadenylated tail and a double-stranded stem-loop structure (51). A microprocessor complex turns the pri-miRNA into a precursor miRNA (pre-miRNA) with mismatches and a loop-structure. The pre-miRNA is transported from nucleus to cytoplasm by Exportin 5, and processed by Dicer to a miRNA duplex of 18-25 nucleotides which can associate with RISC. As the miRNA consist of mismatches, it will have partial complimentary binding to multiple mRNA, resulting in a less specific target than siRNA. Ago2 is activated if a miRNA exhibit high complementarity to an mRNA, but in most cases, Ago2 is not activated because of low complementarity. Silencing still occurs due to translation repression, degradation by deadenylation, decapping or exonuclease action.

1.5.3 Challenges with experimental use of siRNA

Different transfection methods allow entry of siRNA molecules to a cell, but problems may occur inside the cell (52, 53). A challenge with siRNA is that naked and unmodified siRNA is prone to degradation (52). Intracellular RNases can degrade siRNA, but if not degraded by RNases, it must be recognized and incorporated by RISC to achieve silencing. Another challenge is off-target silencing. Off-target silencing refers to silencing of other mRNAs than the target-mRNA, attained when the siRNA is partially complimentary to other mRNA-sequences. Unspecific targeting can result in cell transformation and mutations to the cell, but primarily it will minimize an experimental study with unspecific effects and may lead to wrong conclusions. The third challenge is that ds-siRNA is capable of being detected by PRRs which induces an innate immune response (54). TLR3, PKR and RIG-I are specific PRRs which can recognize ds-siRNA. A solution to the latter problem is to modify the siRNA to reduce immune recognition and response.

2. Objectives

The goal of the Red Flag project, that this master thesis is a part of, is to expand the knowledge on the RBCs of the Salmonidae family. The RBCs can respond to stress and infection, and since the combination of the two is associated with mortality in farmed salmon – and red blood cells are essential for survival - this study may have important implications for salmon health. By increasing the understanding of RBC responses to stress and infection, more reliable biomarkers can be identified.

Antiviral receptors, molecules and mediators are expressed in RBCs, and important for the antiviral response during a viral infection. What are the most important cellular initiators of these responses? The aim of this thesis is to establish methods to silence genes involved in the innate immune responses of salmon RBCs using siRNA, and – if successful - study the effect of silencing on antiviral responses.

Partial goals:

1. Characterize gene expression of the siRNA system in salmonid red blood cells
2. Optimize siRNA transfection in red blood cells
3. Produce GFP mRNA and optimize mRNA transfection as a control
4. Test siRNA effects by silencing GFP mRNA
5. Silence dsRNA receptor genes and MAVS (Mitochondrial antiviral signaling protein)
6. Study effects of transfection and silencing on antiviral responses

3. Materials and Methods

3.1 Isolation of red blood cells

The cellular components of teleost fish blood are RBCs, neutrophils, monocytes, thrombocytes, eosinophils, basophils and lymphocytes (8, p. 31 – 37). Additionally, the blood plasma contains ions, organic molecules and proteins.

3.1.1 Blood sampling

A. salmons ranging from 50 - 300 g were obtained from the Centre for fish trials at the Norwegian University of Life Science (NMBU). Sedation was executed by the Centre of fish trial using Isoeugenol (Aqui-S, 2 mg/mL H_2O) (55). Euthanasia was performed afterwards by adding Tricaine Methanesulfonate (Finquel MS-222, 100mg/L H_2O) (55, 56). Blood was drawn from the caudal vein of the A. salmons, and transferred to a heparinized tube to prevent coagulation (55, 57). The tube was stored on ice prior to isolation of RBCs.

3.1.2 Density gradient centrifugation: Percoll

For *in vitro* experiments exclusively focusing on RBCs, it is essential to achieve the separation and purification of RBCs from other cellular and chemical components in blood. Purification should not harm the cells and contamination has to be avoided (58). The separation and purification are accomplished through a density gradient centrifugation. Density gradient centrifugation is developed to stabilize moving boundaries during sedimentation, enabling cells to migrate within the media to different zones depending on their density. Different media can be employed for density gradient centrifugation, for example, sucrose and salts, polysucrose, iodinated compounds and colloidal silica. The effectiveness of the separation is influenced by different centrifugation factors.

Colloidal silica has been found to be cytotoxic to red blood cells, but the toxic effect can be eliminated by stabilizing the silica (58). Silica particles, when combined with adherent polymers, acquire iso-osmotic ability and pH-neutrality. The discovery of silica stabilization resulted in the Percoll-solution in 1977, where the silica in Percoll is a sodium-stabilized

colloid. Additionally, polyvinylpyrrolidone (PVP) is coated on the particles to minimize cytotoxic effects. During centrifugation, larger particles are concentrated at the bottom while smaller particles accumulate at the top, which is in accordance with the principles of density gradient centrifugation.

3.1.3 RBC isolation by density gradient centrifugation

The protocol described below is designed for isolating and purifying RBCs from 1 mL of A. salmon blood.

- The blood was diluted to a 1:20 ratio with Dulbecco phosphate-buffered saline 1X (DPBS 1X).
- In four 15 mL Falcon tubes, 7.5 mL of a 51% percoll solution was added. The 51% percoll solution was prepared by mixing 18 mL 100% percoll, 3.5 mL DPBS 10X and 13.5 ml sterile water (dH_2O).
- A gradient was created by transferring 5 mL of the diluted blood on top of the 51% Percoll in each 15 mL Falcon tube. The four Falcon tubes were centrifuged at 500g for 20 minutes at 4°C, with the axle setting at 7 and the break setting at 0.
- After centrifugation, the Percoll was aspirated, and the isolated RBCs were transferred to a 50 mL Falcon tube and washed twice by resuspending in 50 mL DPBS 1X. Centrifugation was performed at 500g for 10 minutes at 4°C, with the axle setting at 9 and break setting at 9, after each wash.
- Following the second resuspension, before the second centrifugation after washing, 10 µL of resuspended RBCs were withdrawn and diluted 1:9 in 90 µL DPBS 1X. The resuspension was used for automatic cell counting by Countess, done as in "3.1.4 Cell counting". Cell counting was performed to assess the viability of the cells, and the number of live cells to calculate the amount of media needed for a concentration of $20 * 10^6$ cells/mL.
- After the second centrifugation, the pellet was resuspended in L-15 medium containing 2% fetal calf serum (FCS) and 50 µg/mL gentamicin to $20 * 10^6$ cells/mL. The resuspended RBCs were then transferred 1 mL/well to 12-well plates.

- The 12 well-plates with isolated RBCs were further incubated in a 15ºC incubator under agitation until further use.

3.1.4 Cell counting

From RBCs diluted in DPBS 1X, 10 µL of the diluted cells was mixed with 10 µL of trypan blue. Subsequently, 10 µL of the mixture was transferred to a Countess cell counting chamber slide from Invitrogen. The Countess cell counting chamber slide was inserted into the Countess machine and a clear area with RBCs was identified, and adjusted if needed. Automatic cell counting was performed, once a satisfactory spot was located. This process allowed for the assessment of the total cell count, the number of live cells, the number of dead cells and the percentage of viable cells in the sample.

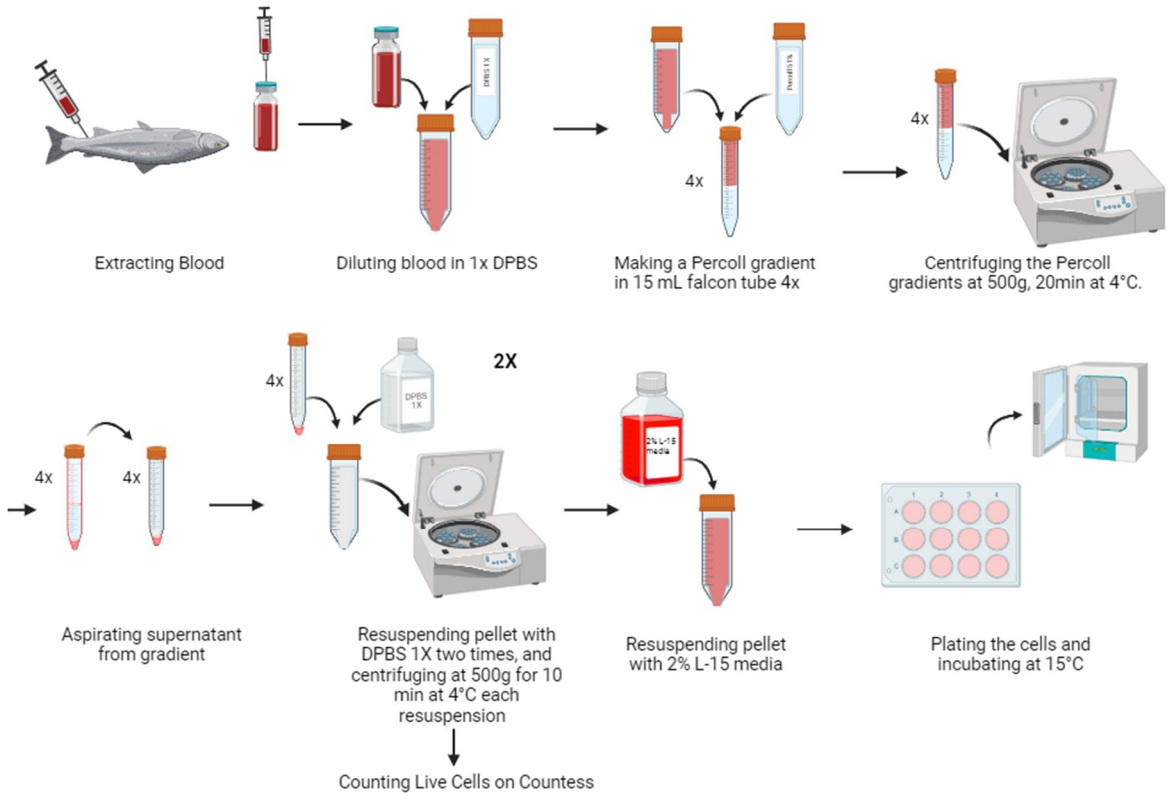

Figure 13. Flowchart of "3.1.3 RBC isolation by density gradient centrifugation" protocol. Made in BioRender.com.

3.2 Working with RNA

RNA is unstable compared to DNA and is prone to degradation (59). Exposure to alkaline pH, high temperatures, metal ions and RNases degrades RNA, and these factors need to be absent to create conditions for working with RNA. The presence of RNase in a sample can originate from the sample itself (endogenous) and from environmental contaminations. To prevent degradation of sample RNA by endogenous RNAse, an RNase inhibitor can be added. Contaminating RNase is a common issue, but solution and equipment used during experiments can be autoclaved or sterile-filtered to minimize RNase contamination, and gloves can be used to prevent contamination from the skin.

3.2.1 Linearization and purification of a GFP encoding DNA plasmid

pVAX1 plasmid (ThermoFischer Scientific) encoding Enhanced Green fluorescent protein (EGFP) was obtained from the research group of E. Rimstad. Restriction enzyme cutting of the GFP encoding plasmid was performed using the restriction enzyme MIuI (Thermofisher Scientific), according to the "fast digestion of Different DNA" protocol with upscaling adjustments (Fast Digestion of Different DNA Protocol (Thermofisher.com)).

- To a 1.5 mL Eppendorf tube, 70 µL nuclease free water, 10 µL 10X FastDigest buffer, 10 µg plasmid DNA and 10 µL FastDigest enzyme was mixed together and incubated at 37°C for 45 min. The mixture was put on ice after the incubation.
- To access the quality of the restricted DNA, an agarose gel was utilized for electrophoresis. The agarose gel was prepared by making an agarose solution containing 50 mL TAE buffer, 5 µL SybrSafe and 0.5 g agarose in an Erlenmeyer flask. The agarose solution was heated up in a microwave oven to dissolve the agarose, and once dissolved, the solution was transferred to an electrophoresis chamber.
- When the gel had solidified, a Generuler 1kb Plus DNA ladder (Thermofisher Scientific) was loaded into the gel for tracking the size of the sample DNA. From the DNA-sample, 5 µL was diluted with 20 µL H_2O, and further mixed with 5 µL 6x loading buffer (Thermofisher Scientific) for visual tracking of the DNA. The diluted DNA was loaded to the gel and electrophoreses was performed at 100V for 1 hour.

- Subsequently, the DNA was purified using NucleoSpin Gel and PCR clean up (MACHEREY-NAGEL), according to manufacturer instructions (Instruction-NucleoSpin-Gel-and-PCR-Clean-up)).
- The quality and quantity of the purified DNA was accessed using a MultiSkan Sky Microplate Spectrophotometer (Thermofisher Scientific), and the linearized GFP plasmid was further continued for in vitro transcription and capping.

3.2.2 In Vitro Transcription

RNA transcripts were achieved from linearized DNA by In vitro transcription (IVT) using the RiboMAX^{TM} Large Scale RNA production system kit (Promega) with SP6 polymerase, following manufacturer's instructions with adjustments (https://no.promega.com/instructions).

- A mixture of 4 µL SP6 transcription 5x buffer, 1 µL of each 25mM rNTPs (ATP, CTP, GTP, UTP), 10 µL of linearized DNA template (1 µg DNA mixed with 9 µL H_2O) and 2 µL of Enzyme Mix (SP6) was prepared in a RNase free tube. The tube was covered with parafilm, to hinder condensation, and incubated at 37°C for 3 hours.
- After incubation, 1 µL DNase was added per µg DNA, and the mRNA was incubated for an additional 15 min at 37°C. After incubation, the mRNA was continued for "mRNA purification".

3.2.3 mRNA purification

The mRNA was purified using the RNeasy Mini Kit (Qiagen).

- Samples were adjusted to a volume of 100 µL with RNase-free water and mixed with 350 µL Buffer RLT. The diluted mRNA was further added 250 µL ethanol (96-100%), and transferred to an RNeasy Mini spin column, further inserted in a 2 mL collection tube.
- The 2 mL collection tube was centrifuged for 30 seconds at 8000g, and after centrifugation, the flow through was discarded.

- To the same RNeasy Mini spin column, 500 µL Buffer RPE was added, and the column was placed in the same collection tube and centrifuged as above.
- After centrifugation, flow through was discarded, and the RNeasy Mini spin column was put into a new collection tube to diminish flow-through remains on the outside of RNeasy spin column. The buffer RPE step was performed again, as above.
- The RNeasy Mini spin column was inserted in a new 2 mL collection tube after repeating the buffer RPE centrifugation step, and centrifuged at 14 500 rpm for 1 min to eliminate carryover of Buffer RPE, and to remove residual flow through on the RNeasy Mini spin column.
- After centrifuging at full speed, RNeasy Mini spin column was put in a 1.5 mL RNase-Free Eppendorf tube. To the RNeasy Mini spin column, 30-50 µL RNase-Free H_2O was added to the spin column membrane, and centrifuged for 1 min at 8000g.
- The elution collected in the 1.5 mL RNase-Free tube was placed on the RNeasy Mini spin column membrane and centrifuged again as before for higher mRNA yield.
- The sample was further quantified on Multiskan sky from Thermofisher Scientific.

3.2.4 mRNA Capping

Capping was executed according to ScriptCap™ Cap 1 Capping System (10 rxn) (CELLSCRIPT™) procedure (Cellscript procedure (cellscript.com)), with three adjustments: 1) the IVT-mRNA was diluted to a total volume of 67 µL instead of 64.5 µL, 2) 2.5 µL S-adenoyl-methionine (SAM) was added in the "enzyme-cocktail" instead of 5 µL and 3) when adding Cocktailed reaction components and ScriptCap Capping enzyme to Heat-denatured RNA, incubation occurred at 37 °C for 2 hours instead of 30 min as it was recommended for incomplete 2'-O-methylated RNA. The reason for the two first adjustments was that an outdated procedure was used during mRNA capping. After capping, the mRNA was purified in the same matter, as described in "3.2.3 mRNA purification". The quantity and quality was accessed using a MultiSkan Sky spectrophotometer from Thermofisher Scientific and TapeStation 4200 from Agilent performing automated electrophoresis. Samples were stored at -20°C until further use.

3.2.5 Spectrophotometric quality and quantity analyses

MultiSkan µDrop Duo plate was washed with ethanol, and ran in MultiSkan Sky Microplate Spectrophotometer after adjusting the absorbance to 450 nm. Channels with absorbance 0.6 ± 0.08 was further used to access the concentration of the DNA or RNA. The protocol used for accessing the DNA or mRNA concentration was available on the SkanIt software (SkanIt Software). An adjustment to the standard RNA protocol was that the concentration formula length was adjusted to 0.051, instead of 0.049. On the plate layout in the protocol, one unknown sample containing 1 µL mRNA sample, and two blank samples blanks containing 1 µL nuclease free water each channel, was chosen to be analysed. The samples were quantified in the MultiSkan Sky Microplate Spectrophotometer assessing the concentration, 260/280-purity and 260/230-purity.

3.2.6 TapeStation 4200 quality analyses

The mRNA was diluted to 250 ng/µL before further preparation for TapeStation 4200. From the diluted mRNA, 1 µL was transferred to a PCR-tube, and mixed with 5 µL RNA Sample buffer. After mixing, the mixed mRNA was vortexed at 2000 rpm for 1 min, then centrifuged for 1 min. The mixed mRNA was further incubated at 72°C for 3 min, and further incubated on ice for 2 min. The sample was centrifuged an additional time for 1 min before being inserted in the TapeStation 4200, together with RNA ScreenTape and Tapestation pippete tip from Agilent for quality assessment of band length, purity and degradation.

3.3 Electroporation

3.3.1 Transfection

Transfection is a procedure for introducing nucleic acids are into eukaryotic cells (52). Different transfection methods exist, falling into three main categories: i) viral based, ii) chemically based and iii) physically based.

Viral-based transfection, also known as transduction, utilizes a viral vector, such as viral envelope, to transport nucleic acid into a host cell (52). Either the transduction could be

stable for long-term expression or transient for short-term expression. The choice between stable and transient transfection depends on the viral vector utilized, for example, retrovirus will lend stable transfection, but adenovirus will give transient transduction.

Chemical transfection can be categorized into two main categories: liposomal and non-lipomosal (52). Liposomal-based transfection involves the use of a positively charged lipid vector that engulf the nucleotide and enter the cell through ionic-interactions and by polarity. Non-liposomal transfection methods utilize the same principles as liposomal-based transfection, but do not employ lipids.

Physical transfection includes different mechanical methods like microinjection, sonoporation, magnetofection, laser irradiation with electroporation being the most common one (52). Electroporation has been utilized for cells termed “difficult-to-transfect” which includes primary cells and stem cells. The application of electrical voltage creates holes in the host cell membrane, increasing the permeability, and allowing the entry of nucleic acids at this point. However, a drawback of electroporation is that the use of high voltage resulting in cell death through necrosis, apoptosis, or permanent alteration of the cell.

3.3.2 Designing siRNAs

From the national library for biotechnology information (NCBI), mRNA sequences of the genes intended for silencing were retrieved in FASTA-format. If the gene had an additional transcript-variant, the variants were assembled in Clustal Omega (clustalo (1.2.4)) with default settings, and only identical parts of the sequence were utilized. After retrieving the sequence, three siRNAs for one gene was designed according to general design guidelines from Thermofisher Scientific (siRNA Design Guideline). Off-target screening was performed using NCBI-BLAST. siRNAs which had high expression of potential off-targets with ≥80% query coverage, were discarded as potential siRNAs. At the end, overhangs were constructed on the antisense-strand of the siRNA, as it increases the potency and increases the antisense strand loading to the RISC (60).

3.3.3 Preparation for the electroporation protocol

- RBCs were transferred from a 12-well plate to a 50 mL Falcon tube, and centrifuged at 300g for 5min at 14˚C. Supernatant was aspirated after centrifugation.
- The RBCs were resuspended in DPBS 1X to a concentration of $5*10^6$ cells/mL. From the resuspension, 10 µL is transferred into a 1.5 mL Eppendorf tube and used for automatic cell counting by Countess, performed as in "3.1.4 Cell counting". Cell counting was performed to assess viability and the amount of T-buffer needed for a concentration of $5 * 10^5$ cells/µL.
- The Falcon tube is centrifuged under the same condition as the last centrifugation. After centrifugation, supernatant is aspirated, and the pellet is resuspended in T-buffer to a concentration of $5 * 10^5$ cells/µL. The resuspended RBCs were then transferred to a 1.5 mL Eppendorf tube, which was put on ice before transfection.

3.3.4 Neon electroporation of A. salmon RBCs

In a 24-well plate, 490 µL of L-15 medium containing 2% FCS was transferred to the wells, depending on the number of transfection executed. For one transfection, RBCs were transferred to a 1.5 mL Eppendorf tube and mixed with corresponding RNA. The solution is then transfected using the Neon™ Transfection system 10 µL kit, following the Invitrogen Neon™ Transfection manual provided by Thermofisher Scientific (Neon Transfection manual (Thermofisher.com)). In an additional well with 490 µL L-15 medium with 2% FCS, 10 µL not electroporated RBCs was added. The 24-well plate was further incubated at 15°C for either "3.4.1 Harvesting of RBCs for flow cytometer" or "3.6.2 Harvesting of RBCs for RNA isolation".

.

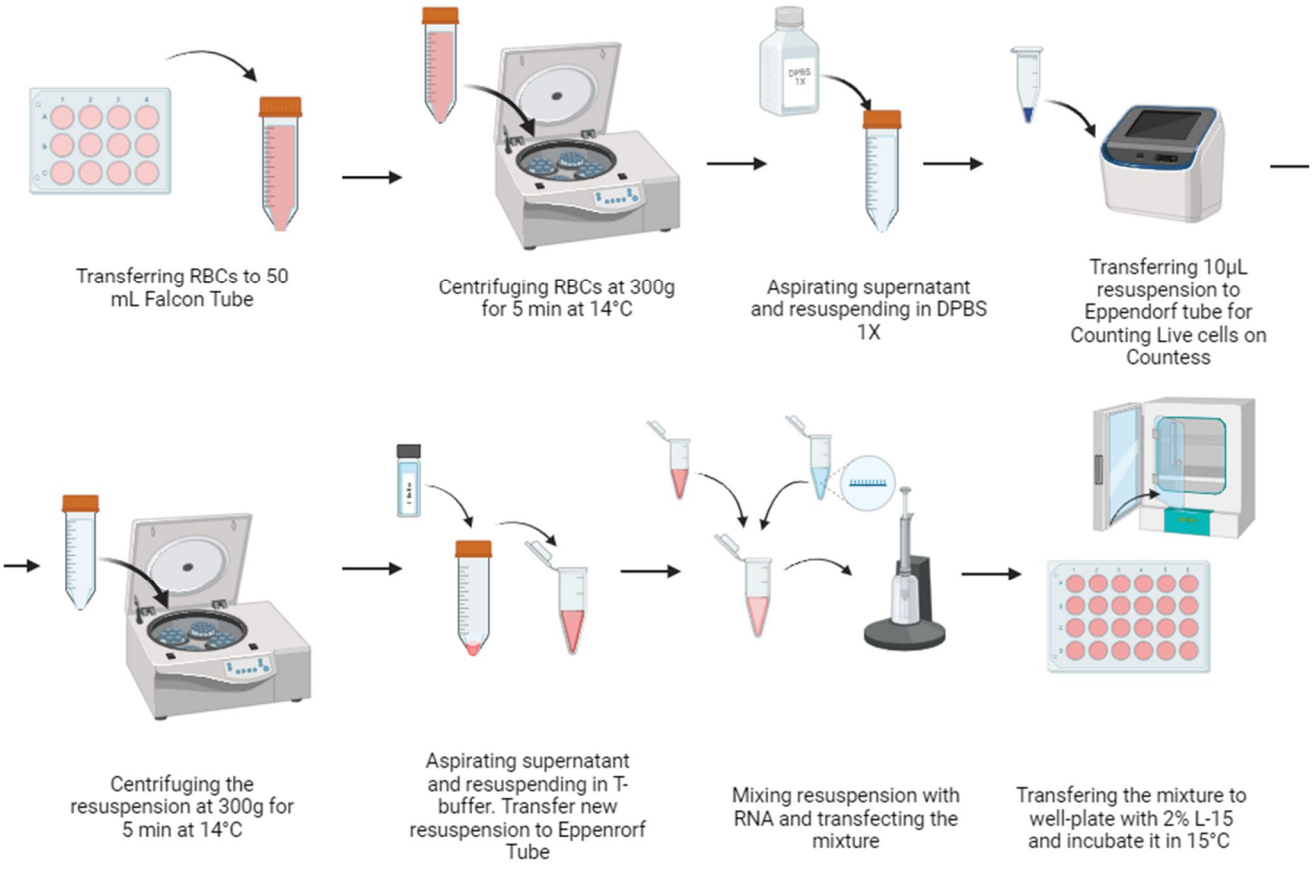

Figure 14. Flowchart of "3.3.3 Preparation for the electroporation protocol" and "3.3.4 Neon electroporation of A. salmon RBCs" protocol. Made in BioRender.com.

3.4 Flow cytometry

Flow cytometry enables multi-parametric analysis of singular cells (61). Fluidic system moves cell-sample in sheath fluid to an optical system consisting of lasers. Lasers are directed through a single cell, one by one, causing scattering of the lasers. Detectors in two different directions, forward scatter (FSC) and side scatter (SSC), read and analyze the scattered lasers. FSS and SSC describe the size and the internal complexity of the cell, respectively. The results from a flow cytometer can be presented as a dot-plot or histogram. By analyzing the results, single cells can be divided into different populations. There are different instruments and reagents that allow flow cytometry to be used for numerous applications in the fields of molecular biology and immunology. For example, flow-cytometry analysis can be utilized to study the expression of fluorescent proteins, e.g. GFP, after transfection of GFP-encoding nucleic acids. Flow cytometer can also be utilized to evaluate cell viability by adding a DNA or RNA binding dye, e.g. propidium iodine (PI), which binds to nonviable RBCs.

3.4.1 Harvesting of cells for flow cytometry analyses

- From the 24-well plate obtained from *"*3.3.4 Neon electroporation of A. salmon RBCs" protocol, 100 µL of each sample was transferred to individual wells in a U-bottom 96 well-plate.
- Samples for auto compensation were also prepared to the 96 well-plate, and consisted of 3 compensation wells: 1) 100 µL of RBCs transfected with fluorescent siRNA, 2) 100 µL of RBCs transfected with mRNA-GFP and 3) 100 µL of dead RBCs. Dead RBCs were prepared by mixing RBCs in a volume containing 1:5 Dimethyl sulfoxide (DMSO).
- The plate was centrifuged at 300g for 5 minutes at 4°C, and the supernatant was aspirated from the wells. The pellets were resuspended with 100 µL DPBS 1x, and centrifuged again as the last condition.
- After centrifugation, supernatant was aspirated, and pellets were resuspended with 100 µL DPBS 1x. Subsequently, 1 µL PI solution was added to all wells, except the RNA transfected compensation wells and the well(s) with un-electroporated RBCs.
- The 96-well plate was further analyzed in Novocyte flow cytometer for assessing cell viability and the amount of fluorescent cells.

3.4.2 Flow cytometry settings

The parameter settings chosen for flow included FSC, SSC, Fluorescein isothiocyanate (FITC), and Phycoerythrin (PE) for both area and height. The stop conditions were set at 10,000 events and 80 µL with a slow flow rate.

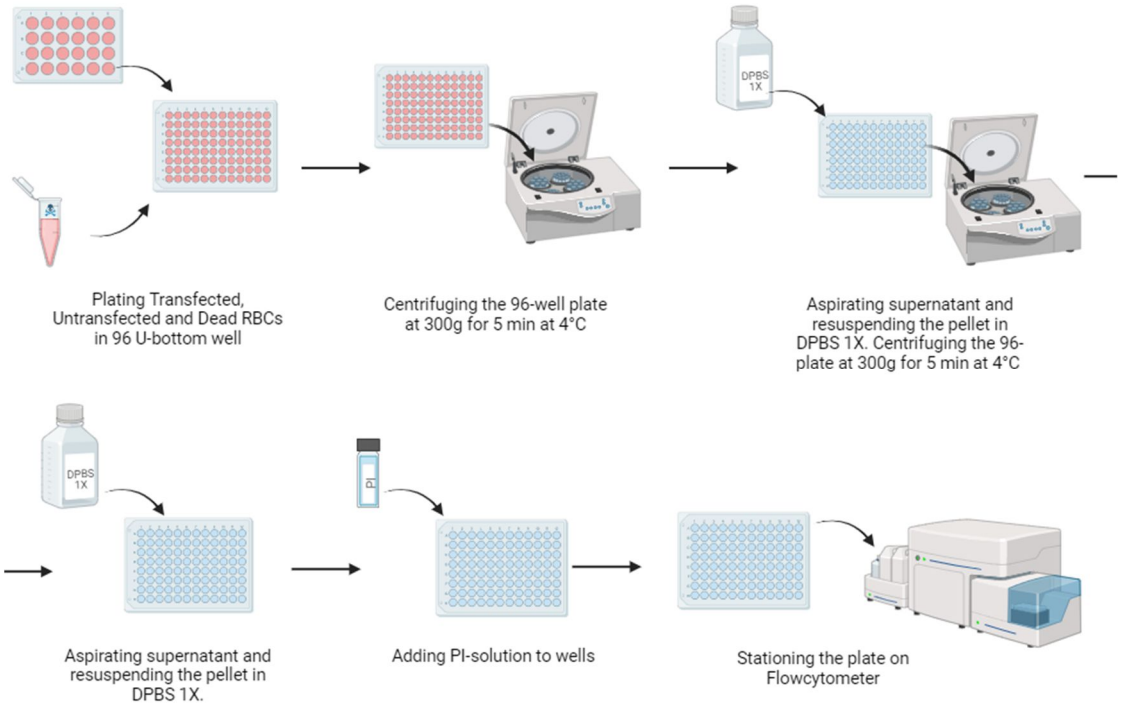

Figure 15. Flowchart of "3.4.1 Harvesting of cells for flow cytometry analyses". Made in BioRender.com.

3.5 Chinook salmon embryo cell line

The Chinook salmon embryonic cell line-214 (CHSE-214) is an epithelial cell line, and is derived from the embryonic tissue of Chinook salmon (*Oncorhynchus tshawytscha*) (62).

3.5.1 Subculturing CHSE-214

CHSE-214 is an adherent cell-line and needs to be transferred to fresh growth media (L-15 media with 5% FCS and antibiotics) to continue growth.

- When the CHSE-214 cells has reached 100% confluence, old growth media is aspirated, and the cells were washed with PBS absent of Ca^{2+} and Mg^{2+}.
- The cells are further detached from the surface using trypsin. Trypsin works by catalyzing the peptide bonds on the CHSE-214 cells used for binding to the surface (63). The trypsination time is dependent on different factors, for example area of flask, cell-line and volume of trypsin added. If incubation occurs for too long, the cells can be damaged. The trypsin added to the CHSE-214 contained ethylenediaminietatraacetic acid (EDTA), which binding to inhibitory cations.

- Inactivation of trypsin was done when fresh growth media with 5% FCS is added.
- Fresh growth media, containing detached CHSE-214 cells, are further transferred to a new cell flask and incubated at 20°C for growth (63, 64).

3.5.2 Preparation of CHSE-214 for electroporation protocol

When the CHSE-214 cells reached 80-100% confluence, electroporation was performed.

- Growth media is aspirated from the cell flask, and cells are washed twice with PBS.
- PBS is aspirated, and trypsin solution containing EDTA was added to the cell flask with CHSE-214. The trypsin solution was distributed quickly by tilting the flask, and then the majority of the solution was aspirated to hinder cell damage.
- Cells were added L-15 media with 5% FCS after enough cells had detached from flask. The cells were further transferred to a 50 mL Falcon tube, which was centrifuged at 500g for 5 min at 15°C.
- Supernatant was aspirated from the 50 mL Falcon tube, and the pellet was resuspended in 1.0 mL PBS, which was transferred to a 1.5 mL Eppendorf tube.
- From the resuspension, 10 µL was withdrawn and transferred to a 1.5 mL Eppendorf which was used for automatic cell counting by Countess, performed as in "3.1.4 Cell counting". Automatic cell counting was performed to assess viability and the opti-MEM™ volume needed for a concentration of $1*10^4$ cells/µL.
- The 1.5 mL Eppendorf tube is further centrifuged at 400g for 5 min at 15°C, and the pellet is resuspended in opti-MEM™ to a concentration of $1*10^4$ cells/µL.
- The opti- MEM™ resuspension is further used for electroporation, performed as in "3.3.4 Neon electroporation of A. salmon RBCs" with one adjustment: 1) Culturing the CHSE-214 cells in 1 mL L-15 media with 5% FCS instead of 490 µL L-15 media with 2% FCS.
- CHSE-214 cells were incubated at 20°C, and after 24 hours, the transfected and not-electroporated CHSE-214 cells were changed to L-15 media with 5% FCS and antibiotics. After 48 hours, the CHSE-214 cells were continued with for "*3.5.3 Harvesting CHSE-214 cells for flow cytometer*".

3.5.3 Harvesting CHSE-214 cells for flow cytometry

- From the 24-well plate with samples containing transfected and not-electroporated CHSE-214 cells, media was aspirated, and the CHSE-214 cells were washed with 1 mL PBS.
- PBS was aspirated from the wells, and 100 µL trypsin was added to each well for detachment of cells. To each well, 500 µL L-15 media with 5% FCS was added when enough cells had detached from the wells.
- The detached cells from each sample in media was further transferred to individual 1.5 mL Eppendorf tube and centrifuged at 400g for 5 min at 15°C.
- The supernatant was aspirated, and the cells were resuspended in 200 µL PBS. The preparation for flow cytometer was done according to "3.4.1 Harvesting of cells for flow cytometry analyses" with same settings as in "3.4.2 Flow cytometry settings"

3.6 RNA isolation

3.6.1 Principle for the MagNA pure RNA isolation system

Isolation of RNA can either be performed with manual methods or automatic systems (64). TRIzol® and Insta-Pure kits are one out of several manual methods for extracting nucleic acid, but automatic systems are more preferred since nucleic acid isolation is technically demanding and labor intensive (65, 66). A high-throughput instrument for automatic extraction is the MagNA Pure system (67). MagNA pure systems purifies RNA using magnetic bead technology (65). Precision pipettors binds to magnetic beads, which again binds to nucleic acid. The bound nucleic acid moves through several washing steps for purification, and after purification, the nucleic acid is eluated. Different bench-top MagNA pure machines is utilized depending on the number of samples. MagNA pure 96 for instance can take up to 96 samples.

3.6.2 Harvesting of RBCs for RNA isolation

- To individual 2 mL Eppendorf tubes, RBCs from "3.3.4 Neon electroporation of A. salmon RBCs" were transferred, and centrifuged at 500g for 5 min at 4°C. After

centrifugation, the supernatant was aspired and the pellets were resuspended in 1 mL DPBS 1X.

- From the resuspension, 10 µL were withdrawn, and assessed for viability through automatic cell counter countess, performed as in "3.1.4 Cell counting".
- The samples were centrifuged an additional time as the last condition, and the supernatant was aspirated. After centrifuging the samples, the pellets were resuspended in 25 µL DPBS 1X and mixed with 175 µL MagNA Pure lysis buffer for lysis of the RBCs. The samples were further stored in -20ºC.

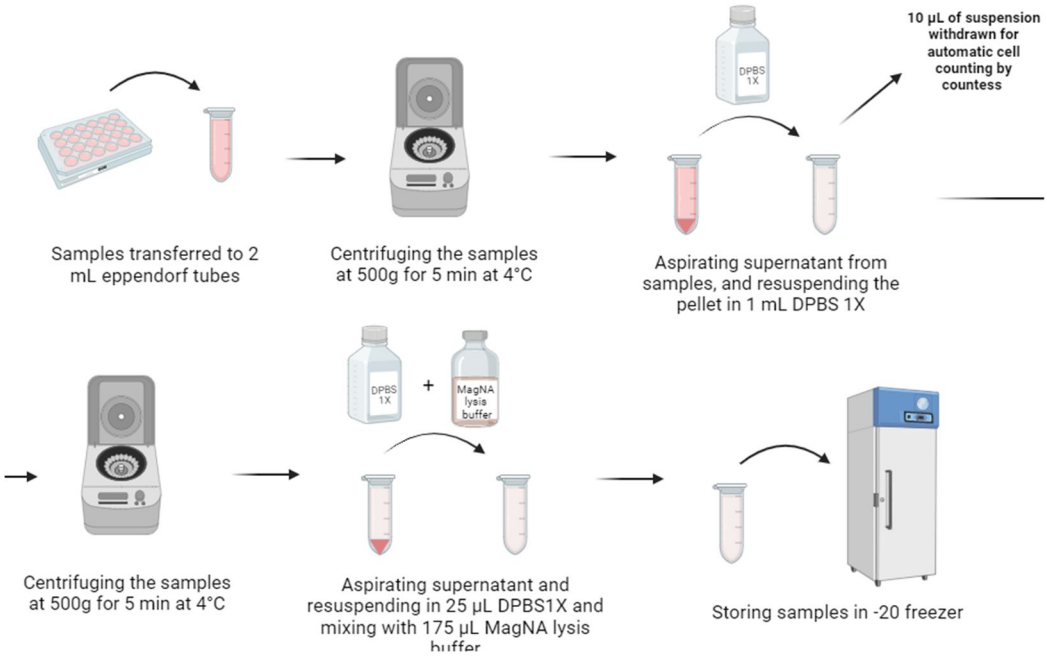

Figure 16. Flowchart of "3.6.2 Harvesting of RBCs for RNA isolation". Made in BioRender.com.

3.6.3 RNA isolation protocol

- In each sample, one 5 mm stainless steel bead (Qiagen), was inserted. The samples were further homogenized using Qiagen TissueLyser II at 22.4 Hz for 3 min.
- After homogenization, samples were centrifuged at 300 rcf for 30 sec, and further transferred to a MagNA Pure 96 Processing Cartridge.
- The isolation was performed using MagNA Pure 96 instrument with the "cellular RNA, Large Volume kit" according to manufacturer (MagNA Pure 96 Cellular RNA Large Volume Kit (roche.com)).

- After isolation, the samples were quantified using Multiskan Sky Microplate Spectrophotometer in the same matter described in “3.2.4 MultiSkan Sky” with following adjustments: 1) Multiskan µdrop plate was utilized instead of µDrop Duo plate, 2) The plate was washed with dH_2O and not ethanol and 3) 2.4 µL RNA sample and nuclease free water was loaded to the channels according to plate layout. The samples were further transferred to individual 1.5 mL Eppendorf tubes, stored at -80°C.

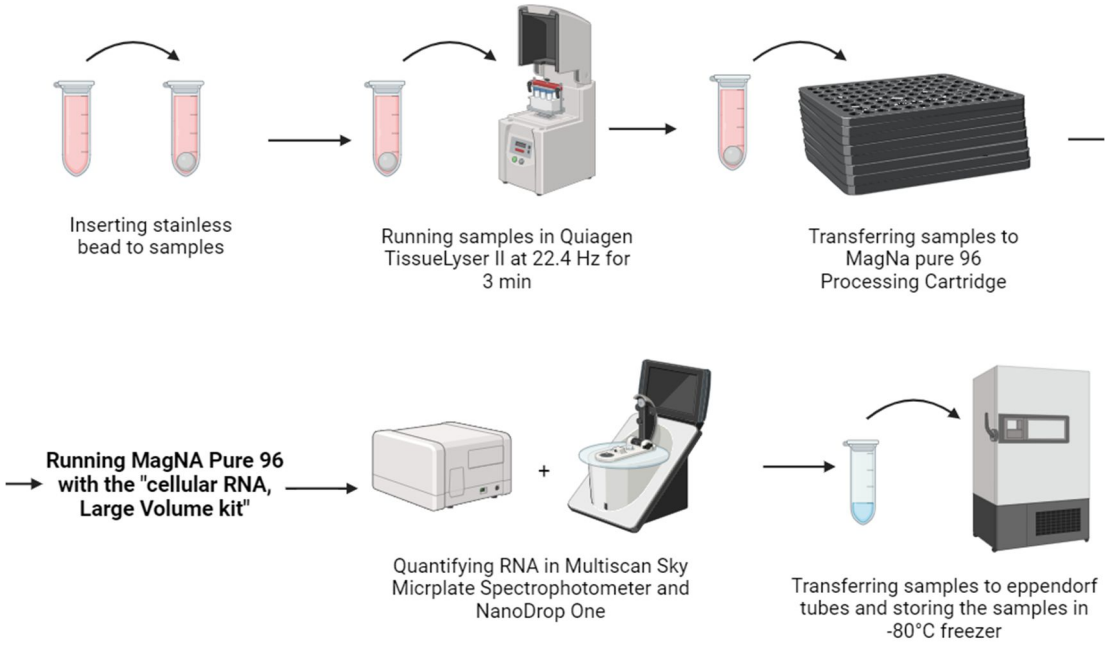

Figure 17. Flowchart for “3.6.3 RNA isolation protocol”. Made in BioRender.com.

3.7 Real time Quantitative polymerase-chain-reaction

Real time Quantitative polymerase-chain-reaction (Real time-qPCR) is a widely recognized technique for studying gene expression (66). The technique amplifies, and simultaneously, quantifies a target DNA-molecule in real time. This differs from original PCR in that it quantifies along with the amplification cycle. qPCR achieves this by monitoring relative quantity by fluorescence through numerous amplification cycles to reach a set threshold-level. The higher expressed a gene is (more mRNA), the fewer amplification cycles is needed to go above threshold-level, and the end-result is a Ct-value which represents the number of amplifications cycles until the threshold was met. The Ct-value can be used to calculate the relative gene-expression from the original sample. For quantification of mRNA through

reverse transcription qPCR (RT-qPCR), isolated RNA is first synthesized into a complimentary DNA (cDNA) template.

Two common florescence quantification methods used for RT- qPCR are SYBR green and TaqMan probes (69). In this thesis, SYBR green was used. The SYBR green dye binds to double stranded DNA during amplification of the target gene by gene-specific primers. Such primers are easy to design, cheap and are able to provide satisfactory results. The drawback of SYBR green is that it is a non-specific dye and could also produce false positive, inaccurate results.

3.7.1 Primer design targeting TLR3, MAVS, RLR3 and RIG-I mRNA

In NCBI-BLAST, the mRNA sequences which were utilized to design siRNA were identified and uploaded into primer-BLAST. The settings were as followed:

1. “Primer Parameters” were adjusted so that “PCR product size” were set at min 100 nt and max 300 nt, and the “primer melting temperatures (T_m)” were set at min 58°C, Opt 60°C, Max 62°C and Max T_m difference at 2°C.

2. “Exon/intron selection” were adjusted to “Exon junction span” set at “Primer must span an exon-exon junction”.

3. The primer-BLAST search was performed in the organism “Salmo salar”.

3.1 If the screening retrieved no results, the “Exon junction span” were changed to “No preference”, and “intron inclusion” in “Exon/intron selection” were adjusted to “Primer pair must be separated by at least one intron on the corresponding genomic DNA”.

3.2 If no results were retrieved again, “intron inclusion” was set on default setting again.

3.7.2 cDNA synthesis protocol

cDNA synthesis was performed using QuantiTect Reverse Transcription kit (Qiagen).

- RNA samples were diluted to 5 – 10 ng/µL with RNAse free water, to a total volume of 10 µL on pcr-strips.
- To each sample, 2 µL gDNA Wipeout Buffer (7X) and 2 µL RNase-free water was added. Samples were inserted in Applied Biosystems Veriti 96 Well Thermal Cycler for 2 min at 42°C, and put on ice.
- To the samples, 6 µL of a reverse transcriptase (RT) mix was added, resulting in a total volume of 20 µL each. The RT-mix contained Quantiscript RT, RT primer mix and Quantiscript RT buffer. The samples were again inserted in Applied Biosystems Veriti 96 Well Thermal Cycler, programmed to synthesize cDNA for 30 min at 42°C, and not 15 min as described in manufacturers protocol, to increase cDNA yield. It was then followed by an incubation step at 95°C for 3 min for inactivation of the Quantiscript RT.

A no template control (NTC) for detection of contamination of PCR reagents, and a no reverse transcriptase control (RTC) for detection of DNA contamination were also prepared during cDNA synthesis. The NTC contained all the reagents except template cDNA, substituted with 10 µL RNase-free water. The RTC had all the reagents except RT-mix, substituted with 6 µL RNase-free water. The NTC and RTC went through all the steps described in the protocol. The newly synthesized cDNA (and NTC and RTC) were diluted with RNase free water to 2.5 ng/µL, and further stored at -20°C for qPCR.

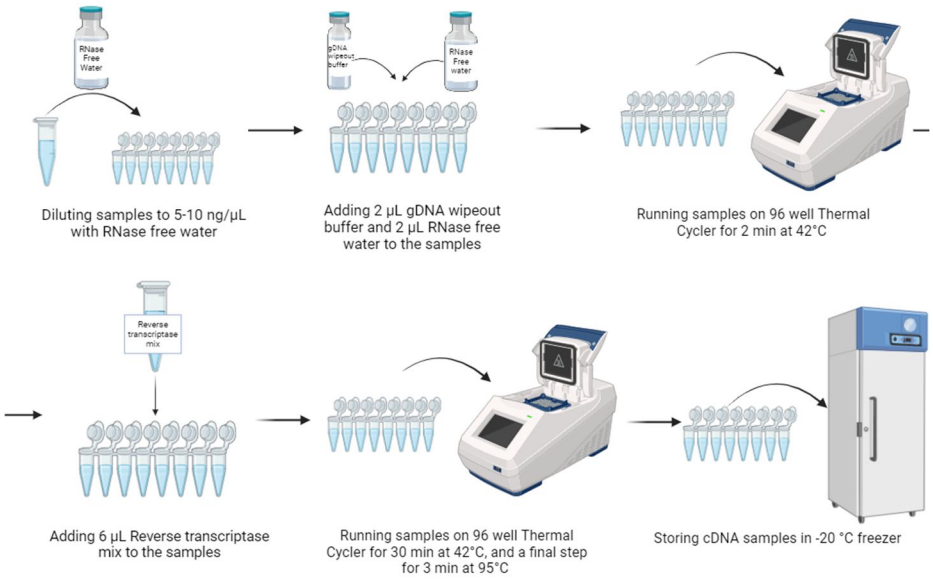

Figure 18. Flowchart of "3.7.2 cDNA synthesis protocol". Made in BioRender.com.

3.7.3 qPCR protocol

- To a 365 qPCR-well plate, 8 µL of a master-mix containing 1:2 SYBR-green (2X), 1:20 reverse primer (10 µM), 1:20 forward primer (10 µM) and 1:4 nuclease free-water was added to parallel wells (two per sample), for creating duplicates .
- In all the wells with master mix, 2 µL cDNA was added to the corresponding primer, resulting in a total volume of 10 µL each well.
- The plate was sealed twice using Bio-Rad PX1 PCR Plate Sealer, and spun in a VWR PCR Plate Spinner.
- After spinning, the plate was loaded onto a Bio-Rad CFX384™ Real-Time System for 1 cycle at 95°C for 30 sec and 40 cycles at 95°C for 15 seconds followed by 60°C for 30 seconds.
- The data generated was uploaded into Bio-Rad CFX Manager 3.1 (3.1.1517.0823) and further processed into an Excel 2007 format for data analysis.

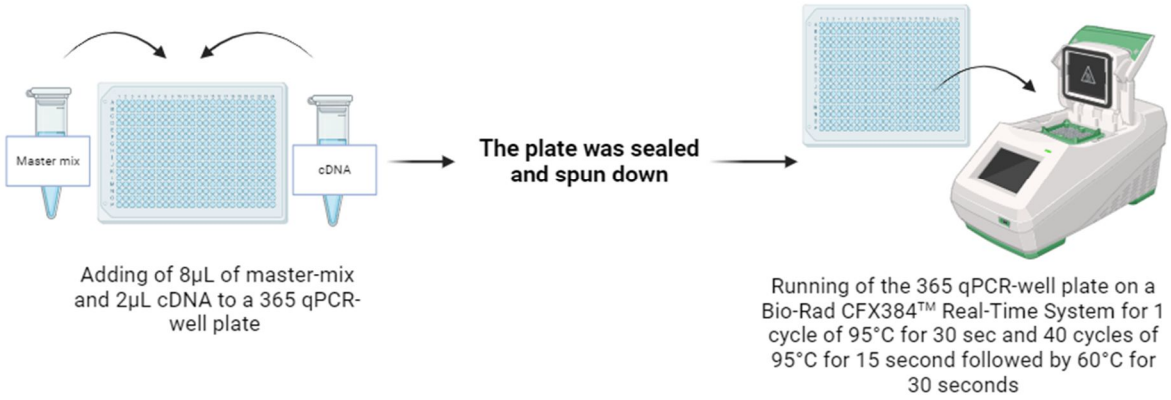

Figure 19. Flowchart of "3.7.3 qPCR protocol". Made in BioRender.com.

3.8 Data Analysis

Graph production of the flow cytometer data and RT-qPCR data was done using Graphpad Prism version 10.2.1. The RT-qPCR data was analyzed using the $2^{-\Delta\Delta Ct}$-method for calculation of relative gene expression. The $2^{-\Delta\Delta Ct}$-method utilizes the Ct-value from the RT-qPCR data, and normalizes it against levels of a reference gene (70). In these experiments EF1α was used as a reference gene. First a ΔCt-value is calculated using formula (1). The ΔCt-value

show the difference in threshold cycles between target gene and reference gene. Next a ΔΔCt-value is calculated using formula (2), calculating the difference in normalized Ct-value of the target samples from the normalized reference sample value. The ΔΔCt-value is equal to 0 for the reference sample, which means that the basal gene expression is set to 1 according to formula (3). Using formula (3) to target samples will then result in a fold-change value relative to the reference sample. An example of calculating fold-change is shown in Appendix A2.

(1) $\Delta CT = CT\ (\text{target gene}) - CT\ (\text{reference gene})$

(2) $\Delta\Delta CT = \Delta CT\ (\text{a target sample}) - \Delta CT\ (\text{a reference sample})$

(3) $\text{Fold change from reference} = 2^{-\Delta\Delta CT}$

Statistical analysis was performed using either one-way ANOVA or two-way ANOVA with alpha-value set to 0.05, in Graphpad Prism version 10.2.1. If a value was missing, mixed effects model was done instead. A multiple comparison test was performed using the test recommended by Graphpad Prism version 10.2.1, which was either a Tukey test or Šídák test.

4 Results

The experiments described in the latter section were performed for three purposes:

1) Optimization of siRNA and mRNA transfection in A. salmon RBCs
2) A control experiment to study if mRNA silencing is achievable in A. salmon RBCs (and CHSE-214).
3) Silencing of TLR3, RIG-I, RLR3 and MAVS in A. salmon RBCs to study the antiviral response compared to basal antiviral response.

Figure 20 gives a more detailed description of which methods have been used for what purpose. “Poly(I:C) stimulation" in Figure 20 has not been described in the latter section, but the experimental design is discussed in “4.8 siRNA silencing of TLR3, RIG-I, RLR3 and MAVS during poly(I:C) stimulation”.

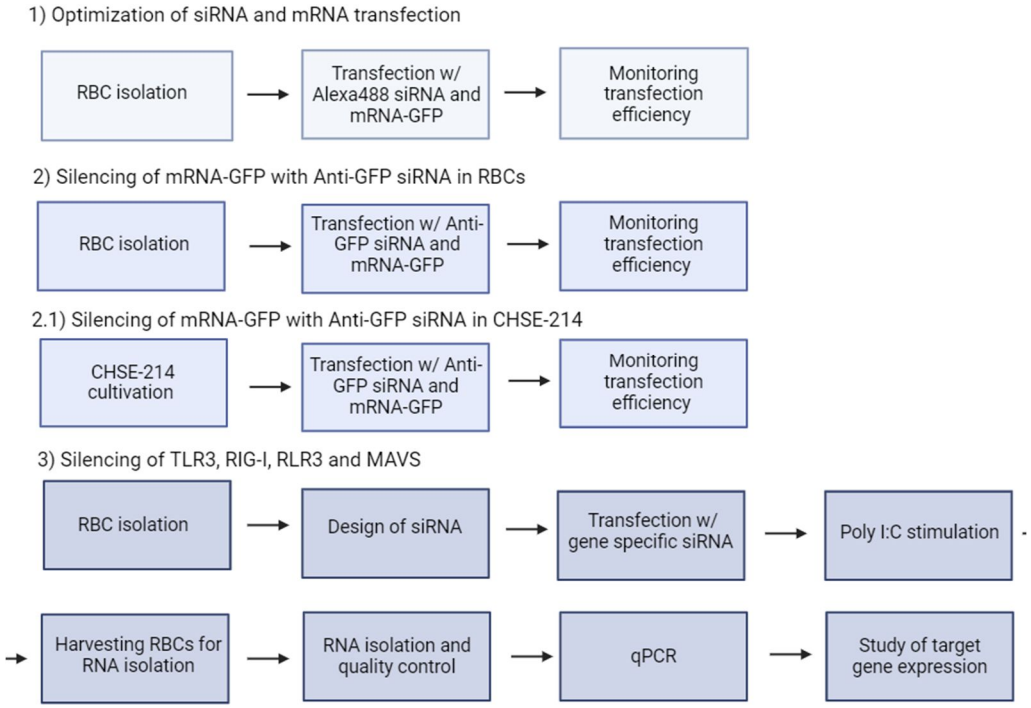

Figure 20. Flowchart of methods utilized for the purpose of 1) Optimization of siRNA and mRNA transfection in A. salmon RBCs, 2) A control experiment to study if mRNA silencing is achievable in A. salmon RBC and CHSE-214 (2.1) and 3) Silencing of TLR3, RIG-I, RLR3 and MAVS in A. salmon RBCs to study the antiviral response compared to basal antiviral response. Made in BioRender.com.

4.1 Gene expression of siRNA effectors in red blood cells

RNA sequencing data (Illumina RNASeq) recently published in Tsoulia *et al*. (36), originating from isolated RBCs from six A. salmon pre-smolts, was used to retrieve expression data on genes encoding proteins involved in the RNAi system (Table 3). For a comparison with two other A. salmon cell lines, Atlantic salmon kidney (ASK) and salmon head kidney-1 (SHK-1), see Appendix Table J1.

Table 3. Mean normalized RBC transcript reads (n= 6 A. salmon) of genes encoding proteins involved in the RNAi mechanism

Gene code	Short name	Full name	Transcript reads
ENSSSAG00000048206	ago2	argonaute RISC catalytic component 2	439
ENSSSAG00000068383	ago1	protein argonaute-1	60
ENSSSAG00000002403	dicer1	endoribonuclease Dicer-like	493
ENSSSAG00000046898	dicer1	endoribonuclease Dicer-like	353
ENSSSAG00000005813	tarbp2	TARBP2 subunit of RISC loading complex	101
ENSSSAG00000026891	snd1	staphylococcal nuclease and tudor domain containing 1	62
ENSSSAG00000050721	lyric	LYRIC protein (AEG-1)	880
ENSSSAG00000066076	mtdha	protein LYRIC-like	3647
ENSSSAG00000079281	taf11	TATA-box binding protein associated factor 11	2440

The number of transcript reads obtained for Ago2 and dicer in A. salmon RBCs are respectively 439 and 493/353. In comparison with ASK and SHK-1 (Appendix J1), Ago2 is transcribed less in RBCs, but dicer is transcribed higher in the kidney cells. Staphylococcal nuclease and tudor domain containing 1 (snd1), LYRIC-protein (lyric), TARBP2 subunit of RISC loading complex, tudor domain containing 1, protein LYRIC-like and TATA-box binding protein associated factor 11 (taf11) are also expressed, and their potential role in the siRNA system is discussed in “5.2.3 Is silencing by siRNA possible in A. salmon RBCs”.

4.2 Optimization of siRNA transfection

The methods utilized to establish and optimize siRNA transfection is shown in Figure 21. Same methods were utilized for establishment and optimization of mRNA transfection in "4.3 mRNA-GFP transfection"

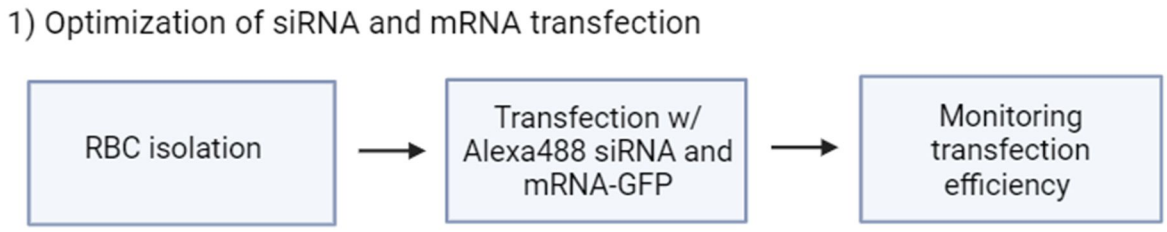

Figure 21. Methods utilized to optimize siRNA and mRNA transfection.

4.2.1 Establishing siRNA transfection in A. salmon RBCs

Transfection efficiency was evaluated by transfecting RBCs with fluorescent Allstars Neg. siRNA AF488 (siRNA-AF488) (Qiagen), and analysing transfected cells by flow cytometry. The amount of siRNA transfected with was 2 µg, which was based on a concentration assay transfecting RBCs with DNA-plasmid (unpublished RED FLAG data). The experimental setup is presented in Figure 22.

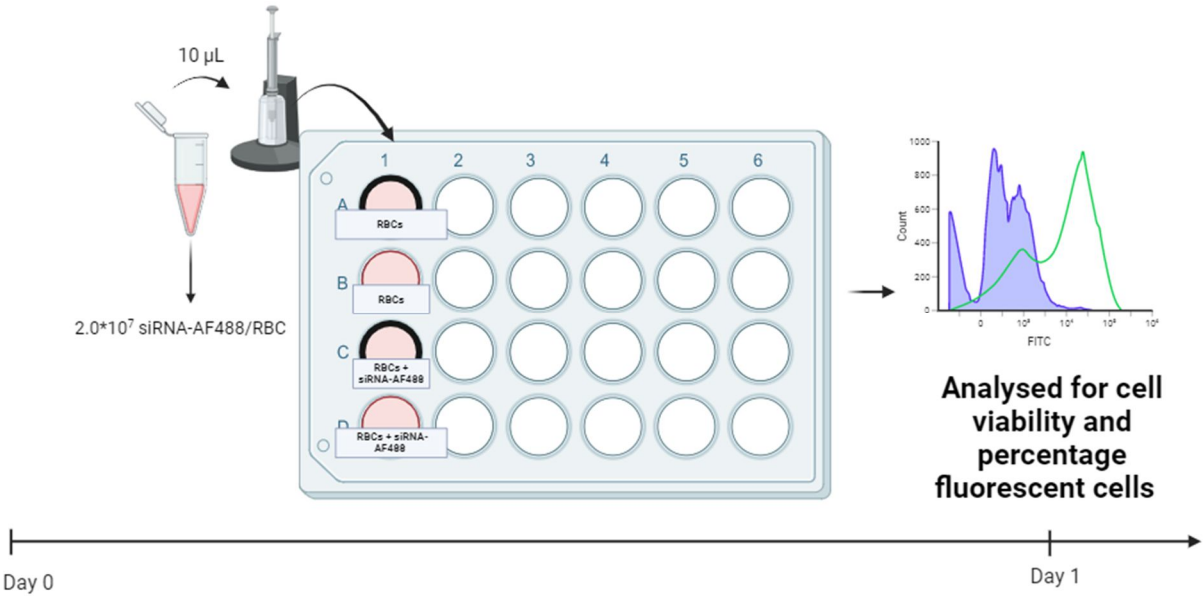

Figure 22. Experimental design of Neon™ transfection for establishing siRNA transfection in A. salmon RBCs. Day 0 is the transfection day. Sample with black border indicate samples that did not undergo electroporation/transfection.

RBCs were isolated from one A. salmon 5 days prior to transfection. One experimental and three control samples containing 0.5 mL L-15 medium with 5 * 10^6 RBCs each were set up. The experimental sample was RBCs transfected with siRNA-AF488. Control samples were

1) RBCs undergoing electroporation as a control of cell viability impacted by the different transfection programs, 2) un-electroporated RBCs incubated with siRNA-AF488 as a control to study false positive staining (siRNA binding to the cell surface), and 3) un-electroporated RBCs as a positive control of cell viability. PI-staining was done prior to analysis to assess cell viability, and cell viability calculation was done as in Appendix A1. PI-solution was added to all samples except to un-electroporated RBCs not incubated with siRNA-AF488, as viability was thought to be identical to the un-electroporated RBCs incubated with siRNA-AF488.

The Neon^{TM} transfection system was set at a program of 1600V, 30ms and 2 pulses. This program had been successful for mRNA-transfections performed in RBCs in the lab, prior to initiating siRNA-transfections in this master thesis. Harvesting was done after 24h, to let the RBCs stabilize after electroporation treatment. PI-positive cells from the siRNA transfected sample is shown in Appendix (Figure B2 b)). The results from establishing siRNA transfection in RBCs, and cell viability from transfection program, is shown in Figure 23.

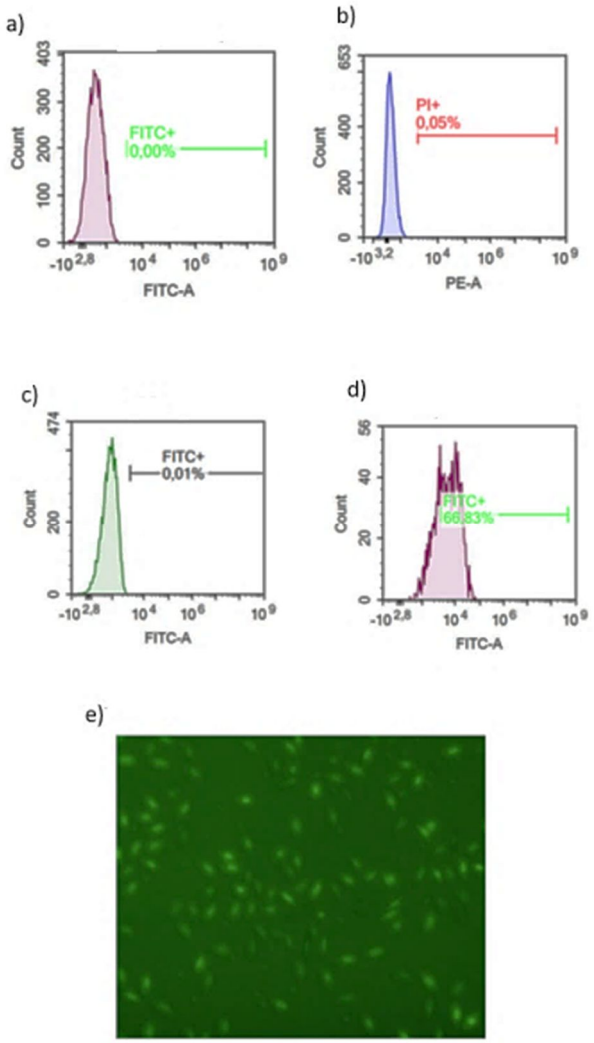

Figure 23. siRNA transfection of A salmon RBC. Analyses were performed 1 day post-transfection. a) Histogram of un-electroporated RBC controls-FITC channel (used for AF488). b) Histogram of electroporated RBC controls PI– channel (live/dead cells). c) Histogram of un-transfected RBCs mixed with siRNA-AF488 - FITC-channel. d) Histogram of RBCs transfected with siRNA-AF488- FITC channel e) Nikon eclipse Ti2-E microscope image (10x/0.30) of RBCs transfected with siRNA-AF488.

A fluorescent signal (FITC+/AF488) is detected in 0.01% of un-electroporated RBCs incubated with siRNA-AF488, (Figure 23 c), compared to the background from RBC in the absence of siRNA (Figure 23 a). For RBCs transfected with siRNA-AF488 (Figure 23 d), 66% of the cells were detected as fluorescent. Nikon eclipse Ti2-E microscope was utilized to capture RBCs transfected with siRNA-AF488 shown in Figure 23 e).

From Figure 23 b), the percentage of PI-stained cells after transfection is 0.05%, indicating a cell viability of 99,5% after transfection with a program of 1600V, 30ms and 2 pulses.

The results from this experiment (Figure 23) indicate that siRNA transfection is successfully established in the RBCs using the 1600V, 30ms and 2 pulses program, and the cell viability was still high one day after transfection.

4.2.2 Optimizing siRNA transfection efficiency in A. salmon RBCs – Experiment 1

To increase the siRNA transfection efficiency, and reduce impact on the cells, different Neon™ programs were tested by varying voltage and pulses (71). Three different programs were tested: P1 set at 1600V, 30ms and 2 pulses (repeated from "4.2.1 Establishing siRNA transfection in A. salmon RBCs"), P2 set at 1500V, 30ms and 2 pulses and, P3 set at 1400V, 30ms, 4 pulses. A lower voltage was tested to see if transfection efficiency would remain similar if voltage was decreased. A higher number of pulses in P3 was to determine if more pulses would increase transfection efficiency. This time, harvesting was done at Day 2 and Day 7 to study the duration of siRNA detection and cell viability of transfected cells over time. The experimental design for the optimization trial is presented in Figure 24.

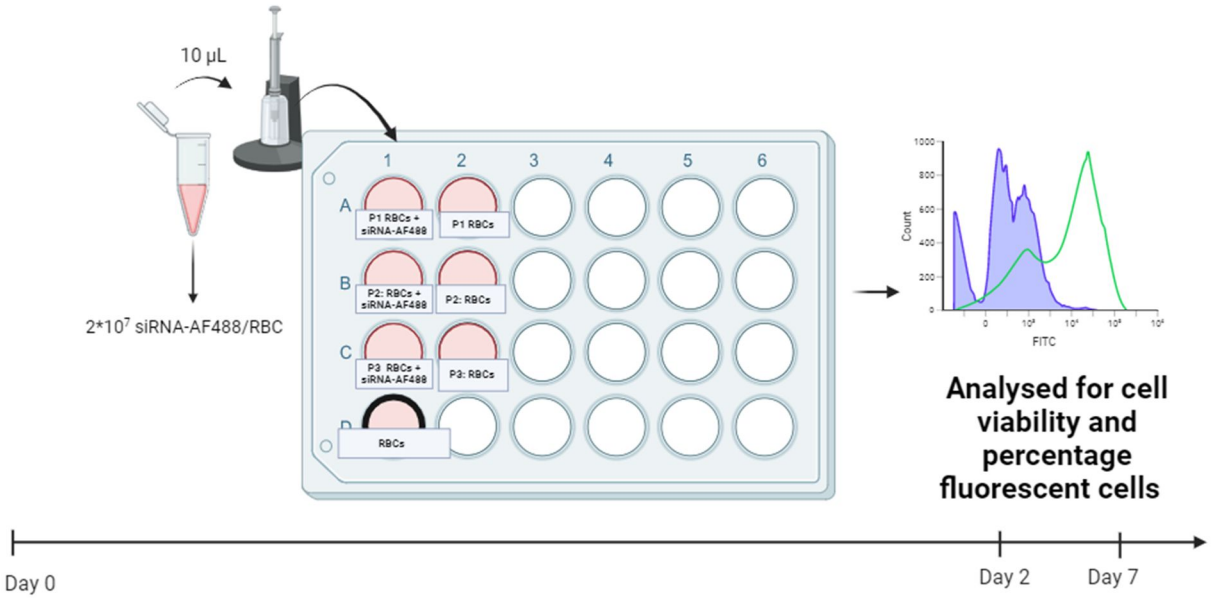

Figure 24. Experimental design of Neon™ transfection setup to increase siRNA transfection. P1, P2 and P3 indicate three different programs: Day 0 is the transfection day. Sample with black border indicate samples that did not undergo electroporation/transfection.

RBCs were isolated from one A. salmon 1 day prior to transfection. The un-electroporated RBCs incubated with siRNA-AF488 control was not added in this experiment, since no fluorescent signal was shown “4.2.1 Establishing siRNA transfection in A. salmon RBCs”. The other two controls (un-electroporated RBCs and electroporated RBCs) was still continued with. The amount of media, numbers of RBCs in each sample, and the siRNA-AF488/RBCs ratio remained identical to previous experiment (“4.2.1 Establishing siRNA transfection in A. salmon RBCs”). Samples were stained with PI as before.

Figure 25 and Figure 26 present the percentage of fluorescent cells (siRNA-AF488 transfected) and cell viability (Total cell count- PI positive cells) analysed at Day 2 and Day 7 post-transfection. Flow cytometer histograms of transfected cells are shown in Appendix Figure B3 and Figure B5.

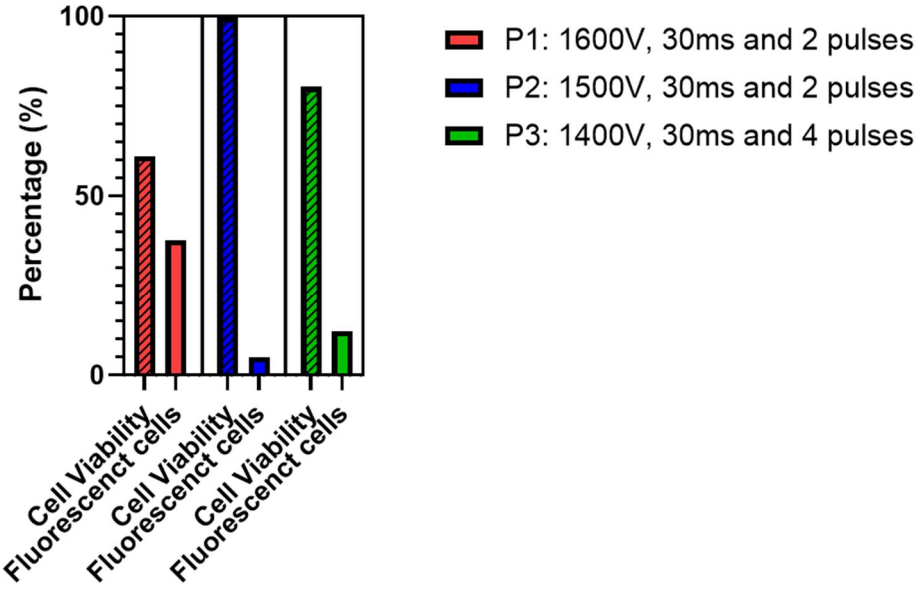

Figure 25. Percentage of fluorescent RBCs (AF488 siRNA transfected) and the cell viability (Total cells – PI positive cells) measured at Day 2 post-transfection. The red bars, blue bars and green bars represent different transfection programs P1, P2 and P3 respectively. The striped left bar presents the cell viability (%) and the right bar presents the fluorescent transfected cells (%).

P1, P2 and P3 transfection led to 38%, 5% and 12% siRNA transfected cells at Day 2. Cell viability were respectively 61%, 100% and 80%. Results indicate that P1, the original program, indicated the best transfection efficiency when analysed at Day 2, but the lowest viability.

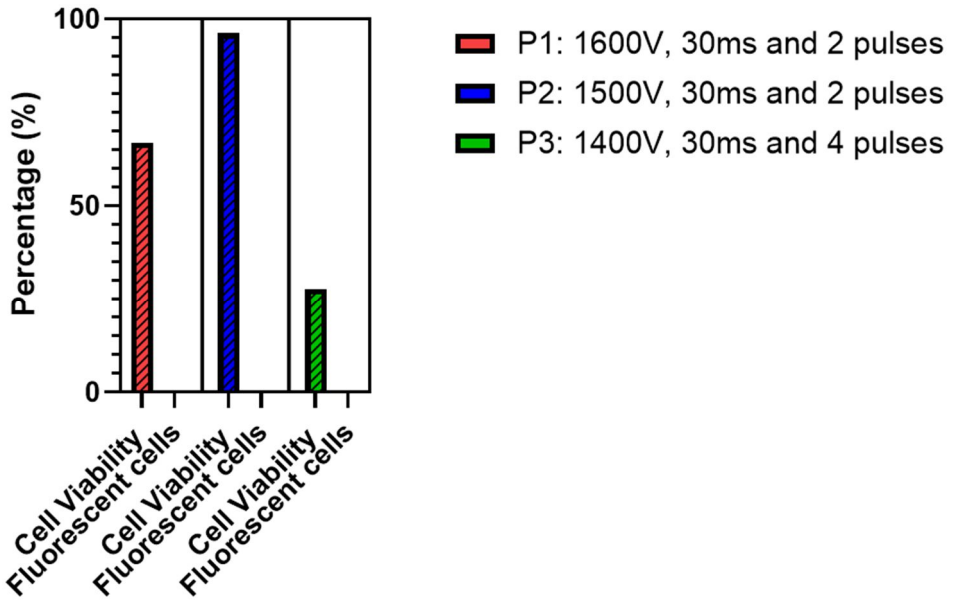

Figure 26. Transfection efficiency and cell viability at Day 7 post-transfection. The red bars, blue bars and green bars illustrate programs P1, P2 and P3 respectively. The left bar of each program (stripe pattern) presents the cell viability (%) and the right bar presents the percentage of siRNA transfected cells (%).

No siRNA transfected cells were detected at Day 7 for all three programs, and cell viability were lower compared to day 2 for all programs. Based on these results, P1 was still considered the best program, and Day 7 was considered too late to detect the siRNA-AF488.

4.2.3 Optimizing siRNA transfection in A. salmon RBCs – Experiment 2

To potentially increase the transfection efficiency, two new programs were tested on three A. salmon individuals. RBCs were isolated and transfected the same day. P1 from the previous optimization experiment was unaltered, but P2 and P3 in this experiment were 1700V, 20ms and 2 pulses and 1800V, 20ms and 3 pulses. A higher voltage was tested in experiment 2, since from "4.2.2 Increasing siRNA transfection efficiency in A. salmon RBCs – Experiment 1", a voltage lower than 1600V resulted to less siRNA transfected cells at Day 2. A higher number of pulses was added to P3, since P3 from experiment 1 (1400V, 30ms and 4 pulses) had a higher number of siRNA transfected cells than P2 (1500V, 30ms and 2 pulses) with higher voltage/fewer pulses. The duration in ms was also altered to see its impact on siRNA transfection.

Harvesting for analysis of fluorescent cells and cell viability were done at Day 1 and Day 3 post-transfection. Day 1 was chosen because a good transfection efficiency and cell viability was assessed at Day 1 when establishing siRNA transfection ("4.2.1 Establishing siRNA transfection in A. salmon RBCs"), and Day 3 was chosen to study siRNA transfected RBCs over a longer duration, but avoid loosing the signal as seen day 7.

The experimental design is presented in Figure 27.

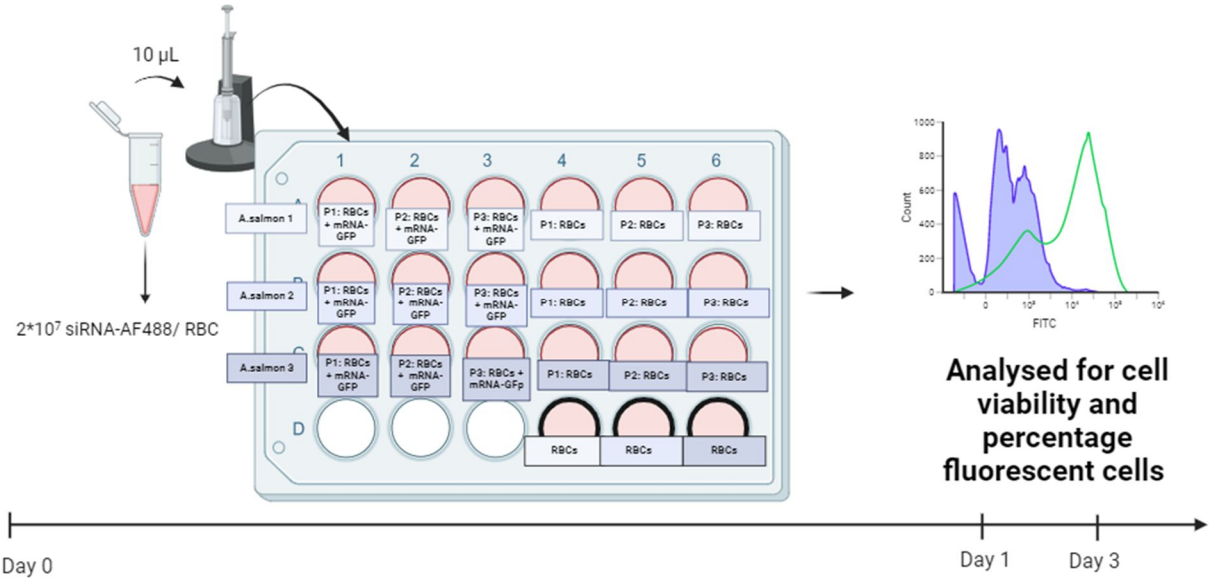

Figure 27. Experimental design of Neon™ transfection from RBCs isolated from three A. salmon. Day 0 is the transfection day and isolation day. Samples with black border indicate samples that did not undergo electroporation/transfection. The color of the "content-box" of each sample indicate the different A. salmon.

Figure 28 shows the number of siRNA transfected cells measured at Day 1 and Day 3. The cell viability was also measured in each experiment, but only shown in the appendix (Appendix Figure B6 – B13).

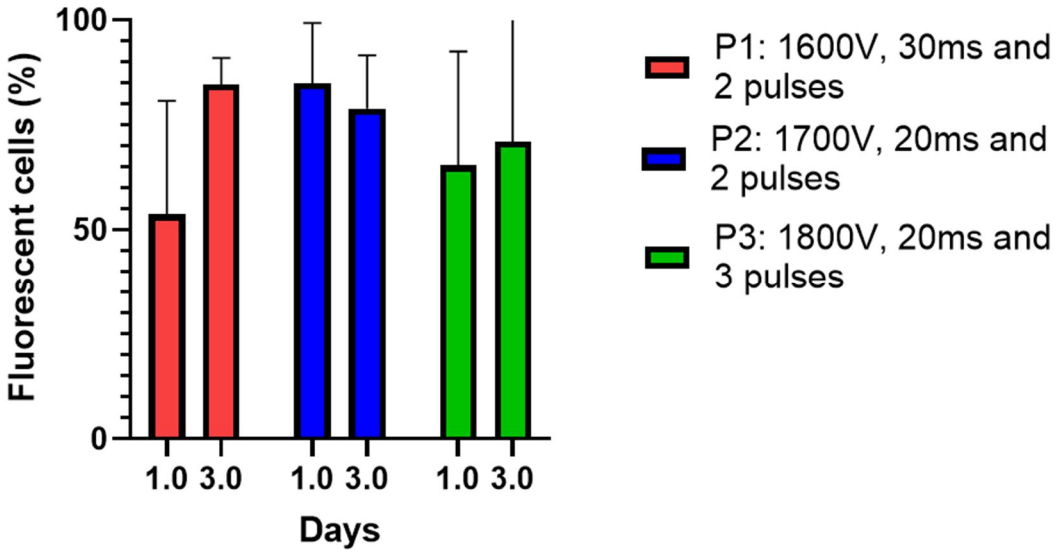

Figure 28. Transfection efficiency (%, n=3 A. salmon) of RBCs at Day 1 and Day 3 post-transfection. Red bars, blue bars and green bars present the percentage of fluorescent cells after transfection with programs P1, P2 and P3 respectively. The left bar presents Day 1 post-transfection, and the right bar presents Day 3 post-transfection. Mean data (n=3) with standard deviation (SD) is presented.

All the programs resulted in a mean transfection efficiency above 50%, as measured both day 1 and day 3. Program P2: 1700V, 20ms and 2 pulses was chosen as the optimized program for siRNA-transfection since analysis showed a mean transfection efficiency above 70% at both time points.

4.3 mRNA-GFP transfection

As a gene silencing control, mRNA encoding GFP (mRNA-GFP) was synthesized and optimized for mRNA transfection. The motive for mRNA transfection was to co-transfect mRNA-GFP with a siRNA, targeting the mRNA-GFP, as a control to study a functional RNAi system in A. salmon RBCs.

The mRNA optimization was performed in collaboration with an exchange PhD student from Chile (Laura Vanessa Solarte Murillo).

4.3.1 mRNA-GFP synthesis

For production of mRNA-GFP, a DNA plasmid encoding GFP had to be linearized, making a template for IVT. The DNA plasmid encoding GFP was ordered from Genscript, using the plasmid pVAX1 (Thermofisher Scientific, pVAX1 Vector (Thermofisher.com)). pVAX1 features a priming site and a multiple cloning site, enabling insertion of a gene and IVT of that gene. More details of the pVAX1 can be assessed in the user guide (PVAX1 user guide (Thermofisher.com)). Sizes of important regions of the linearized pVAX1-GFP mRNA is presented in Figure 29.

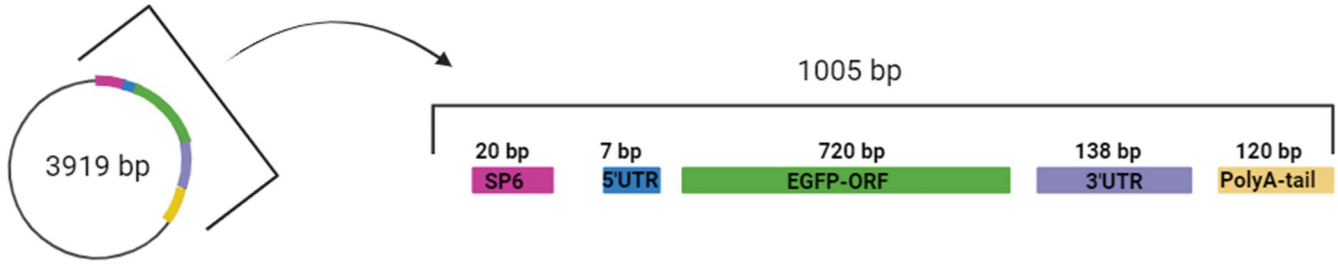

Figure 29. Rough illustration of different regions of the linearized GFP-DNA

The restriction enzyme MIuI cuts the plasmid at basepair position 30 and 1707, creating a 1677bp fragment (pVAX1-GFP). After IVT and capping, the mRNA-transcript derived from the pVAX1-GFP will contain 3 bp from the SP6 promoter, resulting in a final size of 988bp.

The band lengths of pVAX1-GFP cut from pVAX1 DNA is shown in Figure 30.

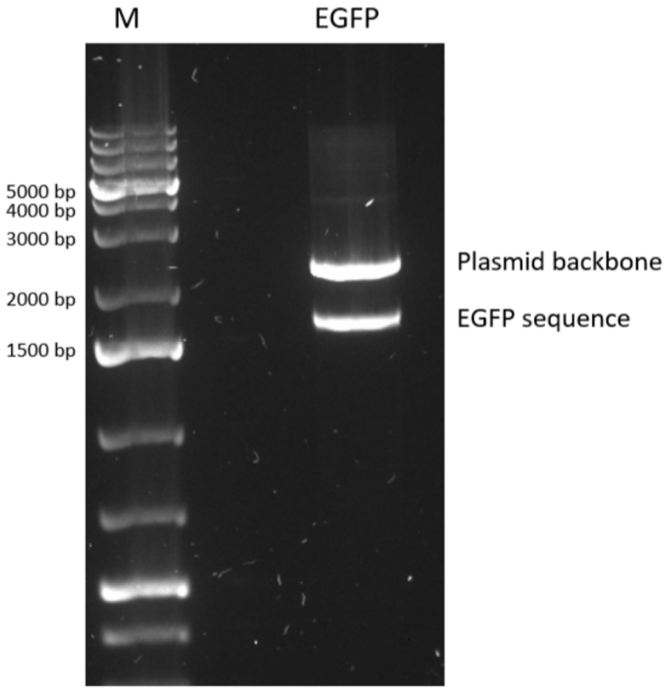

Figure 30. Agarose gel image of pVAX1-GFP (EGFP sequence) and pVAX1 plasmid backbone after linerization. Left well presents the ladder and right well presents the mRNA-GFP sample. Two bands is observed in the sample well, which is the pVAX1-GFP (lower band) and plasmid backbone (upper band).

The pVAX1-GFP band is located according to the expected length of 1677bp, and the pVAX1-GFP was continued for in vitro transcription, mRNA purification and capping. Spectrophotometer analysis of the finalized mRNA-GFP is presented in Table 6, and the Tapestation 4200 electronic gel image of mRNA-GFP is presented in Figure 31.

Table 6. Concentration, 260/280 purity and 260/230 purity of the mRNA-GFP

Concentration (µg/mL)	**Purity 260/280**	**Purity (260/230)**
1077	2.426	2.126

The mRNA-GFP concentration after capping is 1.077 µg/µL. The 260/280-value is above the accepted value (≈2), and 260/230 ratio is in the range of accepted value (2.0 – 2.2). A 260/280 ratio above 2 is not considered a problem, and the mRNA-GFP is considered pure (72).

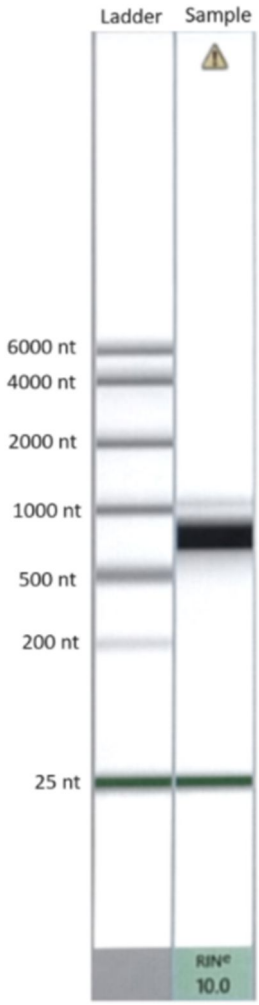

Figure 31. TapeStation 4200 electronic gel image of finalized capped mRNA-GFP. Left well presents the ladder and right well presents the mRNA-GFP sample. The "warning" symbol on the right well is caused by the use of an expired screentape.

From the TapeStation 4200 electronic gel image, two bands are observed from the sample well. The thick black band is at 700 –900 nt, while a weak grey band is above 1000 nt. The black band is the mRNA-GFP, while the grey band is longer RNA transcripts. Failed migration of the mRNA-GFP could be the results of using an expired screentape, since bubble forms in the gel, impacting the migration (73). The RNA integrity number (RIN) from the sample well is 10.0, indicating high quality with no degradation.

4.3.2 Establishing mRNA-GFP transfection

The synthesized mRNA-GFP has to express GFP inside the RBCs for it to be further used for the mRNA-GFP silencing experiment.

The experimental design to establish mRNA-GFP transfection in A. salmon RBCs is presented in Figure 32. Analysis of mRNA-GFP transfected cells was done at Day 1 to let the RBCs stabilize after electroporation treatment. The mRNA-amount transfected with was 2 µg, based on the same concentration assay with DNA plasmid transfection mentioned in "4.2.1 Establishing siRNA transfection in A. salmon RBCs". The Neon™ transfection system was first tested with the electroporation program 1600V, 30ms and 2 pulses, determined from previous experiments.

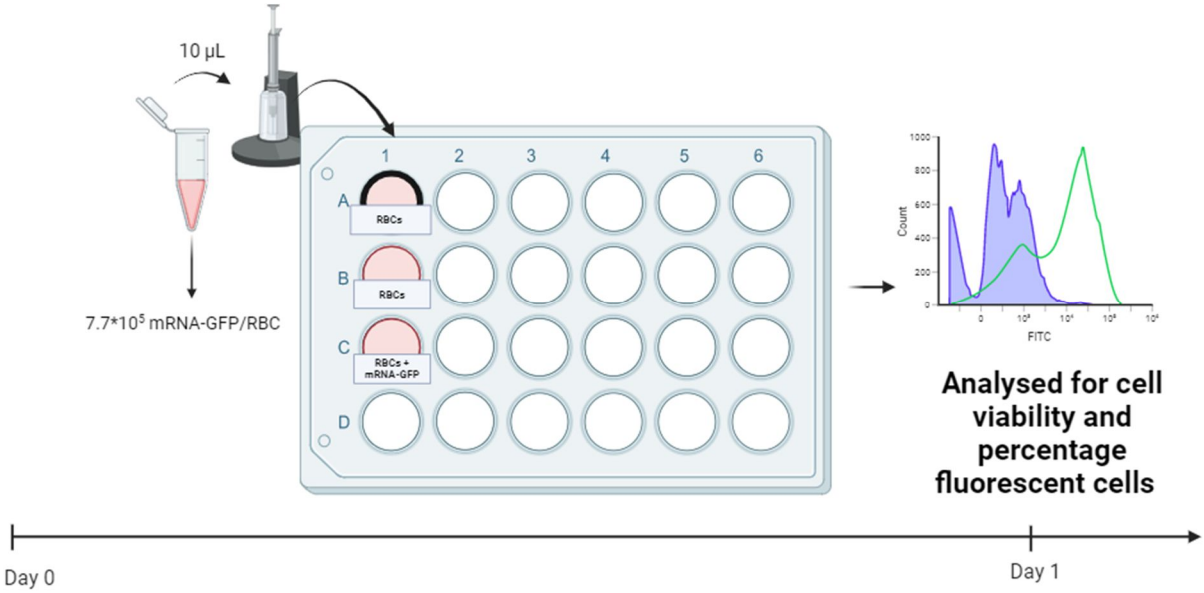

Figure 32. Experimental design of Neon ™ transfection to establish mRNA-GFP transfections in A. salmon RBCs. Day 0 is the transfection day. The sample with black border did not undergo electroporation/transfection.

RBCs were isolated 5 days prior to transfection. The set-up had the same amount of media and same controls as in "4.2.2 Establishing siRNA transfection in A. salmon RBCs", with two differences: 1) the RNA/RBC ratio is different since the mRNA transfection is still done with $5*10^6$ RBCs, and 2) the sample with un-transfected RBCs incubated with RNA (mRNA-GFP e.g.) is not included, since detection of GFP is only possible when mRNA-GFP is translated inside the RBCs.

Figure 33 shows the results from establishing mRNA-GFP transfections in A. salmon RBCs. PI-stained cells from RBCs transfected with mRNA-GFP is shown in Appendix Figure C2 b).

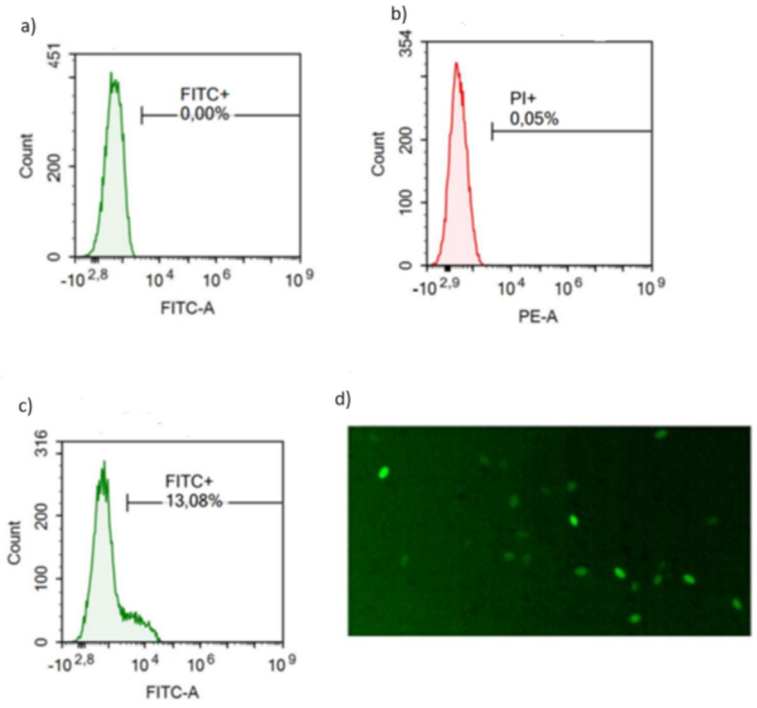

Figure 33. Flow cytometer analysis of RBCs isolated from one A. salmon. a) Histogram of un-electroporated RBCs (control) b) Histogram of the viability of the electroporated RBCs (control) c) Histogram of RBCs transfected with mRNA-GFP. d) Nikon eclipse Ti2-E microscope image (20x/0.45) of RBCs transfected with mRNA-GFP.

Here, 13% of RBCs were determined as transfected with mRNA-GFP, when compared to un-electroporated RBCs (control). To image that the mRNA-GFP is transfected and GFP expressed in the cell, a Nikon eclipse Ti2-E microscope was used (Figure 33 d).

The amount of transfected RBCs stained by PI is 0.05% (Figure 33 b), resulting in a cell viability of 100% from the 1600V, 30ms and 2 pulses transfection program. Note that cells bursted in the transfection process will not be counted as dead cells, and that cell loss was not calculated.

According to this experiment, mRNA-GFP transfection is successfully established in RBCs using the electroporation program 1600V, 30ms and 2 pulses, and a high cell viability is also achieved.

4.3.3 mRNA-GFP optimization

For the silencing control experiment, optimization if mRNA-GFP transfection was done.

4.3.3.1 Optimizing mRNA transfection in A. salmon – Experiment 1

Three programs were tested for further optimization of mRNA-GFP in A. salmon RBCs with varying voltage and pulses (71). The programs were set at 1600V, 30ms and 2 pulses (P1), 1500V, 30ms and 2 pulses (P2) and 1400V, 30ms and 4 pulses (P3). These programs are identical to the programs in "4.2.1.2 Increasing siRNA transfection efficiency in A. salmon RBCs – Experiment 1", with similar testing reasons. The experimental design is shown in Figure 34.

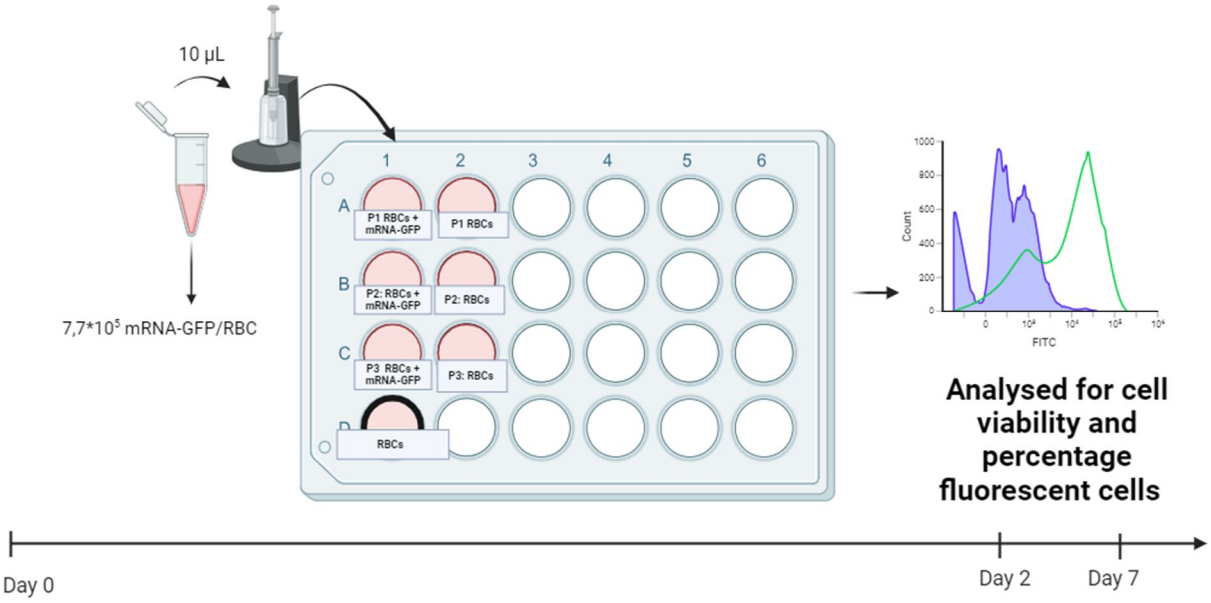

Figure 34. Experimental design of Neon™ transfection to increase mRNA-GFP transfection efficiency in A. salmon RBC. Day 0 is the transfection day. Sample with black border did not undergo electroporation/transfection.

RBCs were transfected one day prior to transfection, and the first optimization trial is done similar to "4.2.2 Establishing mRNA-GFP transfection", with the same number of RBCs, media and identical mRNA-GFP/RBCs ratio. PI-staining was also done to control viability. The main difference is the testing of two additional programs, and that harvesting for analysis of

transfected cells and cell viability was done at Day 2 and Day 7, instead of Day 1, to study GFP expression over time.

The results from the first optimization trial analysed at Day 2 and Day 7 are shown in Figure 35 and Figure 36. Flow-cytometer histograms of the number of PI-positive cells from transfected and electroporated (control) RBCs are shown in Appendix Figure C3 – Figure C6.

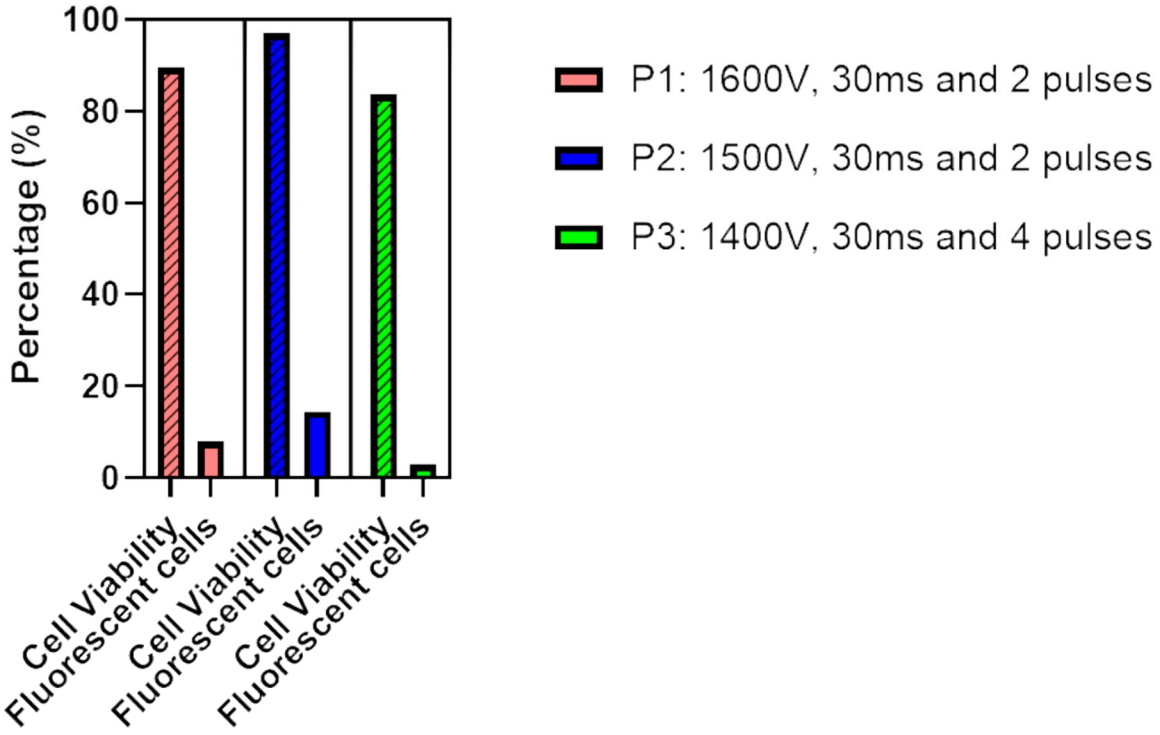

Figure 35. Percentage of fluorescent cells and cell viability 2 days post-transfection of A. salmon RBCs. The red bars, blue bars and green bars presents transfection programs P1, P2 and P3 respectively. The left bar with stripe pattern presents the cell viability (%) and the right bar with no pattern represents the transfected fluorescent cells (%).

The cell viability was 90% for P1, 97% for P2 and 83% for P3 two days after transfection. The percentage of fluorescent transfected cells were highest for P2 with 14%, while P1 and P3 had 8% and 3% fluorescent cells respectively.

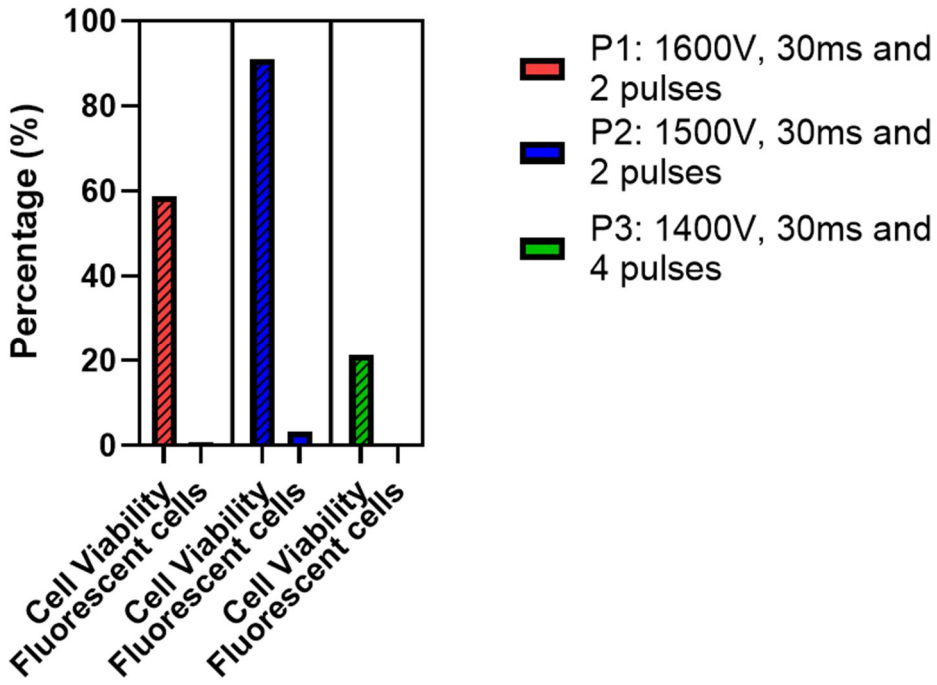

Figure 36. Percentage of fluorescent cells and cell viability (%, n=1 A. salmon) 7 days post-transfection of A. salmon RBCs. The red bar, blue bar and green bar presents transfection programs P1, P2 and P3 respectively. The left bar with stripe pattern presents the cell viability (%) and the right bar with no pattern presents the fluorescent cells (%).

After 7 days post-transfection with mRNA-GFP, the cell-viability decreased for all the programs used compared to 2 days post-transfection. The cell viability was 59%, 91% and 21% for P1, P2 and P3 respectively. The number of fluorescent cells were zero for P1 and P3, and 3% for P2.

Based on these results, P2 gave the highest number of fluorescent cells, and had the highest cell viability at day 2, and Day 7 is too late to study the expression of GFP.

4.3.3.2 Optimizing mRNA transfection in A. salmon – Experiment 2

Four new transfection programs were tested on RBCs isolated from two A. salmon, isolated 1 day prior to transfection. P1, P2, P3 and P4 were respectively set at 1600V, 20ms and 3 pulses, 1500V, 30ms and 3 pulses, 1600V, 10ms and 4 pulses, and 1500V, 10ms and 4 pulses. Either a higher duration in ms, or a higher number of pulses was added to the new

programs, compared to P1 and P2 in the previous optimization experiment, in an attempt to achieve higher transfection efficiency. The experimental design is shown in Figure 37.

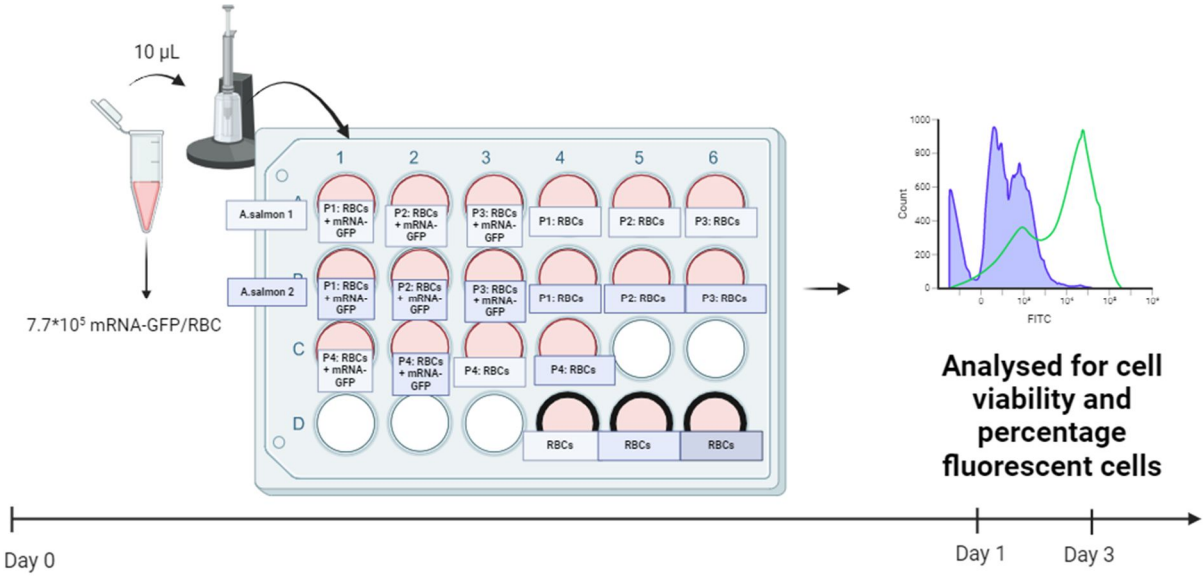

Figure 37. Experimental design of Neon™ transfection to increase mRNA-GFP transfection efficiency in A. salmon RBCs. Day 0 is the day transfection took place. Samples in wells with black border did not undergo transfection/electroporation. The color of the "content-box" on the wells indicate the different A. salmon.

The set-up was identical to "4.2.3.1 Optimizing mRNA transfection in A. salmon – Experiment 1", with the addition of another replicate and two program. Harvesting was performed on Day 1 and Day 3 since detecting GFP-expression at 7 days is too late.

The results of the optimization trial is presented in Figure 36. Cell viability is not presented in Figure 36, and the continuing figures, since transfection with the programs resulted in low amount of PI-stained cells, resulted from change in gating-strategy, shown in Appendix Figure C7 – Figure C14.

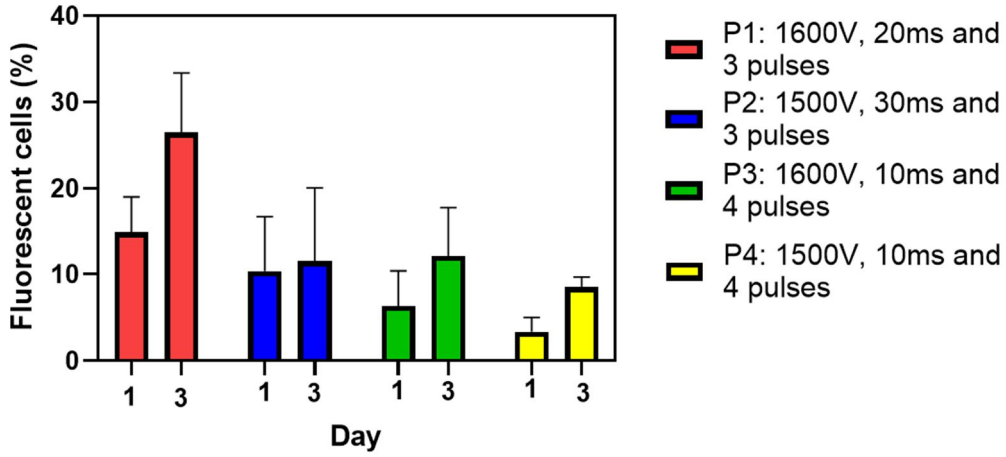

Figure 38. Mean fluorescent cells (%, n=2 A. salmon) analysed at Day 1 and Day 3 post-transfection. Red bars, blue bars, green bars and yellow bars represent the mean number of fluorescent transfected cells using transfection programs P1, P2, P3 and P4 respectively. The left bar of each program presents analyses Day 1 post-transfection, and the right bar presents analyses Day 3 post-transfection. Mean results with standard deviation (SD) is presented.

The mean percentage of fluorescent cells at Day 1 post-transfection using programs P1, P2, P3 and P4 were respectively 15%, 10%, 6% and 3%, with P1 resulting in the highest number of fluorescent cells. After 3 days post-transfection, the mean number of transfected cells increased for all programs, with P1 still having the highest number of 26%. A one-way ANOVA was performed, comparing the means of each program each day (Appendix Table K1). P1 gave a significantly higher number of transfected cells and was continued with for the next optimization trial.

4.3.3.3 Increasing mRNA transfection efficiency in A. salmon – Experiment 3

The aim was to perform a co-transfection using mRNA-GFP and anti-GFP siRNA to test siRNA efficiency in RBC. To identify the best program for this co-transfection, the program found most optimal for siRNA transfection (1700V, 20ms and 2 pulses) was tested for mRNA-GFP transfection. P1 is the optimized program for mRNA in from the latest trial, and P2 the optimized siRNA program. The experimental design is shown in Figure 39.

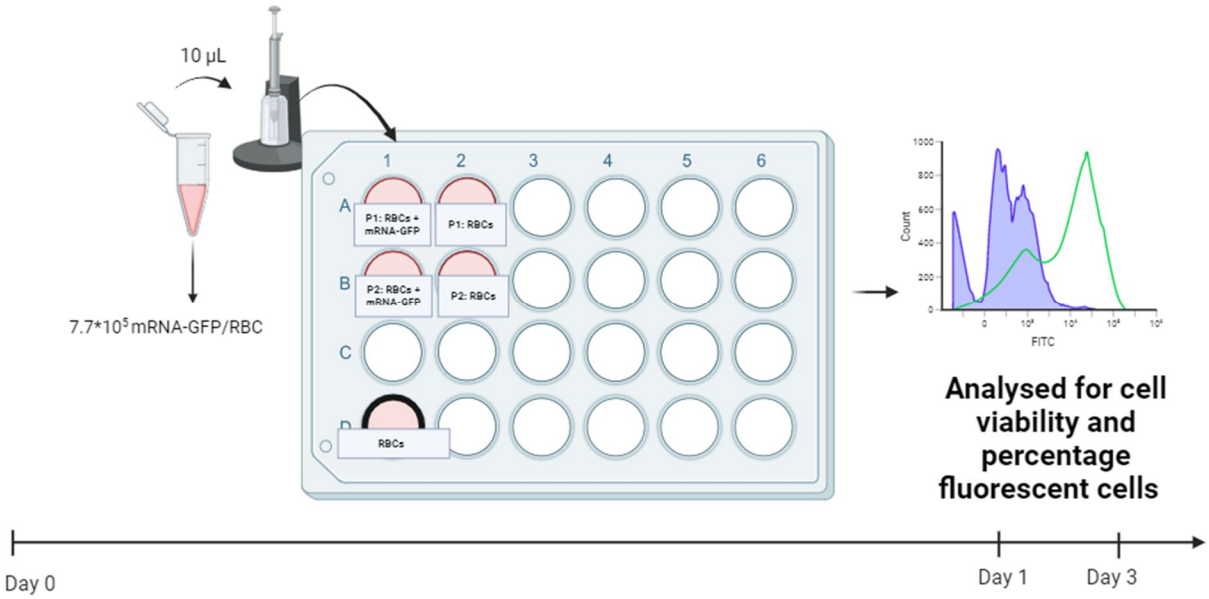

Figure 39. Experimental design of Neon™ transfection to compare P1 against P2 for mRNA-GFP transfection efficiency in A. salmon RBCs. Day 0 is the transfection day. Sample with black border did not experience transfection/electroporation.

The setup is similar to "4.3.3.2 Increasing mRNA transfection efficiency in A. salmon – Experiment 2", with testing of only two programs, and using only one A. salmon individual. RBCs were isolated 8 days prior to transfection.

Figure 40 shows the comparison between effects of transfection program P1 (optimized for mRNA) and P2 (optimized for siRNA). The cell count from day 3 is included in Figure 40, since the set stop condition at 10 000 events was not reached.

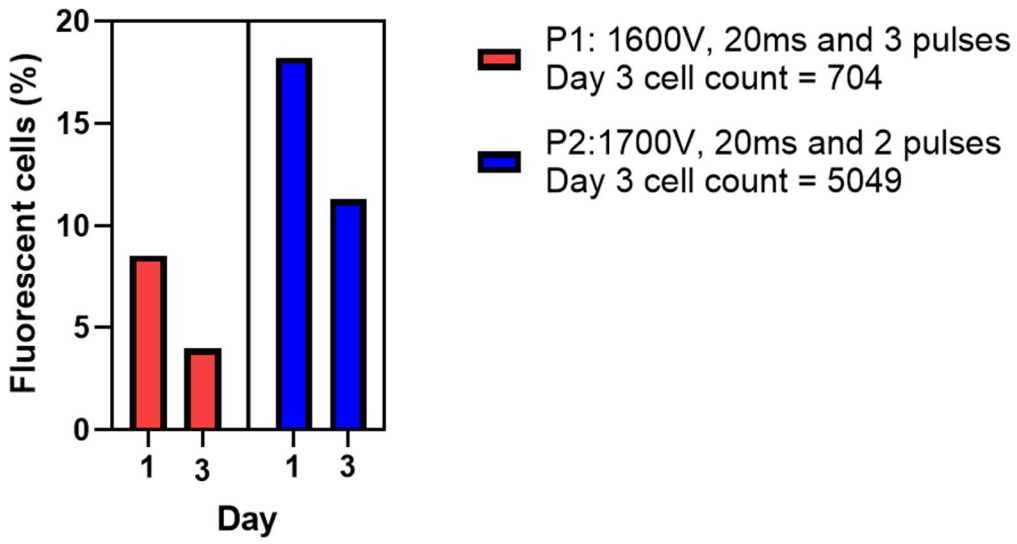

Figure 40. mRNA transfected cells obtained at Day 1 and Day 3 post-transfection with programs P1 and P2 on RBCs. Red bars present P1 transfection efficiency and blue tiles present P2 transfection efficiency. The cell count from each program at Day 3 can be read from the legend.

According to analysis at Day 1, P2 led to a percentage of 18% transfected cells and P1 to 9% transfected cells. The number of fluorescent cells were lower at Day 3. P1 transfection samples had 4% fluorescent cells, and P2 transfection samples had 11% fluorescent cells. Since P2 led to the highest number of fluorescent cells measured at both Day 1 and Day 3, P2 was chosen as the co-transfection program.

4.4 mRNA-GFP silencing control

The functionality of the RNAi mechanism in A. salmon RBCs was studied by co-transfecting Silencer GFP siRNA (anti-GFP siRNA) (Thermofisher Scientific) and mRNA-GFP.

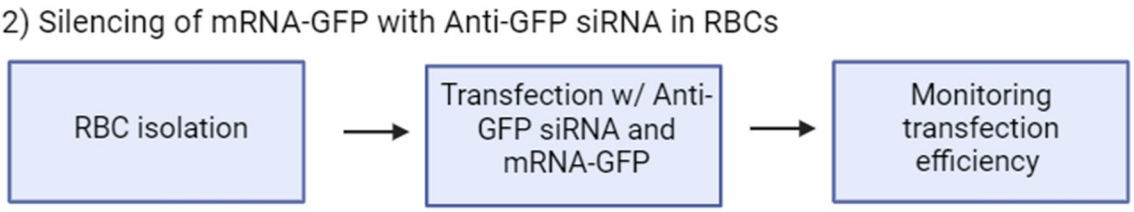

Figure 41. Methods utilized for mRNA-GFP silencing control in A. salmon RBCs.

The anti-GFP siRNA was ordered to target the pEGFP-1 encoded by the mRNA (Accession: U55761 in NCBI). Alignment in Clustal Omega was done to ensure binding of the siRNA to the mRNA-GFP sequence (Appendix Figure D1). The program chosen for transfection was 1700V,

20ms and 2 pulses, based on previous optimizations. The experimental design is shown in Figure 42.

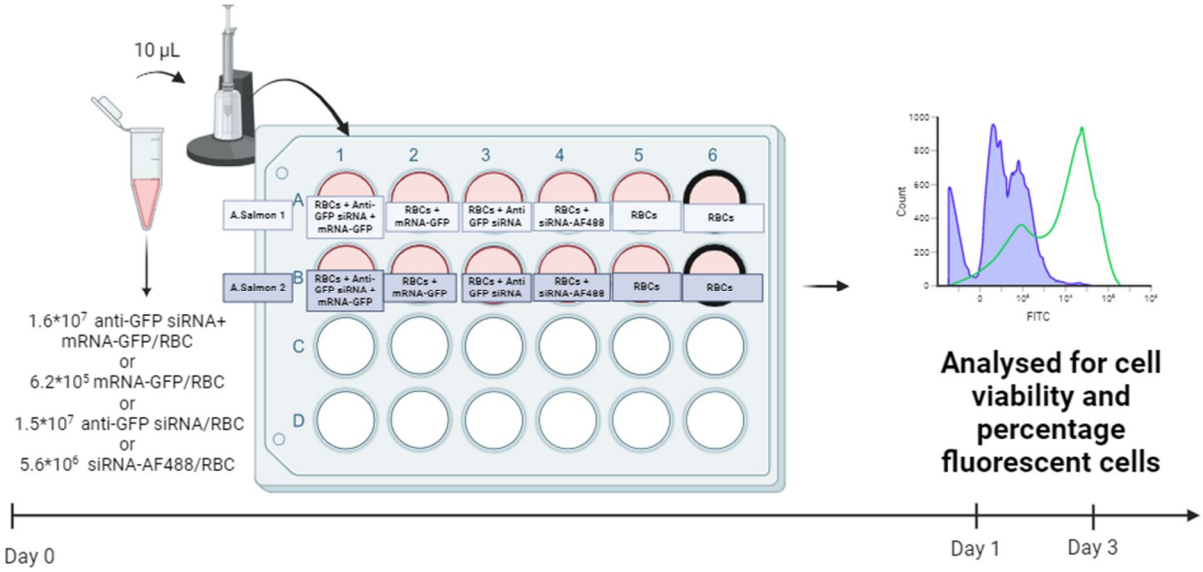

Figure 42. Experimental design of Neon^{TM} transfection for silencing of mRNA-GFP with anti-GFP siRNA in RBCs isolated from two A. salmons. Day 0 is the transfection day. Samples with black border presents wells did not undergo electroporation/transfection. The color of the "content-box" on the wells indicate the different A. salmon.

To the co-transfected RBCs wells, 0.61 µg mRNA-GFP was transfected with 0.63 µg anti-GFP siRNA, resulting in a ratio of 1:24. Control samples transfected with 0.61 µg mRNA-GFP only was used to compare the amount of GFP-expressing fluorescent cells, with the co-transfected sample. The samples were analyzed for the amount of GFP-expressing fluorescent cells and cell viability at Day 1 and Day 3 post transfection. Control transfection with 0.63 µg anti-GFP siRNA only was added to assess any cytotoxic effect from anti-GFP siRNA, and transfection with 0.63 µg siRNA-AF488 was added to indicate transfection efficiency of the "invisible" anti-GFP siRNA. RBCs were isolated 2 days prior to transfection.

The results from the co-transfection, aimed to silence mRNA-GFP, is presented in Figure 43. Flow cytometer histograms of PI-positive and fluorescent cells from each transfected sample is shown in Appendix Figure D2 – D5.

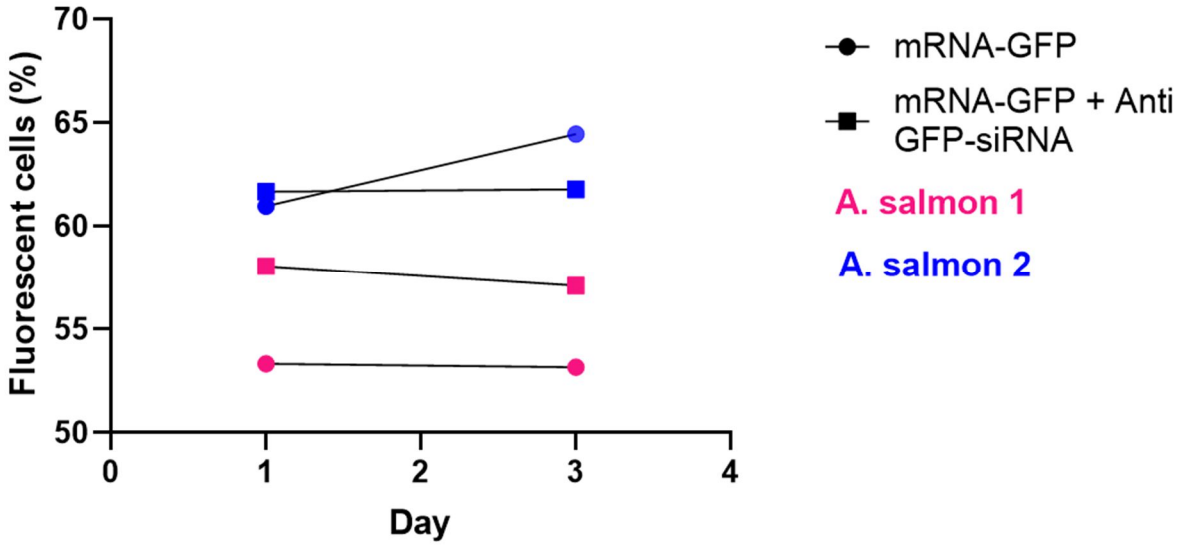

Figure 43. Percentage fluorescent cells (%) from two A. salmon individuals at Day 1 and Day 3 post-transfection in the mRNA-GFP silencing experiment. Square points indicate A. salmon RBCs co-transfected with mRNA-GFP and anti GFP-siRNA, and circular points indicate A. salmon RBCs transfected with mRNA-GFP only. Same colored points indicate the individual A. salmon.

The expected outcome from the mRNA-GFP silencing experiment was a lower percentage of fluorescent cells in the co-transfected sample, compared to the sample only transfected with mRNA-GFP.

A. salmon 1 at Day 1, co-transfected with mRNA-GFP and anti-GFP siRNA, had 58% fluorescent cells, while transfection with mRNA-GFP alone had 53%. Day 3 for A. salmon 1, present similar results.

The percentage of fluorescent cells from A. salmon 2 for transfection with mRNA-GFP only was 61%, while the co-transfected sample had 62%. The number of fluorescent cells increased for the mRNA-GFP transfected sample at Day 3 for A. salmon 2, but decreased for the co-transfected sample. This effect could have been due to silencing, but not convincing. One additional A. salmon individual was tested with similar lack of silencing efficiency since different RNA:RBC –ratio was used. The results from the additional A. salmon individual is only shown in Appendix Figure D6.

4.5 CHSE transfection

4.5.1 siRNA and mRNA establishment in CHSE-214

In order to find out if the lack of silencing was specific to A. salmon RBCs, CHSE-214 was also transfected with siRNA-AF488 and mRNA-GFP, in an attempt to reveal if the RNAi system could be more efficient in another salmonid cell line that was less responsive to intracellular dsRNA (62). Cell-lines with this attribute serve a big interest for host/virus interaction.

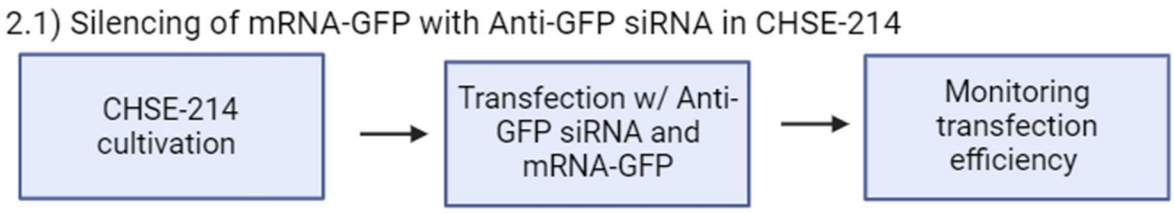

Figure 44. Methods utilized for mRNA-GFP silencing experiment in CHSE-214 cells.

The amount of mRNA-GFP used in each transfection is 2 µg, the same amount used in optimization experiments for mRNA in RBCs. For siRNA-AF488 transfection, identical amount was used for each transfection. The electroporation program was set to 1600V, 10ms and 3 pulses, a program published for these cells earlier (63). Harvesting was done at Day 2, after 24 hours of cultivating in media containing antibiotics, to let the CHSE-214 cells stabilize after transfection. The experimental design is shown in Figure 45.

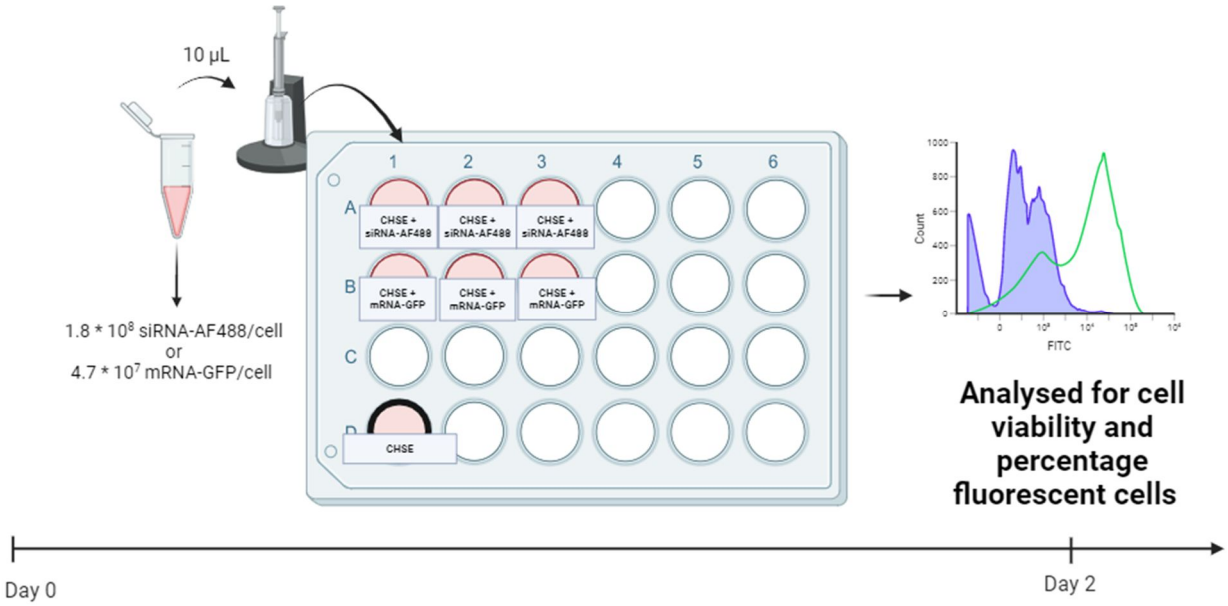

Figure 45. Experimental design of Neon™ transfection to establish mRNA-GFP and siRNA transfection in CHSE-214. Day 0 is the transfection day. Sample with black border did not experience electroporation/transfection.

To three wells with 0.5 mL media, $5*10^5$ cells were transfected with 2 µg siRNA-AF488 per well. Three additional wells of $5*10^5$ cells were transfected with 2 µg mRNA-GFP each well. One control sample with $5*10^5$ un-electroporated cells were added as a positive control of cell viability.

Figure 46 shows the number of fluorescent cells in sample A1, B1 and D1 from Figure 45. Cell viability was found to be >95% for all samples during the transfection and is not added in the following figures of this sub-section, but presented in Appendix Figure E1 – Figure E3.

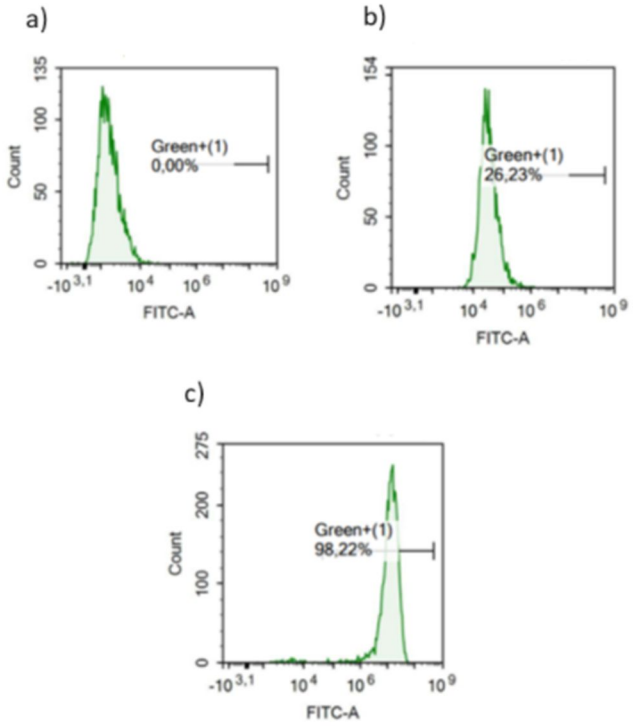

Figure 46. Flow cytometer analysis of CHSE cells with siRNA and mRNA-GFP. a) Histogram of un-electroporated control CHSE-214 cells b) Histogram of CHSE-214 cells transfected with mRNA-GFP only c) Histogram of CHSE-214 cells transfected with mRNA-GFP and siRNA-AF488.

The bar marked “Green+(1)” from Figure 46 presents the number of fluorescent cells from each sample. CHSE-214 cells transfected with mRNA-GFP and siRNA-AF488 had respectively 98% and 26% fluorescent cells. Based on these results, mRNA-GFP and siRNA-AF488 was successfully transfected into the CHSE-214 cells.

Figure 47 shows the mean percentage of fluorescent cells detected in the replicates transfected with siRNA-AF488 and with mRNA-GFP. The total amount of cells counted after mRNA- and siRNA-transfection is shown on top of each bar since the set-stop condition of 10 000 cells counted was not met for any replicates.

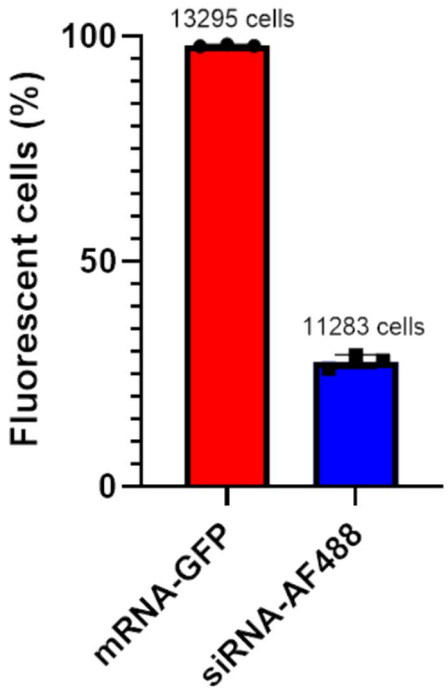

Figure 47. Mean fluorescent cells (%, n = 3 CHSE-214 replicates) detected after mRNA-GFP transfection (red bar) and siRNA-AF488 transfection (blue bar).

The mean percentage of fluorescent CHSE-214 cells transfected with mRNA-GFP is 98%, and the mean percentage of fluorescent cells transfected with siRNA-AF488 is 28%. Since there is a higher number of cells transfected with mRNA-GFP compared to cells transfected with siRNA, silencing of mRNA-GFP with anti-GFP siRNA was considered to be less efficient in these cells.

4.5.2 CHSE silencing experiment

Since the mRNA-GFP silencing did not show positive effects in A. salmon RBCs and this could be caused by less efficient silencing mechanisms in these cells, an mRNA-GFP silencing control experiment was conducted in CHSE-214 cells. The electroporation program chosen was the same as the optimized siRNA electroporation program for A. salmon RBCs, since the

program tested in “4.4.1 siRNA and mRNA establishment in CHSE-214**”** did not achieve optimal siRNA transfection efficiency

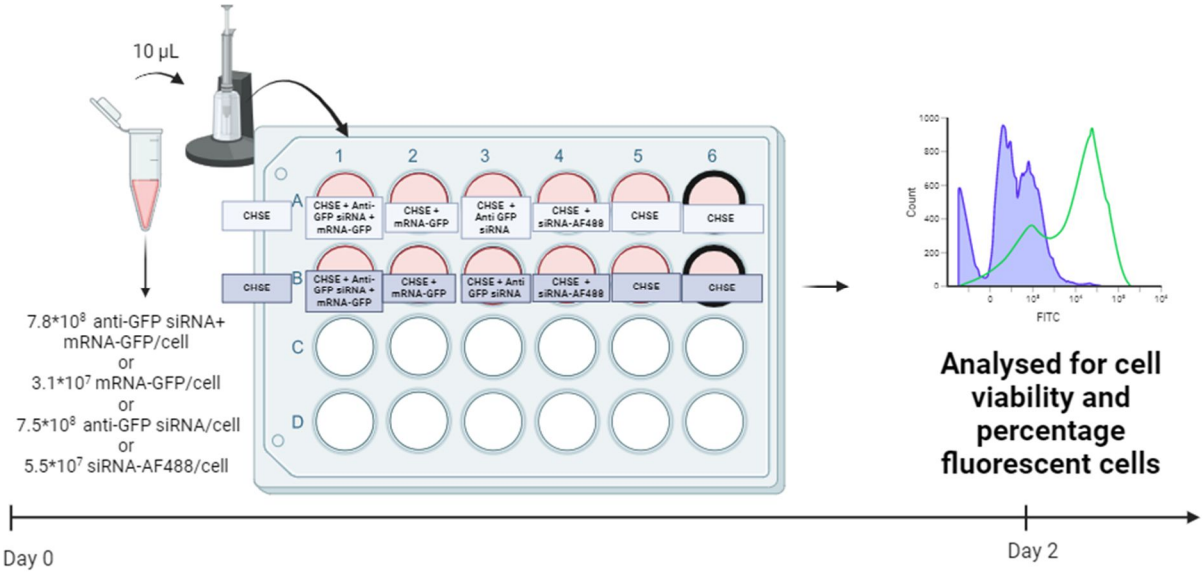

Figure 48. Experimental design of Neon™ transfection for silencing mRNA-GFP with anti-GFP siRNA in CHSE-214 cells. Day 0 is the transfection day. Wells with black border presents control samples that were not electroporated/transfected. The color of the “content-box” on the wells indicates the two parallels.

The setup is similar to “4.3 mRNA-GFP silencing control”, with identical controls, and identical mRNA-GFP and anti-GFP siRNA ratio (1:24). Differences in the setup is the number of cells transfected ($5*10^5$), and harvesting was done at Day 2.

Figure 49 shows the results from the silencing control experiment executed in CHSE-214 cells. The percentage of PI-positive cells are shown in Appendix Figure E4 and Figure E5.

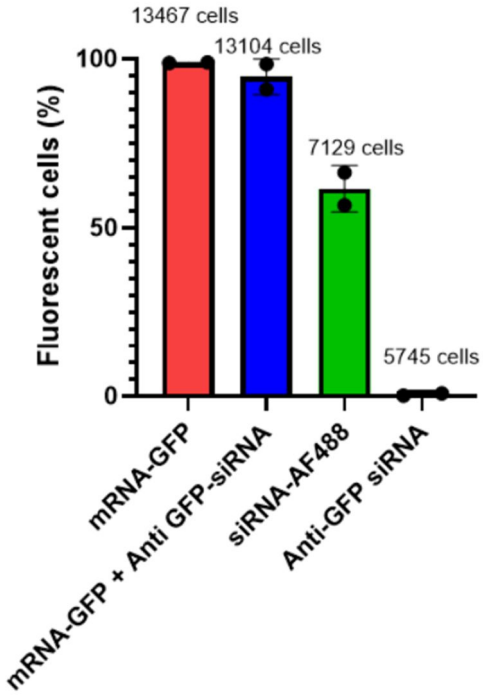

Figure 49. Barplot of the mean percentage of fluorescent CHSE-214 cells (%, n=2 CHSE-214 replicates) after transfecting with mRNA-GFP (red bar), mRNA-GFP + anti-GFP-siRNA (blue bar), siRNA-AF488 only (green bar) and anti-GFP siRNA only (not fluorescent).

The silencing control experiment for CHSE-214 showed a mean of 99% fluorescent cells when transfected with mRNA-GFP only, and a mean of 95% when co-transfected with mRNA-GFP and anti-GFP siRNA. CHSE-214 transfected with siRNA-AF488 with the electroporation program 1700V, 2P and 20ms led to a mean transfection of 62% cells.

Based on these results, a low, but not reliable silencing effect was achieved with CHSE-214 cells.

4.6 Target gene siRNAs and primers

The mRNA-GFP silencing experiments were unsuccessful for A. salmon RBCs and CHSE-214, but due to the previous success in silencing RBC in rainbow trout (74), and silencing of exogenous mRNA could be more difficult to achieve, the attempts to silence endogenous mRNA was still conducted,

The siRNA and primers for this experiment was designed carefully and assessed for quality prior to silencing experiments.

4.6.1 Basal expression versus poly(I:C) stimulated expression of siRNA target genes: TLR3, RIG-I, RLR3 and MAVS:

The genes targeted for silencing are TLR3, RIG-I, RLR3 and MAVS. The reason for selecting TLR3, RIG-I and RLR3 for silencing are because the genes are highly expressed in A. salmon RBCs, and known to initiate an antiviral response to dsRNA (34). MAVS is also targeted to elucidate its role in A. salmon RBCs, since in CHSE-214 cells, knock-down of MAVS by CRISPR/Cas gene editing supposedly stops interferon responses. MAVS is known to be a mediator in the RIG-I signaling pathway (75). The basal expression levels of these target genes in A. salmon RBCs and expression levels when stimulated with poly(I:C) is presented in Table 4 (Unpublished RED FLAG data).

Table 4. The mean basal expression (n= 4) and mean poly(I:C) stimulated expression (n=4) of siRNA target genes. Additional information about the target gene is included: Alternative name of the gene, Gene ID and poly(I:C) fold change from basal expression.

Name	Alternative name	Gene ID/LOC	Mean Expr RBC basal (RNA-Seq reads)	Mean Expr RBC poly(I:C)	Fold change
TLR3		106602560	1556	3226	Up (<2)
RIG-I	Ddx58	100302577	2627	14892	Up (5.3)
RLR3	dhx58	100195148	486	5601	Up (11.8)
MAVS	IPS-1	100316613	1217	1148	No

The fold change from basal expression to poly(I:C) stimulation are TLR3 (<2-fold), RIG-I (5.3-fold) and RLR3 (11.8-fold) respectively. MAVS is expressed in A. salmon RBCs, but not regulated by poly(I:C) stimulation.

4.6.2 siRNA sequences

The siRNAs were designed to target the RNA of TLR3, RIG-I, RLR3 and MAVS. Criteria's from Thermofisher Scientific were followed to enhance features such as dicer recognition and RISC-loading. If more gene copies were present in the genome, all copies were used for the design, making sure the siRNA targeted conserved regions. Different transcripts/splice variants were also considered for targeting all major mRNAs. The design criteria's followed were: 1) UU-overhang and GC-content of 30%-50% for higher siRNA efficiency, 2) Avoiding stretches of >4 T-nucleotide or A-nucleotide for preventing RNA pol III termination, 3) Choosing different mRNA regions to avoid structured areas and 4) Screening of off-targets found in A. salmon RBCs RNA-seq data, explained in "3.3.1 Designing siRNAs". The designed siRNA for TLR3, RLR3 and MAVS, and potential off-targets, are shown in Appendix Table F1 – F3.

For one gene, 3 different 21bp ds-siRNAs targeting a part identical for all copies and main transcript variants was designed. For MAVS, an additional three Dicer substrate interfering RNAs (DsiRNA) was ordered. The DsiRNA targeting MAVS mRNA is termed L-MAVS in this thesis, and was ordered since DsiRNA supports Ago2 loading and increases RISC incorporation rate, resulting to more efficient silencing (76). In Table 5, the sequence of the final siRNAs is presented.

Table 5. siRNA sequences ordered for TLR3, RIG-I, RLR3 and MAVS

Oligo Name	Sense strand sequence (5'-3')	Antisense Strand Sequence (5' - 3')	Antisense Overhang	Start
TLR3-1	UUGGCCAGAUAUAAUCCUC	GAGGAUUAUAUCUGGCCAA	UU	3
TLR3-2	CUAUGACGCGUUCGUCAUU	AAUGACGAACGCGUCAUAG	UU	2293
TLR3-3	ACUCUUCUCGAAGACUCCA	UGGAGUCUUCGAGAAGAGU	UU	2483
RIGI-1	GACUAUAAGGGUCUGUGUG	CACACAGACCCUUAUAGUC	UU	235
RIGI-2	GAGAAAGACCCUGAUAUCA	UGAUAUCAGGGUCUUUCUC	UU	1013
RIGI-3	GUGUAUCUUGGUGUCUGAU	AUCAGACACCAAGAUACAC	UU	2298
RLR3-1	UAAGAUCAUGGGGCGCUAC	GUAGCGCCCCAUGAUCUUA	UU	650
RLR3-2	UGGAACCGACUUCUUCCUG	CAGGAAGAAGUCGGUUCCA	UU	1180
RLR3-3	UUAGCACGUCAGCUUUGUU	AACAAAGCUGACGUGCUAA	UU	3031
MAVS-1	AUUGAAACCGUCAGUCUGG	CCAGACUGACGGUUUCAAU	AG	694
MAVS-2	GUACUUGCUACAGAUGGCG	CGCCAUCUGUAGCAAGUAC	CA	1183
MAVS-3	CGAGGAGUCAUGUAUCUGG	CCAGAUACAUGACUCCUCG	GA	1449
L-MAVS-1	AUUGAAACCGUCAGUCUGGAGGACA	UGUCCUCCAGACUGACGGUUUCAAU	AG	694
L-MAVS-2	GUACUUGCUACAGAUGGCGUGAACC	GGUUCACGCCAUCUGUAGCAAGUAC	CA	1183
L-MAVS-3	CGAGGAGUCAUGUAUCUGGAAUCAA	UUGAUUCCAGAUACAUGACUCCUCG	GA	1449

To ensure the quality of the siRNAs, TLR3-1, RIGI-1, RLR3-1, MAVS-1 and L-MAVS-1, were analyzed on Agilent 2100 Bioanalyzer as duplicate samples to assess the presence of a gel-band of the correct length with no degradation. The kit used was Agilent RNA 6000 Nano kit, according to the protocol "RNA 6000 Nano Kit for 2100 Bioanalyzer Systems". Each sample were further analyzed in Bioanalyzers 2100 Expert software, choosing the assay "Eukaryote Total RNA Nano".

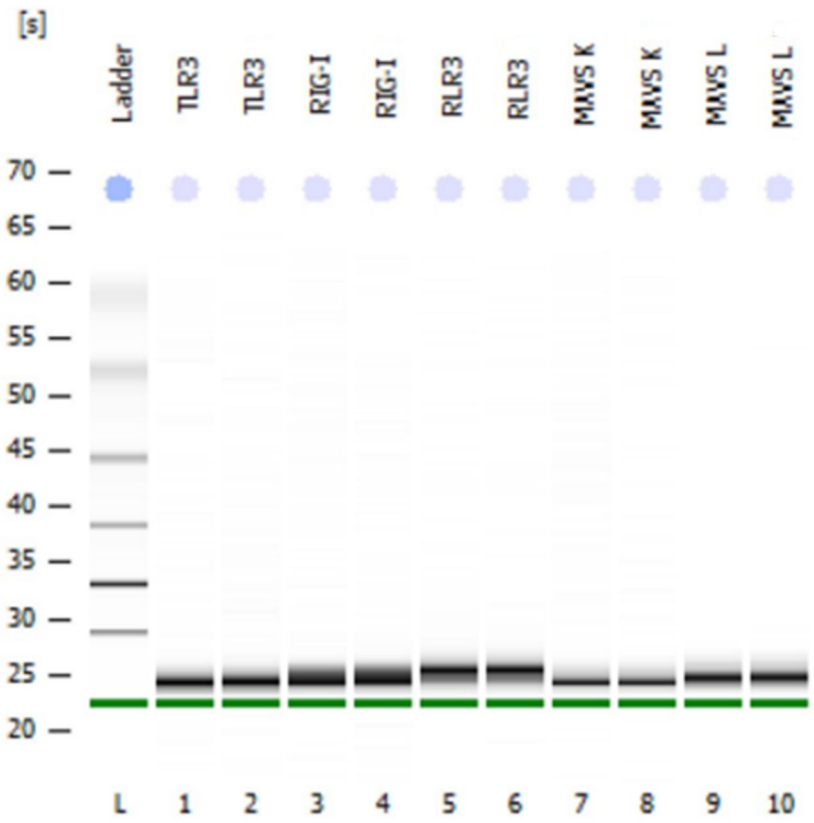

Figure 50. Agilent 2100 Bioanalyzer electronic gel image of siRNA duplicates of TLR3-1, RIGI-1, RLR3-1, MAVS-1 and L-MAVS-1.

From the electronic gel image of each siRNA, a gel bands is observed between 20 – 30 nt for all the siRNAs. The quantitative range of the RNA 6000 Nano kit is at 25 -500 ng/ µL, and the qualitative range is at 5 – 500 ng/µL (77). In each well, 3.97 µg was added of each sample (1 µl), and this overload could explain the strong band and inaccurate size of the band. The quality was considered acceptable, and the analyses was not repeated.

After quality assessment on the Agilent Bioanalyzer 2100, siRNAs targeting the same gene and in same length (e.g. TLR3-1, TLR3-2 and TLR3-3) were pooled together, resulting in a concentration of 1.32 µg/µL per siRNA. The pooled siRNAs will be referred to as siTLR3, siRIG-I, siRLR3, siMAVS and L-siMAVS.

Figure 51 shows the mRNA from TLR3, RIG-I, RLR3 and MAVS, and which regions the siRNAs is complimentary to.

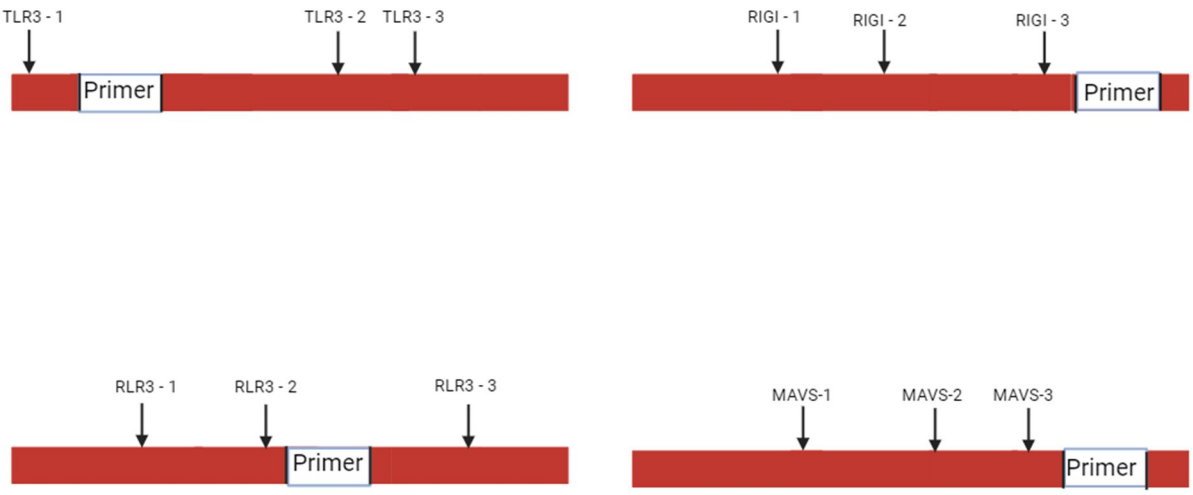

Figure 51. Approximate siRNA target areas on the mRNA of TLR3, RIG-I, RLR3 and MAVS.

4.6.3 Primer sequences for target genes

Primer-sets for the target-genes aimed for silencing (TLR3, RIG-I, RLR3 and MAVS), the antiviral genes (Mx and ISG15) that are regulated by signaling through the siRNA target gene proteins, and the housekeeping gene used for normalization (EF1α) are presented in Table 6. The intention of studying Mx and ISG15 expression is to see if target-specific silencing of dsRNA receptor or MAVS could potentially lead to “shut-down” of the antiviral genes.

Table 6. Primer sequences for TLR3, RIG-I, RLR3, MAVS, Mx, ISG15 and EF1α. Sequence marked with "*" only has partial sequence available.

Gene	Forward primer (5'-3')	Reverse primer (5'-3')	Amplicon length
TLR3	CTCTAACGGCAA*	TTTGATGTTGGC*	181
RIG-I	GCGACCGTCTTACGTCAAAG	TAGAAACACCTGGGCTGCTG	112
RLR3	TTCTCTGTCAGTCTGTGTTGCT	TGTTTGTGTCGCACTGCTTT	187
MAVS	TACGATGGCGTGAACCGTC	CCGTCGTTGTTCTGGATGGA	228
Mx	GGTGATAGGGGACCAGAGT	CTCCTCACGGTCTTGGTAGC	172
ISG15	ATATCTACTGAACATATATCTATCATGGAACTC	CCTCTGCTTTGTTGTGGCCACTT	150
EF1α	TGCCCCTCCAGGATGTCTAC	TCACCAGGCATAGCCCGATTC	174

The primer-sets for TLR3, RIG-I, Mx and ISG-15 were already available in the lab. RLR3 and MAVS primers were designed specifically for this study, and were tested for quality and specificity by qPCR. The primers were tested with concentrations of 1.5 ng, 2.5 ng, 5 ng and 10 ng cDNA derived from A. salmon RBCs. Figure 52 shows the melt curve generated from qPCR analysis of RLR3 and MAVS primer sets.

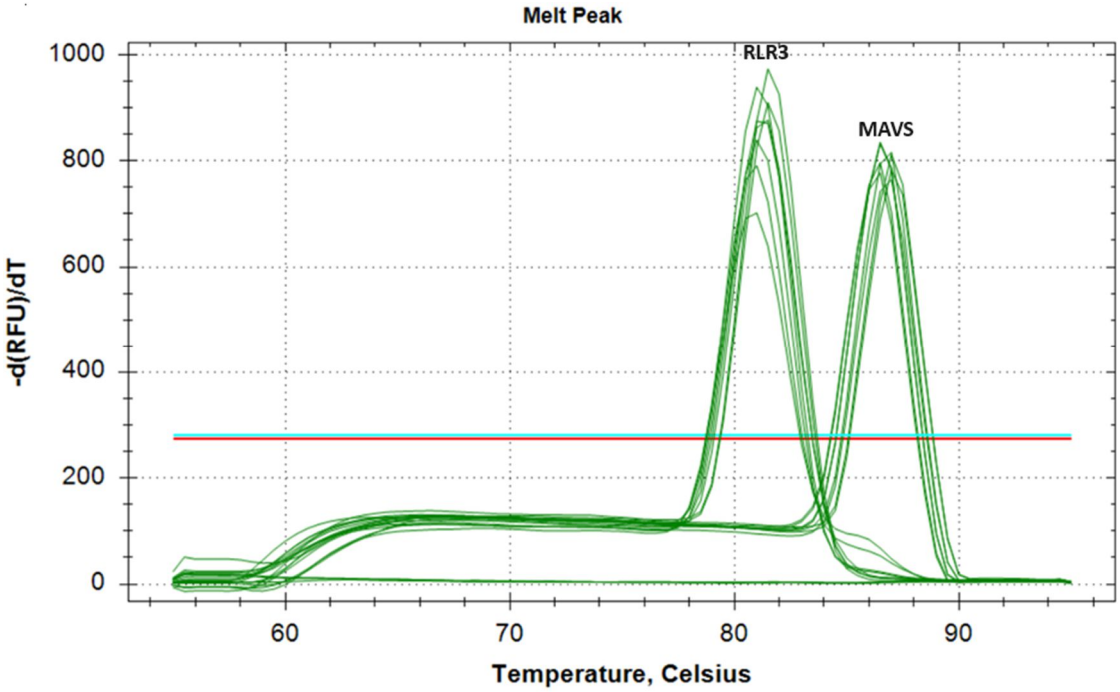

Figure 52. RLR3 and MAVS melt curve from RT-qPCR analysis. Analyzed in Bio-Rad CFX Manager 3.1 (3.1.1517.0823)

From the qPCR analysis, one melt curve peak is observed per assay (shown combined in Figure 52), indicating one specific amplification product. In the figure, the left peak is derived from samples using the RLR3 primer-set, and the right peak is from samples using MAVS primer-set. The melt temperature is in line with a longer amplicon for the MAVS primers (228 bp), compared to RLR3 (187 bp). Ct-values and standard curve from the qPCR analysis are shown in Appendix Table F5 and Figure F1. From Figure F1, the R^2-value could have been higher, but linearity was achieved from the standard curve. The 2.5 ng samples from the qPCR analysis was ran in Agilent 2100 Bioanalyzer as duplicates (One sample in two wells) for quality assessment (length and purity of the amplification product), using the Agilent DNA 12000 Kit.

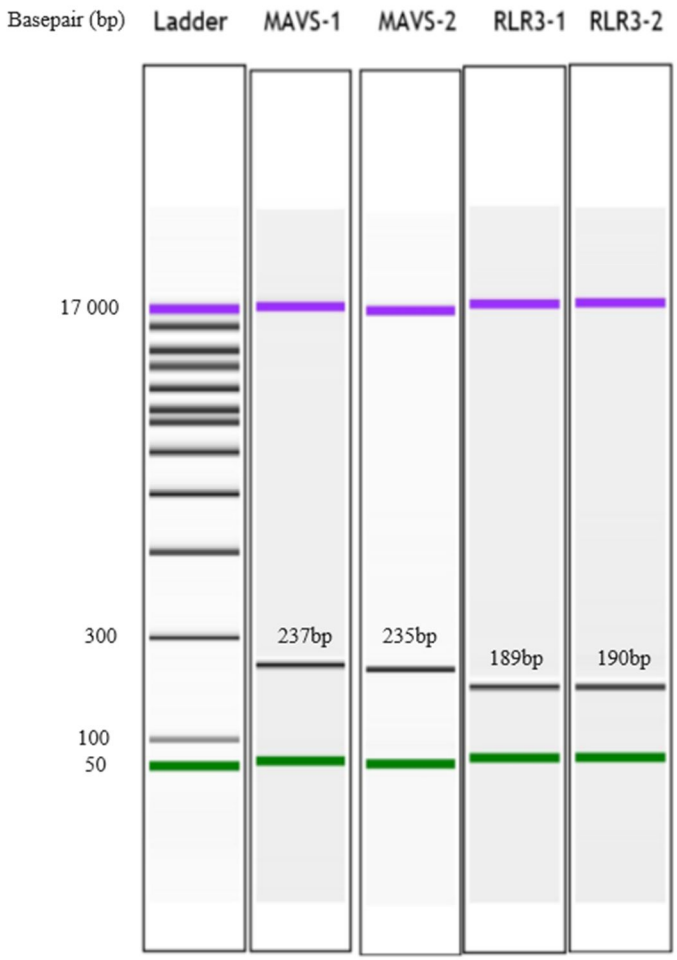

Figure 53. Agilent 2100 Bioanalyzer electronic gel image of the amplification product of primers for MAVS and RLR3 tested against 2.5 ng cDNA from A. salmon RBCs. Approximate size of the band derived from each primer is observed in each well.

Figure 53 shows one band deriving from the duplicates of MAVS 2.5 ng samples, and one band deriving from the duplicates of RLR3 2.5 ng samples, with size approximately correct according to amplicon size.

4.7 siRNA silencing of TLR3, RIG-I, RLR3 and MAVS under basal expression

The methods utilized for silencing TLR3, RIG-I, RLR3 and MAVS are shown in Figure 54. Under basal expression, the step with poly(I:C) stimulation was omitted. Transfection was done 1 day post-isolation during experiments done in this section and "4.8 siRNA silencing of TLR3, RIG-I, RLR3 and MAVS – test of effects on poly on poly(I:C) stimulation". Quantity and quality from "RNA isolation and quality control" can be assessed in Appendix section H, and Ct-values from qPCR can be assessed in Appendix Section I. An example on how fold-change was calculated is shown in Appendix A2

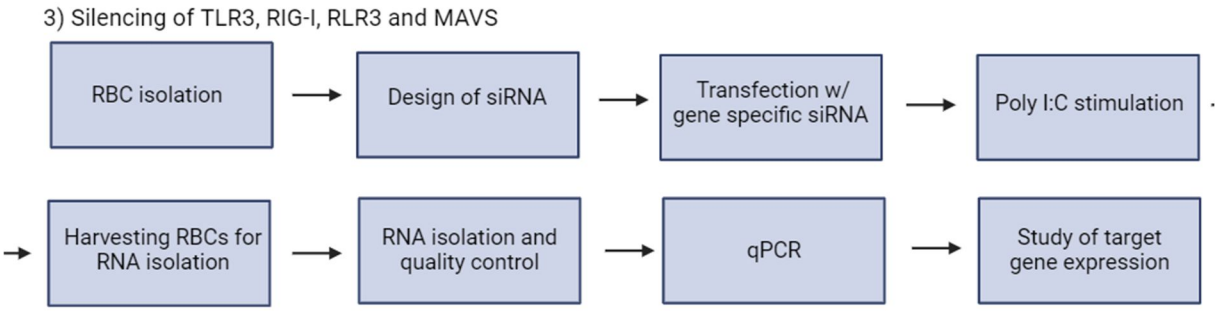

Figure 54. Methods utilized for silencing target genes. Poly(I:C)-stimulation was not done in section "4.7 siRNA silencing of TLR3, RIG-I, RLR3 and Mavs under basal expression", only in section "4.8 siRNA silencing of TLR3, RIG-I, RLR3 and MAVS – test of effects on poly(I:C) stimulation".

4.7.1 Testing knock-down efficiency and responses to transfection at different time points

To find the time-point for optimal knock down and for testing of effects (stimulating with poly(I:C)), the mRNA expression of TLR3, RIG-I, RLR3, MAVS, Mx and ISG15 was analyzed by RT-qPCR after transfecting A. salmon RBCs with siTLR3, siRIG, siRLR3, siMAVS and L-siMAVS. The amount of siRNA used was 3.97 µg. An amount of 2 µg had previously resulted in optimized siRNA transfection, but a higher amount was utilized to increase the RNA:RBC ratio, increasing the probability of an dsRNA interacting with dicer. The time-points chosen for analysis were Day 1, which is considered the earliest possible time for harvesting RBCs after electroporation, Day 3, and Day 6, since a functional study of effects on poly(I:C) stimulation would need analyses at a later time point. Previous experiments had indicated no detection of transfected siRNA at Day 7. The experimental design is shown in Figure 55.

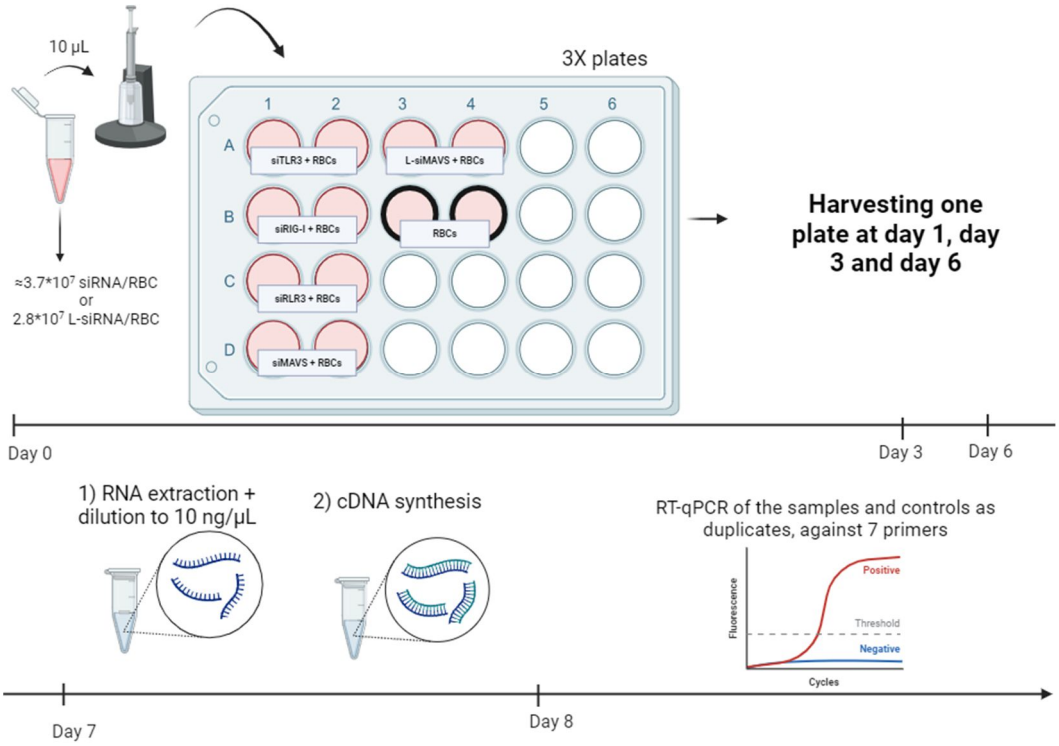

Figure 55. Experimental design of Neon™ transfection to find a time-point where knock-down is detectable and suitable for stimulating with poly(I:C). Day 0 is the day of transfection. Wells with black border represent samples that did not undergo electroporation. Harvesting was done at Day 1, Day 3 and Day 6 post-transfection. The experiment included a total of three 24-well plates, and a total of 30 transfections. From each plate, six samples were harvested, resulting in a total of 18 samples all together. At Day 7, RNA was extracted from all 18 samples and samples were diluted to 10 ng/µL before cDNA-synthesis. From Day 8, gene-expression of TLR3, RIG-I, RLR3, MAVS, Mx, ISG15 and EF1α was analyzed for all 18 samples (and RTC and NTC).

Each siRNA was transfected twice in $5*10^6$ RBC, and added to individual wells with 0.5 mL media, resulting in $10*10^6$ RBC transfected per target mRNA (pooled siRNA). Harvesting was done at Day 1, Day 3 and Day 6, and cell viability from trypan blue staining was assessed at Day 3 and Day 6 using automatic cell counter Countess (Appendix H1). After RNA-extraction, all samples were diluted to 10 ng RNA/µL. All samples were tested for expression of target genes TLR3, RIG-I, RLR3, MAVS, effects on secondary antiviral genes Mx and ISG15, as well as the reference gene EF1α by RT-qPCR using sequence-specific primers.

The transcript level of the target genes after transfecting with siTLR3, siRIG-I, siRLR3, siMAVS and L-siMAVS is shown in Figure 56. “NA” is presented at Day 1 post transfection with siRLR3, since values were missing after running qPCR.

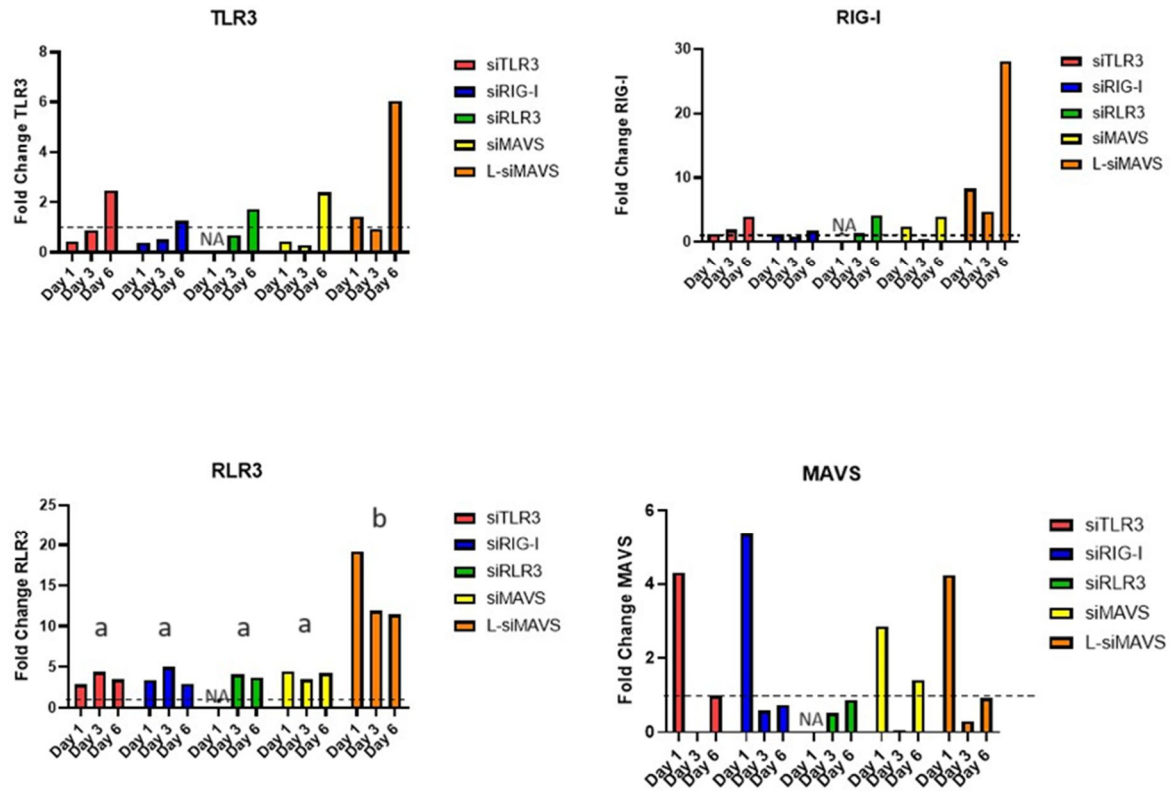

Figure 56. Fold change of TLR3, RIG-I, RLR3 and MAVS mRNA at Day 1, Day 3 and Day 6 post transfection with siRNA normalized against the EF1a reference gene. The dotted line represents the basal expression of each gene in a un-transfected sample. "NA" are presented from Day 1 post transfection with siRLR3. Treatments with significant difference is shown in letters.

There were no convincing signs of specific siRNA knock-down of target mRNA in this experiment, and only RIG-I mRNA appeared to have somewhat lower expression 6 days after siRIG-I transfection, compared to the other siRNA transfections. This difference could be accidental. There were observed some unspecific effects described below.

Levels of TLR3 mRNA were lower than basal expression at Day 1 and Day 3 for all siRNAs transfected, except L-siMAVS, that led to a 1.42-fold upregulation. An increase in TLR3 mRNA is observed at Day 6 after transfection of all siRNAs independent of the target. A one-way ANOVA (mixed models) was performed by comparing the mean fold change of all siRNA treatments at each day against each other (Appendix Table K2). Significant difference was found in TLR3 expression between Day 1 and Day 3, but also between Day 3 and Day 6,

indicating that the effect on TLR3 mRNA levels after transfection is consistent and siRNA independent.

RIG-I mRNA levels were either higher or similar to basal levels for all siRNA transfections except for 3 days after the transfection with siMAVS when RIG-I mRNA was lower (fold 0.42).

RLR3 mRNA had the highest upregulation after siRNA transfection compared to the other dsRNA-receptor and MAVS mRNAs, independent of siRNA targets. All transfected samples were above basal mRNA levels at Day 1, Day 3 and Day 6. A one-way ANOVA test (mixed models since RLR3-value was missing) was performed comparing the means of siRNA transfected cells against each other (Appendix Table K3). A significant difference was found in RLR3 mRNA levels when comparing transfection with L-siMAVS (27 nt) to the 21 nt regular siRNA.

MAVS mRNA increased above basal levels at Day 1 after siRNA transfection independent of target, but decreased to under basal levels at Day 3 and Day 6. The mean fold-change of each siRNA treatment from each day was compared with a one-way ANOVA (Appendix Table K3). Significant difference was found between Day 1 compared to Day 3 and Day 6, indicating siRNA-dependent elevation of MAVS mRNA levels at Day 1 only.

Studying the downstream antiviral genes Mx and ISG15 is a control of basal levels of these genes, to make sure they can be further stimulated by poly(I:C) in a functional test after siRNA transfection, or if the siRNA works as a stimulant.

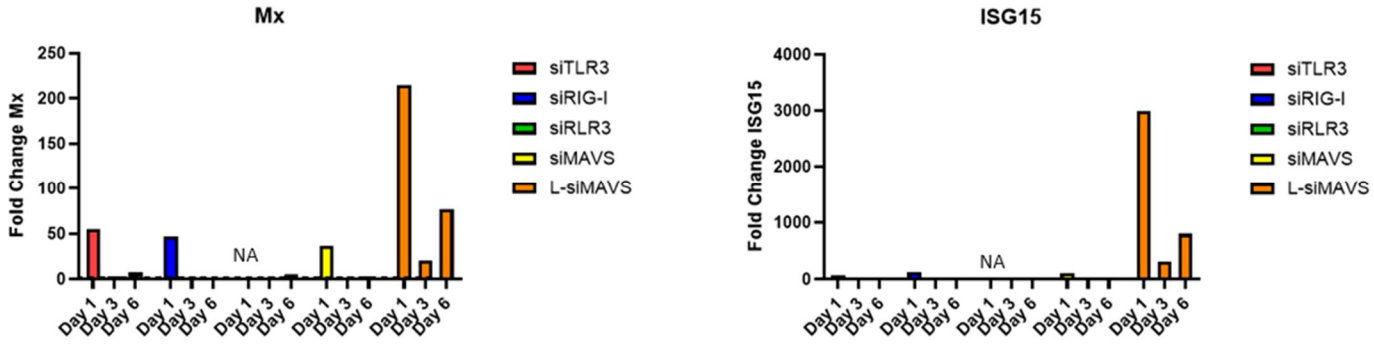

Figure 57. Fold change of Mx and ISG15 mRNA at Day 1, Day 3 and Day 6 post transfection with siRNA normalized against the EF1a reference gene. NA is presented at 1-day post transfection with siRLR3, since the values are missing.

In Figure 57, we observe that Mx-levels increase strongly Day 1 after transfection with siTLR3, siRIG and siMAVS, with a fold-change ranging from 37.0 – 54.8, while L-siMAVS led to a 215-fold increase compared to basal expression. At Day 3, Mx expression decreased. A one-way ANOVA was performed, comparing the mean fold-change caused by siRNA treatment from each time point (Appendix Table K4). Significant differences were found between Day 1 and Day 3, indicating that the high antiviral response at Day 1 after transfecting with siRNA is significantly reduced.

L-siMAVS (27 nt) stimulated ISG15 to a 2994-fold increase in mRNA day 1, while the 21 nt siRNAs all stimulated ISG 15 expression to a fold increase ranging from 71.4 to 127 at Day 1. At Day 3, mRNA decreased to 4.30 – 8.78-fold over basal levels for regular siRNAs and to 315-fold for L-siMAVS. Strong expression of ISG15 is shown from L-siMAVS compared to the other siRNAs.

Based on these findings of strong responses to transfected siRNA particularly on day 1, it was decided that a poly(I:C) stimulation could not be done until Day 3 or later post-transfection. Because of the very strong responses to L-siMAVS, the longer siRNAs were not included for further silencing attempts.

4.7.2 Determine siRNA effectiveness

Aiming to make a final attempt to explore silencing by the siRNAs, RBCs were isolated from 3 A. salmons. The experimental design is shown in Figure 58.

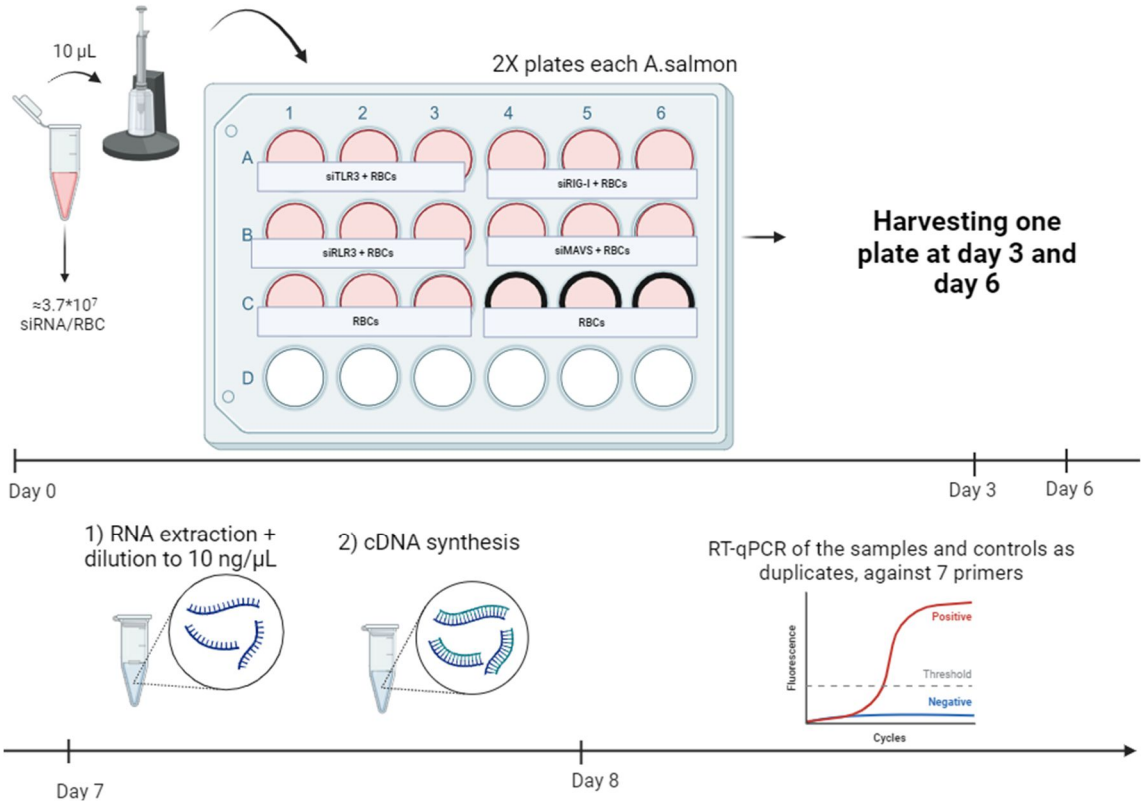

Figure 58. Experimental design of Neon™ transfection to determine the siRNAs silencing efficiency. Day 0 is the day of transfection. Wells with black border show samples that did not undergo electroporation. Harvesting was done at Day 3 and Day 6 post-transfection, making a total of 2 well-plate for each A. salmon. From each plate, six samples were harvested, resulting in a total of 36 samples. At Day 7, RNA was extracted from all 36 samples, and all the samples were diluted to 10 ng/µL. From Day 8, the expression of TLR3, RIG-I, RLR3, MAVS, Mx, ISG15 and EF1α were analyzed for all 36 samples (and RTC and NTC).

The experimental setup was similar to "4.7.1 Testing knock-down efficiency and responses to transfection at different time points". Changes in the setup include addition of electroporated RBC samples (control) without siRNA to determine the effect electroporation itself has on stimulation of target genes. Another change in the setup included that RBCs were transfected with each pooled siRNA mix three times, meaning a total of 15 * 10^6 RBCs transfected per sample. This was done to increase RNA-levels obtained from the samples.

Figure 59 and Figure 60 show the fold change of target genes at Day 3 and Day 6.

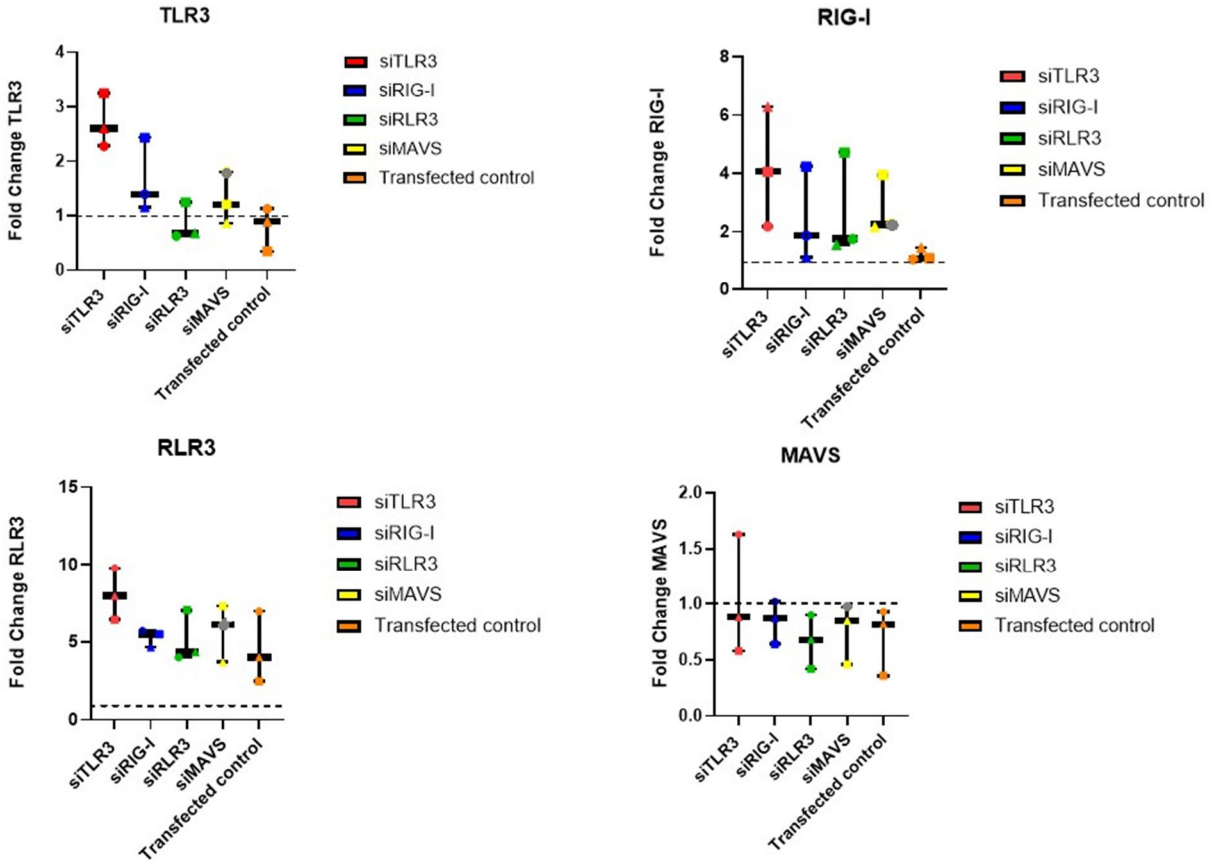

Figure 59. RBC expression of TLR3, RIG-I, RLR3 and MAVS mRNA normalized against the EF1a reference gene, 3 days after transfection with siTLR3, siRIG-I, siRLR3 and siMAVS. Colored points indicate the different siRNAs transfected, and circle, square and triangle points indicate A. salmon 1, A. salmon 2 or A. salmon 3 respectively. Grey points indicate that the EF1α value was slightly divergent from the other values, and the point may be uncertain. The y-axis presents the fold-change. The dotted-line on the y-axis presents the basal expression from the un-electroporated RBCs.

The mean expression of RIG-I and RLR3 is above basal 3 days after transfection independent of the target of the siRNA. RLR3 is upregulated 2.5 – 9.8 -fold, and the electroporated RBCs control also leads to an upregulation of RLR3 mRNA. RIG-I mRNA was upregulated 1.1 – 6.3 fold 3 days after transfection with siRNAs.

The mean TLR3 mRNA expression was also increased above basal expression after transfection with siTLR3, siRIG-I and siMAVS for all the A. salmons. After siRLR3 transfection, and in the transfected control, mRNA levels were slightly below basal expression. A one-way ANOVA test revealed significant difference between the TLR3 expression after transfection with siTLR3 and expression after transfection with siRLR3 and siMAVS (Appendix Table K5).

For MAVS-expression, the mean mRNA level was slightly lower than basal independent of the siRNA used for transfection and in the transfection control.

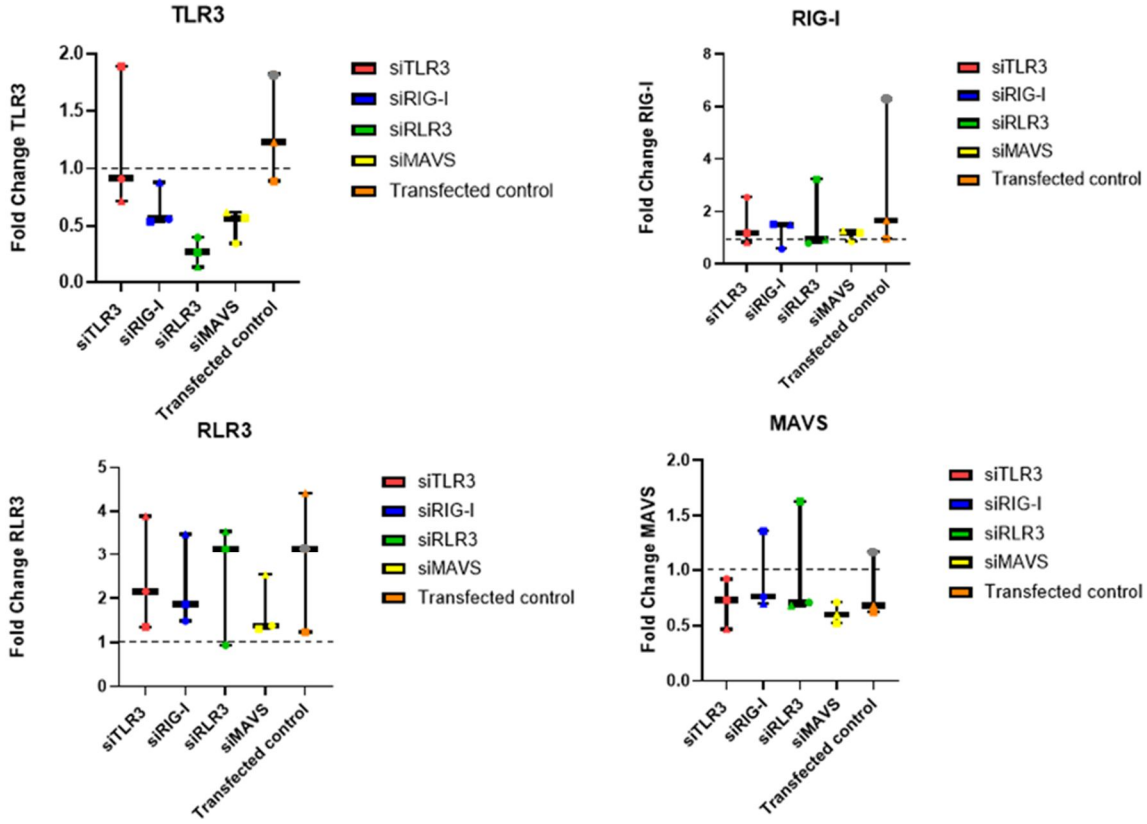

Figure 60. RBC expression of TLR3, RIG-I, RLR3 and MAVS mRNA normalized against the EF1a reference gene, 6 days after transfection with siTLR3, siRIG-I, siRLR3 and siMAVS. Colored points indicate the transfected siRNA, and shaped points (circle, square and triangle) indicates A. salmon 1, A. salmon 2 or A. salmon 3. The y-axis presents the fold-change from basal expression levels, and the dotted-line on the y-axis presents the basal expression from the un-electroporated RBCs. The A. salmon 1 transfected control value is colored grey as it is considered an outlier in the expression of TLR3, RIG-I and MAVS.

At Day 6, the mean expression of TLR3 mRNA when transfected with any siRNA is below basal expression, but above basal expression for the transfected control. Since all the siRNA led to TLR3 expression below basal, no indication of specific TLR3 silencing is shown.

RIG-I and RLR3 mRNA expression was similar to Day 3, with RIG-I mean expression close to basal, and RLR3 still being expressed slightly above basal expression. The mean expression of MAVS mRNA was below basal expression for all siRNAs.

The regulation of the antiviral genes Mx and ISG15 3 and 6 days after transfection is shown in Figure 61.

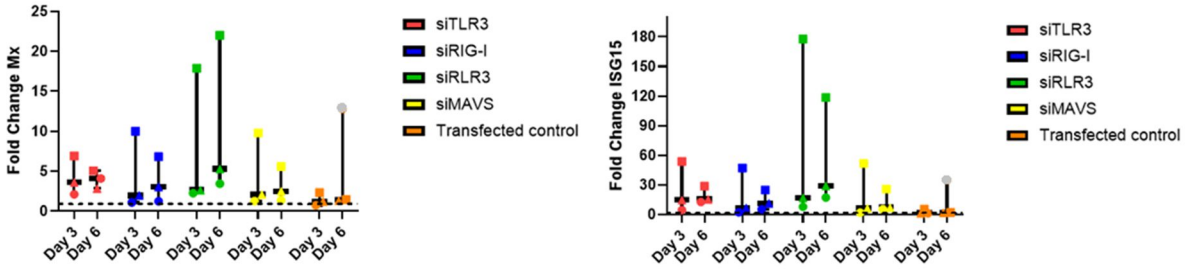

Figure 61. RBC expression of Mx and ISG15 mRNA normalized against the EF1a reference gene, 3 days and 6 days after transfection with siTLR3, siRIG-I, siRLR3 and siMAVS. Common colored points indicate the siRNA transfected with, and circle, square and triangle points indicates A. salmon 1, A. salmon 2 or A. salmon 3, respectively. The dotted line represents the basal expression of each gene in a un-transfected sample. A grey-point is presented at A. salmon 1 transfected control at Day 6, since it presents a high expression of Mx and ISG15.

Mx and ISG15 were upregulated for all three A. salmons at Day 3 and Day 6. A. salmon 2 RBC showed higher expression of Mx and ISG15 at Day 3 and Day 6, compared to A. salmon 1 RBC and A. salmon 3 RBC. Transfected control showed low mRNA expression, except for A. salmon 1 RBC. Difference in antiviral response from the A. salmon individuals RBCs is shown.

Based on these results, silencing did not occur for the targeted genes, but induction of antiviral genes by siRNA depended a lot on the individual.

4.8 siRNA silencing of TLR3, RIG-I, RLR3 and MAVS - test of effects on poly(I:C) stimulation

Silencing of target genes was not observed, but the experiment studying antiviral response from poly(I:C) after siRNA transfection was still done. Poly(I:C) is known to give an antiviral response, and is used as a read-out of Mx and ISG15.

The experimental design is shown in Figure 62.

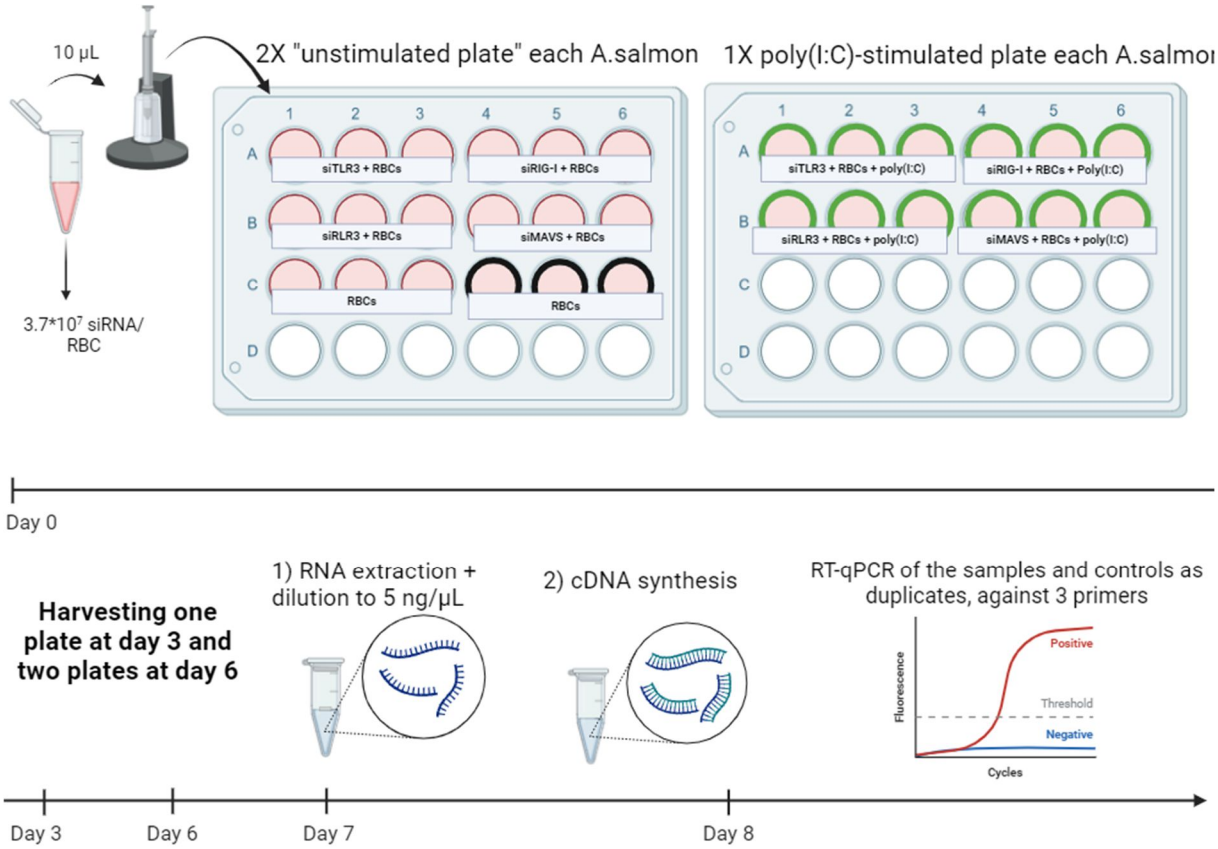

Figure 62. Experimental design of Neon™ transfection to find which dsRNA-receptor (or MAVS) activate an antiviral response after poly(I:C)-stimulation. Day 0 is defined as the day transfection took place. Samples with black border did not undergo electroporation. Samples with green border were stimulated with poly(I:C) 3-days post transfection. One unstimulated plate was harvested at Day 3 and one stimulated and one unstimulated plate at Day 6. From one A. salmon individual, 16 samples were harvested, resulting in a total of 48 samples from all three A. salmons. At Day 7, RNA was extracted from all 48 samples, and all the samples were diluted to 5 ng/µL for cDNA-synthesis. From Day 8, gene-expression of Mx, ISG15 and EF1α was analyzed for all 48 samples (and RTC and NTC)

The experimental design is similar to the to "4.7.2 Determine siRNA effectiveness". A difference in the design is the introduction of a plate transfected with siTLR3, siRIG-I, siRLR3 and siMAVS, but stimulated with 50 µg/mL poly(I:C) at Day 3 post-transfection. After RNA-extraction, all samples were diluted to 5 ng/µL. Only Mx, ISG15 and EF1α expression was assessed by RT-qPCR.

Figure 63 shows the expression of Mx and ISG15 at Day 3, before samples were stimulated with poly(I:C).

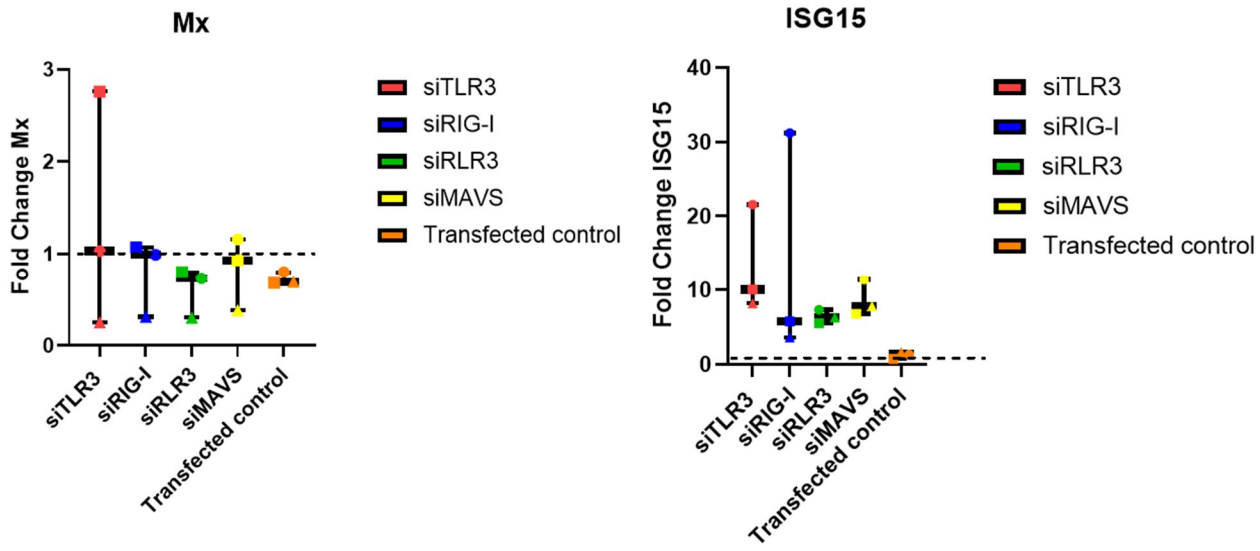

Figure 63. RBC expression of Mx and ISG15 mRNA normalized against the EF1a reference gene, 3 days after transfection with siTLR3, siRIG-I, siRLR3 and siMAVS. Colored points indicate the siRNA transfected , and circle, square and triangle points indicate A. salmon 1, A. salmon 2 or A. salmon 3 respectively. The y-axis presents the fold-change from basal expression (dotted line).

Before poly(I:C) stimulation, all the siRNA transfected samples had a mean expression of Mx similar or below basal. The Mx expression ranged between 0.35 – 2.7 fold. ISG15 ranged between 3.6 – 31 fold after 3 days post-transfection. The transfected control had similar to basal of Mx and ISG15 expression at Day 3.

The Mx and ISG15 expression from siRNA transfected samples stimulated with poly(I:C), and not stimulated with poly(I:C) is presented respectively in Figure 64 and Figure 65.

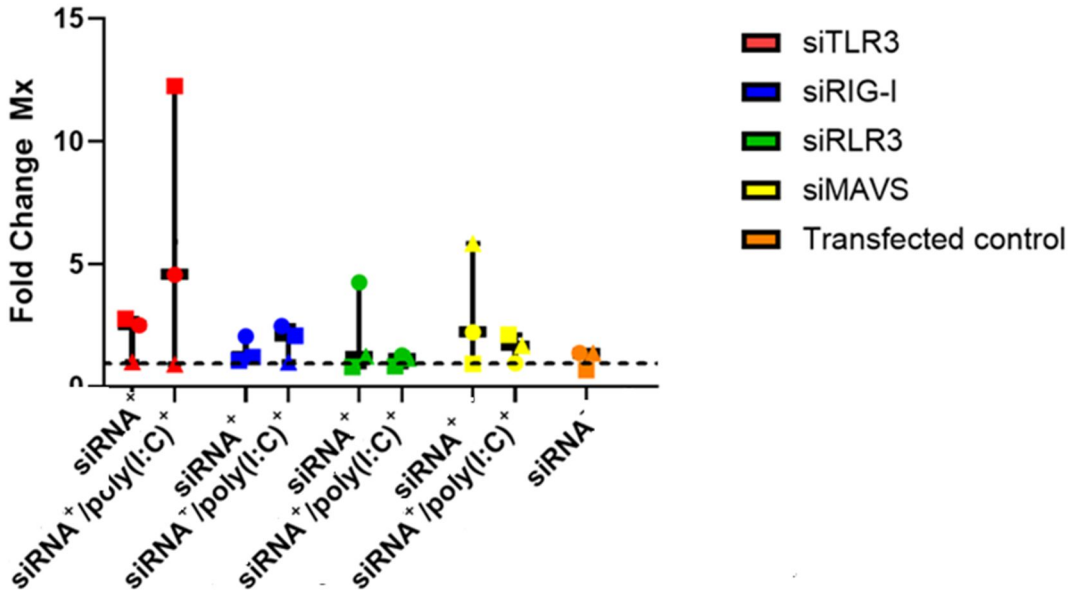

Figure 64. RBC expression of TLR3, RIG-I, RLR3 and MAVS mRNA normalized against the EF1a reference gene, 6 days after transfection with siTLR3, siRIG-I, siRLR3 and siMAVS. X-axis presents if the sample is treated with ($siRNA^+$/$siRNA^-$), and if the sample is stimulated with poly(I:C) ($poly(I:C)^+$).. Common colored points indicate the siRNA-transfected with, and circle, square and triangle points indicate A. salmon 1, A. salmon 2 and A. salmon 3 respectively. The y-axis presents the fold-change from basal expression (dotted line).

At Day 6, the mean fold change of Mx without poly(I:C)-stimulation, after transfecting with siTLR3, siRIG-I, siRLR3 and siMAVS, were 2.08, 1.44, 2.1 and 2.99. After poly(I:C)-stimulation, the fold-change was 5.9, 1.8, 1.08 and 1.58.

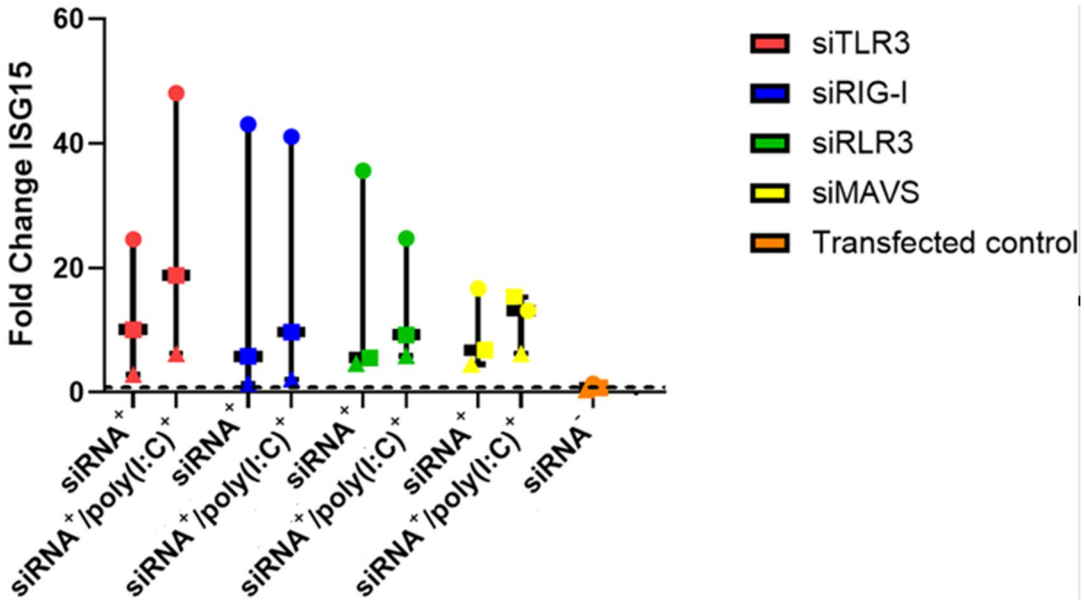

Figure 65. RBC expression of TLR3, RIG-I, RLR3 and MAVS mRNA normalized against the EF1a reference gene, 3 days after transfection with siTLR3, siRIG-I, siRLR3 and siMAVS. X-axis presents if the sample is treated with ($siRNA^+$/$siRNA^-$), and if the sample is stimulated with poly(I:C) ($poly(I:C)^+$). Common colored points indicate the siRNA-transfected with, and circle, square and triangle points indicate A. salmon 1, A. salmon 2 and A. salmon 3 respectively. The y-axis presents the fold-change from basal expression (dotted line).

ISG15 fold-change before poly(I:C) stimulation was 12.5, 16.7, 15.5 and 9.4 respectively from siTLR3, siRIG-I, siRLR3 and siMAVS. After poly(I:C) stimulation, the mean fold-change was 24.4, 17.5, 13.3 and 11.5.

Only siTLR3 and siRIG-I experienced an up-fold of Mx after poly(I:C) stimulation, compared to un-stimulated samples. ISG15 was higher upregulated compared to un-stimulated samples. Transfected control did not experience an up-fold of both ISG15 and Mx.

A control containing un-electroporated RBCs, but underwent poly(I:C)-stimulation at Day 3, was not added in the experimental design, making any speculations hard from this experiment, since distinguishing between siRNA and poly(I:C) stimulated response is not possible. No significant difference was found between poly(I:C) stimulated and not stimulated poly(I:C) samples (Appendix Table K6 – K7), and no significant difference was found between siRNA transfected with when stimulated with poly(I:C) (Appendix Table K8).

5 Discussion and future perspectives

5.1 Discussion of methodologies

5.1.1 Transfection by electroporation

As mentioned in "3.3.1 Transfection", numerous methods could have been utilized for establishing siRNA (and mRNA) in the A. salmon RBCs. Electroporation was chosen since successful siRNA silencing by electroporation has been achieved in Rainbow Trout RBCs by Chico *et al*. (74), discussed in detail in "5.2.5 is the RNAi system functional in fish cells". A lipofectin-based transfection with jetMESSENGER® (Polyplus) has been tried in A. salmon RBCs prior to this thesis, but resulted in low cell viability and transfection efficiency (Unpublished RED FLAG data). Electroporation has also been observed to induce less IFN response than lipofectin-based methods (78).

By varying the electroporation program with increasing voltage, duration and pulse, a higher transfection efficiency can be achieved at the cost of a lower cell viability (71). The cell death caused by electroporation can be divided into two main categories: 1) spontaneous cell death and 2) delayed cell death (71). Spontaneous cell death is generally caused by cells unable to "reseal" after loss of cell plasma membrane barrier function. Delayed cell death, however, results from intracellular changes after resealing, resulting in cell stress initiating apoptosis, necroptosis or autophagy. Viewing viability data after siRNA transfection shown in Figure 25 and Figure 26, estimates on delayed cell death can be made. The earliest time point used for estimating cell viability was Day 2, when the cell viability was measured to 61% when using the electroporation program with the highest voltage and fewest pulses (1600V and 2 pulses). This is most likely a mix of spontaneous and delayed cell death, lacking the count of bursted cells. At Day 7 viability was 66.9%. The program with 1400V and 4 pulses had a cell viability of 80% at Day 2, but at Day 7 viability was reduced to 28%. Delayed cell death is primarily associated with low voltage and a high number for pulses (71), which is in accordance with the data obtained here. Spontaneous cell death only has not been measured. Cells can burst in the transfection process, and can then not be counted as dead cells, just as a loss of cells.

The cell viability was studied at Day 3 using PI staining in a flow cytometer for the final chosen program 1700V, 20ms and 2 pulses , and also with trypan blue staining in automatic cell counter countess (Appendix section G) in the silencing experiments. The cell viability was measured using different dyes (trypan blue and PI), and utilization of different procedures for measurements can result in different estimates of cell viability after electroporation (79, 80). From both procedures, high cell viability was measured, indicating that A. salmon RBCs are robust against electroporation, at least regarding late cell death occurring prior to Day 6 after transfection.

A challenge observed during transfection is arcing (sparks). According to the Neon™ transfection manual (81), sparks could result in low transfection efficiency. When a spark occurs, more cells are lost from RBCs bursting. Transfecting with any of the pooled siRNAs (siTLR3, siRIG, siRLR3, siMAVS or L-siMAVS) resulted in some electrical sparks, also losing a high number of cells from bursting (Appendix Section G). Because of the loss of cells, cell numbers were tripled ($15*10^6$ RBCs) for transfection.

5.1.2 Evaluating transfection efficiency: Flow cytometer and microscope.

Flow cytometry was utilized for evaluating the transfection efficiency of siRNA and mRNA in A. salmon RBCs. Flow cytometry is a quantitative method to measure the number of fluorescent cells, and fluorescence microscopy was utilized as a qualitative approach. Flow cytometry has proven to be a good method for evaluating the relative amount of fluorescent cells, and results corresponded to microscopic images.

A challenge with evaluating transfection efficiency using flow cytometry is the many options for flow-data analysis (82). Computational assistance was not used during analysis, but a manual method was selected. The “gating-strategy” can lead to differences in the results, caused by false positives and negatives. Manual gating can also result in unreproducible results if the gating strategy is not consistent (82). The gating-strategy was changed after the first optimization experiment for siRNA and mRNA transfection (“4.2.2 Optimizing siRNA transfection efficiency in A. salmon RBCs – Experiment 1” and “4.3.3.1 Optimizing mRNA

transfection in A. salmon – Experiment 1"), after consulting with flow cytometry expert Leo Chelappa Gunasekaran at NVI. This explains the sudden rise in cell viability from experiment 1 to experiment 2.

Spectral overlap from the PE and FITC channel can be a challenge in flow cytometer analysis. Spectral-overlap is the spillover resulting from one fluorescent molecule bleeding into the channel where you measure the second (83). Alexa-488 (control-siRNA) or EGFP (expressed from control mRNA) can partly bleed into the PE- channel, in which PI-stained (dead) cells are detected, resulting in false positive cell death data (Figure 66).

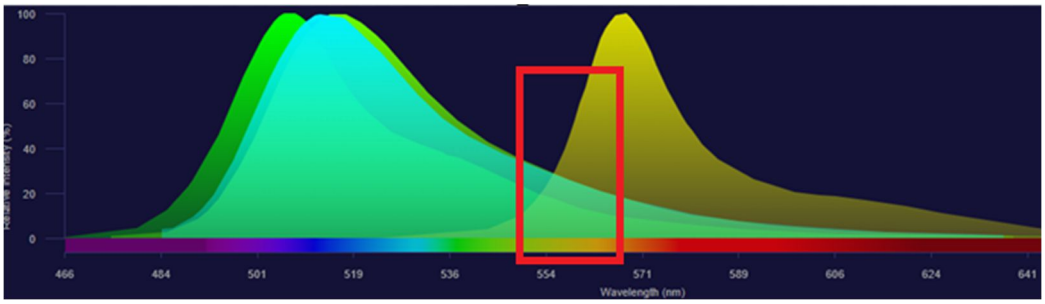

Figure 66. Relative intensity from the fluorophore PE (yellow), FITC (Green), EGFP (Turquoise) and Alexa488 (Lime Green, behind enhanced GFP). Red-square indicate spectral-overlap resulting to potential false positive. Assessed from Thermofisher Scientific Fluorescence SpectraViewer (Fluorescence SpectraViewer (Thermofisher.com))

To discriminate between PI-stained and GFP/AF488 fluorescent cells, auto-compensation was utilized from experiment 2, resulting in less dead cells estimated after transfection.

5.1.3 Measurements of gene-expression: qPCR

RT-qPCR using SYBR green was employed to measure the amount of target-mRNA present in A. salmon RBCs after transfection with siRNA. The results derived from SYBR-green RT-qPCR can be compared with TaqMan RT-qPCR. TaqMan qPCR differentiates from SYBR-green by utilizing a ss-oligonucleotide probe for the target DNA which carry a fluorescent marker (69). The fluorescence signal given from TaqMan qPCR will because of the probe be a bit more specific for the target. Two main advantages of TaqMan qPCR are more specificity and quantification accuracy (69), and that you do not have to perform a melt curve analysis to explore assay specificity. Drawbacks of TaqMan qPCR are that the TaqMan-probe is

expensive compared to just buying primers for SYBR-green qPCR. The evaluation of RLR3 and MAVS primer sets, shows that they produced amplicons with correct length and specific melt curve using the SYBR Green assay (Figure 50). The other primer sets had been tested for specificity earlier.

A challenge with using RT-qPCR for studying RNAi can be that not all primer sets will detect silencing due to partial degradation of the target mRNA (84, 85). In a trial performed by Holmes et al. (84) five primer sets were utilized to detect siRNA silencing of PKCε in human dermal endothelial cells (HDMECs), but only three of the primer sets detected silencing. Holmes *et al.* hypothesized that siRNA silencing resulted in a 3' end template from incomplete degradation and recommended using primer-sets flanking the siRNA target sequence. In this thesis, primer-set problems were minimized by using three siRNAs targeting different regions of the target mRNA (Figure 51). This both reduced the probability that not all three siRNAs can result in silencing, and the risk that the primer set did not detect silencing.

Ultimately, RT-qPCR will only give information about transcription levels/mRNA, and not translation levels/protein. siRNA has the potential to interfere with translation in the same matter as a miRNA, mentioned in "1.5.2 The mechanism of RNAi" (86). If a gene is silenced by siRNA, protein-levels should be assessed to further indicate if silencing has been achieved. Protein detection was not possible in this study since antibodies for salmon TLR3, RIG-I, RLR3 and MAVS was lacking, so we had to settle for a combination of mRNA analyses and functional analyses.

5.2 Discussion of results

From the results we can conclude that siRNA transfection was optimized, and that mRNA-GFP was successfully synthesized by in vitro transcription and optimized for transfection. The test of the RNAi system activity by co-transfecting anti-GFP siRNA with mRNA-GFP was not successful for neither A. salmon RBCs nor CHSE-214 cells. Silencing of endogenous genes TLR3, RIG-I, RLR3 and MAVS was attempted with specifically designed siRNAs, and analysed

for target mRNA expression and function in the dsRNA signaling pathway, but no silencing could be shown.

5.2.1. High amount of fluorescent cells, and viable cells from siRNA transfection

As summarized in “4.2.1 siRNA transfection”, siRNA transfection was successfully optimized. siRNA could be detected earlier than Day 7 after transfection, but was possibly degraded by Day 7.

The optimized siRNA program is 1700V, 20ms and 2 pulses, and from Figure 28, 84% of RBC were transfected when analysed Day 1, and 78% at Day 3, which is considered a good transfection efficiency. Cell viability was generally above 80% (Appendix Figure B7 and B11 at Day 1 and Day 3), indicate that the RBC viability from electroporation is great from the optimized program. Three additional replicates of siRNA-AF488 transfection in experiments “4.3 mRNA-GFP silencing control” indicated >90% siRNA transfected cells, along with a high cell viability (Appendix Figure D2 – Figure D4 and Figure D6). In total, six A. salmon individuals were transfected with siRNA-AF488, using the transfection program 1700V, 20ms and 2 pulses, all showing good transfection efficiency and good cell viability.

5.2.2 Successfully synthesizing in vitro transcribed mRNA-GFP and great mRNA transfection efficiency for co-transfection

As concluded from spectrophotometric measurements (Table 6), the mRNA-GFP transcript was successfully produced, and considered pure and of correct length (73). A functional mRNA-GFP is shown in “4.2.2.2 Establishing mRNA-GFP transfection”, presenting fluorescent cells containing GFP translated from the mRNA.

The optimized siRNA transfection program (1700V, 20ms and 2 pulses) was also suitable for mRNA. GFP expression in mRNA transfected cells increased three days post-transfection with mRNA-GFP (Figure 38), in contrast to siRNA which has the highest detection level early

after transfection. Similar observation has been observed in human T lymphocytes over a shorter period of time (86). In human T lymphocytes, enhanced GFP mRNA transfected with microfluidic vortex shedding (μVS), an increase in mRNA transfected cells was found in measurements between Day 0 to a peak at 19 hours post-transfection, after 19 hours, mRNA transfected cells decreased.

In the first transfection with the optimized siRNA transfected program, a great transfection efficiency was not achieved (Figure 40). The reason for this variation is unknown, but the RBCs had been cultured 8 days before transfection, which is the longest cultured RBC used for transfection in this thesis, and this could potentially be a factor leading to lower efficiency. The transfection efficiency was also shown to differ between A. salmon individuals. A great mRNA transfection efficiency is clearly observed in "4.3 mRNA-GFP silencing control", where the mean fluorescent cell number transfected with mRNA-GFP from two replicates were 57.2% at Day 1 and 58.1% at Day 3 (Figure 43).

5.2.3 Is silencing by siRNA possible in A. salmon RBCs?

From mRNA-GFP silencing experiments, no silencing was achieved in A. salmon RBCs ("4.3 mRNA-GFP silencing control) or in CHSE-214 cells ("4.4.2 CHSE silencing experiment"), indicating a non-functioning RNAi machinery in fish. siRNAs were still designed and ordered ("4.6.2 siRNA sequences"), and the attempt to silence endogenous genes was still conducted and not achieved, seen in "4.6 siRNA silencing of TLR3, RIG-I, RLR3 and MAVS". This puts the question if the siRNA system is present in A. salmon RBCs, and if so, is it functional in A. salmon RBCs or fish in general?

Two of the most important proteins for RNAi are Dicer and Argonaut proteins, discussed in "1.5.2 The mechanism of RNAi". Dicer and AGO2 has been shown to be conserved between species, and vertebrates has been proven to encode those genes, but their specific roles in vertebrates has not been elucidated (88, 89).

RNAi components recognized as important mediators of RNAi in other cells and organisms, are tarbp2, snd1, lyric, mtdha and taff11, shown to be transcribed in A. salmon RBCs (Table 3). Fruit fly (*Drosophila melanogaster*) is one of the species where the RNAi mechanism has been mainly studied. In fruit fly, R2D2 is responsible for stabilizing dicer, and sensing and binding of ds-siRNA (90). The orthologue for R2D2 in human is tarbp2, which is also found in A. salmon. Tarbp2 is important in stabilizing Dicer in humans, which could potentially be its role in A. salmon (91). SND1 has been found to be important for RNAi, functioning as a nuclease in RISC in human cells, and disturbance of SND1 presented disruption of siRNA silencing (92, 93). AEG-1 has been found to be interacting with SND1, showing increasing RISC-activity when both are expressed in human cells (93). mtdha is an orthologue of Metadherin (MTDH), which AEG-1 is also termed as (93). taff11, on the other hand, is involved in RNAi efficiency, facilitating dicer R2D2/tarbp2 tetramization (94). The A. salmon RBCs are then shown to transcribe most essential genes for a functional RNAi system, but still, no silencing has been detected. These genes are also shown to be expressed in A. salmon kidney cell lines SHK-1 and ASK (Appendix Table J1), but if they are involved in RNAi in these cells is not known. However, miRNAs has been identified in A. salmon, involved in different processes such as metabolism, cell division and immunity indicating that RNAi through the miRNA pathway is functional in A. salmon (95).

5.2.4 Stimulation with dsRNA interferes with silencing

A problem arising from silencing genes through siRNA is that siRNA has been shown to induce an interferon response that strongly affect gene expression of many genes (85, 96). Non-specific mRNA regulation was assessed by measuring the RNA-levels of TLR3, RIG-I, RLR3 and MAVS when silencing one gene (e.g. TLR3), since silencing should only diminish target RNA levels, and not the other genes. In this thesis, when trying to silence dsRNA receptors and MAVS, unspecific regulation of the dsRNA receptor genes was rather observed than non-specific silencing (36, 54). Stimulation of the target genes and other antiviral genes involved in dsRNA-sensing could potentially "mask" silencing (97). Silencing of specific dsRNA receptor and antiviral genes is then difficult to monitor.

The dsRNA receptor genes whose RNA levels are increased from most to least at Day 3 and Day 6 are RLR3, RIG-I and TLR3, shown in Figure 59 and Figure 60. The regulation is similar to poly(I:C)-stimulated regulation of the dsRNA receptor (Table 4), presenting that poly(I:C)-stimulation is similar to dsRNA. This is confirmed in Figure 64 and Figure 65 as no significant difference was found between RBCs transfected with siRNA but not-stimulated, and RBCs transfected with siRNA but stimulated with poly(I:C).

Stimulation of RLR3 could potentially impact silencing, as it has been described to interfere with Dicer processing in mammalian cells (98, 99). RLR3 has been shown to interfere with TARBP2 in mammalian cells, influencing RNA silencing, together with RIG-I (100, 101). Lack of functional RNAi machinery has been hypothesized to be attributed by LGP2 to interference with RNAi (102). To draw any speculations if this is also applies for A. salmon RBCs, a study of the RNAi components interaction with RIG-I and RLR3 needs to be executed.

From transfections aiming to silence MAVS RNA, the RNA levels seems to diminish under basal expression at Day 3 and Day 6. These results might indicate that MAVS is downregulated independently of siRNA, but it could be the outcome of detecting a low-expressed gene, which is known to not be up-regulated by poly(I:C) (Table 4). In a study executed by Xing *et al*. (103), degradation of MAVS is observed when introducing dsRNA or poly(I:C) to A549 human lung cancer cells. This could possibly be applied to A. salmon RBCs. The regulation of RNA MAVS from transfected control are also lower than basal expression, which could indicate that any disturbance to RBCs could result in down-regulation of MAVS. A sudden upregulation is however observed at Day 1 (Figure 56), but this could also be the results of stress after electroporation (71, 104).

An interesting, but not a novel finding, was that L-siMAVS stimulated a higher antiviral response than 21-bp siRNAs by inhabiting six extra nucleotides. This corresponds to the literature, whereas 21-bp siRNA supposedly doesn't give a high antiviral response (47). L-siMAVS stimulated even higher antiviral response than RBCs stimulated with poly(I:C) shown in "4.8 siRNA silencing of TLR3, RIG-I, RLR3 and MAVS – test of effects on poly(I:C)

stimulation", signifying that poly(I:C) cannot give a fully similar antiviral response as dsRNA because of molecular dissimilarities (105). The length dependency of dsRNA in fish cells has not been studied a lot, but longer dsRNA are supposedly known to increase antiviral response in Rainbow trout RTG-2 cells (97, 105).

In Human Embryonic Kidney 293-A (HEK-293A) cell line, a proteomics study presented that electroporation treatment induces up-regulation of proteins involved in different biological processes, like the innate immune system (106). In this thesis, electroporation treatment on A. salmon RBCs has been shown to give an upregulation of the dsRNA receptor TLR3, RIG-I and RLR3 in this thesis. The upregulation is more apparent for RLR3. Even if upregulation of dsRNA receptors are observed from electroporation, no apparent upregulation of the antiviral genes Mx or ISG15 is observed, indicating that a ligand must be present to give an antiviral response (54).

5.2.5 Is the RNAi system functional in fish cells?

Compared to mammals, RNAi has not been studied as closely in fish. The RNAi system function has not been shown in neither A. salmon RBCs nor CHSE-214 in this thesis. This could indicate that the RNAi system is not functional in all fish cells. In zebrafish cells (107), rainbow trout cells (74, 96, 108), and A. salmon cells (109) silencing has been achieved. Gruber *et al*. (107) successfully silenced three genes in the zebra fish cell lines ZFL, SJD and ZF4 by microinjection. On the other hand, *in vivo* silencing of the same genes in zebrafish embryos resulted in non-specific silencing.

Au. S (96), tried to silence two exogenous genes and two endogenous genes in Rainbow trout gonadal fibroblast-like cell line (RTG-2) using long dsRNA (600 bp – 750 bp). For avoidance of interferon stimulation, a "soaking" method was used for transfecting the cells, utilizing class-A scavenger receptors (SR-As) expressed on the cell surface of RTG-2, involved in delivering dsRNA in endosomes and in sensing viral dsRNA. Only the exogenous inducible luciferase gene was silenced, and not the exogenous GFP-gene or the endogenous IFN1 and endogenous myelocytomatosis, by sequence-specific regulation. SR-As has not been

identified in A. salmon, making the soaking method not achievable in A. salmon RBCs. Use of "long" dsRNA (27 bp), has been used in this thesis, but shown to strongly stimulate antiviral genes.

In leukocytes isolated from A. salmon spleen, silencing of Eomersodermin was detected by RT-qPCR, and further confirmed using immunostaining (109). The siRNA was 3'-modified with Alexafluor 647 for immunofluorescence analysis, and transfected using electroporation with a Human T cell Nucleofector Kit. Nucleofector combines cell-type specific reagents and electroporation for increasing cell viability, but from this thesis, cell viability was not considered an issue.

A silencing experiment by Collet *et al*. (108) tried to silence luciferase activity from a plasmid in six different fish cell lines using short hairpin RNA (shRNA). shRNA is transcribed by an exogenous vector introduced to the cytoplasm of cells by transfection, which is further transported to the nucleus. The RNA polymerase II transcribes at the RNA polymerase II promotor on the vector, and transcribes pri-shRNA. Pri-shRNA enters the same pathway as the miRNA pathway described in "1.5.2 The mechanism of RNAi", but creates a mature shRNA which is sequence specific, compared to miRNA. The mature shRNA associates with RISC and can silence the mRNA in the same way as siRNA (107). The experiment by Collet B. *et al*. (106) tested different doses of short hairpin RNA (shRNA) and different incubation temperature for the cells to establish factors for silencing efficiency. The transfection was tested by co-transfecting a luciferase encoding plasmid with the shRNA-vector using electroporation. From this experiment, only the Epithelioma papulosum cyprini (EPC) cell line showed consistent silencing. An FHM cell line, originating from the same species, showed no silencing, but rather activation in some samples, showing that RNAi effects might be more cell specific than species specific. Cell lines from the Salmonidae family was also used in the experiment. The cells included were CHSE, RTG-2 and TO-cells. RTG-2 showed silencing when transfected with 4 µg shRNA at 26°C, but also a significant induction of the target when transfected with 2 µg shRNA at 15°C. CHSE showed no significant reduction in luciferase, in line with results from the "4.4.2 CHSE silencing experiment" in this thesis. TO-

cells, deriving from A. salmon Head Kidney, showed significant reduction only with 4 µg shRNA when incubated at 15°C. Results from TO-cells show that some RNAi using shRNA is possible in A. salmon cells. The use of shRNA transfection was considered for this thesis, but since regular siRNA transfection in A. salmon had not been explored, and it was demonstrated functional in Rainbow trout RBCs (74), siRNA was chosen here.

As mentioned, silencing of RNA in Rainbow trout RBCs has been achieved by electroporation by Chico *et al*. (74), part of the research group who are partners in the RED FLAG project. In the rainbow trout RBC experiment, silencing was evaluated by RT-qPCR (as in this thesis), western blot (not done here since antibodies were lacking) and semi-quantitative PCR and gel electrophoresis (not done). The latter method could have been used in this thesis, but since our qPCR revealed stimulation of the target genes, it was not considered necessary. Interaction with Chico V. resulted in the tip to follow her procedure, and if possible, elevate siRNA concentration (Chico Gras personal communication). Apart from this, there are not many differences in the set-up performed by Chico V. *et al*., compared to the set-up in this thesis, except for a higher RNA:RBC-ratio, since transfection by Chico was done with 10-fold fewer cells ($5 * 10^5$ cells), and only slightly less siRNA (≈2.4 µg). In this thesis one could have tried to transfect less cells, which is also recommended by manufacturer (81), but since good transfection efficiency was obtained with $5 * 10^6$ RBCs, diminishing the amount of cells was not thought to be necessary. Assessing RNA-levels by qPCR could be difficult with a lower number of cells since achieving enough RNA for qPCR was already a problem in this thesis, resolved by transfecting a total of $15*10^6$ RBCs per sample instead of $10*10^6$ RBCs.

In summary, RNAi silencing has been found to function in EPC, A. salmon leukocytes, Rainbow trout RBCs, and in some extent RTG-2 cells. Different methods have been used, and some methods like transfection with shRNA, could have been adapted to this thesis to achieve silencing. It has been shown that two cell lines from the same organism can show different silencing efficiency utilizing the RNAi system (108). Further research, must be done to indicate a functional RNAi in the A. salmon RBC.

5.2.6 The difficulty of silencing through siRNA pathway system

Silencing by the RNAi system is considered hard, as there are many factors for successful siRNA silencing. Some challenges are discussed in "1.5.3 Challenges with siRNA" and includes off-targets, degradation of siRNA by RNase and interferon responses. All siRNAs designed for this thesis were tested by screening for potential off-targets in the A salmon genome (Appendix Table F1 – F3). Putative off targets found were tested for expression in RBC using RNA-Seq data obtained in RED FLAG. An experiment was conducted to study when degradation of siRNA occurred ("4.2.1 Increasing siRNA transfection efficiency in A. salmon RBCs – Experiment 1"). Design criteria from Thermofisher were followed, for reasons described in "4.6.2 siRNA sequences". The interferon response problem was thought to be limited because 21-nt siRNA have been shown to have a minimal interferon response due to their size (47). DsiRNA (27-nt) was also used and has been shown to be more potent and longer-lasting than regular siRNA (76). According to literature, 27-nt siRNA can induces higher antiviral responses (47). To further limit the interferon response, we could have added the ribose 2'-position modification to the siRNA (111).

Another challenge for siRNA can be the mRNA secondary structure, which is proven to impact silencing efficiency (112, 113). The mRNA structure could have been further studied assessing the mRNA-structure in Mfold or RNAfold to identify optimal siRNAs binding regions. By designing three siRNA for each gene, this problem was minimized.

In results from «4.2.1 Establishing siRNA transfection in A. salmon RBCs», the microscope image indicates that siRNA-AF488 is transfected into the nucleus. siRNA has its main function in the cytoplasm, but in human cells, silencing by siRNA has been achieved in both cytoplasm and nucleus (114, 115). In *C. elegans*, an Argonaut NRDE-3 protein is involved in relocating siRNA from cytoplasm to nucleus for functional nucleus RNAi (116). This could potentially be the fate of siRNA in A. salmon RBCs.

5.2.7 The potential role of RNAi system in RBCs

In this thesis, RNAi has been mostly discussed as a tool for gene studies with siRNA, but RNAi is responsible for endogenous regulatory mechanism for example with miRNA and piRNA. The pathway of siRNA, miRNA and piRNA differs in protein involved, and the proteins transcribed for the siRNA pathway is initially thought to be transcribed as an antiviral defense mechanism, now utilized as a gene tool (88). When viral RNA is exposed in the cells, dicer cuts viral RNA to siRNA. The siRNA is further loaded onto Argonaut 2, creating RISC, resulting in slicing of viral RNA with the complimentary sequence. This antiviral mechanism is found in invertebrates (117), but is not as thoroughly described in vertebrates. Since RNAi is an antiviral mechanism in some organisms (118), viruses have evolved and adapted a defense mechanism by expressing viral suppressors of RNAi (VSR) (88). In insects and plants, VSR can function by inhibiting dicer or Argonaut, increasing viral replication. In fish, the RNAi system against viruses has not been studied, but proteins from fish viruses involved in suppressing RNAi has been observed for red spotted grouper nervous necrosis virus (119) and ISAV that infect A. salmon (120), strengthening the presence of the RNAi pathway as an antiviral defense mechanism (88). Dicer has also been found to be upregulated in rare minnow when infected by grass carp reovirus (121).

5.2.8 TLR3 possibly interacts with poly(I:C)

The dsRNA-receptor interacting with poly(I:C) in A. salmon RBCs was not confirmed during this thesis, but it is believed that poly(I:C) interacts with TLR3. Interaction with poly(I:C) probably happen after endocytosis, making the endosomal TLR3 a good candidate (122). Poly(I:C) interaction with TLR3 could activate the type I IFN signaling pathway, which results in an antiviral response from the RBCs (112). Even if there is a high possibility that TLR3 is activated by poly(I:C) in A. salmon RBCs, it has still not been confirmed.

Comparing Tsoulia *et al*. (36) PRV-1 infection data with poly(I:C)-stimulation data (Table 4), similar stimulation of dsRNA receptor is observed. The receptor activating an antiviral response from PRV-1 is not confirmed, but as explained in “1.4.2.2 RBC innate antiviral responses to PRV”, IFN-responses indicate RIG-I activation from PRV, and not TLR3, even if

similar regulation of the dsRNA receptors is observed. Tsoulia *et al*. transcriptomic findings shows that RLR3 is significantly induces, but it's involvement in antiviral responses in fish is not well understood.

5.3 Future perspectives

5.3.1 What could have been achieved from siRNA silencing in A. salmon RBCs?

Silencing by siRNA has not been successful in A. salmon RBCs in this thesis, which could mean that silencing by the RNAi pathway is not possible in the RBCs. This would in case limit a potential method for gene studies in A. salmon RBCs. The possibility of performing gene studies with siRNA could elucidate the roles of different genes in the A. salmon RBCs, for functional genomics studies, in a cost-effective way. In this thesis, siRNA was used aiming to find out which receptors interacted with and led to the effects of dsRNA, and this could have been adapted to find which dsRNA receptor was important for PRV-1 effects in A. salmon RBCs. By identifying the dsRNA-receptor interacting with the PRV-1 genome, we could gain insight in the responses of RBCs to virus.

5.3.2 What can we gain from these results?

From the results in this thesis, the establishment of a high transfection efficiency of siRNA was achieved in A. salmon RBCs, even if silencing was not accomplished. From successful RNAi experiments, modification to the siRNA has been done to not activate the interferon response, and some have used a plasmid based method instead, synthesizing shRNA. To examine if such methods could be applied to A. salmon RBCs, further research must be done.

mRNA transfection were optimized during this thesis for a control experiment, and good expression of GFP was achieved from the mRNA. mRNA transfection has the potential to be used for different applications such as disease treatment (123), regenerative medicine (124) and vaccination (125). Application of mRNA can be limited due to stability and immunogenicity, but different modifications, such as pseudouridine can limits these issues (126).

6 Conclusions

- siRNA transfection in A. salmon RBCs were optimized to >80% siRNA transfected RBCs.
- mRNA-GFP was successfully synthesized, transfected and translated in A. salmon RBC, with >50% mRNA transfected RBCs.
- Silencing of transfected mRNA-GFP was not accomplished in A. salmon RBCs or CHSE-214 cells.
- Silencing of dsRNA-receptors and MAVS was not accomplished.
- Transfection of siRNAs leads to an antiviral response in A. salmon RBCs, and unspecific regulation of TLR3, RIG-I, RLR3 and MAVS genes.
- Long siRNAs (27 nt) are much stronger inducers of antiviral responses than regular 21 nt siRNAs

7 References

1. Aas Ø, Klemetsen A, Einum S, Skurdal J. Atlantic salmon ecology: John Wiley & Sons; 2010.
2. Stead SM, Laird L. The handbook of salmon farming: Springer Science & Business Media; 2002.
3. Björnsson BT, Einarsdottir IE, Power D. Is salmon smoltification an example of vertebrate metamorphosis? Lessons learnt from work on flatfish larval development. Aquaculture. 2012;362:264-72.
4. Jonsson N, Jonsson B, Hansen L. The relative role of density-dependent and density-independent survival in the life cycle of Atlantic salmon Salmo salar. Journal of Animal Ecology. 1998;67(5):751-62.
5. Halttunen E. Staying alive: the survival and importance of Atlantic salmon post-spawners. 2011.
6. Lærøy Seafood., *How do we produce salmon?* How do we produce salmon? (leroyseafood.com). Accessed November 4, 2023
7. I. Sommerset *et al*., *Fiskehelserapporten 2023. nr 8a/2024*. The Norwegian Veterinary Institute, 2024. Fiskehelserapporten 2023 (vetinst.no). Accessed April 20, 2024
8. Roberts RJ. Fish pathology: John Wiley & Sons; 2012.
9. Esmaeili N. Blood performance: a new formula for fish growth and health. Biology. 2021;10(12):1236.
10. Kryvi, H., Poppe, T. Fiskeanatomi: Vigmostad & Bjørke AS; 2021
11. Fánge R. 1 Fish Blood Cells. Fish physiology. 12: Elsevier; 1992. p. 1-54.
12. Rozas-Serri M, Correa R, Walker-Vergara R, Coñuecar D, Barrientos S, Leiva C, et al. Reference intervals for blood biomarkers in farmed atlantic salmon, coho salmon and rainbow trout in Chile: promoting a preventive approach in aquamedicine. Biology. 2022;11(7):1066.
13. Cogswell A, Benfey T, Sutterlin A. The hematology of diploid and triploid transgenic Atlantic salmon (Salmo salar). Fish Physiology and Biochemistry. 2001;24:271-7.
14. Uzoigwe C. The human erythrocyte has developed the biconcave disc shape to optimise the flow properties of the blood in the large vessels. Medical hypotheses. 2006;67(5):1159-63.

15. Nombela I, Ortega-Villaizan MDM. Nucleated red blood cells: Immune cell mediators of the antiviral response. PLoS pathogens. 2018;14(4):e1006910.

16. Ginhoux F, Jung S. Monocytes and macrophages: developmental pathways and tissue homeostasis. Nature Reviews Immunology. 2014;14(6):392-404.

17. Stout RD, Suttles J. Functional plasticity of macrophages: reversible adaptation to changing microenvironments. Journal of leukocyte biology. 2004;76(3):509-13.

18. Gomez D, Sunyer JO, Salinas I. The mucosal immune system of fish: the evolution of tolerating commensals while fighting pathogens. Fish & shellfish immunology. 2013;35(6):1729-39.

19. Kindt, T.J., Goldsby, R.A., Osborne B.A. 2007. IMMUNOLOGY: W.H. Freeman and Company; 2007

20. Abbas AK, Lichtman AH, Pillai S. Basic immunology: functions and disorders of the immune system: Elsevier Health Sciences; 2014.

21. Dahle MK, Jørgensen JB. Antiviral defense in salmonids–Mission made possible? Fish & Shellfish Immunology. 2019;87:421-37.

22. Wessel Ø, Krasnov A, Timmerhaus G, Rimstad E, Dahle MK. Antiviral responses and biological concequences of piscine orthoreovirus infection in salmonid erythrocytes. Frontiers in Immunology. 2019;9:3182.

23. Lund M, Krudtaa Dahle M, Timmerhaus G, Alarcon M, Powell M, Aspehaug V, et al. Hypoxia tolerance and responses to hypoxic stress during heart and skeletal muscle inflammation in Atlantic salmon (Salmo salar). PloS one. 2017;12(7):e0181109.

24. Haatveit HM, Hodneland K, Braaen S, Hansen EF, Nyman IB, Dahle MK, Frost P, Rimstad E. DNA vaccine expressing the non-structural proteins of Piscine orthoreovirus delay the kinetics of PRV infection and induces moderate protection against heart-and skeletal muscle inflammation in Atlantic salmon (Salmo salar). Vaccine. 2018 Nov 29;36(50):7599-608.

25. Wessel Ø, Haugland Ø, Rode M, Fredriksen BN, Dahle MK, Rimstad E. Inactivated Piscine orthoreovirus vaccine protects against heart and skeletal muscle inflammation in Atlantic salmon. Journal of fish diseases. 2018 Sep;41(9):1411-9.

26. Olsen AB, Hjortaas M, Tengs T, Hellberg H, Johansen R. First description of a new disease in rainbow trout. Oncorhynchus mykiss.

27. Bohle H, Bustos P, Leiva L, Grothusen H, Navas E, Sandoval A, Bustamante F, Montecinos K, Gaete A, Mancilla M. First complete genome sequence of piscine orthoreovirus variant 3 infecting coho salmon (Oncorhynchus kisutch) farmed in southern Chile. Genome Announcements. 2018 Jun 14;6(24):10-128.

28. Vallejos-Vidal E, Reyes-López FE, Sandino AM, Imarai M. Sleeping With the Enemy? The Current Knowledge of Piscine Orthoreovirus (PRV) Immune Response Elicited to Counteract Infection. Frontiers in Immunology. 2022;13:768621.

29. Haatveit HM, Nyman IB, Markussen T, Wessel Ø, Dahle MK, Rimstad E. The non-structural protein μNS of piscine orthoreovirus (PRV) forms viral factory-like structures. Veterinary research. 2016;47:1-11.

30. Finstad ØW, Dahle MK, Lindholm TH, Nyman IB, Løvoll M, Wallace C, et al. Piscine orthoreovirus (PRV) infects Atlantic salmon erythrocytes. Veterinary research. 2014;45:1-13.

31. Di Cicco E, Ferguson HW, Kaukinen KH, Schulze AD, Li S, Tabata A, et al. The same strain of Piscine orthoreovirus (PRV-1) is involved in the development of different, but related, diseases in Atlantic and Pacific Salmon in British Columbia. Facets. 2018;3(1):599-641.

32. Kniert J, Lin QF, Shmulevitz M. Captivating Perplexities of Spinareovirinae 5′ RNA Caps. Viruses. 2021;13(2):294.

33. Bjørgen H, Wessel Ø, Fjelldal PG, Hansen T, Sveier H, Sæbø HR, et al. Piscine orthoreovirus (PRV) in red and melanised foci in white muscle of Atlantic salmon (Salmo salar). Veterinary Research. 2015;46:1-12.

34. Garseth Å, Fritsvold C, Opheim M, Skjerve E, Biering E. Piscine reovirus (PRV) in wild Atlantic salmon, Salmo salar L., and sea-trout, Salmo trutta L., in Norway. Journal of fish diseases. 2013;36(5):483-93.

35. Morera D, Roher N, Ribas L, Balasch JC, Doñate C, Callol A, et al. RNA-Seq reveals an integrated immune response in nucleated erythrocytes. PloS one. 2011;6(10):e26998.

36. Tsoulia T, Sundaram AY, Braaen S, Jørgensen JB, Rimstad E, Wessel Ø, et al. Transcriptomics of early responses to purified Piscine orthoreovirus-1 in Atlantic salmon (Salmo salar L.) red blood cells compared to non-susceptible cell lines. Frontiers in Immunology. 2024;15:1359552.

37. Robertsen B. The role of type I interferons in innate and adaptive immunity against viruses in Atlantic salmon. Developmental & Comparative Immunology. 2018;80:41-52.

38. Dahle MK, Wessel Ø, Timmerhaus G, Nyman IB, Jørgensen SM, Rimstad E, et al. Transcriptome analyses of Atlantic salmon (Salmo salar L.) erythrocytes infected with piscine orthoreovirus (PRV). Fish & shellfish immunology. 2015;45(2):780-90.

39. Sadler AJ, Williams BR. Interferon-inducible antiviral effectors. Nature reviews immunology. 2008 Jul;8(7):559-68.

40. Sen GL, Blau HM. A brief history of RNAi: the silence of the genes. The FASEB journal. 2006;20(9):1293-9.

41. Napoli C, Lemieux C, Jorgensen R. Introduction of a chimeric chalcone synthase gene into petunia results in reversible co-suppression of homologous genes in trans. The plant cell. 1990 Apr 1;2(4):279-89.

42. Romano N, Macino G. Quelling: transient inactivation of gene expression in Neurospora crassa by transformation with homologous sequences. Molecular microbiology. 1992 Nov;6(22):3343-53.

43. Guo S, Kemphues KJ. par-1, a gene required for establishing polarity in C. elegans embryos, encodes a putative Ser/Thr kinase that is asymmetrically distributed. Cell. 1995 May 19;81(4):611-20.

44. Fire A, Xu S, Montgomery MK, Kostas SA, Driver SE, Mello CC. Potent and specific genetic interference by double-stranded RNA in Caenorhabditis elegans. nature. 1998 Feb 19;391(6669):806-11.

45. Hammond SM, Bernstein E, Beach D, Hannon GJ. An RNA-directed nuclease mediates post-transcriptional gene silencing in Drosophila cells. Nature. 2000 Mar 16;404(6775):293-6.

46. Zamore PD, Tuschl T, Sharp PA, Bartel DP. RNAi: double-stranded RNA directs the ATP-dependent cleavage of mRNA at 21 to 23 nucleotide intervals. cell. 2000 Mar 31;101(1):25-33.

47. Elbashir SM, Lendeckel W, Tuschl T. RNA interference is mediated by 21-and 22-nucleotide RNAs. Genes & development. 2001;15(2):188-200.

48. Bernstein E, Caudy AA, Hammond SM, Hannon GJ. Role for a bidentate ribonuclease in the initiation step of RNA interference. Nature. 2001 Jan 18;409(6818):363-6.

49. Bantounas I, Phylactou L, Uney J. RNA interference and the use of small interfering RNA to study gene function in mammalian systems. Journal of molecular endocrinology. 2004;33(3):545-57.

50. Kutter C, Svoboda P. miRNA, siRNA, piRNA: Knowns of the unknown. Taylor & Francis; 2008.

51. Lam JK, Chow MY, Zhang Y, Leung SW. siRNA versus miRNA as therapeutics for gene silencing. Molecular Therapy-Nucleic Acids. 2015;4.

52. Chong ZX, Yeap SK, Ho WY. Transfection types, methods and strategies: A technical review. PeerJ. 2021;9:e11165.

53. Gavrilov K, Saltzman WM. Therapeutic siRNA: principles, challenges, and strategies. The Yale journal of biology and medicine. 2012;85(2):187.

54. Whitehead KA, Dahlman JE, Langer RS, Anderson DG. Silencing or stimulation? siRNA delivery and the immune system. Annual review of chemical and biomolecular engineering. 2011;2:77-96.

55. Fraser T, Mayer I, Skjæraasen J, Hansen T, Fjelldal P. The effect of triploidy on the efficacy and physiological response to anesthesia with MS 222 and isoeugenol in Atlantic salmon post-smolts. Aquaculture international. 2014;22:1347-59.

56. Smith S. Fish diagnostics for the private practitioner. 2015.

57. Biran R, Pond D. Heparin coatings for improving blood compatibility of medical devices. Advanced drug delivery reviews. 2017;112:12-23.

58. Pertoft H. Fractionation of cells and subcellular particles with Percoll. Journal of biochemical and biophysical methods. 2000;44(1-2):1-30.

59. Nielsen H. Working with RNA. RNA: Methods and Protocols. 2011:15-28.

60. Sano M, Sierant M, Miyagishi M, Nakanishi M, Takagi Y, Sutou S. Effect of asymmetric terminal structures of short RNA duplexes on the RNA interference activity and strand selection. Nucleic acids research. 2008;36(18):5812-21.

61. McKinnon KM. Flow cytometry: an overview. Current protocols in immunology. 2018;120(1):5.1. -5.1. 11.

62. Monjo A, Poynter S, DeWitte-Orr S. CHSE-214: A model for studying extracellular dsRNA sensing in vitro. Fish & shellfish immunology. 2017;68:266-71.

63. Ploss FB. Methods to study fusion activation of infectious salmon anaemia virus: Norwegian University of Life Sciences, Ås; 2022.

64. Sigma Aldrich. LLC, *Fundamental Techniques in Cell culture*, 3rd ed.: Sigma-Aldrich Co.LLC, 2016, p.82. Fundamental Techniques in Cell Culture (sigmaaldrich.com) Accessed January 3, 2024

65. Hindiyeh M, Mor O, Pando R, Mannasse B, Kabat A, Assraf-Zarfati H, et al. Comparison of the new fully automated extraction platform eMAG to the MagNA PURE 96 and the well-established easyMAG for detection of common human respiratory viruses. PLoS One. 2019;14(2):e0211079.

66. Fiebelkorn KR, Lee BG, Hill CE, Caliendo AM, Nolte FS. Clinical evaluation of an automated nucleic acid isolation system. Clinical chemistry. 2002;48(9):1613-5.

67. Roche Diagnostics. *MagNA Pure 96 system*. MagNA Pure 96 Instrument, High-throughput robotic workstation for fully automated purification of nucleic acids from up to 96 samples. (roche.com). Accessed February 20, 2024

68. Pabinger S, Rödiger S, Kriegner A, Vierlinger K, Weinhäusel A. A survey of tools for the analysis of quantitative PCR (qPCR) data. Biomolecular Detection and Quantification. 2014;1(1):23-33.

69. Cao H, Shockey JM. Comparison of TaqMan and SYBR Green qPCR methods for quantitative gene expression in tung tree tissues. Journal of agricultural and food chemistry. 2012;60(50):12296-303.

70. Rao X, Huang X, Zhou Z, Lin X. An improvement of the 2ˆ (–delta delta CT) method for quantitative real-time polymerase chain reaction data analysis. Biostatistics, bioinformatics and biomathematics. 2013;3(3):71.

71. Jakstys B, Jakutaviciute M, Uzdavinyte D, Satkauskiene I, Satkauskas S. Correlation between the loss of intracellular molecules and cell viability after cell electroporation. Bioelectrochemistry. 2020;135:107550.

72. Matlock B. Assessment of nucleic acid purity. Technical Note. 2015;52646:1-2.

73. Agilent. *Agilent TapeStation Software Displays a Different ScreenTape Expiration Date*. Agilent TapeStation Software Displays a Different ScreenTape Expiration Date - Articles - Automated Electrophoresis Portal - Agilent Community. Assessed April 06, 2024

74. Chico V, Salvador-Mira ME, Nombela I, Puente-Marin S, Ciordia S, Mena MC, et al. Ifit5 participates in the antiviral mechanisms of rainbow trout red blood cells. Frontiers in immunology. 2019;10:613.

75. Van der Wal YA, Nordli H, Akandwanaho A, Greiner-Tollersrud L, Kool J, Jørgensen JB. CRISPR-Cas–induced IRF3 and MAVS knockouts in a salmonid cell line disrupt PRR signaling and affect viral replication. Frontiers in Immunology. 2023;14:1214912.

76. Kim D-H, Behlke MA, Rose SD, Chang M-S, Choi S, Rossi JJ. Synthetic dsRNA Dicer substrates enhance RNAi potency and efficacy. Nature biotechnology. 2005;23(2):222-6.

77. Agilent. *RNA 6000 Nano Kit for 2100 Bioanalyzer Systems*. RNA 6000 Nano Kit for 2100 Bioanalyzer Systems Kit Guide (agilent.com). Accessed January 30, 2024

78. Jensen K., Anderson J. A., Glass E. J. Comparison of Small Interfering RNA (siRNA) Delivery into Bovine Monocyte-Derived Macrophages by Transfection and Electroporation. *Vet. Immunol. Immunopathol*. 2014, 158, 224–232.

79. Mascotti K, McCullough J, Burger SR. HPC viability measurement: trypan blue versus acridine orange and propidium iodide. Transfusion. 2000;40(6):693-6.

80. Koç E, Çelik-Uzuner S, Uzuner U, Çakmak R. The detailed comparison of cell death detected by annexin V-PI counterstain using fluorescence microscope, flow cytometry and automated cell counter in mammalian and microalgae cells. Journal of Fluorescence. 2018;28:1393-404.

81. Invitrogen. *Neon™ Transfection System User Guide*. Neon Transfection System User Guide (Pub. No. MAN0001557 C.0) (Thermofisher.com). Accessed April 04, 2024

82. Verschoor CP, Lelic A, Bramson JL, Bowdish DM. An introduction to automated flow cytometry gating tools and their implementation. Frontiers in immunology. 2015;6:154622.

83. Roederer M. Spectral compensation for flow cytometry: visualization artifacts, limitations, and caveats. Cytometry: The Journal of the International Society for Analytical Cytology. 2001;45(3):194-205.

84. Holmes K, Williams CM, Chapman EA, Cross MJ. Detection of siRNA induced mRNA silencing by RT-qPCR: considerations for experimental design. BMC research notes. 2010;3:1-5.

85. Herbert M, Coppieters N, Lasham A, Cao H, Reid G. The importance of RT-qPCR primer design for the detection of siRNA-mediated mRNA silencing. BMC Research Notes. 2011;4:1-7.

86. Doench JG, Petersen CP, Sharp PA. siRNAs can function as miRNAs. Genes & development. 2003;17(4):438-42.

87. Jarrell JA, Twite AA, Lau KH, Kashani MN, Lievano AA, Acevedo J, Priest C, Nieva J, Gottlieb D, Pawell RS. Intracellular delivery of mRNA to human primary T cells with microfluidic vortex shedding. Scientific reports. 2019 Mar 1;9(1):3214.

88. Obbard DJ, Gordon KH, Buck AH, Jiggins FM. The evolution of RNAi as a defence against viruses and transposable elements. Philosophical Transactions of the Royal Society B: Biological Sciences. 2009;364(1513):99-115.

89. Obbard DJ, Gordon KH, Buck AH, Jiggins FM. The evolution of RNAi as a defence against viruses and transposable elements. Philosophical Transactions of the Royal Society B: Biological Sciences. 2009;364(1513):99-115.

90. Tang G. siRNA and miRNA: an insight into RISCs. Trends in biochemical sciences. 2005;30(2):106-14.

91. Chen C, Zhu C, Huang J, Zhao X, Deng R, Zhang H, et al. SUMOylation of TARBP2 regulates miRNA/siRNA efficiency. Nature communications. 2015;6(1):8899.

92. Tsuchiya N, Ochiai M, Nakashima K, Ubagai T, Sugimura T, Nakagama H. SND1, a component of RNA-induced silencing complex, is up-regulated in human colon cancers and implicated in early stage colon carcinogenesis. Cancer research. 2007;67(19):9568-76.

93. Yoo BK, Santhekadur PK, Gredler R, Chen D, Emdad L, Bhutia S, et al. Increased RNA-induced silencing complex (RISC) activity contributes to hepatocellular carcinoma. Hepatology. 2011;53(5):1538-48.

94. Liang C, Wang Y, Murota Y, Liu X, Smith D, Siomi MC, et al. TAF11 assembles the RISC loading complex to enhance RNAi efficiency. Molecular cell. 2015;59(5):807-18.

95. Barozai MYK. Identification and characterization of the microRNAs and their targets in Salmo salar. Gene. 2012;499(1):163-8.

96. Schyth BD. RNAi-mediated gene silencing in fishes? Journal of Fish Biology. 2008;72(8):1890-906.

97. Au S. Investigation of RNA interference (RNAi)-mediated gene silencing in rainbow trout. 2020.

98. Quicke KM, Kim KY, Horvath CM, Suthar MS. RNA helicase LGP2 negatively regulates RIG-I signaling by preventing TRIM25-mediated caspase activation and recruitment domain ubiquitination. Journal of Interferon & Cytokine Research. 2019;39(11):669-83.

99. Van der Veen AG, Maillard PV, Schmidt JM, Lee SA, Deddouche-Grass S, Borg A, et al. The RIG-I-like receptor LGP2 inhibits Dicer-dependent processing of long double-stranded RNA and blocks RNA interference in mammalian cells. The EMBO journal. 2018;37(4):e97479.

100. Takahashi T, Nakano Y, Onomoto K, Yoneyama M, Ui-Tei K. LGP2 virus sensor enhances apoptosis by upregulating apoptosis regulatory genes through TRBP-bound miRNAs during viral infection. Nucleic acids research. 2020;48(3):1494-507.

101. Takahashi T, Nakano Y, Onomoto K, Yoneyama M, Ui-Tei K. Virus sensor RIG-I represses RNA interference by interacting with TRBP through LGP2 in mammalian cells. Genes. 2018;9(10):511.

102. Sanchez David RY, Combredet C, Najburg V, Millot GA, Beauclair G, Schwikowski B, et al. LGP2 binds to PACT to regulate RIG-I–and MDA5-mediated antiviral responses. Science signaling. 2019;12(601):eaar3993.

103. Xing F, Matsumiya T, Onomoto K, Hayakari R, Imaizumi T, Yoshida H, et al. Foreign RNA induces the degradation of mitochondrial antiviral signaling protein (MAVS): the role of intracellular antiviral factors. 2012.

104. Wiseman S, Osachoff H, Bassett E, Malhotra J, Bruno J, VanAggelen G, Mommsen TP, Vijayan MM. Gene expression pattern in the liver during recovery from an acute stressor in rainbow trout. Comparative Biochemistry and Physiology Part D: Genomics and Proteomics. 2007 Sep 1;2(3):234-44.

105. Poynter SJ, DeWitte-Orr SJ. Length-dependent innate antiviral effects of double-stranded RNA in the rainbow trout (Oncorhynchus mykiss) cell line, RTG-2. Fish & Shellfish Immunology. 2015;46(2):557-65.

106. Zhao M, Zhao D, Ma Y, Hu Z, Wei Z. Quantitative proteomic analysis of cell responses to electroporation, a classical gene delivery approach. Proteomics. 2018;18(16):1800127.

107. Gruber J, Manninga H, Tuschl T, Osborn M, Weber K. Specific RNAi mediated gene knockdown in zebrafish cell lines. RNA biology. 2005;2(3):101-5.

108. Collet B, Collins C, Cheyne V, Lester K. Plasmid-driven RNA interference in fish cell lines. In Vitro Cellular & Developmental Biology-Animal. 2022;58(3):189-93.

109. Kumari J, Bøgwald J, Dalmo RA. Eomesodermin of Atlantic salmon: an important regulator of cytolytic gene and interferon gamma expression in spleen lymphocytes. PLoS One. 2013;8(2):e55893.

110. Rao DD, Vorhies JS, Senzer N, Nemunaitis J. siRNA vs. shRNA: similarities and differences. Advanced drug delivery reviews. 2009;61(9):746-59.

111. Alagia A, Eritja R. siRNA and RNAi optimization. Wiley Interdisciplinary Reviews: RNA. 2016;7(3):316-29.

112. Gredell JA, Berger AK, Walton SP. Impact of target mRNA structure on siRNA silencing efficiency: A large-scale study. Biotechnology and bioengineering. 2008;100(4):744-55.

113. Luo KQ, Chang DC. The gene-silencing efficiency of siRNA is strongly dependent on the local structure of mRNA at the targeted region. Biochemical and biophysical research communications. 2004;318(1):303-10.

114. Robb GB, Brown KM, Khurana J, Rana TM. Specific and potent RNAi in the nucleus of human cells. Nature structural & molecular biology. 2005;12(2):133-7.

115. Dudley NR, Goldstein B. RNA interference: silencing in the cytoplasm and nucleus. Curr Opin Mol Ther. 2003;5(2):113-7.

116. Guang S, Bochner AF, Pavelec DM, Burkhart KB, Harding S, Lachowiec J, et al. An Argonaute transports siRNAs from the cytoplasm to the nucleus. Science. 2008;321(5888):537-41.

117. Galiana-Arnoux D, Dostert C, Schneemann A, Hoffmann JA, Imler J-L. Essential function in vivo for Dicer-2 in host defense against RNA viruses in drosophila. Nature immunology. 2006;7(6):590-7.

118. Reshi ML, Wu J-L, Wang H-V, Hong J-R. RNA interference technology used for the study of aquatic virus infections. Fish & shellfish immunology. 2014;40(1):14-23.

119. Wu H-C, Wu J-L, Chu H-L, Su Y-C, Hong J-R. RGNNV induces mitochondria-mediated cell death via newly synthesized protein dependent pathway in fish cells. Fish & shellfish immunology. 2010;29(3):451-63.

120. Vandana Thukral VT, Bhavna Varshney BV, Ramly R, Ponia S, Mishra S, Olsen C, et al. s8ORF2 protein of infectious salmon anaemia virus is a RNA-silencing suppressor and interacts with Salmon salar Mov10 (SsMov10) of the host RNAi machinery. 2018.

121. Su J, Zhu Z, Wang Y, Zou J, Wang N, Jang S. Grass carp reovirus activates RNAi pathway in rare minnow, Gobiocypris rarus. Aquaculture. 2009;289(1-2):1-5.

122. Matsumoto M, Seya T. TLR3: interferon induction by double-stranded RNA including poly (I: C). Advanced drug delivery reviews. 2008;60(7):805-12.

123. Kormann MS, Hasenpusch G, Aneja MK, Nica G, Flemmer AW, Herber-Jonat S, et al. Expression of therapeutic proteins after delivery of chemically modified mRNA in mice. Nature biotechnology. 2011;29(2):154-7.

124. Mandal PK, Rossi DJ. Reprogramming human fibroblasts to pluripotency using modified mRNA. Nature protocols. 2013;8(3):568-82.

125. Petsch B, Schnee M, Vogel AB, Lange E, Hoffmann B, Voss D, et al. Protective efficacy of in vitro synthesized, specific mRNA vaccines against influenza A virus infection. Nature biotechnology. 2012;30(12):1210-6.

126. Kariko K, Weissman D. Naturally occurring nucleoside modifications suppress the immunostimulatory activity of RNA: implication for therapeutic RNA development. Current Opinion in Drug Discovery and Development. 2007;10(5):523.

Appendix

A Calculations

A1. Cell viabilty from PI-staining after Flow Cytometer analysis

$$(1)\ \ 100\% - PI\ stained\ cells\ (\%) = Cell\ Viability$$

Example from calculating Cell viabilty from Figure B1 b):

$$100\% - 0.05\% = 99.5\%\ Cell\ viability$$

A2. Fold Change of gene when normalized against reference gene

$$(1) \qquad \Delta CT = CT\ (target\ gene) - CT\ (reference\ gene)$$

$$(2) \qquad \Delta\Delta CT = \Delta CT\ (a\ target\ sample) - \Delta CT\ (a\ reference\ sample)$$

$$(3) \qquad 2^{-\Delta\Delta CT}$$

Un-electroporated RBCs:

$Ct_{EF1\alpha}$ = 21.59

Ct_{Mx}= 29.14

$$(1) \qquad \Delta CT = 29.14 - 21.59 = 7.55$$

$$(2) \qquad \Delta\Delta CT = 7.55 - 7.55 = 0$$

$$(3) \qquad 2^0 = 0$$

RBCs Transfected with siRNA:

$Ct_{EF1\alpha}$ = 22.59

Ct_{Mx}= 30.10

$$(1) \qquad \Delta CT = 30.10 - 22.59 = 7.51$$

$$(2) \qquad \Delta\Delta CT = 7.51 - 7.55 = -0.05$$

$$(3) \qquad 2^{-0.05} = 1.03\ fold\ change$$

B - siRNA optimization in A.salmon RBCs

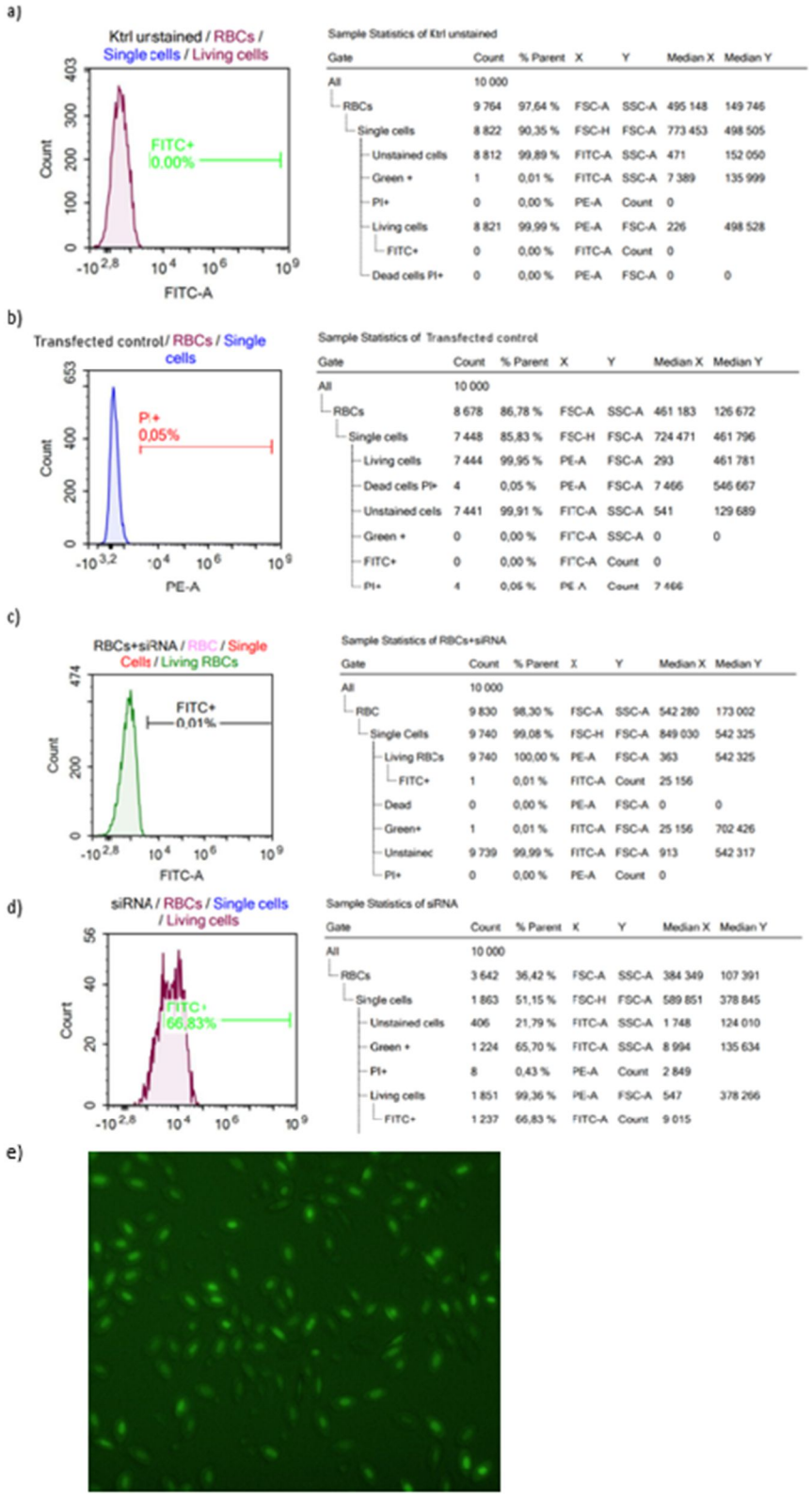

Figure B1. Flow cytometer histogram and corresponding sample statistics from siRNA-AF488 establishment in A. salmon RBCs. a) not-electroporated RBCs. b) Electroporated RBCs. c) Not-transfected RBCs mixed with

siRNA-AF488. d) RBCs transfected with siRNA-AF488. e) Microscope picture of RBCs transfected with siRNA-AF488.

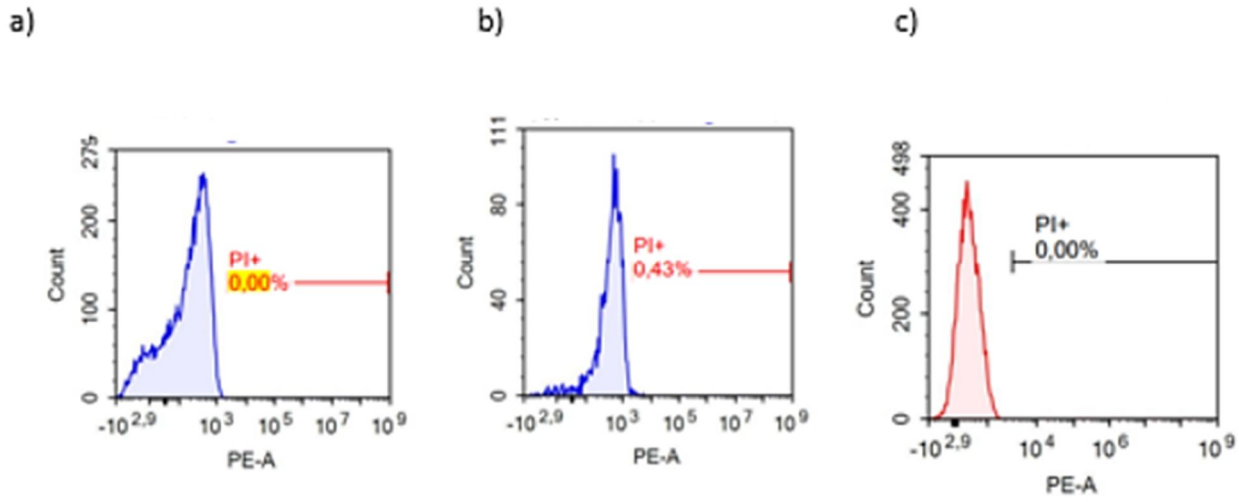

Figure B2. Flow cytometer histogram from "4.2.1 Establishing siRNA transfection in A. salmon RBCs" a) not-electroporated RBCs. b) RBCs transfected with siRNA-AF488. c) Not-electroporated RBCs incubated with siRNA-AF488

a)

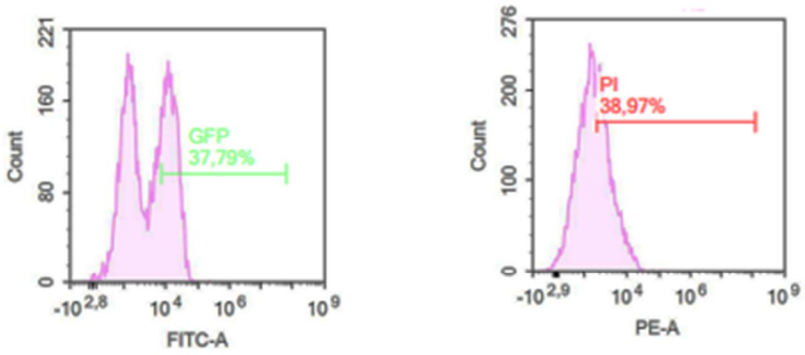

b)

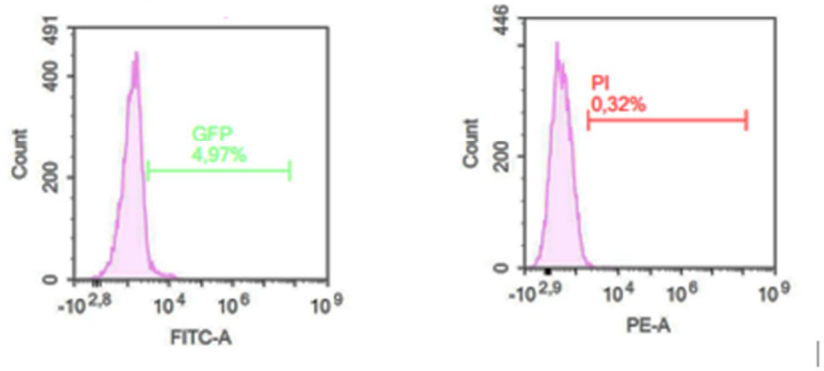

c)

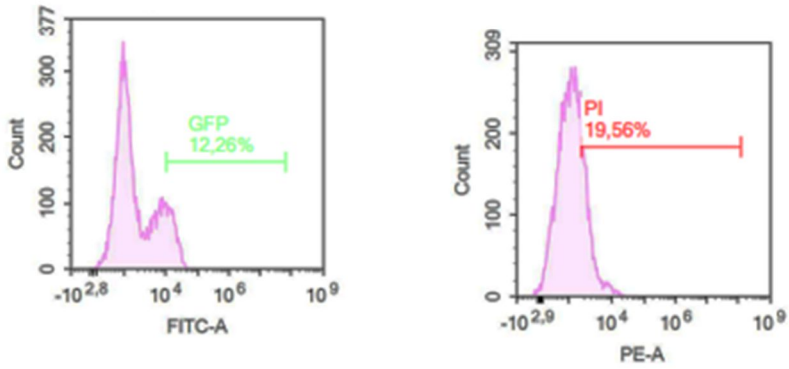

Figure B3. Flow cytometer histogram of siRNA transfected cells (Termed GFP in this Figure) and PI-positive RBCs from "4.2.2 Optimizing siRNA transfection in A. salmon RBCs – Experiment 1" at Day 2 a) P1. b) P2. c) P3.

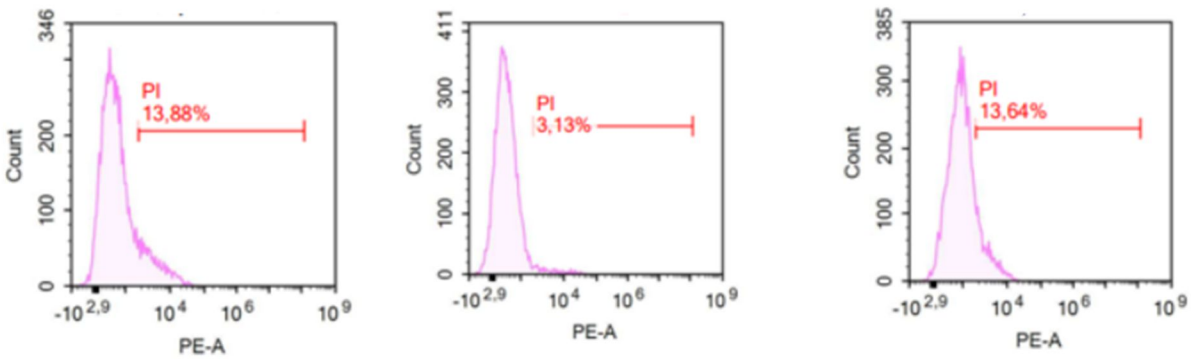

Figure B4. Flow cytometer histogram of PI-positive RBCs in transfected control RBCs from "4.2.2 Optimizing siRNA transfection in A. salmon RBCs – Experiment 1" at Day 2 a) P1. b) P2. c) P3.

Only transfected RBCs stained with PI is shown, and not electroporated RBCs from "Optimizing siRNA transfection efficency in A. salmon RBCs – Experiment 1)", since data is missing.

a)

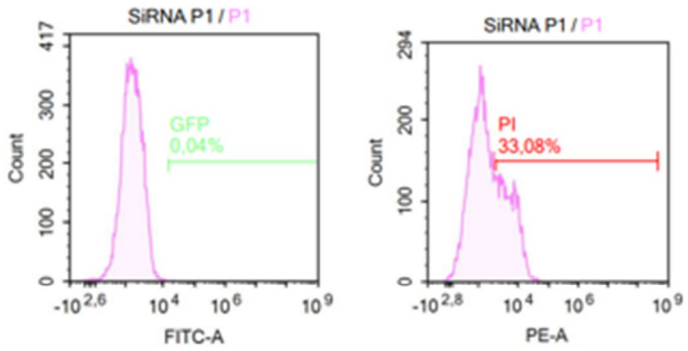

b)

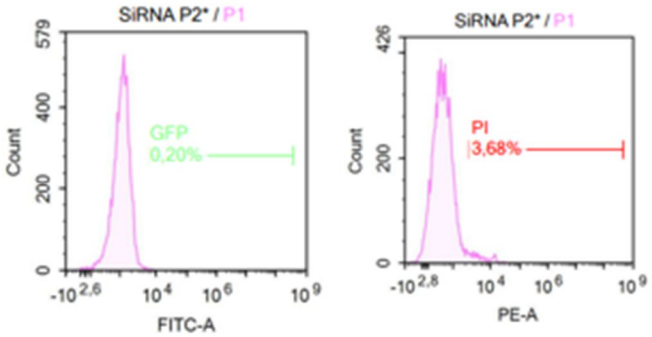

c)

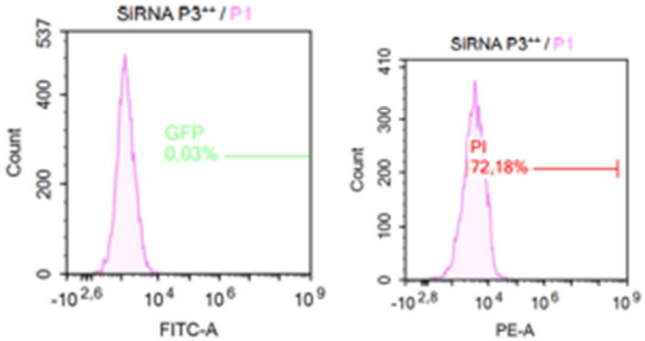

Figure B5. Flow cytometer histogram of siRNA transfected cells (Termed GFP in this Figure) and PI-positive RBCs from "4.2.2 Optimizing siRNA transfection in A. salmon RBCs – Experiment 1" at Day 7 a) P1. b) P2. c) P3.

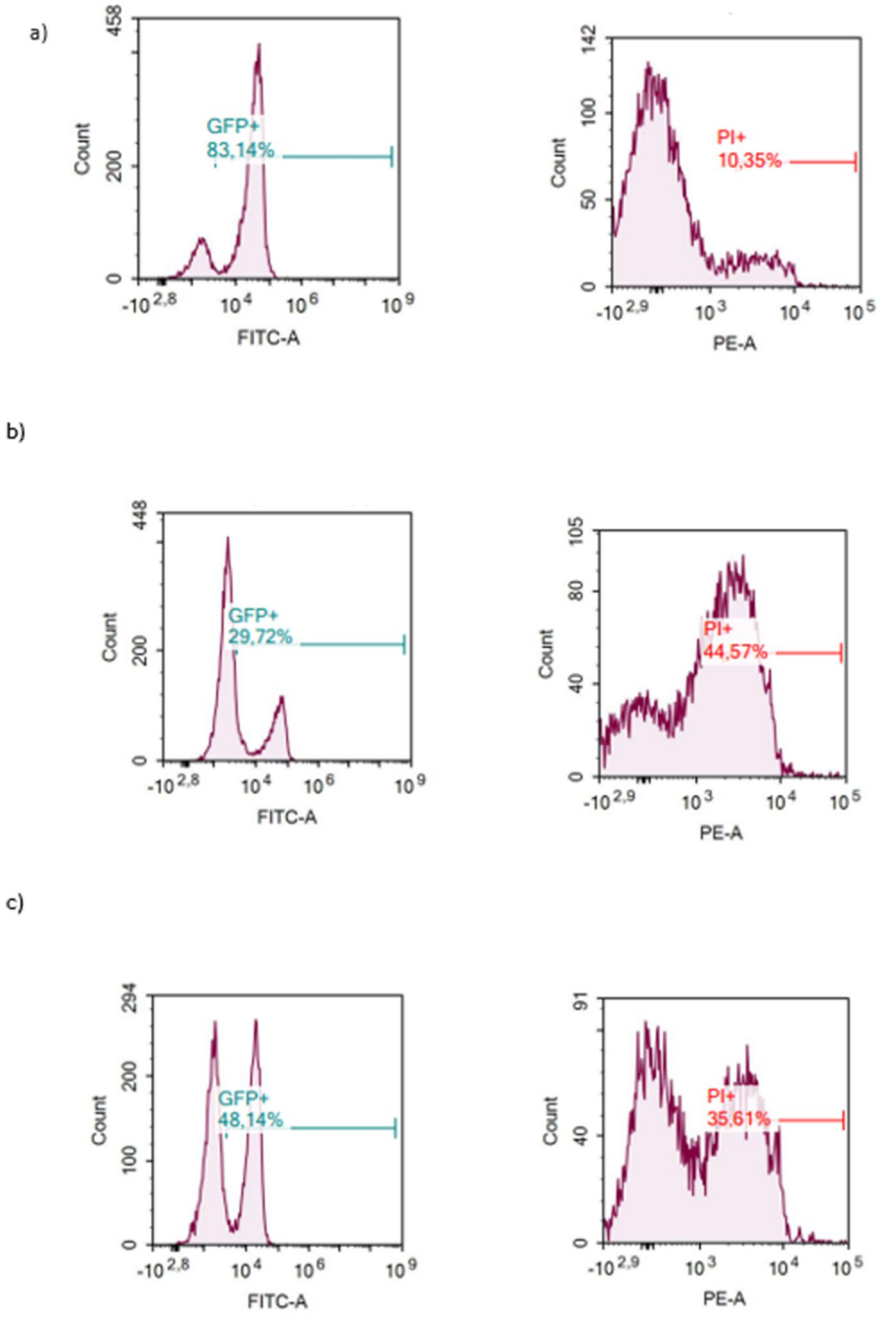

Figure B6. Flow cytometer histogram of siRNA transfected cells (Termed GFP in this Figure) and PI-positive RBCs from "4.2.3 Optimizing siRNA transfection in A. salmon RBCs – Experiment 2" at Day 1 from P1 a) A. salmon individual 1. b) A. salmon individual 2 c) A. salmon individual 3

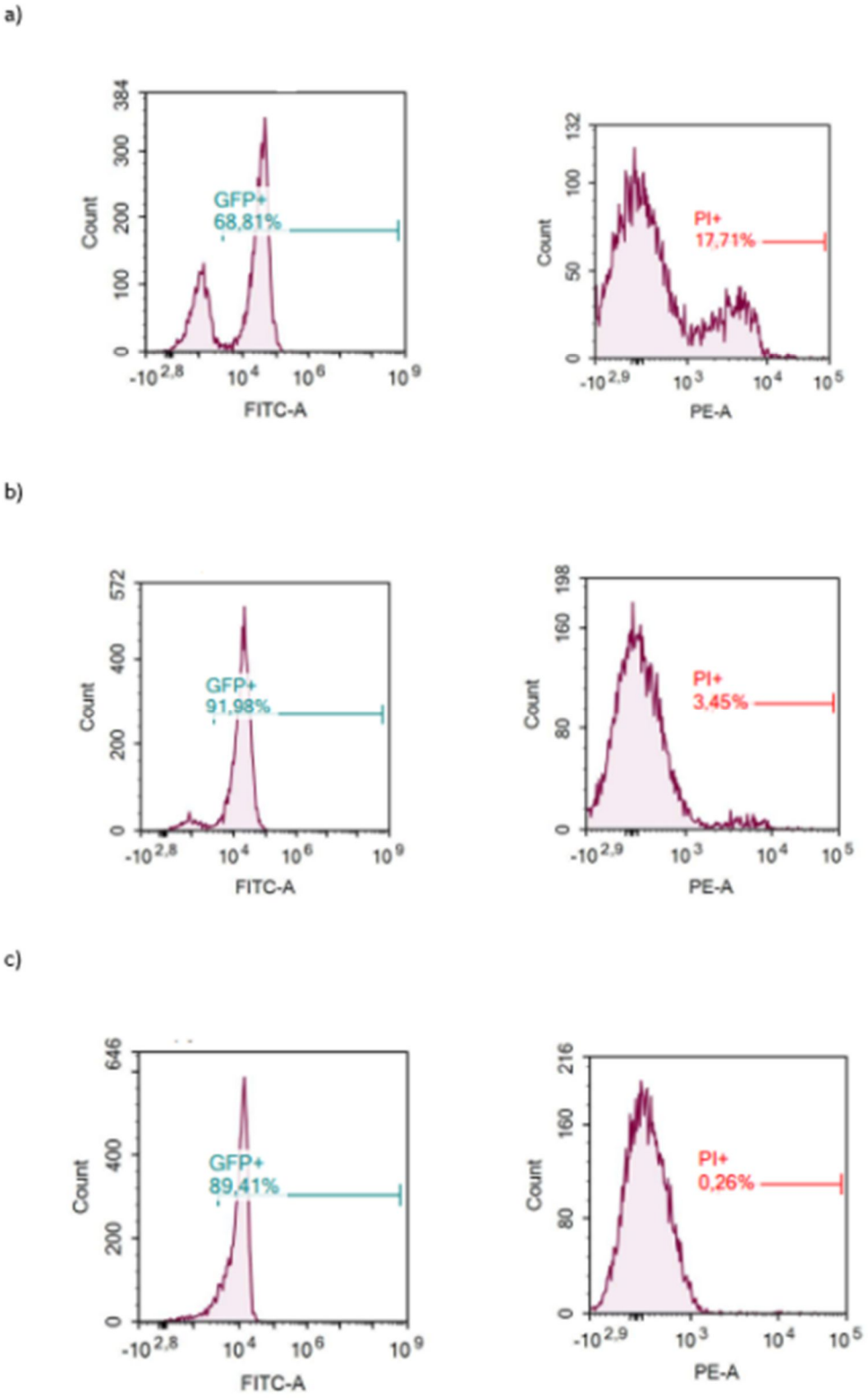

Figure B7. Flow cytometer histogram of siRNA transfected cells (Termed GFP in this Figure) and PI-positive RBCs from "4.2.3 Optimizing siRNA transfection in A. salmon RBCs – Experiment 2" at Day 1 from P2 a) A. salmon individual 1. b) A. salmon individual 2 c) A. salmon individual 3

a)

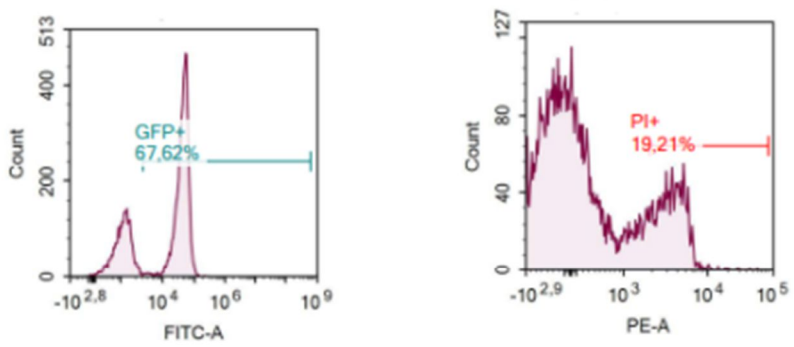

b)

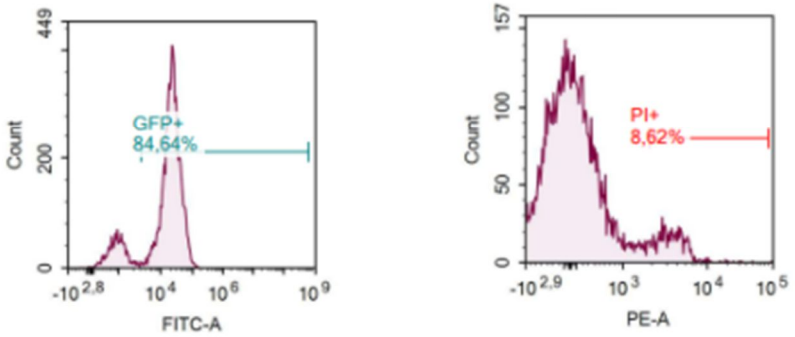

c)

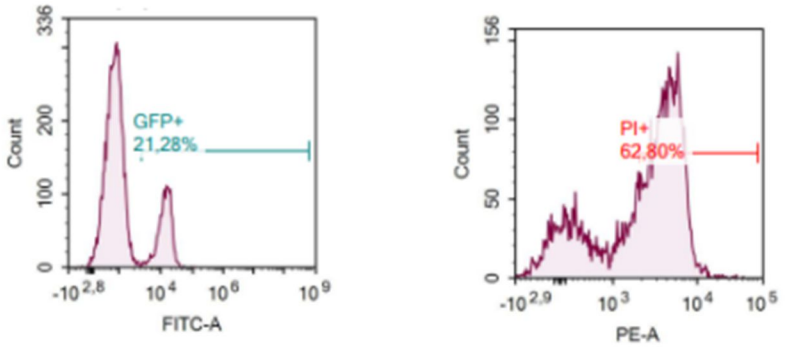

Figure B8. Flow cytometer histogram of siRNA transfected cells (Termed GFP in this Figure) and PI-positive RBCs from "4.2.3 Optimizing siRNA transfection in A. salmon RBCs – Experiment 2" at Day 1 from P3 a) A. salmon individual 1. b) A. salmon individual 2 c) A. salmon individual 3

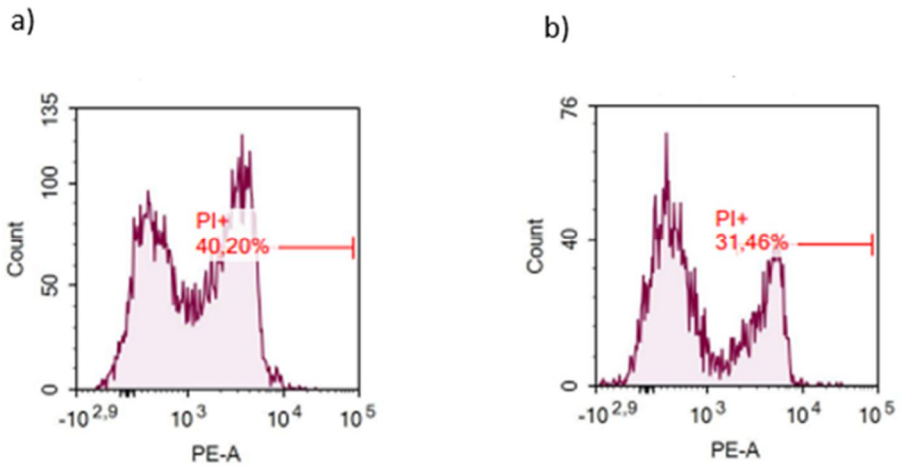

Figure B9. Flow cytometer histogram of PI-positive in transfected control from "4.2.3 Optimizing siRNA transfection in A. salmon RBCs – Experiment 2" A. salmon 1 at Day 1 a) P1 b) P2. P3 is not included since values are missing

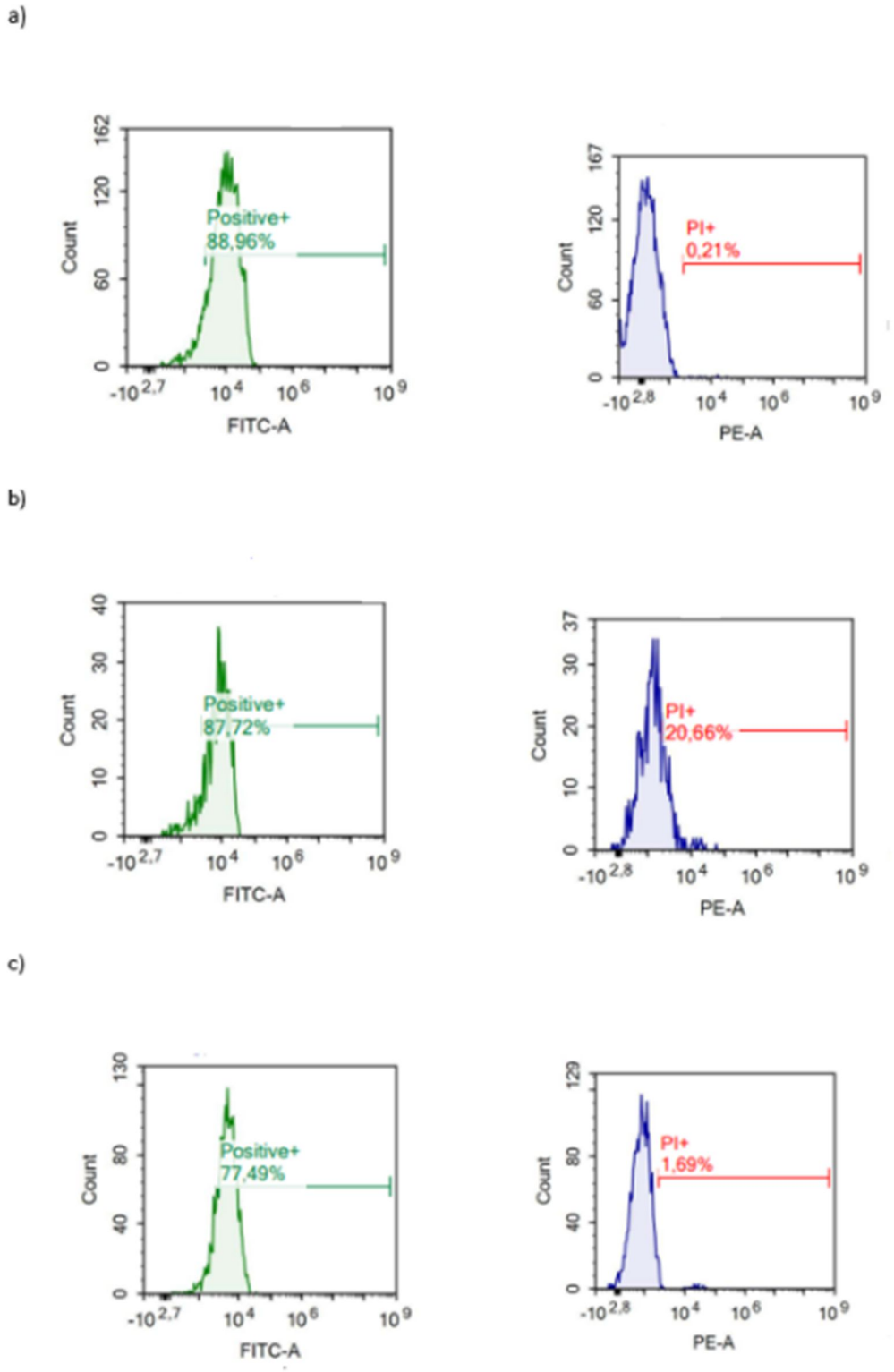

Figure B10. Flow cytometer histogram of siRNA transfected cells (Termed GFP in this Figure) and PI-positive RBCs from "4.2.3 Optimizing siRNA transfection in A. salmon RBCs – Experiment 2" at Day 3 from P1 a) A. salmon individual 1. b) A. salmon individual 2 c) A. salmon individual 3

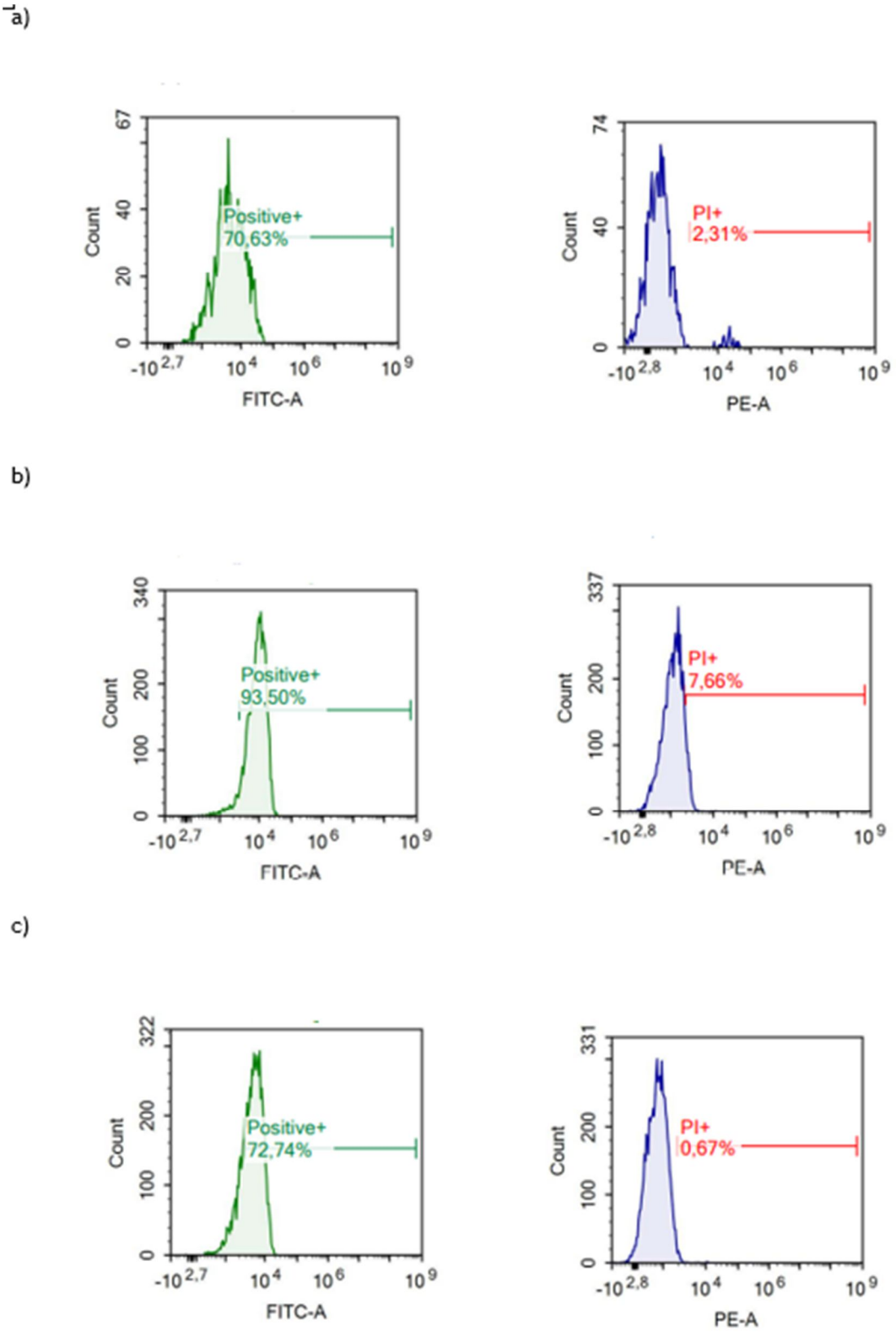

Figure B11. Flow cytometer histogram of siRNA transfected cells (Termed GFP in this Figure) and PI-positive RBCs from "4.2.3 Optimizing siRNA transfection in A. salmon RBCs – Experiment 2" at Day 3 from P2 a) A. salmon individual 1. b) A. salmon individual 2 c) A. salmon individual 3

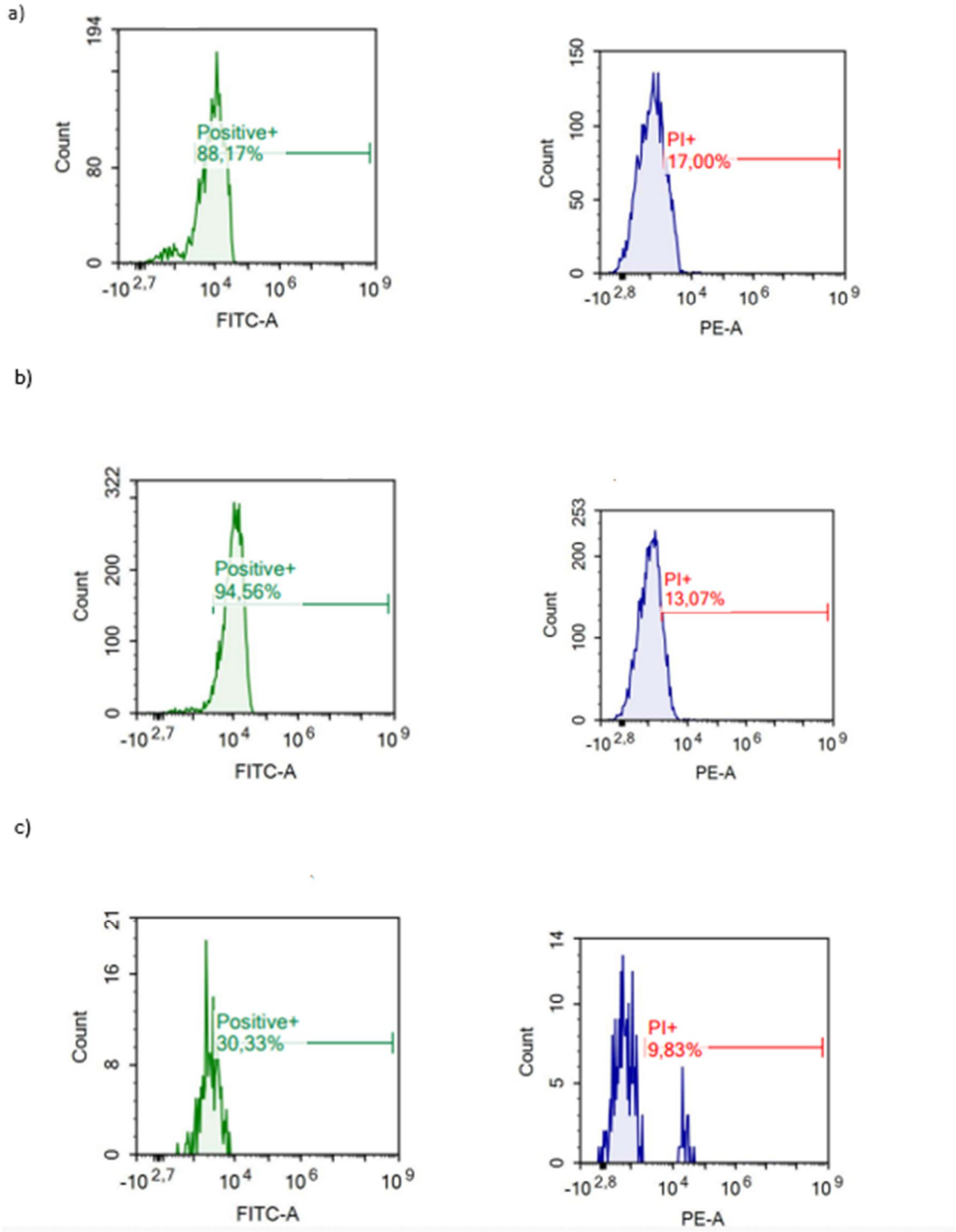

Figure B12. Flow cytometer histogram of siRNA transfected cells (Termed GFP in this Figure) and PI-positive RBCs from "4.2.3 Optimizing siRNA transfection in A. salmon RBCs – Experiment 2" at Day 3 from P3 a) A. salmon individual 1. b) A. salmon individual 2 c) A. salmon individal 3

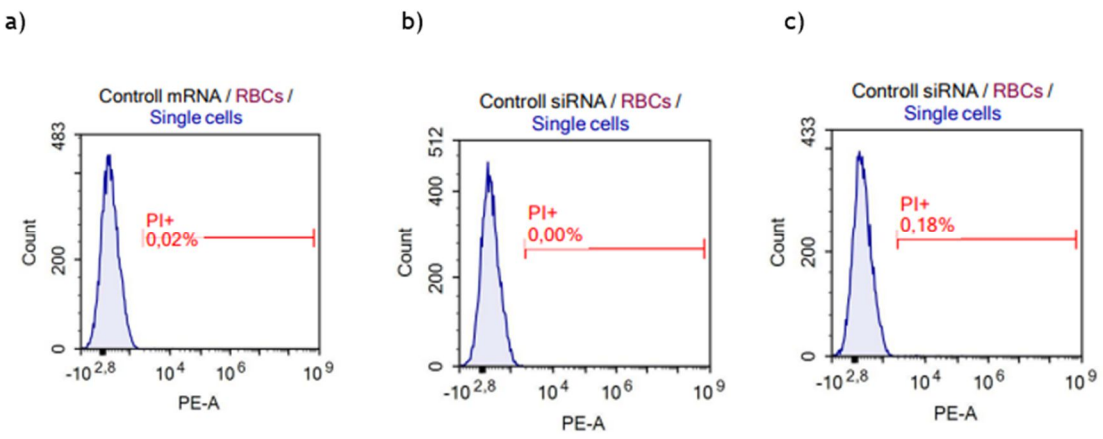

Figure B13. Flow cytometer histogram of PI-positive RBCs in transfected control from "4.2.3 Optimizing siRNA transfection in A. salmon RBCs – Experiment 2" at Day 3. a) P1 b) P2 c) P3

C - mRNA optimization in A salmon RBCs

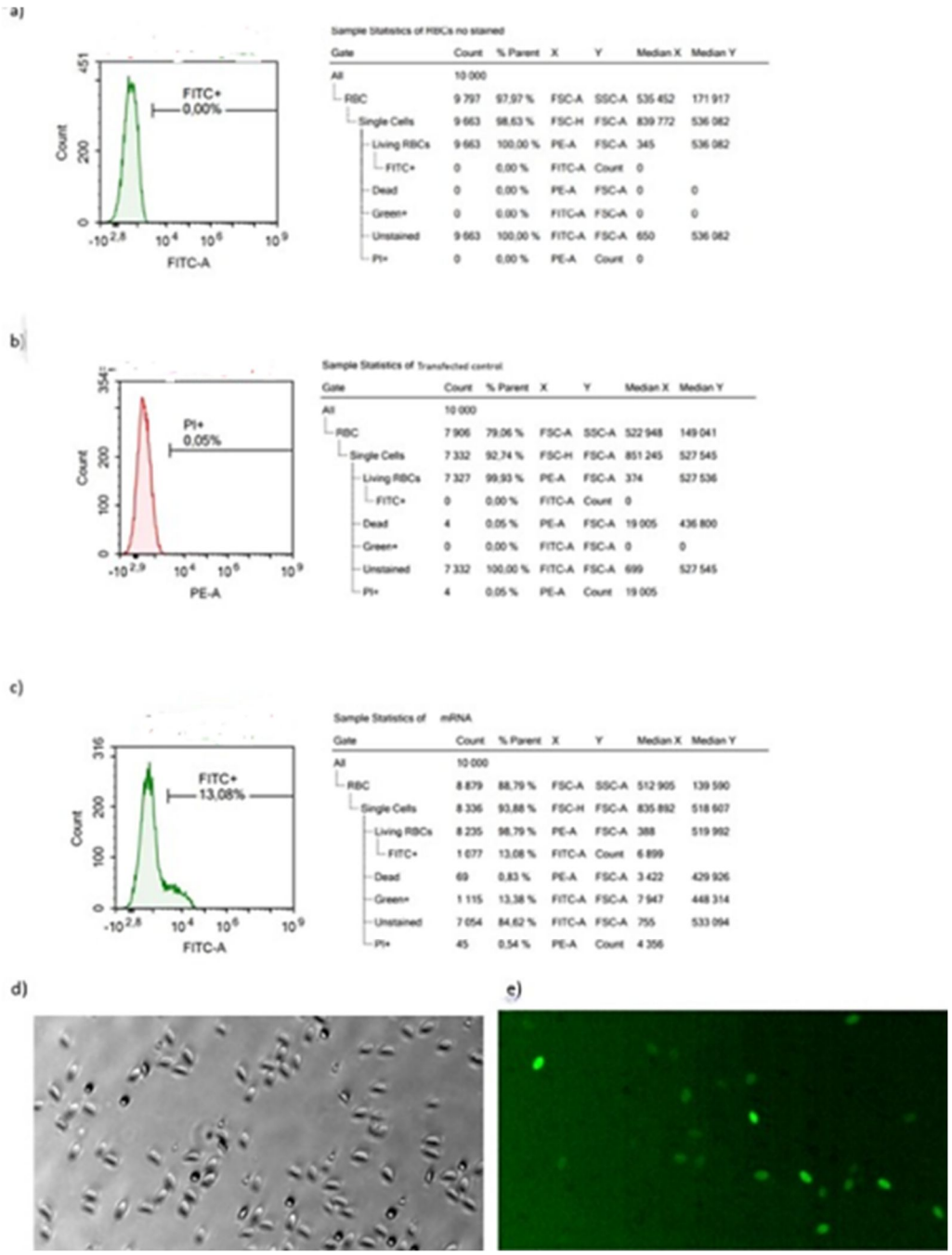

Figure C1. Flow cytometer histogram and corresponding sample statistics from mRNA-GFP establishment in A. salmon RBCs. a) not-electroporated RBCs. b) Electroporated RBCs (PI-stained). c) Not-transfected RBCs mixed with siRNA-AF488. Microscope picture of RBCs transfected with siRNA-AF488 in d) Bright-field Channel and e) FITC-channel.

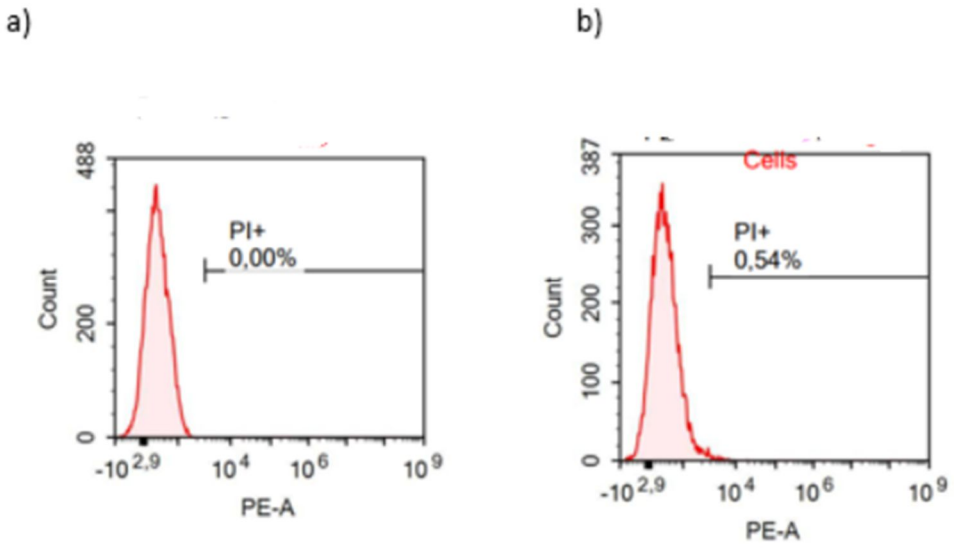

Figure C2. Flow cytometer histogram from "4.3.2 Establishing mRNA-GFP transfection" a) not-electroporated RBCs. b) RBCs transfeceted with mRNA-GFP.

a)

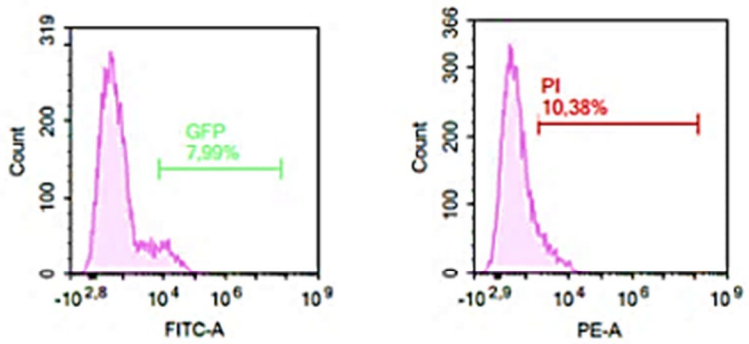

b)

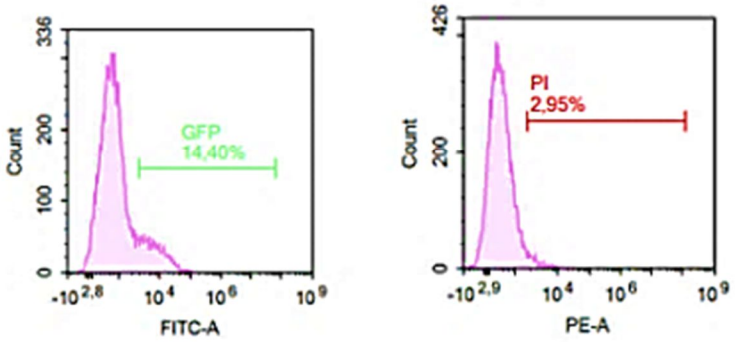

c)

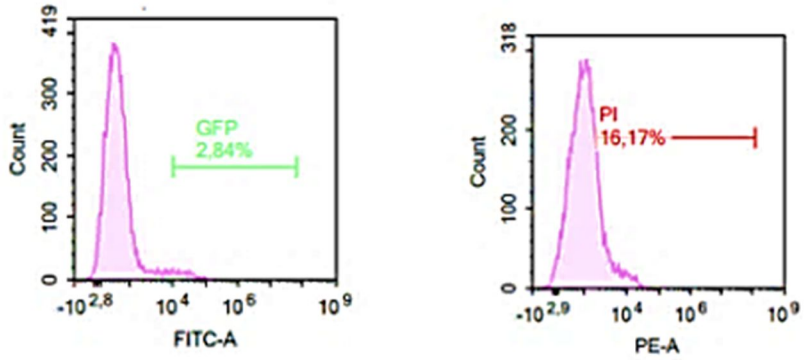

Figure C3. Flow cytometer histogram of mRNA transfected cells (Termed GFP in this Figure) and PI-positive RBCs from "4.3.3.1 Optimizing mRNA transfection in A. salmon RBCs – Experiment 1" a) P1. b) P2. c) P3.

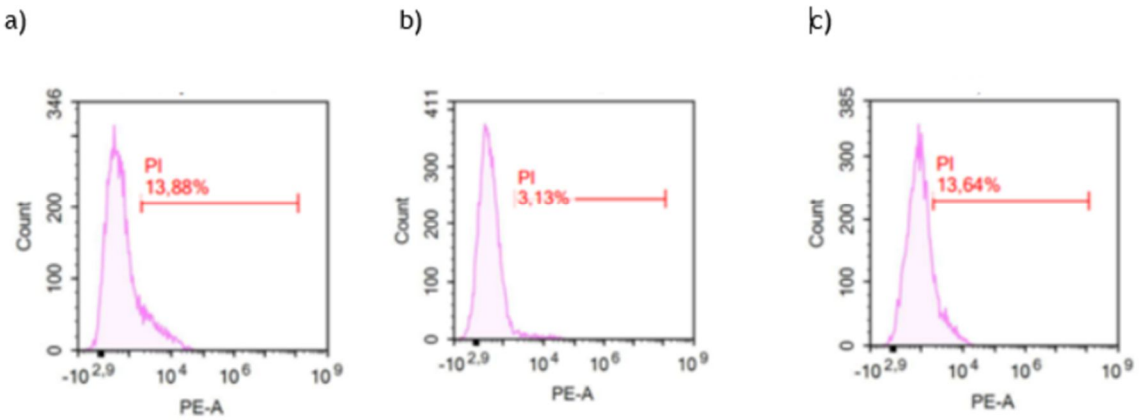

Figure C4. Flow cytometer histogram of PI-positive RBCs in transfected control RBCs from "4.3.3.1 Optimizing mRNA transfection in A. salmon RBCs – Experiment 1" at Day 2 a) P1. b) P2. c) P3.

a)

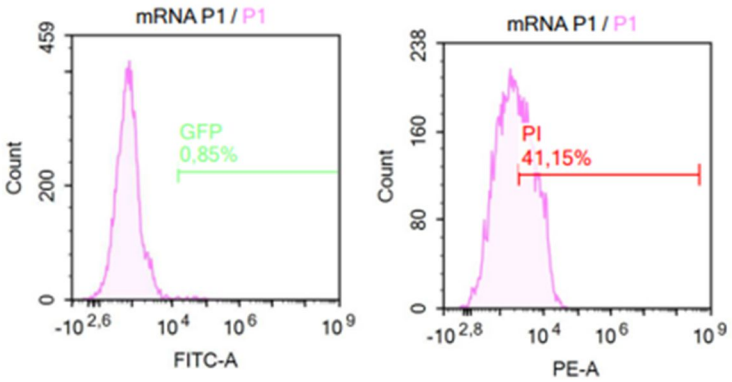

b)

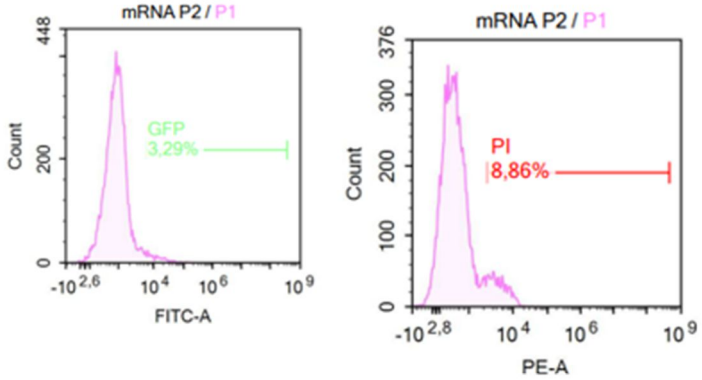

c)

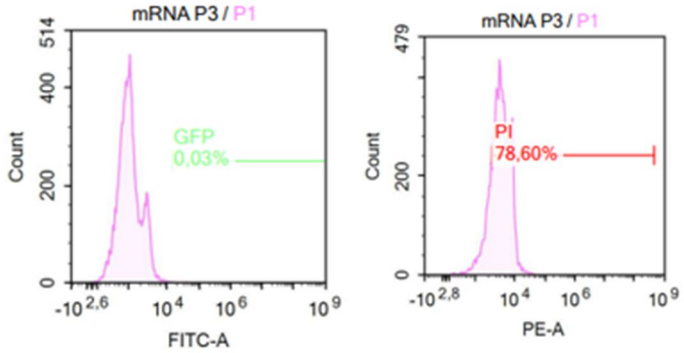

Figure C5. Flow cytometer histogram of mRNA transfected cells (Termed GFP in this Figure) and PI-positive RBCs from "4.3.3.2 Optimizing mRNA transfection in A. salmon RBCs – Experiment 1" at Day 7 a) P1 b) P2 c) P3

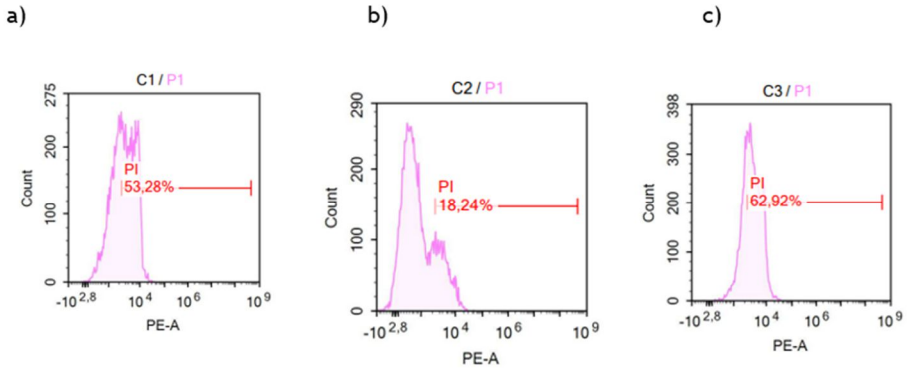

Figure C6. Flow cytometer histogram of PI-positive RBCs in transfected control RBCs from "4.3.3.1 Optimizing mRNA transfection in A. salmon RBCs – Experiment 1" at Day 7 a) P1. b) P2. c) P3.

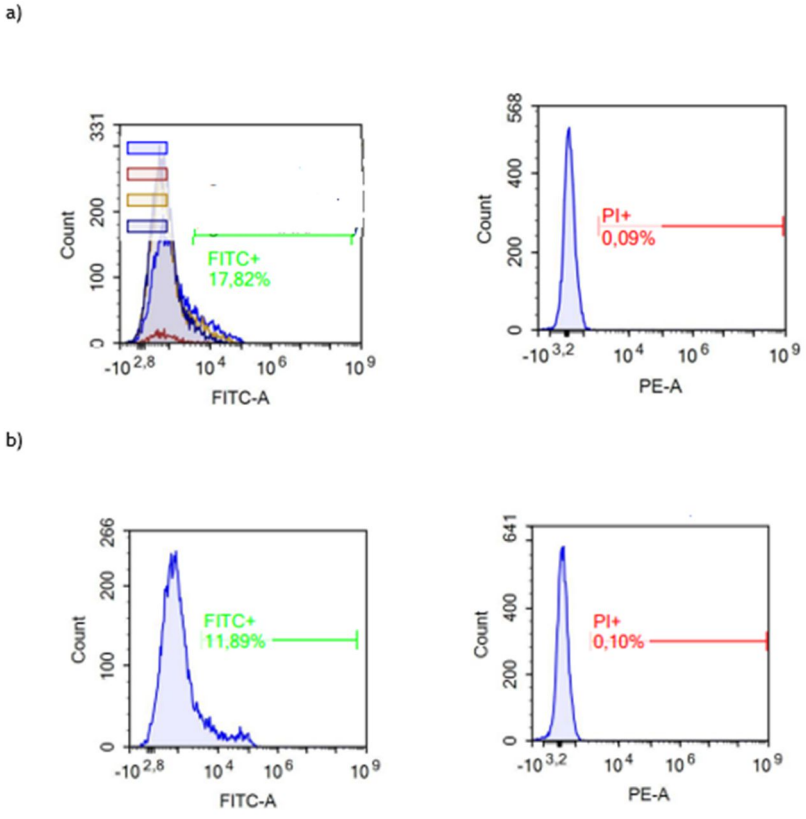

Figure C7. Flow cytometer histogram of mRNA transfected cells and PI-positive RBCs from "4.3.3.2 Optimizing mRNA transfection in A. salmon RBCs – Experiment 2" at Day 1 from P1 a) A. salmon individual 1. b) A. salmon individual 2.

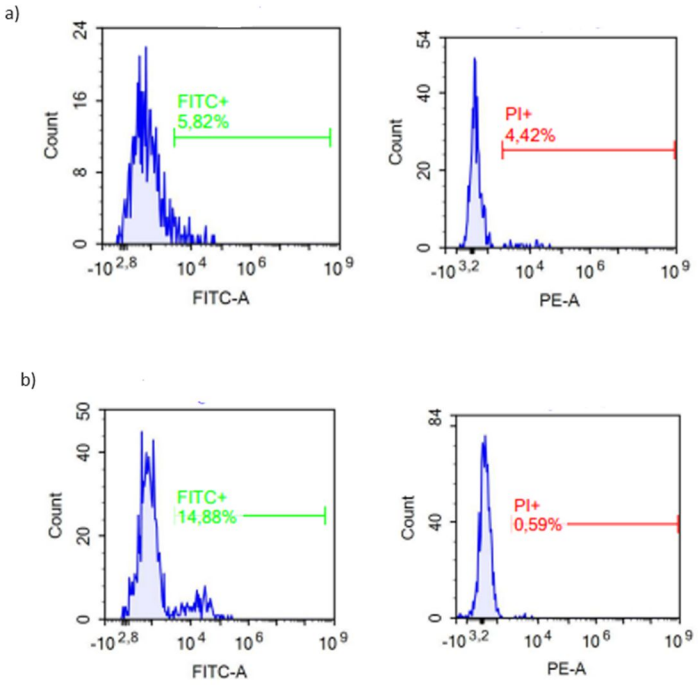

Figure C8. Flow cytometer histogram of mRNA transfected cells and PI-positive RBCs from "4.3.3.2 Optimizing mRNA transfection in A. salmon RBCs – Experiment 2" at Day 1 from P2 a) A. salmon individual 1. b) A. salmon individual 2.

a)

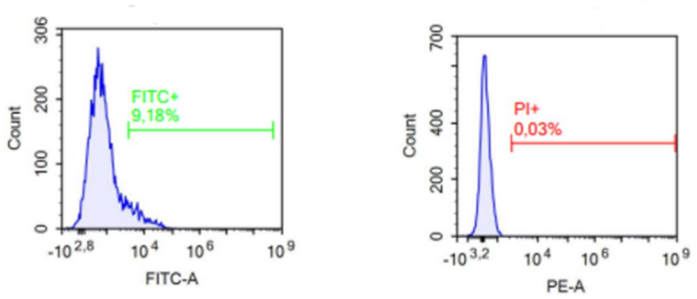

b)

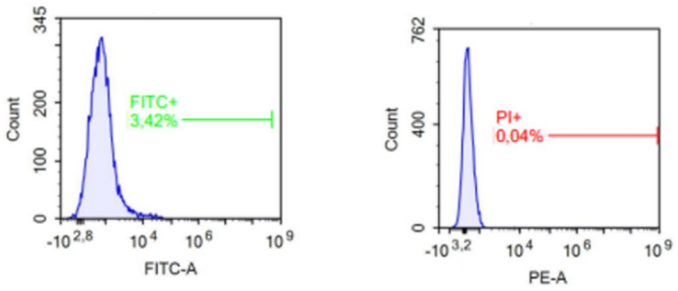

Figure C10. Flow cytometer histogram of mRNA transfected cells and PI-positive RBCs from "4.3.3.2 Optimizing mRNA transfection in A. salmon RBCs – Experiment 2" at Day 1 from P3 a) A. salmon individual 1. b) A. salmon individual 2.

a)

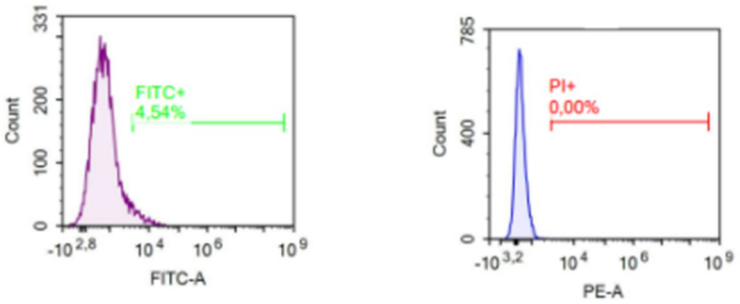

b)

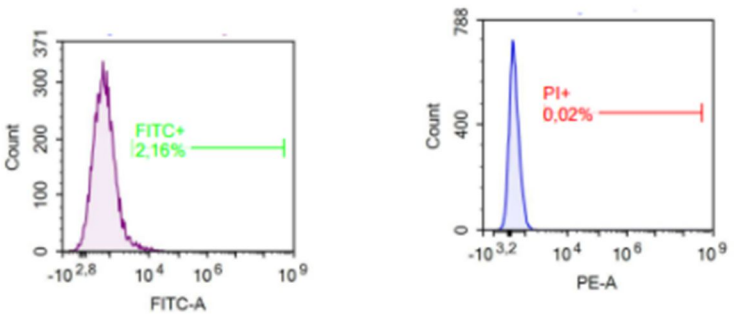

Figure C11. Flow cytometer histogram of mRNA transfected cells and PI-positive RBCs from "4.3.3.2 Optimizing mRNA transfection in A. salmon RBCs – Experiment 2" at Day 1 from P4 a) A. salmon individual 1. b) A. salmon individual 2.

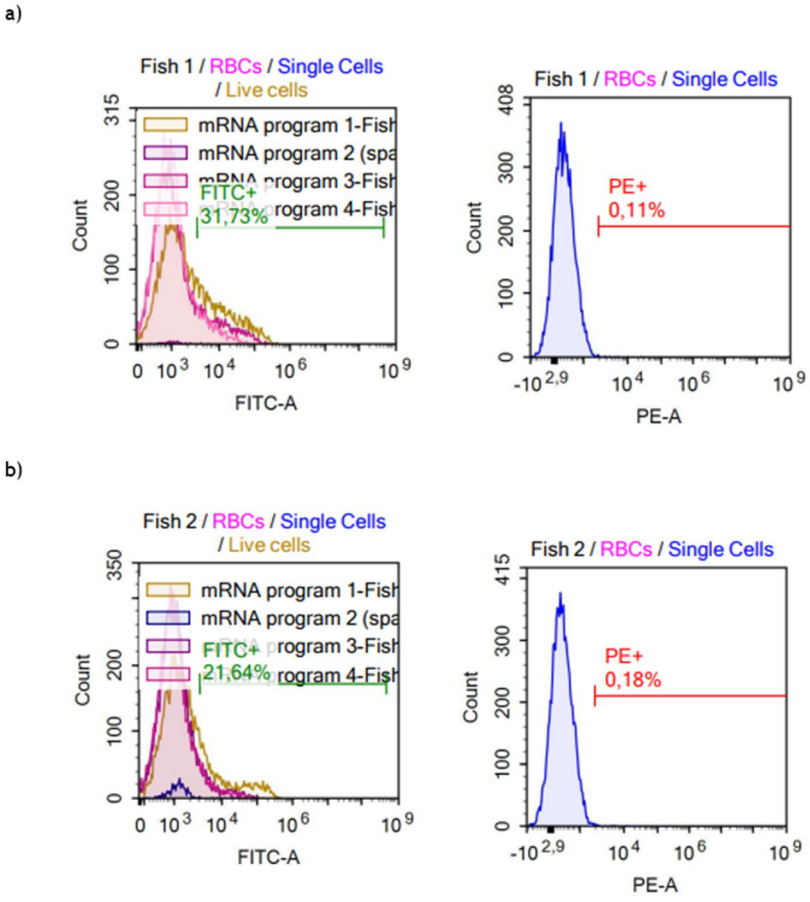

Figure C11. Flow cytometer histogram of mRNA transfected cells and PI-positive RBCs from "4.3.3.2 Optimizing mRNA transfection in A. salmon RBCs – Experiment 2" at Day 3 from P1 a) A. salmon individual 1. b) A. salmon individual 2.

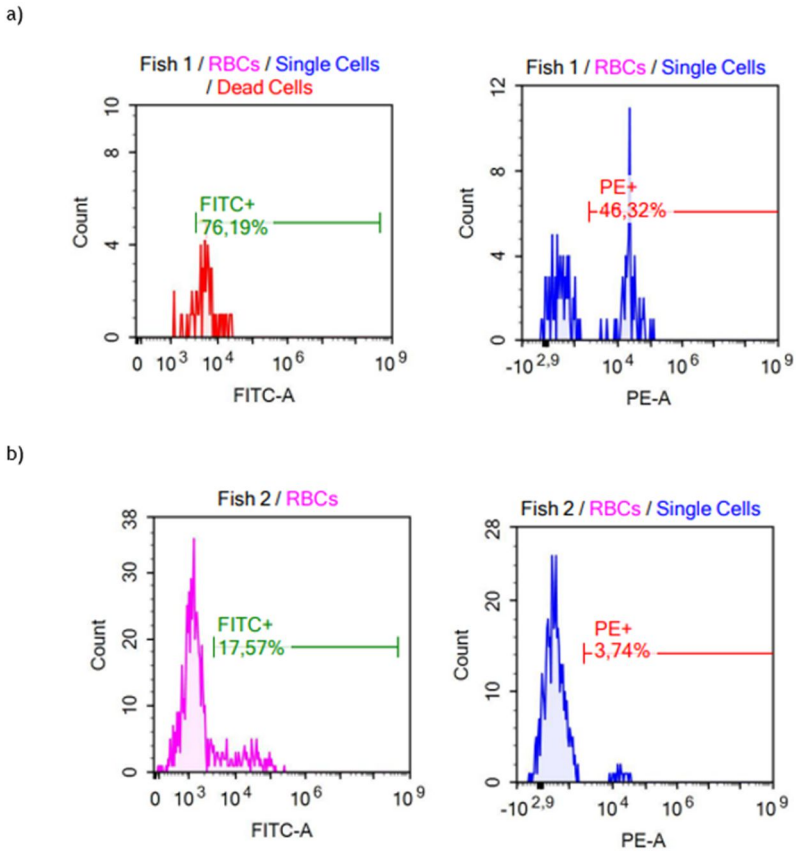

Figure C12. Flow cytometer histogram of mRNA transfected cells and PI-positive RBCs from "4.3.3.2 Optimizing mRNA transfection in A. salmon RBCs – Experiment 2" at Day 3 from P2 a) A. salmon individual 1. b) A. salmon individual 2

a)

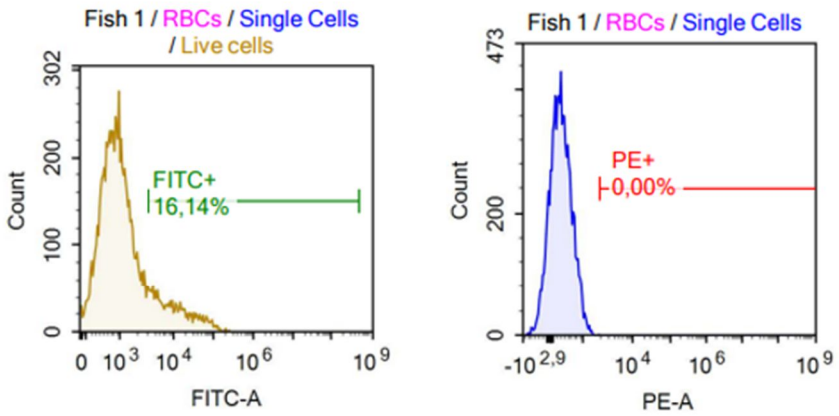

b)

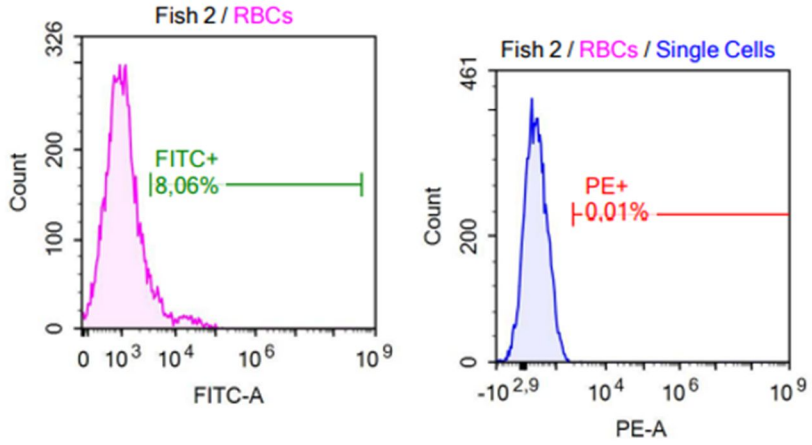

Figure C13. Flow cytometer histogram of mRNA transfected cells and PI-positive RBCs from "4.3.3.2 Optimizing siRNA transfection in A. salmon RBCs – Experiment 2" at Day 3 from P3 a) A. salmon individual 1. b) A. salmon individual 2

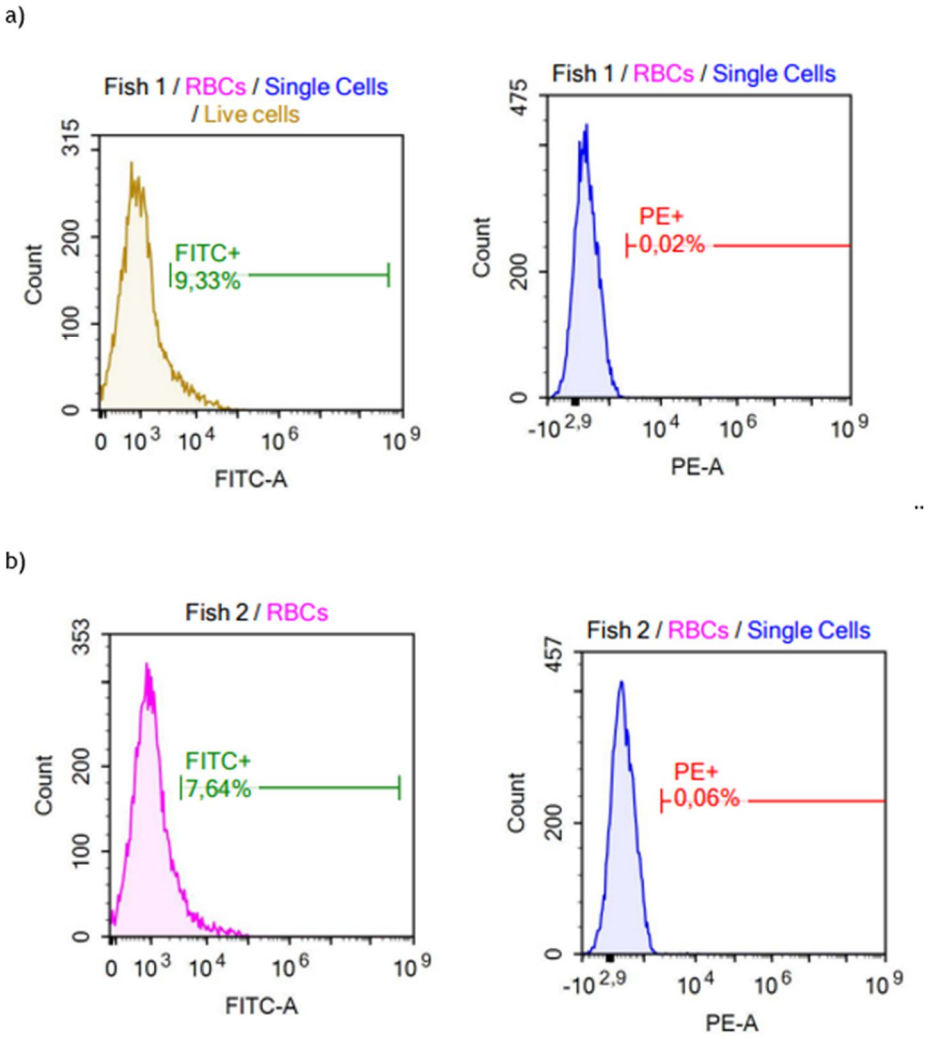

Figure C14. Flow cytometer histogram of mRNA transfected cells and PI-positive RBCs from "4.3.3.2 Optimizing siRNA transfection in A. salmon RBCs – Experiment 2" at Day 3 from P4 a) A. salmon individual 1. b) A. salmon individual 2

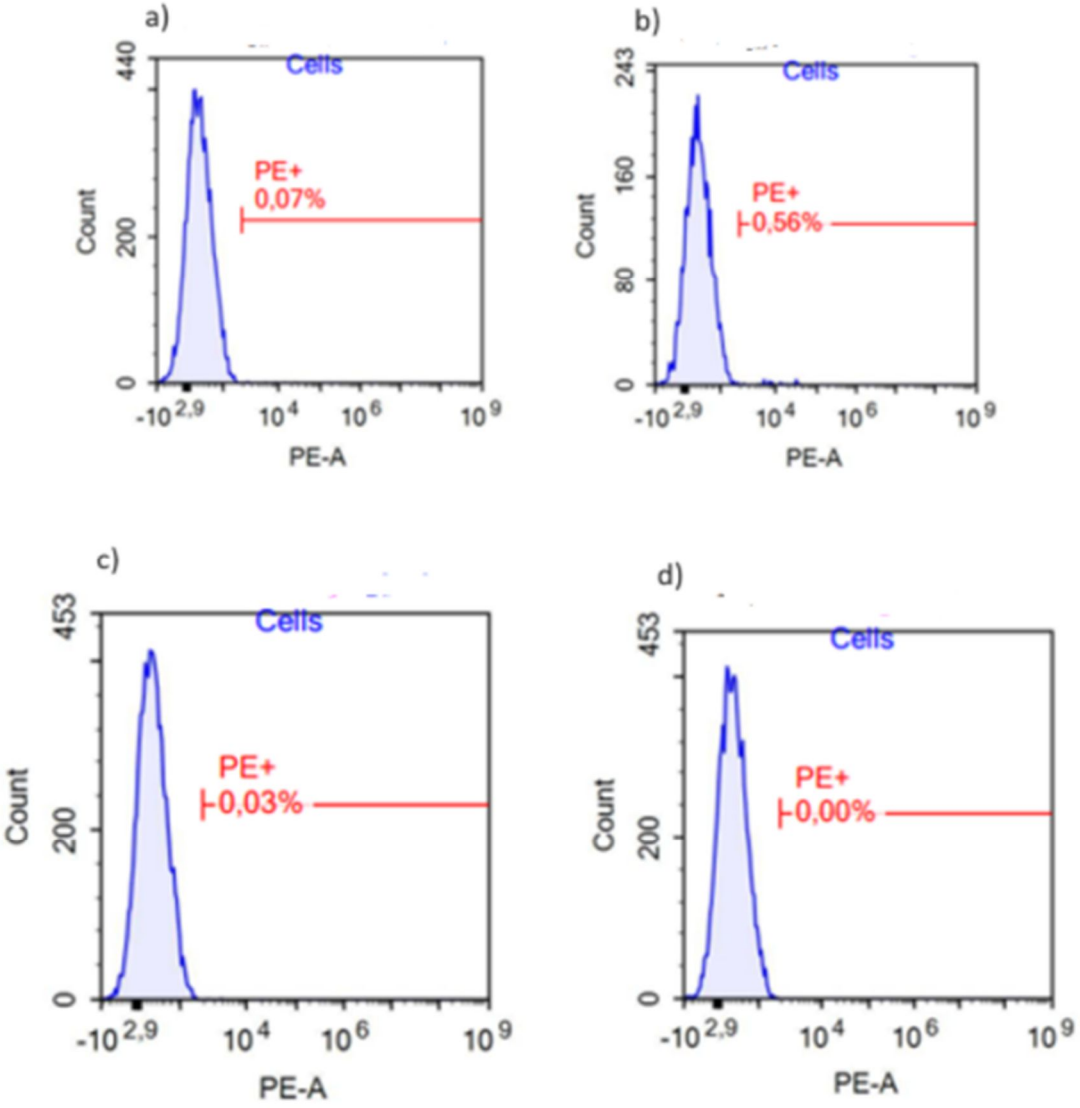

Figure C14. Flow cytometer histogram of PI-positive transfected control RBCs from "4.3.3.2 Optimizing siRNA transfection in A. salmon RBCs – Experiment 2" at Day 3 from P4 a) P1. b) P2. c) P3. d) P4.

a)

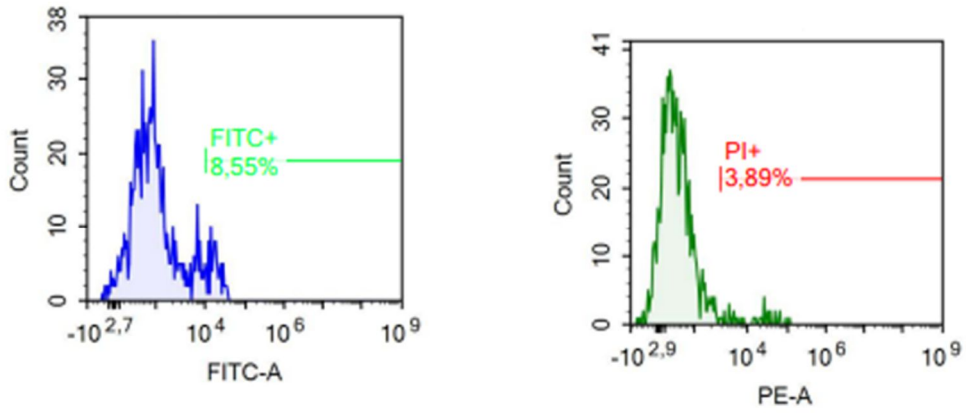

b)

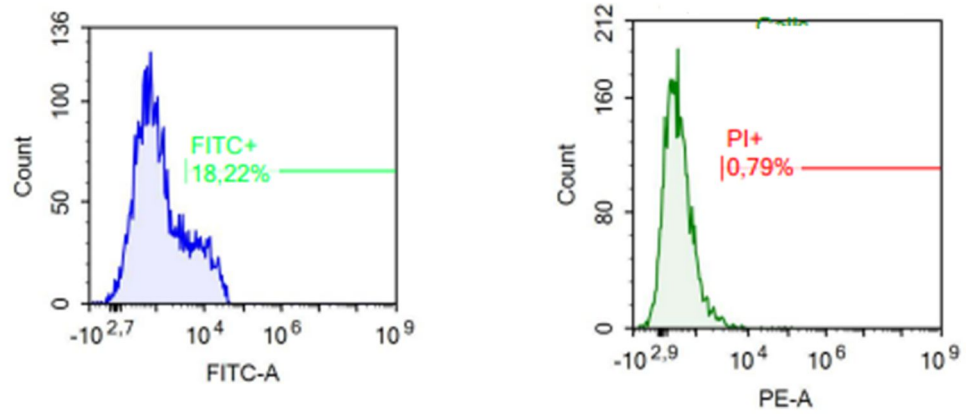

Figure C15. Flow cytometer histogram of mRNA transfected cells and PI-positive RBCs from "4.3.3.3 Optimizing siRNA transfection in A. salmon RBCs – Experiment 3" at Day 1 a) P1. b) P2

a)

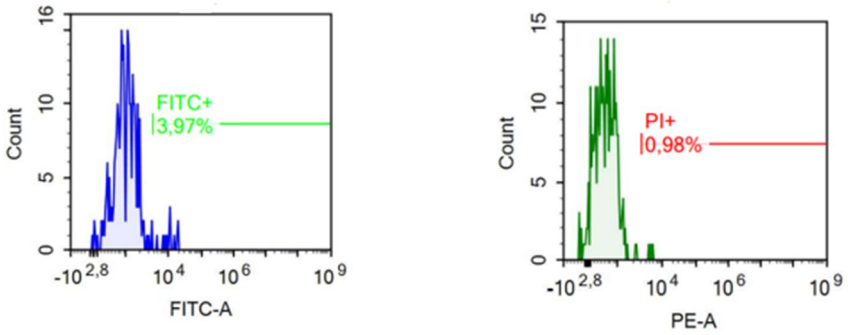

b)

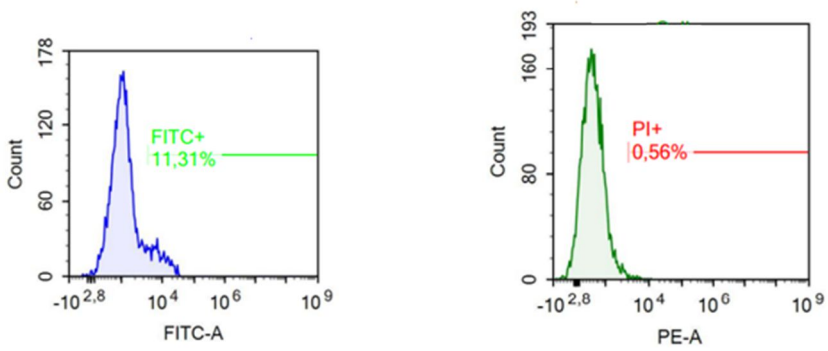

Figure C14. Flow cytometer histogram of mRNA transfected cells and PI-positive RBCs from "4.3.3.3 Optimizing siRNA transfection in A. salmon RBCs – Experiment 3" at Day 3 a) P1. b) P2

D – Silencing Experiment in A.salmon RBCs

```
mRNA-GFP    ----------------------------------ATGGTGAGCAAGGGCGAGGAGCTG      24
Cloning     ACGGTACCGCGGGCCCGGGATCCACCGGTCGCCACCATGGTGAGCAAGGGCGAGGAGCTG      120
                                              ************************

mRNA-GFP    TTCACCGGGGTGGTGCCCATCCTGGTCGAGCTGGACGGCGACGTAAACGGCCACAAGTTC      84
Cloning     TTCACCGGGGTGGTGCCCATCCTGGTCGAGCTGGACGGCGACGTAAACGGCCACAAGTTC      180
            ************************************************************

mRNA-GFP    AGCGTGTCCGGCGAGGGCGAGGGCGATGCCACCTACGGCAAGCTGACCCTGAAGTTCATC      144
Cloning     AGCGTGTCCGGCGAGGGCGAGGGCGATGCCACCTACGGCAAGCTGACCCTGAAGTTCATC      240
            ************************************************************

mRNA-GFP    TGCACCACCGGCAAGCTGCCCGTGCCCTGGCCCACCCTCGTGACCACCCTGACCTACGGC      204
Cloning     TGCACCACCGGCAAGCTGCCCGTGCCCTGGCCCACCCTCGTGACCACCCTGACCTACGGC      300
            ************************************************************

mRNA-GFP    GTGCAGTGCTTCAGCCGCTACCCCGACCACATGAAGCAGCACGACTTCTTCAAGTCCGCC      264
Cloning     GTGCAGTGCTTCAGCCGCTACCCCGACCACATGAAGCAGCACGACTTCTTCAAGTCCGCC      360
            ************************************************************

mRNA-GFP    ATGCCCGAAGGCTACGTCCAGGAGCGCACCATCTTCTTCAAGGACGACGGCAACTACAAG      324
Cloning     ATGCCCGAAGGCTACGTCCAGGAGCGCACCATCTTCTTCAAGGACGACGGCAACTACAAG      420
            ************************************************************

mRNA-GFP    ACCCGCGCCGAGGTGAAGTTCGAGGGCGACACCCTGGTGAACCGCATCGAGCTGAAGGGC      384
Cloning     ACCCGCGCCGAGGTGAAGTTCGAGGGCGACACCCTGGTGAACCGCATCGAGCTGAAGGGC      480
            ************************************************************

mRNA-GFP    ATCGACTTCAAGGAGGACGGCAACATCCTGGGGCACAAGCTGGAGTACAACTACAACAGC      444
Cloning     ATCGACTTCAAGGAGGACGGCAACATCCTGGGGCACAAGCTGGAGTACAACTACAACAGC      540
            ************************************************************

mRNA-GFP    CACAACGTCTATATCATGGCCGACAAGCAGAAGAACGGCATCAAGGTGAACTTCAAGATC      504
Cloning     CACAACGTCTATATCATGGCCGACAAGCAGAAGAACGGCATCAAGGTGAACTTCAAGATC      600
            ************************************************************

mRNA-GFP    CGCCACAACATCGAGGACGGCAGCGTGCAGCTCGCCGACCACTACCAGCAGAACACCCCC      564
Cloning     CGCCACAACATCGAGGACGGCAGCGTGCAGCTCGCCGACCACTACCAGCAGAACACCCCC      660
            ************************************************************

mRNA-GFP    ATCGGCGACGGCCCCGTGCTGCTGCCCGACAACCACTACCTGAGCACCCAGTCCGCCCTG      624
Cloning     ATCGGCGACGGCCCCGTGCTGCTGCCCGACAACCACTACCTGAGCACCCAGTCCGCCCTG      720
            ************************************************************

mRNA-GFP    AGCAAAGACCCCAACGAGAAGCGCGATCACATGGTCCTGCTGGAGTTCGTGACCGCCGCC      684
Cloning     AGCAAAGACCCCAACGAGAAGCGCGATCACATGGTCCTGCTGGAGTTCGTGACCGCCGCC      780
            ************************************************************

mRNA-GFP    GGGATCACTCTCGGCATGGACGAGCTGTACAAGTAA----------------------      720
Cloning     GGGATCACTCTCGGCATGGACGAGCTGTACAAGTAAAGCGGCCGCGACTCTAGATCATAA      840
            ***********************************
```

Figure D1. Clustal Omega alligment of mRNA-GFP sequence against anti-GFP siRNA target

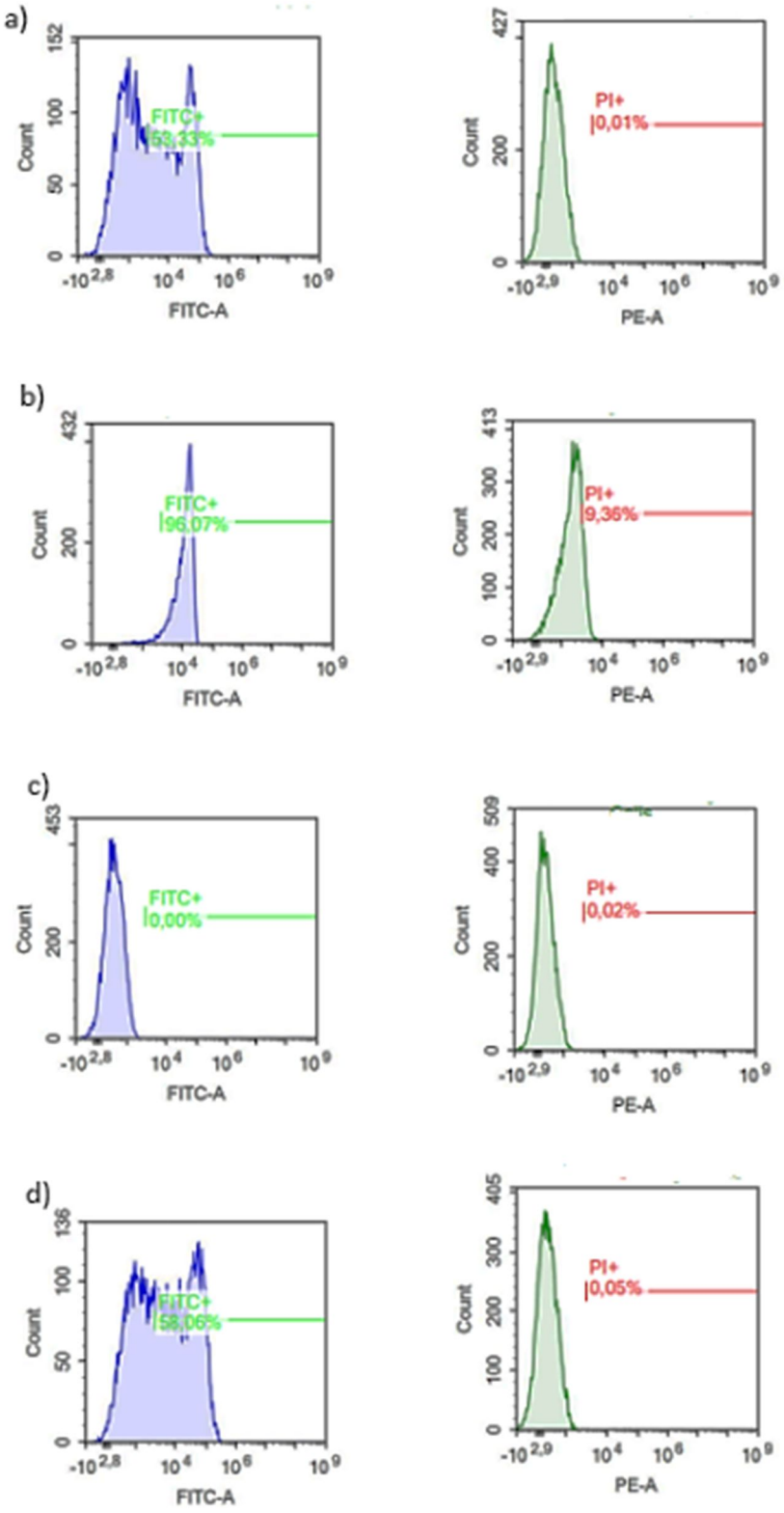

Figure D2. Flow cytometer histogram of fluorescent cells and PI-stained cells RBCs from "4.4 mRNA-GFP silencing control" at Day 1 a) mRNA-GFP transfected b) siRNA-AF488 transfected c) anti-GFP siRNA transfected d) mRNA-GFP + anti-GFP siRNA transfected

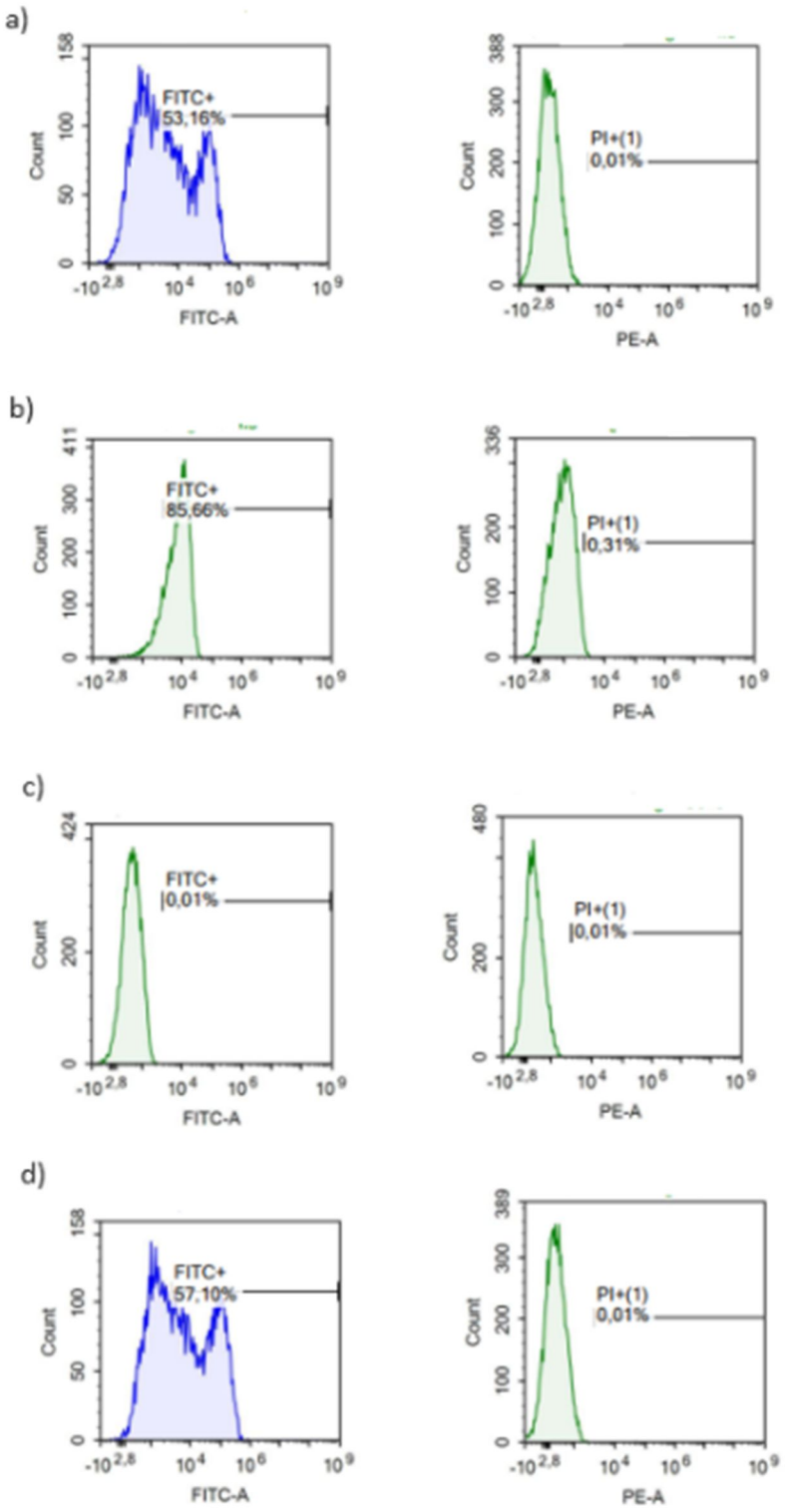

Figure D3. Flow cytometer histogram of fluorescent cells and PI-stained cells A. salmon 1 RBCs from "4.4 mRNA-GFP silencing control" at Day 3 a) mRNA-GFP transfected b) siRNA-AF488 transfected c) anti-GFP siRNA transfected d) mRNA-GFP + anti-GFP siRNA transfected

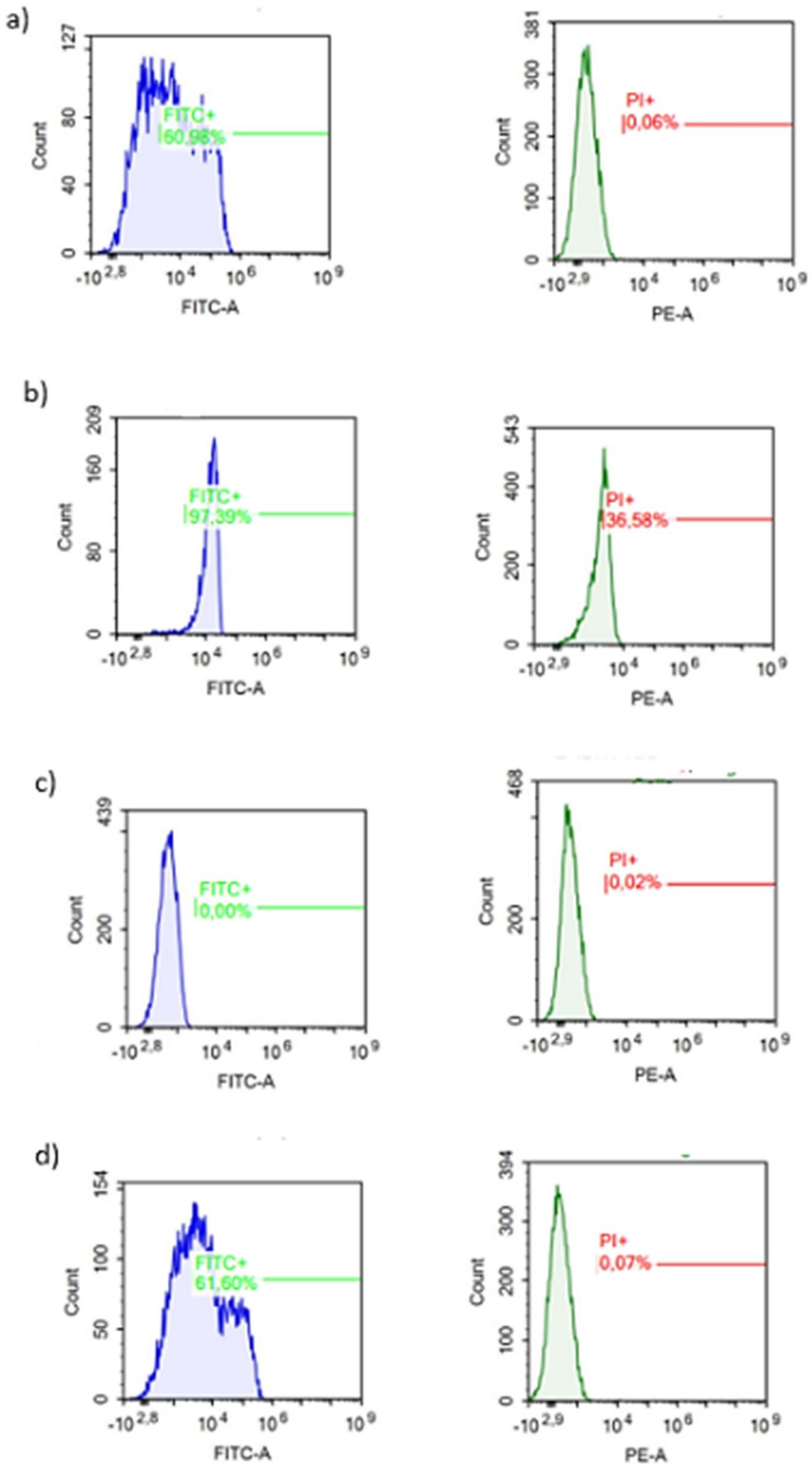

Figure D4. Flow cytometer histogram of fluorescent cells and PI-stained cells A. salmon 2 RBCs from "4.4 mRNA-GFP silencing control" at Day 1 a) mRNA-GFP transfected b) siRNA-AF488 transfected c) anti-GFP siRNA transfected d) mRNA-GFP + anti-GFP siRNA transfected

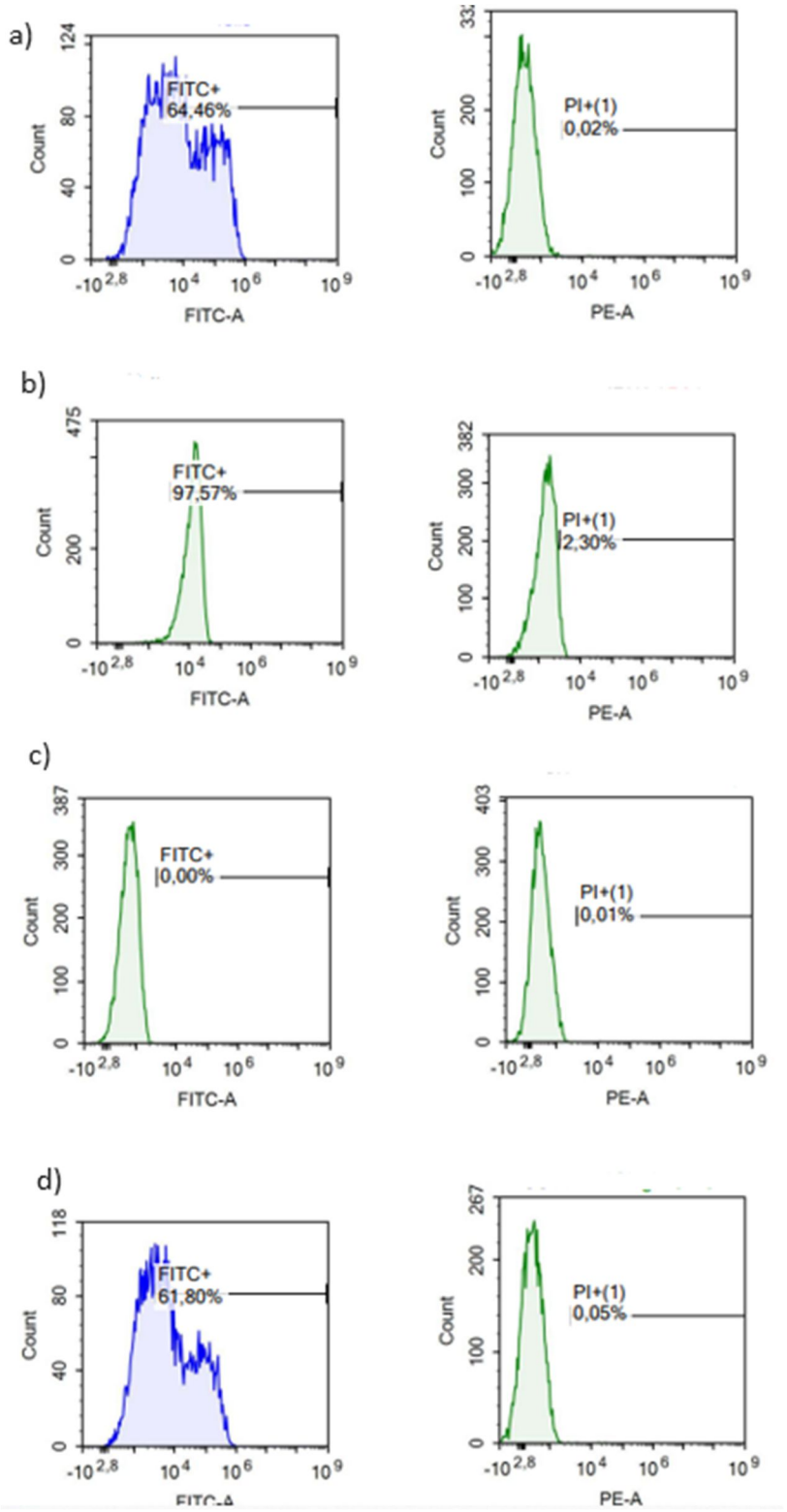

Figure D5. Flow cytometer histogram of fluorescent cells and PI-stained cells A. salmon 2 RBCs from "4.4 mRNA-GFP silencing control" at Day 3 a) mRNA-GFP transfected b) siRNA-AF488 transfected c) anti-GFP siRNA transfected d) mRNA-GFP + anti-GFP siRNA transfected

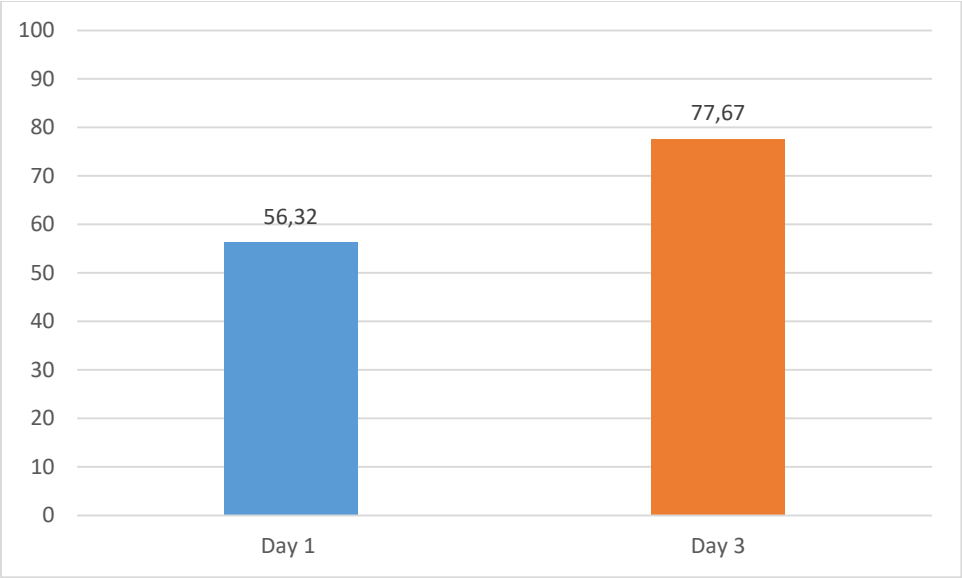

Figure D6. Barplot of an additional A. salmon individual after transfection with mRNA-GFP during co-transfection experiment. The individual was not included because of different RNA:RBC ratio. Blue bar-plot presents at Day 1, and orange bar-plot presents Day 3.

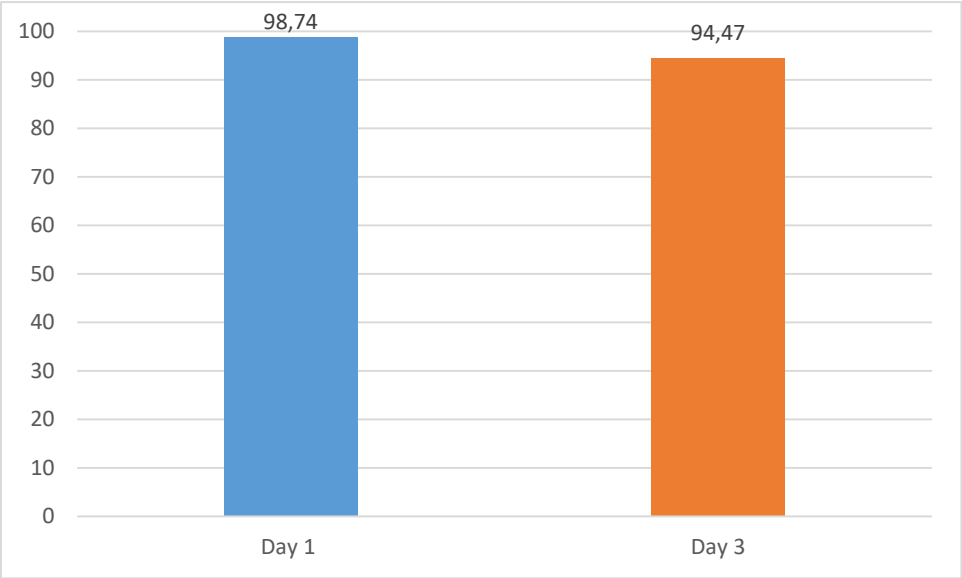

Figure D7. Barplot of an additional A. salmon individual after transfection with siRNA-AF488 during co-transfection experiment. The individual was not included because of different RNA:RBC ratio. Blue bar-plot presents at Day 1, and orange bar-plot presents Day 3.

E – CHSE-214 transfections

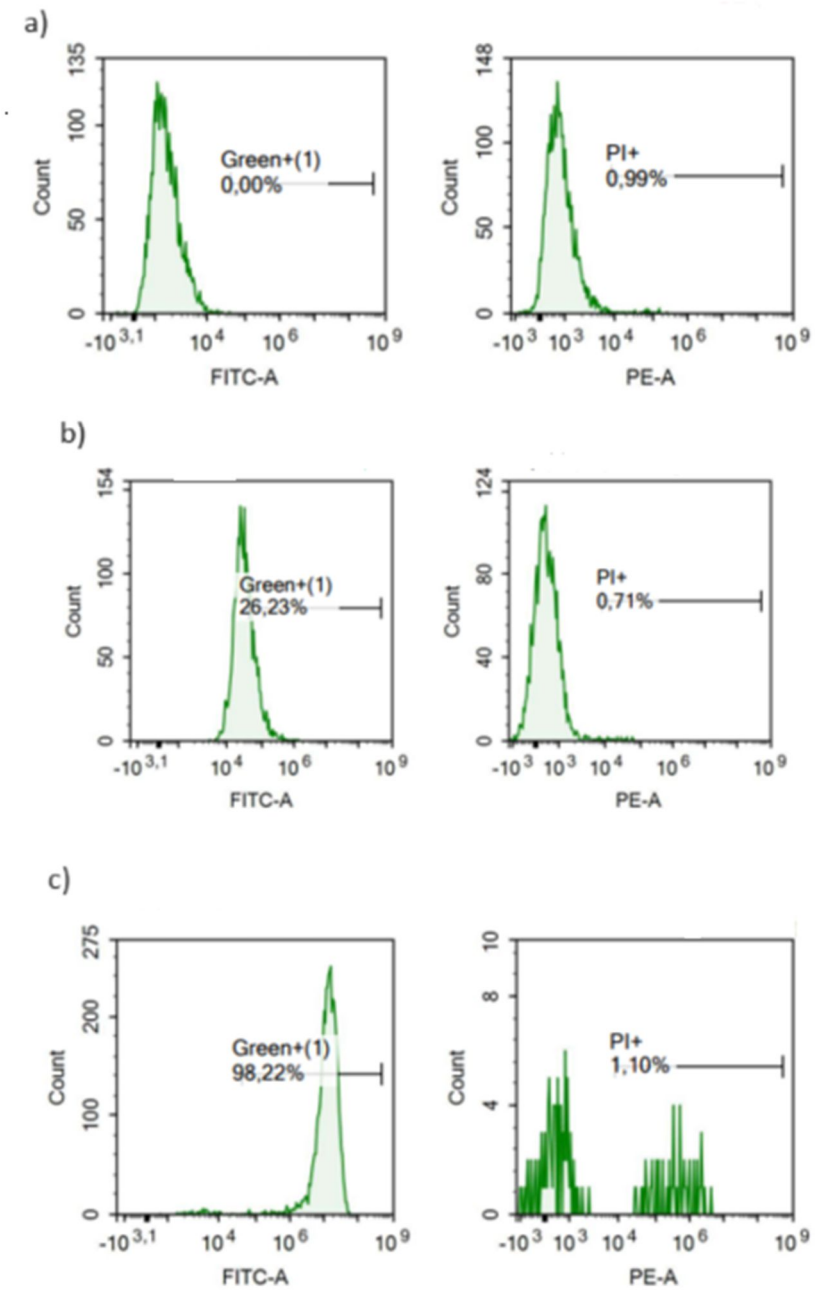

Figure E1. Flow cytometer histogram of CHSE-214 cells 2 days post-transfection**.** a) un-electroporated b) siRNA-AF488 transfected c) mRNA-GFP transfected

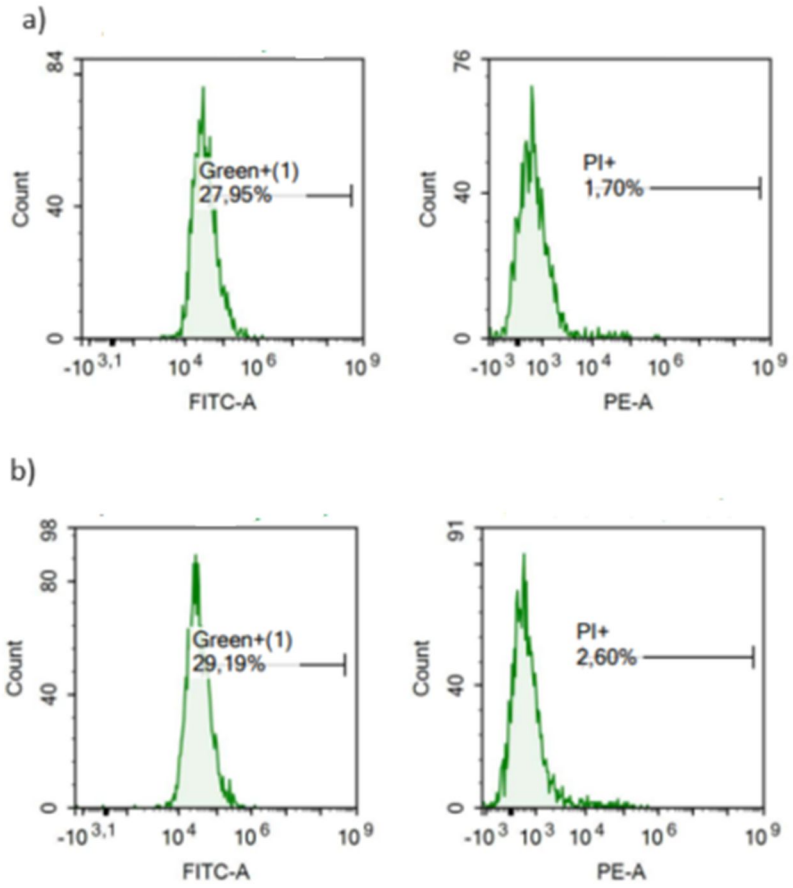

Figure E2. Flow cytometer histogram of CHSE-214 cells (n=2) 2 days post-transfection with siRNA-AF488**.** a) Replicate 1 b) Replicate 2

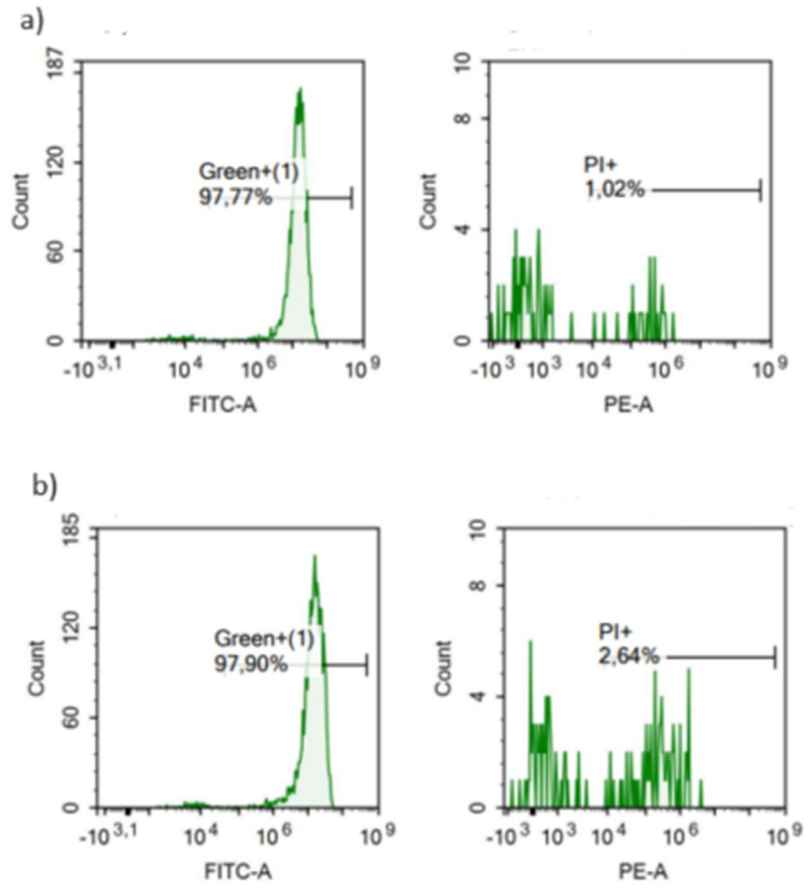

Figure E3. Flow cytometer histogram of CHSE-214 cells (n=2) 2 days post-transfection with mRNA-GFP**.** a) Replicate 1 b) Replicate 2

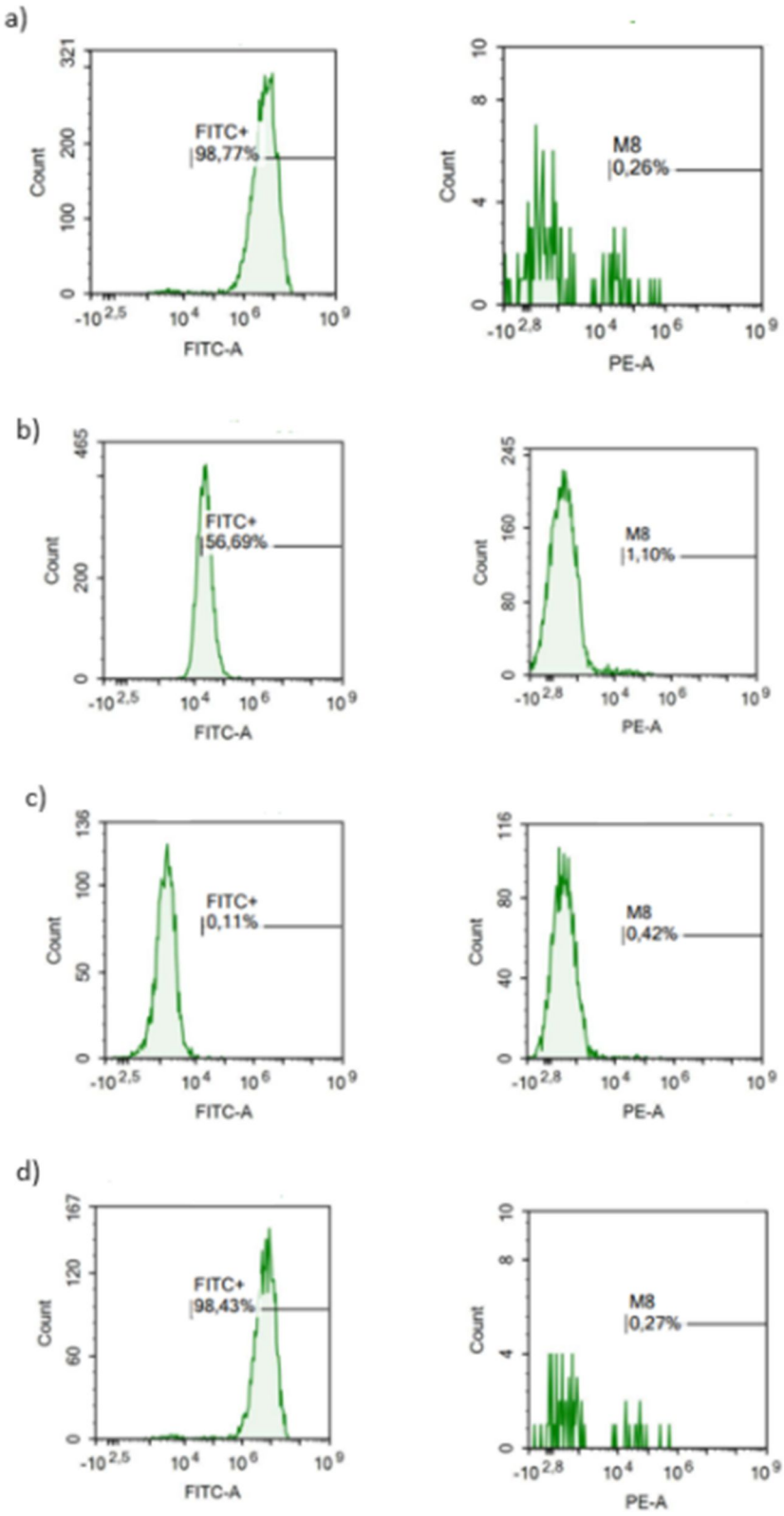

Figure E4. Flow cytometer histogram of fluorescent cells and PI-stained cells (M8) from "4.5.2 CHSE silencing experiment" replicate 1 at Day 2 a) mRNA-GFP transfected b) siRNA-AF488 transfected c) anti-GFP siRNA transfected d) mRNA-GFP + anti-GFP siRNA transfected

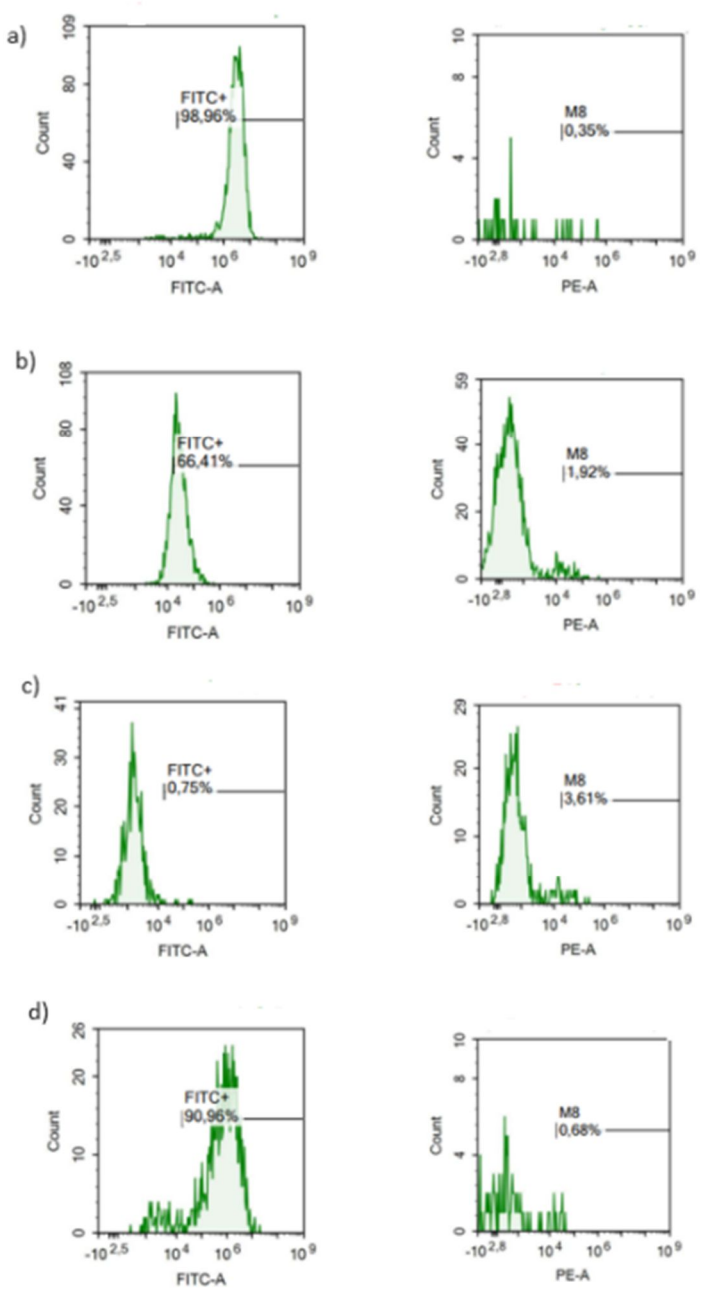

Figure E5. Flow cytometer histogram of fluorescent cells and PI-stained cells (M8) from "4.5.2 CHSE silencing experiment" replicate 1 at Day 2 a) mRNA-GFP transfected b) siRNA-AF488 transfected c) anti-GFP siRNA transfected d) mRNA-GFP + anti-GFP siRNA transfected

F - siRNA design and primer design

The design of RIG-I is not included since it is not avaiable.

Table F1. siRNA sequences for TLR3 with posistion and potential off targets

Gene	Sequences	Posistion (nt)	Off targets	Query Coverage	SI%
TLR3 Accession :BK008646	AATTGGCCAGATATAA TCCTC	3 - 23	GeneID:100286425	66%	100%
	AACTATGACGCGTTCG TCATT	2293 - 2313	GeneID:106575120 GeneID:106575365	76% 66%	93,75% 100%
	AAACTCTTCTCGAAGA CTCCA	2483 - 2503	GeneID:106564127 GeneID:106564130 GeneID:106595501 GeneID:106589048 GeneID:106587506 GeneID:106599036	80% 80% 80% 76% 76% 71%	94,12% 94,12% 94,12% 93,75% 93,75% 100%

Table F2. siRNA sequences for RLR3 with posistion and potential off targets

Gene	Sequences	Posistion (nt)	Off targets	Query Coverage	SI%
RLR3 Accession: 1.XM_045720586 2.XM_014204107 Assembled in Clustal W	AATAAGATCATG GGGCGCTAC	650 - 670	None		
	AATGGAACCGAC TTCTTCCTG	1180 - 1200	GeneID:106588944 GeneID:106571143	66% 66%	100% 100%
	AATTAGCACGTC AGCTTTGTT	3031 - 3051	GeneID:106583387 GeneID:106580367	76% 76%	93,75% 93,75%

Table F3. siRNA sequences for MAVS with posistion and potential off targets

Gene	Sequences	Posistion (nt)	Off targets	Query Coverage	SI%
MAVS Accession: FN178458		1449-1474	None		
		1183-1208	GeneID:123724551	68%	94,12%
		694-719	None		

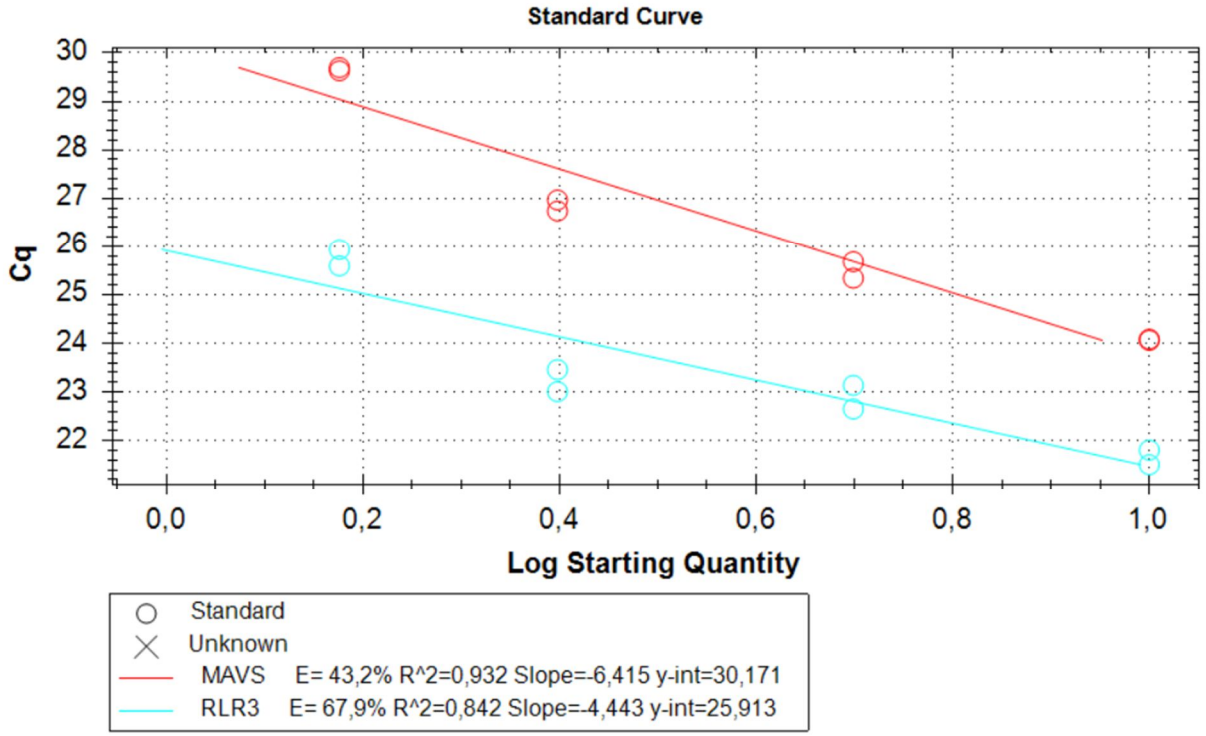

Figure F1. Standard curve of RLR3 and MAVS after qPCR analysis

Table F5. Ct-value from RLR3 and MAVS samples.

Well	Fluor	Target	Content	Sample	Cq	Cq Mean	Cq Std. Dev	Starting Quantity (SQ)	Log Starting Quantity	SQ Mean	SQ Std. Dev
A02	SYBR	RLR3	Std	1.5 ng	26,27	26,27	0,000	1,500E+00	0,176	1,50E+00	0,00E+00
A03	SYBR	RLR3	Std	1.5 ng	26,04	26,04	0,000	1,500E+00	0,176	1,50E+00	0,00E+00
A04	SYBR	RLR3	Std	2.5 ng	23,88	23,88	0,000	2,500E+00	0,398	2,50E+00	0,00E+00
A05	SYBR	RLR3	Std	2.5 ng	23,32	23,32	0,000	2,500E+00	0,398	2,50E+00	0,00E+00
A06	SYBR	RLR3	Std	5 ng	23,48	23,48	0,000	5,000E+00	0,699	5,00E+00	0,00E+00
A07	SYBR	RLR3	Std	5 ng	23,07	23,07	0,000	5,000E+00	0,699	5,00E+00	0,00E+00
A08	SYBR	RLR3	Std	10 ng	22,21	22,21	0,000	1,000E+01	1,000	1,00E+01	0,00E+00
A09	SYBR	RLR3	Std	10 ng	21,95	21,95	0,000	1,000E+01	1,000	1,00E+01	0,00E+00
A10	SYBR	RLR3	Unkn	RTN	N/A	0,00	0,000	N/A	N/A	0,00E+00	0,00E+00
B02	SYBR	MAVS	Std	1.5 ng	29,56	29,56	0,000	1,500E+00	0,176	1,50E+00	0,00E+00
B03	SYBR	MAVS	Std	1.5 ng	29,63	29,63	0,000	1,500E+00	0,176	1,50E+00	0,00E+00
B04	SYBR	MAVS	Std	2.5 ng	26,66	26,66	0,000	2,500E+00	0,398	2,50E+00	0,00E+00
B05	SYBR	MAVS	Std	2.5 ng	26,89	26,89	0,000	2,500E+00	0,398	2,50E+00	0,00E+00
B06	SYBR	MAVS	Std	5 ng	25,61	25,61	0,000	5,000E+00	0,699	5,00E+00	0,00E+00
B07	SYBR	MAVS	Std	5 ng	25,28	25,28	0,000	5,000E+00	0,699	5,00E+00	0,00E+00
B08	SYBR	MAVS	Std	10 ng	24,03	24,03	0,000	1,000E+01	1,000	1,00E+01	0,00E+00
B09	SYBR	MAVS	Std	10 ng	24,01	24,01	0,000	1,000E+01	1,000	1,00E+01	0,00E+00
B10	SYBR	MAVS	Unkn	RTN	N/A	0,00	0,000	N/A	N/A	0,00E+00	0,00E+00
B11	SYBR	MAVS	Unkn	NTC	N/A	0,00	0,000	N/A	N/A	0,00E+00	0,00E+00

G - Countess-measurments after transfection

Table G1. Cell viability and cells/mL after measuring in automatic cell counter at Day 3 and Day 6 from "4.7.1 Testing knock-down efficiency and responses to transfection at different time points". Day 1 is not added, since great viabilty has been shown at Day 1. Cells/mL and Cell viabilty are numbers directly from countess.

FISH 1	RBCs				Day 3		Day 6	
					Countess		Countess	
Well		Voltage (V)	Width (ms)	Number of p	*Cells/mL*	*Cell Viability*	*Cells/mL*	*Cell Viability*
TLR3		1700	20	2	1,2*10^6	95	1,1 *10^6	94
RIG-I		1700	20	2	5,5*10^5	94	3,8*10^5	85
RLR3		1700	20	2	1,0*10^6	93	8,0*10^5	89
MAVS-K		1700	20	2	6,1*10^5	97	4,6*10^5	89
MAVS-L		1700	20	2	8,4*10^5	95	5,9*10^5	89
Kontroll		1700	20	2	1*10^6	93	1,1*10^6	87
					Diluted in 2mL DPBS			Diluted in 2mL DPBS

Table G2. Cell viability and cells/mL after measuring in automatic cell counter at Day 3 and Day 6 from "4.7.2 Determine siRNA effectivness" from A. salmon individual 1. Cells/mL and Cell viabilty are numbers directly from countess, but total cells are the total number of cells of each sample.

FISH 1	RBCs				Day 3			Day 6		
					Countess			Countess		
Well		Voltage (V)	Width (ms)	Number of pi	*Cells/mL*	*Cell Viability*	*Total Cells*	*Cells/mL*	*Cell Viability*	*Total Cells*
TLR3		1700	20	2	430000,00	84,00	6450000,00	570000,00	86	8550000
RIG-I		1700	20	2	410000,00	72,00	6150000,00	530000,00	78	7950000
RLR3		1700	20	2	460000,00	85,00	6900000,00	580000,00	77	8700000
MAVS-K		1700	20	2	590000,00	83,00	8850000,00	650000,00	77	9750000
Tkontroll		1700	20	2	570000,00	76,00	8550000,00	720000,00	80	10800000
Kontroll		1700	20	2	1300000,00	92,00	19500000,00	1300000,00	90	19500000

Table G3. Cell viability and cells/mL after measuring in automatic cell counter at Day 3 and Day 6 from "4.7.2 Determine siRNA effectivness" from A. salmon individual 2. Cells/mL and Cell viabilty are numbers directly from countess, but total cells are the total number of cells of each sample.

FISH 2	RBCs				Day 3			Day 6		
					Countess			Countess		
Well		Voltage (V)	Width (ms)	Number of pi	*Cells/mL*	*Cell Viability*	*Total Cells*	*Cells/mL*	*Cell Viability*	*Total Cells*
TLR3		1700	20	2	530000,00	82	7950000	660000,00	92	9900000
RIG-I		1700	20	2	520000,00	95	7800000	1300000,00	94	19500000
RLR3		1700	20	2	660000,00	93	9900000	800000,00	92	12000000
MAVS-K		1700	20	2	1100000,00	97	16500000	760000,00	92	11400000
Tkontroll		1700	20	2	560000,00	97	8400000	1100000,00	95	16500000
Kontroll		1700	20	2	370000,00	96	5550000	1600000,00	93	24000000

Table G4. Cell viability and cells/mL after measuring in automatic cell counter at Day 3 and Day 6 from "4.7.2 Determine siRNA effectivness" from A. salmon individual 3. Cells/mL and Cell viabilty are numbers directly from countess, but total cells are the total number of cells of each sample.

FISH 3	RBCs				Day 3			Day 6		
					Countess			Countess		
Well		Voltage (V)	Width (ms)	Number of pu	Cells/mL	Cell Viability	Total Cells	Cells/mL	Cell Viability	Total Cells
TLR3		1700	20	2	530000,00	88	7950000	740000,00	63	11100000
RIG-I		1700	20	2	700000,00	91	10500000	1600000,00	65	24000000
RLR3		1700	20	2	530000,00	91	7950000	490000,00	87	7350000
MAVS-K		1700	20	2	720000,00	87	10800000	940000,00	89	14100000
Tkontroll		1700	20	2	1100000,00	77	16500000	1300000,00	75	19500000
Kontroll		1700	20	2	410000,00	71	6150000	1700000,00	95	25500000

Table G5. Cell viability and cells/mL after measuring in automatic cell counter at Day 3 and Day 6 from "4.8 siRNA silencing of TLR3, RIG-I, RLR3 and MAVS – test of effects on poly(I:C) stimulation" from A. salmon individual 1. Cells/mL and Cell viabilty are numbers directly from countess, but total cells are the total number of cells of each sample.

FISH 1	RBCs				Day 3			Day 6			Day 6 - Poly I:C		
					Countess			Countess			Countess		
Well		Voltage (V)	Width (ms)	Number of p	Cells/mL	Cell Viability	Total cells	Cells/mL	Cell Viability	Total cells	Cells/mL	Cell Viability	Total cells
TLR3		1700	20	2	330000,00	78,00	4950000,00	1100000,00	94,00	16500000	810000,00	92,00	12150000
RIG-I		1700	20	2	130000,00	60,00	1950000,00	570000,00	92,00	8550000	600000,00	91,00	9000000
RLR3		1700	20	2	250000,00	88,00	3750000,00	120000,00	84,00	1800000	720000,00	86,00	10800000
MAVS-K		1700	20	2	460000,00	94,00	6900000,00	510000,00	91,00	7650000	770000,00	86,00	11550000
Tkontroll		1700	20	2	370000,00	83,00	5550000,00	120000,00	62,00	1800000			
Kontroll		1700	20	2	520000,00	93,00	7800000,00	8000000,00	92,00	120000000			

Table G6. Cell viability and cells/mL after measuring in automatic cell counter at Day 3 and Day 6 from "4.8 siRNA silencing of TLR3, RIG-I, RLR3 and MAVS – test of effects on poly(I:C) stimulation" from A. salmon individual 2. Cells/mL and Cell viabilty are numbers directly from countess, but total cells are the total number of cells of each sample.

FISH 2	RBCs				Day 3			Day 6			Day 6 - Poly I:C		
					Countess			Countess			Countess		
Well		Voltage (V)	Width (ms)	Number of p	Cells/mL	Cell Viability	Cells original	Cells/mL	Cell Viability	Cells/mL	Cells/mL	Cell Viability	Cells/mL
TLR3		1700	20	2	670000,00	95,00	10050000,00	1300000,00	89,00	19500000	980000,00	91,00	14700000
RIG-I		1700	20	2	360000,00	87,00	5400000,00	280000,00	80,00	4200000	420000,00	91,00	6300000
RLR3		1700	20	2	110000,00	88,00	1650000,00	160000,00	75,00	2400000	70000,00	100,00	1050000
MAVS-K		1700	20	2	80000,00	62,00	1200000,00	80000,00	48,00	1200000	70000,00	78,00	1050000
Tkontroll		1700	20	2	270000,00	92,00	4050000,00	60000,00	73,00	900000			
Kontroll		1700	20	2	920000,00	92,00	13800000,00	1900000,00	87,00	28500000			

Table G7. Cell viability and cells/mL after measuring in automatic cell counter at Day 3 and Day 6 from "4.8 siRNA silencing of TLR3, RIG-I, RLR3 and MAVS – test of effects on poly(I:C) stimulation" from A. salmon individual 3. Cells/mL and Cell viabilty are numbers directly from countess, but total cells are the total number of cells of each sample.

FISH 3	RBCs				Day 3			Day 6			Day 6 - Poly I:C		
					Countess			Countess			Countess		
Well		Voltage (V)	Width (ms)	Number of p	Cells/mL	Cell Viability	Cells original	Cells/mL	Cell Viability	Cells/mL	Cells/mL	Cell Viability	Cells/mL
TLR3		1700	20	2	380000,00	85,00	5700000,00	400000,00	82,00	6000000	840000,00	92,00	12600000
RIG-I		1700	20	2	590000,00	94,00	8850000,00	1700000,00	83,00	25500000	1600000,00	85,00	24000000
RLR3		1700	20	2	910000,00	89,00	13650000,00	600000,00	83,00	9000000	340000,00	91,00	5100000
MAVS-K		1700	20	2	200000,00	84,00	3000000,00	310000,00	80,00	4650000	230000,00	79,00	3450000
Tkontroll		1700	20	2	310000,00	94,00	4650000,00	330000,00	96,00	4950000			
Kontroll		1700	20	2	1000000,00	83,00	15000000,00	940000,00	83,00	14100000,00			

H – RNA extraction and quantification

Table H1. RNA concentration, 260/280-ratio and 260/230-ratio of the RNA from "4.7.1 Testing knock-down efficiency and responses to transfection at different time points". Volume (µL) of RNA and RNase-free water used for each sample, to gain a cocentration of 10 ng/µL, is shown in the two right-most coloumns.

Sample ID cDNA	Well	RNA Conc. (ng/ul)	(A260/A280)	(A260/A230)	RNA	Water
D1.TLR3	A3	18,20	2,046	1,327	5,5	4,5
D1.RIGI	B3	10,52	2,146	1,170	9,5	0,5
D1.RLR3	C3	14,94	2,033	1,220	6,7	3,3
D1.MAVSK	D3	10,29	1,97	0,977	9,7	0,3
D1.MAVSL	E3	11,35	1,986	1,13	8,8	1,2
D1.Con	G3	20,90	2,081	1,552	4,8	5,2
D3.TLR3	H3	12,98	2,092	1,639	7,7	2,3
D3.RIGI	A4	10,20	1,736	0,839	9,8	0,2
D3.RLR3	B4	15,59	2,054	1,29	6,4	3,6
D3.MAVSK	C4	13,22	2,025	1,095	7,6	2,4
D3.MAVSL	D4	11,67	2,043	1,126	8,6	1,4
D3.Con	F4	17,71	2,047	1,199	5,6	4,4
D6.TLR3	G4	15,43	2,077	1,410	6,5	3,5
D6.RIGI	H4	5,88	1,756	1,059	17,0	-7,0
D6.RLR3	A5	14,37	2,05	0,936	7,0	3,0
D6.MAVSK	B5	10,04	2,2	1,053	10,0	0,0
D6.MAVSL	C5	10,69	2,015	0,541	9,4	0,6
D6.Con	E5	13,63	2,012	1,201	3,7	6,3

Table H2 RNA concentration, 260/280-ratio and 260/230-ratio of the RNA from "4.7.2 Determine siRNA effectiveness". Volume (µL) of RNA and RNase-free water used for each sample, to gain a cocentration of 10 ng/µL, is shown in the two right-most coloumns.

Sample ID cDNA	Well	RNA Conc. (ng/ul)	(A260/A280)	(A260/A230)	RNA	Water
F1.D3.TLR3	A1	21,71	2,046	1,385	4,6	5,4
F1.D3.RIGI	B1	21,22	2,114	1,566	4,7	5,3
F1.D3.RLR3	C1	17,8	2,096	1,557	5,6	4,4
F1.D3.MAVS	D1	17,71	2,149	1,682	5,6	4,4
F1.D3.TKON	E1	20,65	2,108	1,543	4,8	5,2
F1.D3.KON	F1	43,59	2,127	1,88	2,3	7,7
F2.D3.TLR3	G1	12,49	2,068	0,8947	8,0	2,0
F2.D3.RIGI	H1	14,37	2,047	1,586	7,0	3,0
F2.D3.RLR3	A2	23,43	1,952	1,341	4,3	5,7
F2.D3.MAVS	B2	27,92	2,085	1,685	3,6	6,4
F2.D3.TKON	C2	27,18	2,094	1,448	3,7	6,3
F2.D3.KON	D2	53,88	2,025	1,575	1,9	8,1
F3.D3.TLR3	E2	17,22	2,069	1,379	5,8	4,2
F3.D3.RIGI	F2	21,06	2,048	1,277	4,7	5,3
F3.D3.RLR3	G2	16,98	2,059	1,253	5,9	4,1
F3.D3.MAVS	H2	22,45	2,037	1,687	4,5	5,5
F3.D3.TKON	A3	25,63	2,093	1,688	3,9	6,1
F3.D3.KON	B3	33,96	2,144	1,755	2,9	7,1
F1.D6.TLR3	C3	17,88	2,086	1,576	5,6	4,4
F1.D6.RIGI	D3	12,08	2,056	1,41	8,3	1,7
F1.D6.RLR3	E3	28,82	2,277	1,093	3,5	6,5
F1.D6.MAVS	F3	15,1	2,056	1,555	6,6	3,4
F1.D6.TKON	G3	16,73	2,135	1,424	6,0	4,0
F1.D6.KON	H3	38,45	2,039	2,057	2,6	7,4
F2.D6.TLR3	A4	16,49	1,924	1,058	6,1	3,9
F2.D6.RIGI	B4	18,12	2,114	1,337	5,5	4,5
F2.D6.RLR3	C4	22,29	2,1	1,372	4,5	5,5
F2.D6.MAVS	D4	24	2,07	1,455	4,2	5,8
F2.D6.TKON	E4	34,61	2,131	1,82	2,9	7,1
F2.D6.KON	F4	44,9	2,124	1,833	2,2	7,8
F3.D6.TLR3	G4	16,65	2,082	1,275	6,0	4,0
F3.D6.RIGI	H4	15,76	2,053	1,532	6,3	3,7
F3.D6.RLR3	A5	14,53	2,07	1,29	6,9	3,1
F3.D6.MAVS	B5	20,65	2,144	1,654	4,8	5,2
F3.D6.TKON	C5	29,47	2,087	1,861	3,4	6,6
F3.D6.KON	D5	33,55	2,097	2,025	3,0	7,0

Table H3. RNA concentration, 260/280-ratio and 260/230-ratio of the RNA from "4.8 siRNA silencing of TLR3, RIG-I, RLR3 and MAVS – test of effects on poly(I:C) stimulation". Volume (µL) of RNA and RNase-free water used for each sample, to gain a cocentration of 5 ng/µL, is shown in the two right-most coloumns. Yellow-rows were quantified again in NanoDrop One because of bad-purity in RNA-sample.

Sample ID cDNA	Well	RNA Conc. (ng/ul)	(A260/A280)	(A260/A230)	Water	RNA
F1.D3.TLR3	A1	21,63	2,137	1,699	7,7	2,3
F1.D3.RIGI	B1	15,92	2,191	1,773	6,9	3,1
F1.D3.RLR3	C1	18,2	2,104	1,973	7,3	2,7
F1.D3.MAVS	D1	18,78	2,11	2,018	7,3	2,7
F1.D3.TKON	E1	12,08	2,114	1,626	5,9	4,1
F1.D3.KON	F1	40,73	2,123	2,105	8,8	1,2
F2.D3.TLR3	G1	19,02	2,100	1,991	7,4	2,6
F2.D3.RIGI	H1	14,2	2,071	1,776	6,5	3,5
F2.D3.RLR3	A2	12,65	2,162	0,9118	6,0	4,0
F2.D3.MAVS	B2	9,551	2,127	0,9669	4,8	5,2
F2.D3.TKON	C2	13,71	2,154	1,191	6,4	3,6
F2.D3.KON	D2	29,47	2,124	1,633	8,3	1,7
F3.D3.TLR3	E2	18,45	2,112	1,439	7,3	2,7
F3.D3.RIGI	F2	26,12	2	1,517	8,1	1,9
F3.D3.RLR3	G2	13,8	2,086	1,119	6,4	3,6
F3.D3.MAVS	H2	12,41	2,111	1,267	6,0	4,0
F3.D3.TKON	A3	26,61	2,159	1,895	8,1	1,9
F3.D3.KON	B3	41,8	2,169	2,169	8,8	1,2
F1.D6.TLR3	C3	16,65	2,103	1,759	7,0	3,0
F1.D6.RIGI	D3	10,3	2,001	1,44	5,1	4,9
F1.D6.RLR3	E3	12,57	2,081	1,556	6,0	4,0
F1.D6.MAVS	F3	12,57	2,139	1,791	6,0	4,0
F1.D6.TKON	G3	7,347	2	1,233	3,2	6,8
F1.D6.KON	H3	30,86	2,088	2,088	8,4	1,6
F2.D6.TLR3	A4	18,61	2,073	1,365	7,3	2,7
F2.D6.RIGI	B4	13,47	2,143	1,447	6,3	3,7
F2.D6.RLR3	C4	6,612	2,132	0,871	2,4	7,6
F2.D6.MAVS	D4	5,061	2,067	0,7126	0,1	9,9
F2.D6.TKON	E4	10,1	1,95	1,13	5,0	5,0
F2.D6.KON	F4	21,55	2,079	1,475	7,7	2,3
F3.D6.TLR3	G4	12,16	2,069	1,231	5,9	4,1
F3.D6.RIGI	H4	17,22	2,049	1,407	7,1	2,9
F3.D6.RLR3	A5	14,2	1,99	1,5	6,5	3,5
F3.D6.MAVS	B5	8,2	1,92	0,86	3,9	6,1
F3.D6.TKON	C5	22,53	2,156	1,828	7,8	2,2
F3.D6.KON	D5	28,82	2,139	2,206	8,3	1,7
F1.D6.TLR3.poly	E5	14,29	1,902	1,591	6,5	3,5
F1.D6.RIGI.poly	F5	10,69	2,148	1,578	5,3	4,7
F1.D6.RLR3.poly	G5	15,59	2,054	1,326	6,8	3,2
F1.D6.MAVS.poly	H5	16,08	2,118	1,589	6,9	3,1
F2.D6.TLR3.poly	A6	20,16	1,945	1,307	7,5	2,5
F2.D6.RIGI.poly	B6	11,6	2,011	1,03	5,7	4,3
F2.D6.RLR3.poly	C6	6,367	2,364	0,9286	2,1	7,9
F2.D6.MAVS.poly	D6	5,8	2	0,6	1,4	8,6
F3.D6.TLR3.poly	E6	11,18	2,141	1,28	5,5	4,5
F3.D6.RIGI.poly	F6	16,57	2,071	1,18	7,0	3,0
F3.D6.RLR3.poly	G6	9,714	2,125	1,044	4,9	5,1
F3.D6.MAVS.poly	H6	8,408	2,06	1,03	4,1	5,9

I – qPCR

Yellow row represents values in which had a Ct-value of EF1α higher than average, or not achieved (“NA”). Values were considered representative or not, and if not representative, they were marked as grey-points.

a)

siRNA-primer	Day	Ct	Average
Kontroll-EFa	Day 1	20,64	
Kontroll-EFa	Day 1	20,67	20,65
TLR3-EFa	Day 1	21,94	
TLR3-EFa	Day 1	21,58	21,76
RIGI-EFa	Day 1	21,96	
RIGI-EFa	Day 1	22,00	21,98
RLR3-EFa	Day 1	32,18	
RLR3-EFa	Day 1	31,78	31,98
MAVSK-EFa	Day 1	23,32	
MAVSK-EFa	Day 1	23,29	23,30
MAVSL-EFa	Day 1	22,34	
MAVSL-EFa	Day 1	22,33	22,33

b)

siRNA-primer	Day	Ct	Average
Kontroll-TLR3	Day 1	26,53	
Kontroll-TLR3	Day 1	24,05	25,29
TLR3-TLR3	Day 1	27,93	
TLR3-TLR3	Day 1	27,26	27,60
RIGI-TLR3	Day 1	28,13	
RIGI-TLR3	Day 1	27,77	27,95
RLR3-TLR3	Day 1		
RLR3-TLR3	Day 1		
MAVSK-TLR3	Day 1	29,00	
MAVSK-TLR3	Day 1	29,26	29,13
MAVSL-TLR3	Day 1	26,77	
MAVSL-TLR3	Day 1	26,15	26,46

c)

siRNA-primer	Day	Ct	Average
Kontroll-RIGI	Day 1	25,65	
Kontroll-RIGI	Day 1	25,80	25,72
TLR3-RIGI	Day 1	26,56	
TLR3-RIGI	Day 1	26,36	26,46
RIGI-RIGI	Day 1	26,81	
RIGI-RIGI	Day 1	26,88	26,85
RLR3-RIGI	Day 1		
RLR3-RIGI	Day 1		
MAVSK-RIGI	Day 1	27,13	
MAVSK-RIGI	Day 1	27,11	27,12
MAVSL-RIGI	Day 1	24,31	
MAVSL-RIGI	Day 1	24,37	24,34

d)

siRNA-primer	Day	Ct	Average
Kontroll-RLR3	Day 1	24,61	
Kontroll-RLR3	Day 1	24,69	24,65
TLR3-RLR3	Day 1	24,40	
TLR3-RLR3	Day 1	24,11	24,25
RIGI-RLR3	Day 1	24,45	
RIGI-RLR3	Day 1	24,01	24,23
RLR3-RLR3	Day 1		
RLR3-RLR3	Day 1		
MAVSK-RLR3	Day 1	25,13	
MAVSK-RLR3	Day 1	25,18	25,15
MAVSL-RLR3	Day 1	22,19	
MAVSL-RLR3	Day 1	21,95	22,07

e)

siRNA-primer	Day	Ct	Average
Kontroll-MAVS	Day 1	32,48	
Kontroll-MAVS	Day 1	30,22	31,35
TLR3-MAVS	Day 1	30,04	
TLR3-MAVS	Day 1	30,66	30,35
RIGI-MAVS	Day 1	30,32	
RIGI-MAVS	Day 1	30,17	30,25
RLR3-MAVS	Day 1		
RLR3-MAVS	Day 1		
MAVSK-MAVS	Day 1	32,58	
MAVSK-MAVS	Day 1	32,38	32,48
MAVSL-MAVS	Day 1	30,97	
MAVSL-MAVS	Day 1	30,92	30,94

f)

siRNA - primer	Day 1	Ct	Average
Kontroll-MX	Day 1	26,04	
Kontroll-MX	Day 1	25,91	25,97
TLR3-MX	Day 1	26,80	
TLR3-MX	Day 1	26,56	26,68
RIGI-MX	Day 1	27,36	
RIGI-MX	Day 1	26,90	27,13
RLR3-MX	Day 1		
RLR3-MX	Day 1		
MAVSK-MX	Day 1	28,84	
MAVSK-MX	Day 1	28,73	28,79
MAVSL-MX	Day 1	25,41	
MAVSL-MX	Day 1	25,14	25,27

g)

siRNA-primer	Day	Ct	Average
Kontroll-ISG15	Day 1	26,04	
Kontroll-ISG15	Day 1	25,96	26,00
TLR3-ISG15	Day 1	26,49	
TLR3-ISG15	Day 1	26,10	26,30
RIGI-ISG15	Day 1	25,69	
RIGI-ISG15	Day 1	25,66	25,68
RLR3-ISG15	Day 1		
RLR3-ISG15	Day 1		
MAVSK-ISG15	Day 1	27,24	
MAVSK-ISG15	Day 1	27,13	27,18
MAVSL-ISG15	Day 1	21,47	
MAVSL-ISG15	Day 1	21,48	21,48

Figure I1. Ct-values at Day 1 from “Testing knowck-down efficiency and responses to transfection at different time points”) a) EF1α. b) TLR3. c) RIG-I. d) RLR3. e) MAVS. f) Mx. g) ISG15

a)

siRNA-primer	Day	Ct	Average
Kontroll-EFa	Day 3	21,41	
Kontroll-EFa	Day 3	21,17	21,29
TLR3-EFa	Day 3	22,16	
TLR3-EFa	Day 3	21,75	21,95
RIGI-EFa	Day 3	22,58	
RIGI-EFa	Day 3	21,86	22,22
RLR3-EFa	Day 3	21,39	
RLR3-EFa	Day 3	21,55	21,47
MAVSK-EFa	Day 3	23,08	
MAVSK-EFa	Day 3	22,46	22,77
MAVSL-EFa	Day 3	21,90	
MAVSL-EFa	Day 3	21,31	21,60

b)

siRNA-primer	Day	Ct	Average
Kontroll-TLR3	Day 3	26,39	
Kontroll-TLR3	Day 3	26,21	26,30
TLR3-TLR3	Day 3	27,21	
TLR3-TLR3	Day 3	27,07	27,14
RIGI-TLR3	Day 3	28,63	
RIGI-TLR3	Day 3	27,80	28,21
RLR3-TLR3	Day 3	27,10	
RLR3-TLR3	Day 3	27,04	27,07
MAVSK-TLR3	Day 3	29,80	
MAVSK-TLR3	Day 3	29,46	29,63
MAVSL-TLR3	Day 3	27,07	
MAVSL-TLR3	Day 3	26,41	26,74

c)

siRNA-primer	Day	Ct	Average
Kontroll-RIGI	Day 3	25,80	
Kontroll-RIGI	Day 3	25,81	25,81
TLR3-RIGI	Day 3	25,64	
TLR3-RIGI	Day 3	25,42	25,53
RIGI-RIGI	Day 3	27,14	
RIGI-RIGI	Day 3	26,80	26,97
RLR3-RIGI	Day 3	25,72	
RLR3-RIGI	Day 3	25,37	25,54
MAVSK-RIGI	Day 3	29,05	
MAVSK-RIGI	Day 3	28,04	28,54
MAVSL-RIGI	Day 3	24,28	
MAVSL-RIGI	Day 3	23,46	23,87

d)

siRNA-primer	Day	Ct	Average
Kontroll-RLR3	Day 3	24,89	
Kontroll-RLR3	Day 3	24,51	24,70
TLR3-RLR3	Day 3	23,39	
TLR3-RLR3	Day 3	23,05	23,22
RIGI-RLR3	Day 3	23,43	
RIGI-RLR3	Day 3	23,18	23,31
RLR3-RLR3	Day 3	23,03	
RLR3-RLR3	Day 3	22,65	22,84
MAVSK-RLR3	Day 3	24,59	
MAVSK-RLR3	Day 3	24,18	24,38
MAVSL-RLR3	Day 3	21,44	
MAVSL-RLR3	Day 3	21,44	21,44

e)

siRNA-primer	Day	Ct	Average
Kontroll-MAVS	Day 3	29,36	
Kontroll-MAVS	Day 3	28,10	28,73
TLR3-MAVS	Day 3	36,78	
TLR3-MAVS	Day 3	32,59	34,69
RIGI-MAVS	Day 3	30,01	
RIGI-MAVS	Day 3	30,85	30,43
RLR3-MAVS	Day 3	29,84	
RLR3-MAVS	Day 3	29,91	29,88
MAVSK-MAVS	Day 3	34,02	
MAVSK-MAVS	Day 3	34,66	34,34
MAVSL-MAVS	Day 3	30,59	
MAVSL-MAVS	Day 3	31,00	30,79

f)

siRNA-primer	Day	Ct	Average
Kontroll-MX	Day 3	27,07	
Kontroll-MX	Day 3	26,94	27,00
TLR3-MX	Day 3	26,30	
TLR3-MX	Day 3	26,09	26,19
RIGI-MX	Day 3	27,32	
RIGI-MX	Day 3	27,39	27,35
RLR3-MX	Day 3	26,06	
RLR3-MX	Day 3	26,14	26,10
MAVSK-MX	Day 3	28,57	
MAVSK-MX	Day 3	28,52	28,55
MAVSL-MX	Day 3	22,80	
MAVSL-MX	Day 3	23,08	22,94

g)

siRNA-primer	Day	Ct	Average
Kontroll-ISG15	Day 3	27,23	
Kontroll-ISG15	Day 3	27,15	27,19
TLR3-ISG15	Day 3	24,96	
TLR3-ISG15	Day 3	24,60	24,78
RIGI-ISG15	Day 3	25,14	
RIGI-ISG15	Day 3	24,92	25,03
RLR3-ISG15	Day 3	24,42	
RLR3-ISG15	Day 3	24,05	24,24
MAVSK-ISG15	Day 3	26,83	
MAVSK-ISG15	Day 3	26,31	26,57
MAVSL-ISG15	Day 3	19,40	
MAVSL-ISG15	Day 3	19,01	19,20

Figure I2. Ct-values at Day 3 from "Testing knowck-down efficiency and responses to transfection at different time points") a) EF1α. b) TLR3. c) RIG-I. d) RLR3. e) MAVS. f) Mx. g) ISG15

a)

siRNA-prime	Day	Ct	Average
KTRL-EFa	Day 6	22,65	
KTRL-EFa	Day 6	22,53	22,59
TLR3-EFa	Day 6	21,46	
TLR3-EFa	Day 6	21,30	21,38
RIGI-EFa	Day 6	22,89	
RIGI-EFa	Day 6	22,82	22,85
RLR3-EFa	Day 6	22,21	
RLR3-EFa	Day 6	22,15	22,18
MAVSK-EFa	Day 6	22,74	
MAVSK-EFa	Day 6	22,62	22,68
MAVSL-EFa	Day 6	22,14	
MAVSL-EFa	Day 6	22,06	22,10

b)

siRNA-prime	Day	Ct	Average
KTRL-TLR3	Day 6	28,57	28,57
TLR3-TLR3	Day 6	26,14	
TLR3-TLR3	Day 6	25,98	26,06
RIGI-TLR3	Day 6	28,52	28,52
RLR3-TLR3	Day 6	27,37	27,37
MAVSK-TLR	Day 6	27,39	27,39
MAVSL-TLR	Day 6	25,48	25,48

c)

siRNA-prime	Day	Ct	Average
KTRL-RIGI	Day 6	29,29	
KTRL-RIGI	Day 6	29,47	29,38
TLR3-RIGI	Day 6	27,01	
TLR3-RIGI	Day 6	25,33	26,17
RIGI-RIGI	Day 6	29,02	
RIGI-RIGI	Day 6	28,61	28,82
RLR3-RIGI	Day 6	27,05	
RLR3-RIGI	Day 6	26,73	26,89
MAVSK-RIG	Day 6	27,64	
MAVSK-RIG	Day 6	27,32	27,48
MAVSL-RIG	Day 6	24,15	
MAVSL-RIG	Day 6	24,01	24,08

d)

siRNA-prime	Day	Ct	Average
KTRL-RLR3	Day 6	26,32	
KTRL-RLR3	Day 6	26,31	26,31
TLR3-RLR3	Day 6	23,54	
TLR3-RLR3	Day 6	23,05	23,30
RIGI-RLR3	Day 6	25,21	
RIGI-RLR3	Day 6	24,80	25,00
RLR3-RLR3	Day 6	23,99	
RLR3-RLR3	Day 6	24,03	24,01
MAVSK-RLF	Day 6	24,28	
MAVSK-RLF	Day 6	24,34	24,31
MAVSL-RLF	Day 6	22,40	
MAVSL-RLF	Day 6	22,21	22,30

e)

siRNA-prime	Day	Ct	Average
KTRL-MAVS	Day 6	27,40	
KTRL-MAVS	Day 6	27,42	27,41
TLR3-MAVS	Day 6	26,30	
TLR3-MAVS	Day 6	26,17	26,24
RIGI-MAVS	Day 6	28,12	
RIGI-MAVS	Day 6	28,11	28,12
RLR3-MAVS	Day 6	27,02	
RLR3-MAVS	Day 6	27,38	27,20
MAVSK-MA	Day 6	27,06	
MAVSK-MA	Day 6	26,94	27,00
MAVSL-MA	Day 6	26,95	
MAVSL-MA	Day 6	27,09	27,02

f)

siRNA-prime	Day	Ct	Average
KTRL-MX	Day 6	29,63	
KTRL-MX	Day 6	29,42	29,52
TLR3-MX	Day 6	25,78	
TLR3-MX	Day 6	25,16	25,47
RIGI-MX	Day 6	29,36	
RIGI-MX	Day 6	28,78	29,07
RLR3-MX	Day 6	26,91	
RLR3-MX	Day 6	26,47	26,69
MAVSK-MX	Day 6	27,96	
MAVSK-MX	Day 6	28,10	28,03
MAVSL-MX	Day 6	22,84	
MAVSL-MX	Day 6	22,71	22,77

g)

siRNA-prime	Day	Ct	Average
KTRL-ISG15	Day 6	29,29	
KTRL-ISG15	Day 6	29,69	29,49
TLR3-ISG15	Day 6	24,22	
TLR3-ISG15	Day 6	23,80	24,01
RIGI-ISG15	Day 6	25,60	
RIGI-ISG15	Day 6	25,61	25,60
RLR3-ISG15	Day 6	25,04	
RLR3-ISG15	Day 6	24,88	24,96
MAVSK-ISG	Day 6	26,46	
MAVSK-ISG	Day 6	26,46	26,46
MAVSL-ISG	Day 6	19,15	
MAVSL-ISG	Day 6	19,29	19,22

Figure I3. Ct-values at Day 6 from "Testing knowck-down efficiency and responses to transfection at different time points") a) EF1α. b) TLR3. c) RIG-I. d) RLR3. e) MAVS. f) Mx. g) ISG15

a)

siRNA-primer	Fish-Day	Ct	Average
Kontroll-EFa	F1-day 3	21,43	
Kontroll-EFa	F1-day 3	21,30	21,37
TLR3-EFa	F1-day 3	22,20	
TLR3-EFa	F1-day 3	22,00	22,10
RIGI-EFa	F1-day 3	24,75	
RIGI-EFa	F1-day 3	24,79	24,77
RLR3-EFa	F1-day 3	22,05	
RLR3-EFa	F1-day 3	21,96	22,01
MAVS-EFa	F1-day 3	24,54	
MAVS-EFa	F1-day 3	24,68	24,61
TK-EFa	F1-day 3	22,32	
TK-EFa	F1-day 3	22,08	22,20

b)

siRNA-primer	Fish-Day	Ct	Average
Kontroll-TLR3	F1-day 3	27,30	
Kontroll-TLR3	F1-day 3	27,35	27,33
TLR3-TLR3	F1-day 3	27,13	
TLR3-TLR3	F1-day 3	26,61	26,87
RIGI-TLR3	F1-day 3	30,43	
RIGI-TLR3	F1-day 3	30,07	30,25
RLR3-TLR3	F1-day 3	28,92	
RLR3-TLR3	F1-day 3	28,37	28,64
MAVS-TLR3	F1-day 3	29,72	
MAVS-TLR3	F1-day 3	29,73	29,73
TK-TLR3	F1-day 3	28,39	
TK-TLR3	F1-day 3	27,56	27,98

c)

siRNA-primer	Fish-Day	Ct	Average
Kontroll-RIGI	F1-day 3	26,04	
Kontroll-RIGI	F1-day 3	25,87	25,96
TLR3-RIG-I	F1-day 3	26,24	
TLR3-RIG-I	F1-day 3	24,90	25,57
RIGI-RIGI	F1-day 3	28,61	
RIGI-RIGI	F1-day 3	28,32	28,46
RLR3-RIGI	F1-day 3	25,75	
RLR3-RIGI	F1-day 3	25,82	25,79
MAVS-RIGI	F1-day 3	28,07	
MAVS-RIGI	F1-day 3	27,98	28,02
TK-RIGI	F1-day 3	26,84	
TK-RIGI	F1-day 3	26,59	26,72

d)

siRNA-primer	Fish-Day	Ct	Average
Kontroll-RLR3	F1-day 3	25,27	
Kontroll-RLR3	F1-day 3	26,32	25,80
TLR3-RLR3	F1-day 3	23,36	
TLR3-RLR3	F1-day 3	23,12	23,24
RIGI-RLR3	F1-day 3	26,91	
RIGI-RLR3	F1-day 3	26,47	26,69
RLR3-RLR3	F1-day 3	24,46	
RLR3-RLR3	F1-day 3	24,40	24,43
MAVS-RLR3	F1-day 3	26,46	
MAVS-RLR3	F1-day 3	26,40	26,43
TK-RLR3	F1-day 3	23,94	
TK-RLR3	F1-day 3	23,72	23,83

e)

siRNA-primer	Fish-Day	Ct	Average
Kontroll-MAVS	F1-day 3	27,61	
Kontroll-MAVS	F1-day 3	26,70	27,16
TLR3-MAVS	F1-day 3	27,29	
TLR3-MAVS	F1-day 3	27,08	27,19
RIGI-MAVS	F1-day 3	30,45	
RIGI-MAVS	F1-day 3	30,63	30,54
RLR3-MAVS	F1-day 3	27,90	
RLR3-MAVS	F1-day 3	28,01	27,95
MAVS-MAVS	F1-day 3	30,54	
MAVS-MAVS	F1-day 3	30,35	30,44
TK-MAVS	F1-day 3	28,11	
TK-MAVS	F1-day 3	28,07	28,09

f)

siRNA-primer	Fish-Day	Ct	Average
Kontroll-MX	F1-day 3	26,11	
Kontroll-MX	F1-day 3	25,88	25,99
TLR3-MX	F1-day 3	25,69	
TLR3-MX	F1-day 3	25,59	25,64
RIGI-MX	F1-day 3	29,20	
RIGI-MX	F1-day 3	29,32	29,26
RLR3-MX	F1-day 3	25,75	
RLR3-MX	F1-day 3	25,16	25,46
MAVS-MX	F1-day 3	28,90	
MAVS-MX	F1-day 3	28,95	28,92
TK-MX	F1-day 3	27,31	
TK-MX	F1-day 3	27,20	27,25

g)

siRNA-primer	Fish-Day	Ct	Average
Kontroll-ISG15	F1-day 3	26,01	
Kontroll-ISG15	F1-day 3	25,78	25,89
TLR3-ISG15	F1-day 3	24,76	
TLR3-ISG15	F1-day 3	24,11	24,43
RIGI-ISG15	F1-day 3	28,22	
RIGI-ISG15	F1-day 3	28,07	28,15
RLR3-ISG15	F1-day 3	23,79	
RLR3-ISG15	F1-day 3	23,33	23,56
MAVS-ISG15	F1-day 3	28,25	
MAVS-ISG15	F1-day 3	28,10	28,17
TK-ISG15	F1-day 3	26,60	
TK-ISG15	F1-day 3	26,38	26,49

Figure I4. Ct-values from at Day 3 from "4.7.2 Determine siRNA effectiveness" for A. salmon 1 a) EF1α. b) TLR3. c) RIG-I. d) RLR3. e) MAVS. f) Mx. g) ISG15

a)

siRNA-primer	Fish - Day	Ct	Average
Kontroll-EFa	F1 day 6	21,65	
Kontroll-EFa	F1 day 6	21,54	21,60
TLR3-EFa	F1 day 6	23,18	
TLR3-EFa	F1 day 6	22,56	22,87
RIGI-EFa	F1 day 6	22,51	
RIGI-EFa	F1 day 6	21,60	22,06
RLR3-EFa	F1 day 6	22,89	
RLR3-EFa	F1 day 6	22,74	22,81
MAVS-EFa	F1 day 6	21,98	
MAVS-EFa	F1 day 6	21,70	21,84
TK-EFa	F1 day 6	21,93	
TK-EFa	F1 day 6	21,64	21,78

b)

siRNA-primer	Fish - Day	Ct	Average
Kontroll-TLR3	F1 day 6	26,95	
Kontroll-TLR3	F1 day 6	27,11	27,11
TLR3-TLR3	F1 day 6	27,48	
TLR3-TLR3	F1 day 6	28,52	28,52
RIGI-TLR3	F1 day 6	28,29	
RIGI-TLR3	F1 day 6	28,41	28,41
RLR3-TLR3	F1 day 6	29,61	
RLR3-TLR3	F1 day 6	29,66	29,66
MAVS-TLR3	F1 day 6	28,97	
MAVS-TLR3	F1 day 6	28,88	28,88
TK-TLR3	F1 day 6	26,71	
TK-TLR3	F1 day 6	26,43	26,43

c)

siRNA-primer	Fish - Day	Ct	Average
Kontroll-RIGI	F1 day 6	26,12	
Kontroll-RIGI	F1 day 6	26,12	26,12
TLR3-RIG-I	F1 day 6	26,38	
TLR3-RIG-I	F1 day 6	26,05	26,05
RIGI-RIGI	F1 day 6	27,53	
RIGI-RIGI	F1 day 6	27,36	27,36
RLR3-RIGI	F1 day 6	28,07	
RLR3-RIGI	F1 day 6	27,67	27,67
MAVS-RIGI	F1 day 6	27,21	
MAVS-RIGI	F1 day 6	26,59	26,59
TK-RIGI	F1 day 6	24,18	
TK-RIGI	F1 day 6	23,66	23,66

d)

siRNA-primer	Fish - Day	Ct	Average
Kontroll-RLR3	F1 day 6	24,51	
Kontroll-RLR3	F1 day 6	24,39	24,39
TLR3-RLR3	F1 day 6	24,44	
TLR3-RLR3	F1 day 6	24,56	24,56
RIGI-RLR3	F1 day 6	24,38	
RIGI-RLR3	F1 day 6	24,28	24,28
RLR3-RLR3	F1 day 6	25,52	
RLR3-RLR3	F1 day 6	25,69	25,69
MAVS-RLR3	F1 day 6	24,81	
MAVS-RLR3	F1 day 6	24,17	24,17
TK-RLR3	F1 day 6	22,97	
TK-RLR3	F1 day 6	22,94	22,94

e)

siRNA-primer	Fish - Day	Ct	Average
Kontroll-MAVS	F1 day 6	26,40	
Kontroll-MAVS	F1 day 6	26,37	26,38
TLR3-MAVS	F1 day 6	27,98	
TLR3-MAVS	F1 day 6	27,57	27,78
RIGI-MAVS	F1 day 6	27,21	
RIGI-MAVS	F1 day 6	27,28	27,24
RLR3-MAVS	F1 day 6	28,06	
RLR3-MAVS	F1 day 6	28,14	28,10
MAVS-MAVS	F1 day 6	27,15	
MAVS-MAVS	F1 day 6	27,11	27,13
TK-MAVS	F1 day 6	26,41	
TK-MAVS	F1 day 6	26,28	26,35

f)

siRNA-primer	Fish - Day	Ct	Average
Kontroll-MX	F1 day 6	27,17	
Kontroll-MX	F1 day 6	27,12	27,15
TLR3-MX	F1 day 6	26,54	
TLR3-MX	F1 day 6	26,24	26,39
RIGI-MX	F1 day 6	27,15	
RIGI-MX	F1 day 6	27,48	27,31
RLR3-MX	F1 day 6	26,64	
RLR3-MX	F1 day 6	26,52	26,58
MAVS-MX	F1 day 6	27,00	
MAVS-MX	F1 day 6	26,87	26,93
TK-MX	F1 day 6	23,69	
TK-MX	F1 day 6	23,62	23,66

g)

siRNA-primer	Fish - Day	Ct	Average
Kontroll-ISG15	F1 day 6	27,91	
Kontroll-ISG15	F1 day 6	27,77	27,84
TLR3-ISG15	F1 day 6	25,31	
TLR3-ISG15	F1 day 6	25,59	25,45
RIGI-ISG15	F1 day 6	25,78	
RIGI-ISG15	F1 day 6	26,00	25,89
RLR3-ISG15	F1 day 6	25,16	
RLR3-ISG15	F1 day 6	24,74	24,95
MAVS-ISG15	F1 day 6	25,63	
MAVS-ISG15	F1 day 6	25,68	25,66
TK-ISG15	F1 day 6	23,02	
TK-ISG15	F1 day 6	22,79	22,91

Figure I5. Ct-values from at Day 6 from "4.7.2 Determine siRNA effectiveness" for A. salmon 1 a) EF1α. b) TLR3. c) RIG-I. d) RLR3. e) MAVS. f) Mx. g) ISG15

a)

siRNA-primer	Fish-Day	Ct	Average
Kontroll-EFa	F2-day 3	21,29	
Kontroll-EFa	F2-day 3	21,31	21,30
TLR3-EFa	F2-day 3	24,19	
TLR3-EFa	F2-day 3	23,04	23,04
RIGI-EFa	F2-day 3	22,78	
RIGI-EFa	F2-day 3	22,24	22,51
RLR3-EFa	F2-day 3	22,03	
RLR3-EFa	F2-day 3	21,73	21,88
MAVS-EFa	F2-day 3	21,77	
MAVS-EFa	F2-day 3	21,36	21,57
TK-EFa	F2-day 3	21,39	
TK-EFa	F2-day 3	21,15	21,27

b)

siRNA-primer	Fish-Day	Ct	Average
Kontroll-TLR3	F2-day 3	28,27	
Kontroll-TLR3	F2-day 3	28,68	28,48
TLR3-TLR3	F2-day 3	28,65	
TLR3-TLR3	F2-day 3	28,38	28,52
RIGI-TLR3	F2-day 3	28,42	
RIGI-TLR3	F2-day 3	28,39	28,41
RLR3-TLR3	F2-day 3	29,19	
RLR3-TLR3	F2-day 3	28,30	28,74
MAVS-TLR3	F2-day 3	28,71	
MAVS-TLR3	F2-day 3	28,22	28,47
TK-TLR3	F2-day 3	30,36	
TK-TLR3	F2-day 3	29,60	29,98

c)

siRNA-primer	Fish-Day	Ct	Average
Kontroll-RIGI	F2-day 3	25,56	
Kontroll-RIGI	F2-day 3	25,57	25,57
TLR3-RIG-I	F2-day 3	26,01	
TLR3-RIG-I	F2-day 3	24,56	25,29
RIGI-RIGI	F2-day 3	24,94	
RIGI-RIGI	F2-day 3	24,46	24,70
RLR3-RIGI	F2-day 3	23,72	
RLR3-RIGI	F2-day 3	24,11	23,92
MAVS-RIGI	F2-day 3	24,27	
MAVS-RIGI	F2-day 3	23,45	23,86
TK-RIGI	F2-day 3	25,52	
TK-RIGI	F2-day 3	25,32	25,42

d)

siRNA-primer	Fish-Day	Ct	Average
Kontroll-RLR3	F2-day 3	25,07	
Kontroll-RLR3	F2-day 3	24,87	24,97
TLR3-RLR3	F2-day 3		
TLR3-RLR3	F2-day 3	24,02	24,02
RIGI-RLR3	F2-day 3	24,13	
RIGI-RLR3	F2-day 3	23,31	23,72
RLR3-RLR3	F2-day 3	23,05	
RLR3-RLR3	F2-day 3	22,43	22,74
MAVS-RLR3	F2-day 3	22,34	
MAVS-RLR3	F2-day 3	22,40	22,37
TK-RLR3	F2-day 3	23,86	
TK-RLR3	F2-day 3	23,40	23,63

e)

siRNA-primer	Fish-Day	Ct	Average
Kontroll-MAVS	F2-day 3	26,76	
Kontroll-MAVS	F2-day 3	26,34	26,55
TLR3-MAVS	F2-day 3	28,13	
TLR3-MAVS	F2-day 3	28,08	28,11
RIGI-MAVS	F2-day 3	27,51	
RIGI-MAVS	F2-day 3	27,36	27,43
RLR3-MAVS	F2-day 3	27,56	
RLR3-MAVS	F2-day 3	27,25	27,41
MAVS-MAVS	F2-day 3	27,11	
MAVS-MAVS	F2-day 3	26,80	26,96
TK-MAVS	F2-day 3	27,18	
TK-MAVS	F2-day 3	26,84	27,01

f)

siRNA-primer	Fish-Day	Ct	Average
Kontroll-MX	F2-day 3	25,24	
Kontroll-MX	F2-day 3	25,07	25,16
TLR3-MX	F2-day 3	24,33	
TLR3-MX	F2-day 3	23,89	24,11
RIGI-MX	F2-day 3	23,21	
RIGI-MX	F2-day 3	22,88	23,05
RLR3-MX	F2-day 3	21,70	
RLR3-MX	F2-day 3	21,46	21,58
MAVS-MX	F2-day 3	22,23	
MAVS-MX	F2-day 3	22,04	22,14
TK-MX	F2-day 3	23,92	
TK-MX	F2-day 3	23,90	23,91

g)

siRNA-primer	Fish-Day	Ct	Average
Kontroll-ISG15	F2-day 3	24,74	
Kontroll-ISG15	F2-day 3	24,85	24,80
TLR3-ISG15	F2-day 3	21,48	
TLR3-ISG15	F2-day 3	20,82	21,15
RIGI-ISG15	F2-day 3	21,04	
RIGI-ISG15	F2-day 3	20,58	20,81
RLR3-ISG15	F2-day 3	18,26	
RLR3-ISG15	F2-day 3	18,28	18,27
MAVS-ISG15	F2-day 3	19,63	
MAVS-ISG15	F2-day 3	19,84	19,74
TK-ISG15	F2-day 3	22,68	
TK-ISG15	F2-day 3	22,73	22,70

Figure I6. Ct-values from at Day 3 from "4.7.2 Determine siRNA effectiveness" for A. salmon 2 a) EF1α. b) TLR3. c) RIG-I. d) RLR3. e) MAVS. f) Mx. g) ISG15

a)

siRNA-primer	Fish - day	Ct	Average
Kontroll-EFa	F2 day 6	21,49	
Kontroll-EFa	F2 day 6	21,70	21,60
TLR3-EFa	F2 day 6	23,26	
TLR3-EFa	F2 day 6	22,85	23,05
RIGI-EFa	F2 day 6	22,65	
RIGI-EFa	F2 day 6	22,19	22,42
RLR3-EFa	F2 day 6	22,37	
RLR3-EFa	F2 day 6	22,79	22,58
MAVS-EFa	F2 day 6	22,02	
MAVS-EFa	F2 day 6	21,78	21,90
TK-EFa	F2 day 6	21,78	
TK-EFa	F2 day 6	21,49	21,63

b)

siRNA-primer	Fish - day	Ct	Average
Kontroll-TLR3	F2 day 6	27,97	
Kontroll-TLR3	F2 day 6	27,29	27,63
TLR3-TLR3	F2 day 6	28,19	
TLR3-TLR3	F2 day 6	28,16	28,17
RIGI-TLR3	F2 day 6	29,56	
RIGI-TLR3	F2 day 6	29,14	29,35
RLR3-TLR3	F2 day 6	30,97	
RLR3-TLR3	F2 day 6	30,03	30,50
MAVS-TLR3	F2 day 6	28,81	
MAVS-TLR3	F2 day 6	28,70	28,76
TK-TLR3	F2 day 6	27,96	
TK-TLR3	F2 day 6	27,72	27,84

c)

siRNA-primer	Fish - day	Ct	Average
Kontroll-RIGI	F2 day 6	24,49	
Kontroll-RIGI	F2 day 6	24,60	24,55
TLR3-RIG-I	F2 day 6	26,00	
TLR3-RIG-I	F2 day 6	25,54	25,77
RIGI-RIGI	F2 day 6	25,02	
RIGI-RIGI	F2 day 6	24,53	24,77
RLR3-RIGI	F2 day 6	24,11	
RLR3-RIGI	F2 day 6	23,58	23,84
MAVS-RIGI	F2 day 6	24,96	
MAVS-RIGI	F2 day 6	24,24	24,60
TK-RIGI	F2 day 6	24,81	
TK-RIGI	F2 day 6	24,47	24,64

d)

siRNA-primer	Fish - day	Ct	Average
Kontroll-RLR3	F2 day 6	23,54	
Kontroll-RLR3	F2 day 6	23,13	23,33
TLR3-RLR3	F2 day 6	24,67	
TLR3-RLR3	F2 day 6	24,04	24,36
RIGI-RLR3	F2 day 6	23,47	
RIGI-RLR3	F2 day 6	23,03	23,25
RLR3-RLR3	F2 day 6	23,15	
RLR3-RLR3	F2 day 6	22,19	22,67
MAVS-RLR3	F2 day 6	23,26	
MAVS-RLR3	F2 day 6	23,23	23,25
TK-RLR3	F2 day 6	23,01	
TK-RLR3	F2 day 6	23,11	23,06

e)

siRNA-primer	Fish - day	Ct	Average
Kontroll-MAVS	F2 day 6	26,12	
Kontroll-MAVS	F2 day 6	25,52	25,82
TLR3-MAVS	F2 day 6	27,93	
TLR3-MAVS	F2 day 6	27,55	27,74
RIGI-MAVS	F2 day 6	26,13	
RIGI-MAVS	F2 day 6	26,27	26,20
RLR3-MAVS	F2 day 6	26,11	
RLR3-MAVS	F2 day 6	26,10	26,10
MAVS-MAVS	F2 day 6	27,28	
MAVS-MAVS	F2 day 6	26,84	27,06
TK-MAVS	F2 day 6	26,64	
TK-MAVS	F2 day 6	26,45	26,55

f)

siRNA-primer	Fish - day	Ct	Average
Kontroll-MX	F2 day 6	24,69	
Kontroll-MX	F2 day 6	24,91	24,80
TLR3-MX	F2 day 6	24,80	
TLR3-MX	F2 day 6	24,71	24,75
RIGI-MX	F2 day 6	22,88	
RIGI-MX	F2 day 6	22,83	22,85
RLR3-MX	F2 day 6	21,32	
RLR3-MX	F2 day 6	21,34	21,33
MAVS-MX	F2 day 6	22,61	
MAVS-MX	F2 day 6	22,64	22,62
TK-MX	F2 day 6	24,26	
TK-MX	F2 day 6	24,36	24,31

g)

siRNA-primer	Fish - day	Ct	Average
Kontroll-ISG15	F2 day 6	24,22	
Kontroll-ISG15	F2 day 6	24,21	24,21
TLR3-ISG15	F2 day 6	21,02	
TLR3-ISG15	F2 day 6	20,65	20,83
RIGI-ISG15	F2 day 6	20,36	
RIGI-ISG15	F2 day 6	20,44	20,40
RLR3-ISG15	F2 day 6	18,31	
RLR3-ISG15	F2 day 6	18,30	18,31
MAVS-ISG15	F2 day 6	20,12	
MAVS-ISG15	F2 day 6	19,54	19,83
TK-ISG15	F2 day 6	23,25	
TK-ISG15	F2 day 6	23,10	23,17

Figure I7. Ct-values from at Day 6 from "4.7.2 Determine siRNA effectiveness" for A. salmon 2 a) EF1α. b) TLR3. c) RIG-I. d) RLR3. e) MAVS. f) Mx. g) ISG15

a)

siRNA-primer	Fish - Day	Ct	Average
Kontroll-EFa	F3 - D3	21,49	
Kontroll-EFa	F3 - D3	21,49	21,49
TLR3-EFa	F3 - D3	23,48	
TLR3-EFa	F3 - D3	23,34	23,41
RIGI-EFa	F3 - D3	22,82	
RIGI-EFa	F3 - D3	22,68	22,75
RLR3-EFa	F3 - D3	22,82	
RLR3-EFa	F3 - D3	22,38	22,60
MAVS-EFa	F3 - D3	22,18	
MAVS-EFa	F3 - D3	22,14	22,16
TK-EFa	F3 - D3	22,12	
TK-EFa	F3 - D3	22,14	22,13

b)

siRNA-primer	Fish - day	Ct	Average
Kontroll-TLR3	F3 - D3	27,96	
Kontroll-TLR3	F3 - D3	28,01	27,98
TLR3-TLR3	F3 - D3	28,82	
TLR3-TLR3	F3 - D3	28,24	28,53
RIGI-TLR3	F3 - D3	29,04	
RIGI-TLR3	F3 - D3	29,03	29,03
RLR3-TLR3	F3 - D3	29,61	
RLR3-TLR3	F3 - D3	29,66	29,64
MAVS-TLR3	F3 - D3	28,83	
MAVS-TLR3	F3 - D3	28,90	28,87
TK-TLR3	F3 - D3	28,95	
TK-TLR3	F3 - D3	28,63	28,79

c)

siRNA-primer	Fish - day	Ct	Average
Kontroll-RIGI	F3 - D3	25,98	
Kontroll-RIGI	F3 - D3	26,07	26,03
TLR3-RIGI	F3 - D3	29,09	
TLR3-RIGI	F3 - D3	21,50	25,30
RIGI-RIGI	F3 - D3	27,32	
RIGI-RIGI	F3 - D3	26,92	27,12
RLR3-RIGI	F3 - D3	26,81	
RLR3-RIGI	F3 - D3	26,19	26,50
MAVS-RIGI	F3 - D3	25,60	
MAVS-RIGI	F3 - D3	25,55	25,58
TK-RIGI	F3 - D3	25,97	
TK-RIGI	F3 - D3	26,25	26,11

d)

siRNA-primer	Fish - day	Ct	Average
Kontroll-RLR3	F3 - D3	25,17	
Kontroll-RLR3	F3 - D3	25,22	25,20
TLR3-RLR3	F3 - D3	24,23	
TLR3-RLR3	F3 - D3	24,03	24,13
RIGI-RLR3	F3 - D3	24,36	
RIGI-RLR3	F3 - D3	24,11	24,24
RLR3-RLR3	F3 - D3	24,27	
RLR3-RLR3	F3 - D3	24,09	24,18
MAVS-RLR3	F3 - D3	23,93	
MAVS-RLR3	F3 - D3	24,02	23,98
TK-RLR3	F3 - D3	23,86	
TK-RLR3	F3 - D3	23,80	23,83

e)

siRNA-primer	Fish - day	Ct	Average
Kontroll-MAVS	F3 - D3	26,32	
Kontroll-MAVS	F3 - D3	26,50	26,41
TLR3-MAVS	F3 - D3	28,91	
TLR3-MAVS	F3 - D3	28,12	28,52
RIGI-MAVS	F3 - D3	27,70	
RIGI-MAVS	F3 - D3	28,05	27,88
RLR3-MAVS	F3 - D3	28,01	
RLR3-MAVS	F3 - D3	28,14	28,07
MAVS-MAVS	F3 - D3	27,39	
MAVS-MAVS	F3 - D3	27,25	27,32
TK-MAVS	F3 - D3	27,27	
TK-MAVS	F3 - D3	27,39	27,33

f)

siRNA-primer	Fish - day	Ct	Average
Kontroll-MX	F3 - D3	26,33	
Kontroll-MX	F3 - D3	26,30	26,32
TLR3-MX	F3 - D3	26,43	
TLR3-MX	F3 - D3	26,32	26,38
RIGI-MX	F3 - D3	26,74	
RIGI-MX	F3 - D3	26,48	26,61
RLR3-MX	F3 - D3	26,08	
RLR3-MX	F3 - D3	25,96	26,02
MAVS-MX	F3 - D3	25,86	
MAVS-MX	F3 - D3	25,99	25,92
TK-MX	F3 - D3	26,67	
TK-MX	F3 - D3	26,68	26,68

g)

siRNA-primer	Fish - day	Ct	Average
Kontroll-ISG15	F3 - D3	25,96	
Kontroll-ISG15	F3 - D3	26,01	25,98
TLR3-ISG15	F3 - D3	24,16	
TLR3-ISG15	F3 - D3	23,89	24,02
RIGI-ISG15	F3 - D3	24,55	
RIGI-ISG15	F3 - D3	24,44	24,50
RLR3-ISG15	F3 - D3	23,10	
RLR3-ISG15	F3 - D3	22,93	23,02
MAVS-ISG15	F3 - D3	23,80	
MAVS-ISG15	F3 - D3	24,21	24,01
TK-ISG15	F3 - D3	26,32	
TK-ISG15	F3 - D3	26,10	26,21

Figure I8. Ct-values from at Day 3 from "4.7.2 Determine siRNA effectiveness" for A. salmon 3 a) EF1α. b) TLR3. c) RIG-I. d) RLR3. e) MAVS. f) Mx. g) ISG15

a)

siRNA-primer	Fish - Day	Ct	Average
Kontroll-EFa	F3 - D6	21,43	
Kontroll-EFa	F3 - D6	21,14	21,29
TLR3-EFa	F3 - D6	22,83	
TLR3-EFa	F3 - D6	22,59	22,71
RIGI-EFa	F3 - D6	23,03	
RIGI-EFa	F3 - D6	23,00	23,02
RLR3-EFa	F3 - D6	23,07	
RLR3-EFa	F3 - D6	22,58	22,83
MAVS-EFa	F3 - D6	22,91	
MAVS-EFa	F3 - D6	22,31	22,61
TK-EFa	F3 - D6	22,73	
TK-EFa	F3 - D6	22,29	22,51

b)

siRNA-primer	Fish - Day	Ct	Average
Kontroll-TLR3	F3 - D6	26,49	
Kontroll-TLR3	F3 - D6	26,43	26,46
TLR3-TLR3	F3 - D6	28,50	
TLR3-TLR3	F3 - D6	28,20	28,35
RIGI-TLR3	F3 - D6	28,72	
RIGI-TLR3	F3 - D6	28,02	28,37
RLR3-TLR3	F3 - D6	31,69	
RLR3-TLR3	F3 - D6	30,09	30,89
MAVS-TLR3	F3 - D6	28,67	
MAVS-TLR3	F3 - D6	28,27	28,47
TK-TLR3	F3 - D6	27,41	
TK-TLR3	F3 - D6	27,37	27,39

c)

siRNA-primer	Fish - Day	Ct	Average
Kontroll-RIGI	F3 - D6	25,15	
Kontroll-RIGI	F3 - D6	25,04	25,09
TLR3-RIGI	F3 - D6	27,76	
TLR3-RIGI	F3 - D6	25,82	26,79
RIGI-RIGI	F3 - D6	26,55	
RIGI-RIGI	F3 - D6	25,93	26,24
RLR3-RIGI	F3 - D6	27,19	
RLR3-RIGI	F3 - D6	26,31	26,75
MAVS-RIGI	F3 - D6	26,29	
MAVS-RIGI	F3 - D6	25,87	26,08
TK-RIGI	F3 - D6	25,70	
TK-RIGI	F3 - D6	25,47	25,58

d)

siRNA-primer	Fish - Day	Ct	Average
Kontroll-RLR3	F3 - D6	25,17	
Kontroll-RLR3	F3 - D6	23,54	24,36
TLR3-RLR3	F3 - D6	23,66	
TLR3-RLR3	F3 - D6	23,98	23,82
RIGI-RLR3	F3 - D6	24,25	
RIGI-RLR3	F3 - D6	24,33	24,29
RLR3-RLR3	F3 - D6	24,14	
RLR3-RLR3	F3 - D6	24,01	24,08
MAVS-RLR3	F3 - D6	24,43	
MAVS-RLR3	F3 - D6	24,24	24,33
TK-RLR3	F3 - D6	23,55	
TK-RLR3	F3 - D6	23,32	23,44

e)

siRNA-primer	Fish - Day	Ct	Average
Kontroll-MAVS	F3 - D6	25,46	
Kontroll-MAVS	F3 - D6	25,05	25,25
TLR3-MAVS	F3 - D6	27,81	
TLR3-MAVS	F3 - D6	27,70	27,75
RIGI-MAVS	F3 - D6	27,50	
RIGI-MAVS	F3 - D6	27,51	27,51
RLR3-MAVS	F3 - D6	27,33	
RLR3-MAVS	F3 - D6	27,36	27,35
MAVS-MAVS	F3 - D6	27,50	
MAVS-MAVS	F3 - D6	27,13	27,31
TK-MAVS	F3 - D6	27,19	
TK-MAVS	F3 - D6	26,88	27,03

f)

siRNA-primer	Fish - Day	Ct	Average
Kontroll-MX	F3 - D6	28,04	
Kontroll-MX	F3 - D6	26,34	27,19
TLR3-MX	F3 - D6	26,34	
TLR3-MX	F3 - D6	26,21	26,28
RIGI-MX	F3 - D6	27,31	
RIGI-MX	F3 - D6	27,30	27,31
RLR3-MX	F3 - D6	26,45	
RLR3-MX	F3 - D6	26,21	26,33
MAVS-MX	F3 - D6	27,41	
MAVS-MX	F3 - D6	26,98	27,20
TK-MX	F3 - D6	27,96	
TK-MX	F3 - D6	28,07	28,01

g)

siRNA-primer	Fish - Day	Ct	Average
Kontroll-ISG15	F3 - D6	26,39	
Kontroll-ISG15	F3 - D6	26,08	26,24
TLR3-ISG15	F3 - D6	24,15	
TLR3-ISG15	F3 - D6	23,27	23,71
RIGI-ISG15	F3 - D6	24,43	
RIGI-ISG15	F3 - D6	24,49	24,46
RLR3-ISG15	F3 - D6	22,88	
RLR3-ISG15	F3 - D6	22,96	22,92
MAVS-ISG15	F3 - D6	25,02	
MAVS-ISG15	F3 - D6	24,51	24,77
TK-ISG15	F3 - D6	26,69	
TK-ISG15	F3 - D6	26,62	26,65

Figure I9. Ct-values from each sample at Day 6 for testing siRNA-efficency for A. salmon 3 a) EF1α-expression. b) TLR3-expression. c) RIG-I-expresiion. d) RLR3-Expression. e) MAVS-expression. f) Mx-expression. g) ISG15-expression

a)

siRNA-primer	Fish - Day	Ct	Average
Kontroll-EFA	F1 - D3	22,06	
Kontroll-EFA	F1 - D3	21,12	21,59
TLR3-EFA	F1 - D3	22,77	
TLR3-EFA	F1 - D3	22,41	22,59
RIGI-EFA	F1 - D3	23,37	
RIGI-EFA	F1 - D3	22,76	23,06
RLR3-EFA	F1 - D3	22,87	
RLR3-EFA	F1 - D3	21,92	22,40
MAVS-EFA	F1 - D3	22,68	
MAVS-EFA	F1 - D3	22,03	22,36
TK-EFA	F1 - D3	22,76	
TK-EFA	F1 - D3	22,11	22,44

b)

siRNA-primer	Fish - Day	Ct	Average
Kontroll-MX	F1 - D3	28,93	
Kontroll-MX	F1 - D3	29,35	29,14
TLR3-MX	F1 - D3	29,98	
TLR3-MX	F1 - D3	30,21	30,10
RIGI-MX	F1 - D3	31,00	
RIGI-MX	F1 - D3	30,27	30,64
RLR3-MX	F1 - D3	30,39	
RLR3-MX	F1 - D3	30,41	30,40
MAVS-MX	F1 - D3	29,75	
MAVS-MX	F1 - D3	29,64	29,70
TK-MX	F1 - D3	31,11	
TK-MX	F1 - D3	29,50	30,31

c)

siRNA-primer	Fish - Day	Ct	Average
Kontroll-ISG15	F1 - D3	27,81	
Kontroll-ISG15	F1 - D3	26,79	27,30
TLR3-ISG15	F1 - D3	24,13	
TLR3-ISG15	F1 - D3	23,60	23,87
RIGI-ISG15	F1 - D3	24,44	
RIGI-ISG15	F1 - D3	23,18	23,81
RLR3-ISG15	F1 - D3	26,08	
RLR3-ISG15	F1 - D3	24,40	25,24
MAVS-ISG15	F1 - D3	25,15	
MAVS-ISG15	F1 - D3	23,97	24,56
TK-ISG15	F1 - D3	28,09	
TK-ISG15	F1 - D3	27,37	27,73

Figure I10. Ct-values from each sample at Day 3 from "4.8 siRNA silencing of TLR3, RIG-I, RLR3 and MAVS – test of effects on poly(I:C) stimulationfor A. salmon 1 a) EF1α. b) Mx. c) ISG15

a)

siRNA primer	Fish - Day/poly	Ct	Average
Kontroll-EFA	F1-D6	21,33	
Kontroll-EFA	F1-D6	20,10	20,71
TLR3-EFA	F1-D6	22,32	
TLR3-EFA	F1-D6	21,57	21,94
RIGI-EFA	F1-D6	22,93	
RIGI-EFA	F1-D6	22,72	22,83
RLR3-EFA	F1-D6	22,14	
RLR3-EFA	F1-D6	38,62	22,14
MAVS-EFA	F1-D6	21,38	
MAVS-EFA	F1-D6	20,90	21,14
TK-EFA	F1-D6	23,57	
TK-EFA	F1-D6	22,92	23,24
TLR3-EFA	F1-Poly	21,59	
TLR3-EFA	F1-Poly	21,43	21,51
RIGI-EFA	F1-Poly	21,74	
RIGI-EFA	F1-Poly	21,35	21,55
RLR3-EFA	F1-Poly	21,52	
RLR3-EFA	F1-Poly	21,32	21,42
MAVS-EFA	F1-Poly	20,99	
MAVS-EFA	F1-Poly	21,28	21,13

b)

siRNA primer	Fish - Day/poly(I:C)	Ct	Average
Kontroll-MX	F1-D6	29,98	
Kontroll-MX	F1-D6	27,27	28,62
TLR3-MX	F1-D6	28,57	
TLR3-MX	F1-D6	28,50	28,53
RIGI-MX	F1-D6	30,14	
RIGI-MX	F1-D6	29,25	29,70
RLR3-MX	F1-D6	28,51	
RLR3-MX	F1-D6	27,39	27,95
MAVS-MX	F1-D6	28,49	
MAVS-MX	F1-D6	27,32	27,90
TK-MX	F1-D6	31,45	
TK-MX	F1-D6	29,95	30,70
TLR3-MX	F1-Poly	27,31	
TLR3-MX	F1-Poly	27,13	27,22
RIGI-MX	F1-Poly	28,39	
RIGI-MX	F1-Poly	27,93	28,16
RLR3-MX	F1-Poly	29,16	
RLR3-MX	F1-Poly	28,80	28,98
MAVS-MX	F1-Poly	29,16	
MAVS-MX	F1-Poly	29,03	29,09

c)

siRNA primer	Fish - Day/poly(I:C)	Ct	Average
Kontroll-ISG15	F1-D6	27,74	
Kontroll-ISG15	F1-D6	27,02	27,38
TLR3-ISG15	F1-D6	24,73	
TLR3-ISG15	F1-D6	23,24	23,99
RIGI-ISG15	F1-D6	24,66	
RIGI-ISG15	F1-D6	23,46	24,06
RLR3-ISG15	F1-D6	23,93	
RLR3-ISG15	F1-D6	23,37	23,65
MAVS-ISG15	F1-D6	24,32	
MAVS-ISG15	F1-D6	23,16	23,74
TK-ISG15	F1-D6	28,09	
TK-ISG15	F1-D6	27,51	27,80
TLR3-ISG15	F1-Poly	22,59	
TLR3-ISG15	F1-Poly	22,59	22,59
RIGI-ISG15	F1-Poly	23,08	
RIGI-ISG15	F1-Poly	22,62	22,85
RLR3-ISG15	F1-Poly	24,09	
RLR3-ISG15	F1-Poly	22,82	23,45
MAVS-ISG15	F1-Poly	24,81	
MAVS-ISG15	F1-Poly	23,38	24,09

Figure I11. Ct-values from each sample at Day 6 from "4.8 siRNA silencing of TLR3, RIG-I, RLR3 and MAVS – test of effects on poly(I:C) stimulationfor A. salmon 1 a) EF1α. b) Mx. c) ISG15. Red-value was not added in the analysis.

a)

siRNA-primer	Fish-Day	Ct	Average
Kontroll-EFA	F2-D6	22,99	
Kontroll-EFA	F2-D6	21,85	22,42
TLR3-EFA	F2-D6	23,90	
TLR3-EFA	F2-D6	22,11	23,00
RIGI-EFA	F2-D6	24,05	
RIGI-EFA	F2-D6	22,41	23,23
RLR3-EFA	F2-D6	24,21	
RLR3-EFA	F2-D6	23,45	23,83
MAVS-EFA	F2-D6	24,83	
MAVS-EFA	F2-D6	23,47	24,15
TK-EFA	F2-D6	25,02	
TK-EFA	F2-D6	23,71	24,36

b)

siRNA-primer	Fish-Day	Ct	Average
Kontroll-MX	F2-D6	28,21	
Kontroll-MX	F2-D6	27,56	27,89
TLR3-MX	F2-D6	27,95	
TLR3-MX	F2-D6	26,07	27,01
RIGI-MX	F2-D6	29,25	
RIGI-MX	F2-D6	27,94	28,60
RLR3-MX	F2-D6	29,73	
RLR3-MX	F2-D6	29,50	29,62
MAVS-MX	F2-D6	30,16	
MAVS-MX	F2-D6	29,28	29,72
TK-MX	F2-D6	31,33	
TK-MX	F2-D6	29,43	30,38

c)

siRNA-primer	Fish-Day	Ct	Average
Kontroll-ISG15	F2-D6	27,00	
Kontroll-ISG15	F2-D6	25,20	26,10
TLR3-ISG15	F2-D6	23,75	
TLR3-ISG15	F2-D6	22,95	23,35
RIGI-ISG15	F2-D6	24,72	
RIGI-ISG15	F2-D6	24,05	24,39
RLR3-ISG15	F2-D6	25,80	
RLR3-ISG15	F2-D6	24,28	25,04
MAVS-ISG15	F2-D6	25,79	
MAVS-ISG15	F2-D6	24,34	25,06
TK-ISG15	F2-D6	28,73	
TK-ISG15	F2-D6	28,31	28,52

Figure I12. Ct-values from each sample at Day 3 from "4.8 siRNA silencing of TLR3, RIG-I, RLR3 and MAVS – test of effects on poly(I:C) stimulationfor A. salmon 2 a) EF1α. b) Mx. c) ISG15

a)

siRNA-primer	Fish - Day/poly(I:C)	Ct	Average
Kontroll-EFA	F2-D6	22,99	
Kontroll-EFA	F2-D6	21,85	22,42
TLR3-EFA	F2-D6	23,90	
TLR3-EFA	F2-D6	22,11	23,00
RIGI-EFA	F2-D6	24,05	
RIGI-EFA	F2-D6	22,41	23,23
RLR3-EFA	F2-D6	24,21	
RLR3-EFA	F2-D6	23,45	23,83
MAVS-EFA	F2-D6	24,83	
MAVS-EFA	F2-D6	23,47	24,15
TK-EFA	F2-D6	25,02	
TK-EFA	F2-D6	23,71	24,36
TLR3-EFA	F2-Poly	21,96	
TLR3-EFA	F2-Poly	22,09	22,02
RIGI-EFA	F2-Poly	22,98	
RIGI-EFA	F2-Poly	22,98	22,98
RLR3-EFA	F2-Poly	23,48	
RLR3-EFA	F2-Poly	23,35	23,42
MAVS-EFA	F2-Poly	23,78	
MAVS-EFA	F2-Poly	23,80	23,79

b)

siRNA-primer	Fish - Day/poly(I:C)	Ct	Average
Kontroll-MX	F2-D6	28,21	
Kontroll-MX	F2-D6	27,56	27,89
TLR3-MX	F2-D6	27,95	
TLR3-MX	F2-D6	26,07	27,01
RIGI-MX	F2-D6	29,25	
RIGI-MX	F2-D6	27,94	28,60
RLR3-MX	F2-D6	29,73	
RLR3-MX	F2-D6	29,50	29,62
MAVS-MX	F2-D6	30,16	
MAVS-MX	F2-D6	29,28	29,72
TK-MX	F2-D6	31,33	
TK-MX	F2-D6	29,43	30,38
TLR3-MX	F2-Poly	23,58	
TLR3-MX	F2-Poly	24,17	23,87
RIGI-MX	F2-Poly	27,53	
RIGI-MX	F2-Poly	27,25	27,39
RLR3-MX	F2-Poly	28,94	
RLR3-MX	F2-Poly	29,36	29,15
MAVS-MX	F2-Poly	28,22	
MAVS-MX	F2-Poly	28,13	28,18

c)

siRNA-primer	Fish - Day/poly(I:C)	Ct	Average
Kontroll-ISG15	F2-D6	27,00	
Kontroll-ISG15	F2-D6	25,20	26,10
TLR3-ISG15	F2-D6	23,75	
TLR3-ISG15	F2-D6	22,95	23,35
RIGI-ISG15	F2-D6	24,72	
RIGI-ISG15	F2-D6	24,05	24,39
RLR3-ISG15	F2-D6	25,80	
RLR3-ISG15	F2-D6	24,28	25,04
MAVS-ISG15	F2-D6	25,79	
MAVS-ISG15	F2-D6	24,34	25,06
TK-ISG15	F2-D6	28,73	
TK-ISG15	F2-D6	28,31	28,52
TLR3-ISG15	F2-Poly	21,24	
TLR3-ISG15	F2-Poly	21,69	21,46
RIGI-ISG15	F2-Poly	23,36	
RIGI-ISG15	F2-Poly	23,42	23,39
RLR3-ISG15	F2-Poly	23,84	
RLR3-ISG15	F2-Poly	23,96	23,90
MAVS-ISG15	F2-Poly	23,55	
MAVS-ISG15	F2-Poly	23,51	23,53

Figure I13. Ct-values from each sample at Day 6 from "4.8 siRNA silencing of TLR3, RIG-I, RLR3 and MAVS – test of effects on poly(I:C) stimulationfor A. salmon 2 a) EF1α. b) Mx. c) ISG15

a)

siRNA-primer	Fish - Day	Ct	Average
Kontroll-EFa	F3 - D3	20,86	
Kontroll-EFa	F3 - D3	21,32	21,09
TLR3-EFa	F3 - D3	21,71	
TLR3-EFa	F3 - D3	21,65	21,68
RIGI-EFa	F3 - D3	22,07	
RIGI-EFa	F3 - D3	21,46	21,76
RLR3-EFa	F3 - D3	22,40	
RLR3-EFa	F3 - D3	21,93	22,17
MAVS-EFa	F3 - D3	22,40	
MAVS-EFa	F3 - D3	22,34	22,37
TK-EFa	F3 - D3	21,29	
TK-EFa	F3 - D3	21,63	21,46

b)

siRNA-primer	Fish - Day	Ct	Average
Kontroll-MX	F3 - D3	25,21	
Kontroll-MX	F3 - D3	24,90	25,06
TLR3-MX	F3 - D3	28,05	
TLR3-MX	F3 - D3	27,29	27,67
RIGI-MX	F3 - D3	28,41	
RIGI-MX	F3 - D3	26,44	27,42
RLR3-MX	F3 - D3	27,74	
RLR3-MX	F3 - D3	28,00	27,87
MAVS-MX	F3 - D3	28,26	
MAVS-MX	F3 - D3	27,23	27,75
TK-MX	F3 - D3	26,86	
TK-MX	F3 - D3	25,05	25,96

c)

siRNA-primer	Fish - Day	Ct	Average
Kontroll-ISG15	F3 - D3	25,62	
Kontroll-ISG15	F3 - D3	24,82	25,22
TLR3-ISG15	F3 - D3	23,74	
TLR3-ISG15	F3 - D3	21,81	22,77
RIGI-ISG15	F3 - D3	24,64	
RIGI-ISG15	F3 - D3	23,43	24,04
RLR3-ISG15	F3 - D3	24,00	
RLR3-ISG15	F3 - D3	23,29	23,65
MAVS-ISG15	F3 - D3	24,25	
MAVS-ISG15	F3 - D3	22,83	23,54
TK-ISG15	F3 - D3	24,77	
TK-ISG15	F3 - D3	25,03	24,90

Figure I15. Ct-values from each sample at Day 3 from "4.8 siRNA silencing of TLR3, RIG-I, RLR3 and MAVS – test of effects on poly(I:C) stimulationfor A. salmon 3 a) EF1α. b) Mx. c) ISG15

a)

siRNA-primer	Fish - Day/poly(I:C)	Ct	Average
Kontroll-EFa	F3 - D6	21,48	
Kontroll-EFa	F3 - D6	21,60	21,54
TLR3-EFa	F3 - D6	22,12	
TLR3-EFa	F3 - D6	21,79	21,96
RIGI-EFa	F3 - D6	22,20	
RIGI-EFa	F3 - D6	21,84	22,02
RLR3-EFa	F3 - D6	24,81	
RLR3-EFa	F3 - D6	24,53	24,67
MAVS-EFa	F3 - D6	29,28	
MAVS-EFa	F3 - D6	28,58	28,93
TK-EFa	F3 - D6	21,63	
TK-EFa	F3 - D6	21,27	21,45
TLR3-EFa	F3 - Poly	22,29	
TLR3-EFa	F3 - Poly	22,08	22,19
RIGI-EFa	F3 - Poly	21,64	
RIGI-EFa	F3 - Poly	21,37	21,51
RLR3-EFa	F3 - Poly	23,41	
RLR3-EFa	F3 - Poly	23,06	23,24
MAVS-EFa	F3 - Poly	23,28	
MAVS-EFa	F3 - Poly	23,13	23,20

b)

siRNA-primer	Fish - Day/poly(I:C)	Ct	Average
Kontroll-MX	F3 - D6	27,75	
Kontroll-MX	F3 - D6	27,08	27,41
TLR3-MX	F3 - D6	28,25	
TLR3-MX	F3 - D6	27,37	27,81
RIGI-MX	F3 - D6	27,81	
RIGI-MX	F3 - D6	27,41	27,61
RLR3-MX	F3 - D6	30,55	
RLR3-MX	F3 - D6	29,94	30,25
MAVS-MX	F3 - D6	32,34	
MAVS-MX	F3 - D6	32,17	32,25
TK-MX	F3 - D6	26,97	
TK-MX	F3 - D6	26,82	26,90
TLR3-MX	F3 - Poly	28,25	
TLR3-MX	F3 - Poly	28,16	28,21
RIGI-MX	F3 - Poly	27,29	
RIGI-MX	F3 - Poly	27,48	27,39
RLR3-MX	F3 - Poly	28,60	
RLR3-MX	F3 - Poly	29,23	28,91
MAVS-MX	F3 - Poly	28,28	
MAVS-MX	F3 - Poly	28,40	28,34

c)

siRNA-primer	Fish - Day/poly(I:C)	Ct	Average
Kontroll-ISG15	F3 - D6	25,01	
Kontroll-ISG15	F3 - D6	24,39	24,70
TLR3-ISG15	F3 - D6	24,17	
TLR3-ISG15	F3 - D6	23,08	23,62
RIGI-ISG15	F3 - D6	25,00	
RIGI-ISG15	F3 - D6	24,34	24,67
RLR3-ISG15	F3 - D6	25,92	
RLR3-ISG15	F3 - D6	25,34	25,63
MAVS-ISG15	F3 - D6	30,17	
MAVS-ISG15	F3 - D6	29,67	29,92
TK-ISG15	F3 - D6	26,55	
TK-ISG15	F3 - D6	25,38	25,96
TLR3-ISG15	F3 - Poly	22,58	
TLR3-ISG15	F3 - Poly	22,85	22,71
RIGI-ISG15	F3 - Poly	24,08	
RIGI-ISG15	F3 - Poly	23,13	23,61
RLR3-ISG15	F3 - Poly	24,22	
RLR3-ISG15	F3 - Poly	23,46	23,84
MAVS-ISG15	F3 - Poly	23,91	
MAVS-ISG15	F3 - Poly	23,55	23,73

Figure I16. Ct-values from each sample at Day 6 from "4.8 siRNA silencing of TLR3, RIG-I, RLR3 and MAVS – test of effects on poly(I:C) stimulationfor A. salmon 3 a) EF1α. b) Mx. c) ISG15

J – siRNA effectors in A. salmon RBCs, SHK-1 and ASK

Table J1. Transcript expression of essentail proteins involved in the RNAi-system from A. salmon RBCs, SHK-1 and ASK. Green "boxes" indicate which cell has the highest expression of the gene.

Gene	RBCs Transcripts	ASK Transcripts	SHK-1 Transcripts
argonaute RISC catalytic component 2	439	520	648
protein argonaute-1	60	257,5	141
endoribonuclease Dicer-like	493	424,5	156
endoribonuclease Dicer-like	353	310	235,5
TARBP2 subunit of RISC loading complex	101	182,5	189
staphylococcal nuclease and tudor domain containing 1	62	389	482
tudor domain containing 1	14	4,5	111
LYRIC protein (AEG-1)	880	2918,5	1407,5
protein LYRIC-like	3647	3766	5018,5
TATA-box binding protein associated factor 11	2440	3659,5	2867

Table J1. Transcript expression of essentail proteins involved in the RNAi-system from RBCs, SHK-1 and ASK. Green "boxes" indicate which cell has the highest expression of the gene.

K – Statistical tests

The tables in this section presents which groups-means were compared against each other for statistical analysis. Columns in same color represents one group-mean, which were compared with the other group-means of different color.

The tables in this section presents which groups-means were compared against each other for statistical analysis. Columns in same color represents one group-mean, which were compared with the other group-means of different color.

Table K1. Comparison of P1, P2, P3 and P4 from "4.3.3.2 Optimizing mRNA transfection in A.salmon – Experiment 2"

	P1		**P2**		**P3**		**P4**	
	A. salmon 1	A. salmon 2	A. salmon 1	A. salmon 2	A. salmon 1	A. salmon 2	A. salmon 1	A. salmon 2
Day 1	17.82	11.89	5.82	14.88	9.18		4.54	
Day 3	31.3		5.48		16.14		9.33	

Mean Mean Mean Mean

Table K2. Comparison of Day 1, Day 3 and Day 6 TLR3 fold change from "4.7.1 Testing knock-down efficiency and responses to transfection at different time points"

	Day 1	Day 3	Day 6
siTLR3	0.44	0.89	2.46
siRIG-I	0.39	0.51	1.24
siRLR3	"N	0.6	1.7
siMAVS	0.44	0.28	2.40
L-siMAVS	1.42	0.92	6.06

Mean Mean Mean

Table K3. Comparison of siTLR3, siRIG-I, siRLR3, siMAVS and L-siMAVS RLR3 fold-change from "4.7.1 Testing knock-down efficiency and responses to transfection at different time points".

	siTLR3	siRIG-I	siRLR3	siMAVS	siLMAVS
Day 1	2.84	3.36	NA	4.44	19.20
Day 3					
Day 6	3.49	2.97	3.71	4.25	11.45

Table K4. Comparison of Day 1, Day 3 and Day 6 MAVS fold change from "4.7.1 Testing knock-down efficiency and responses to transfection at different time points"

	Day 1	Day 3	Day 6
siTLR3	4.30	0.03	0.98
siRIG-I	5.37	0.59	0.74
siRLR3			
siMAVS	2.86	0.06	1.41
siLMAVS	4.24	0.30	0.93

Table K5. Comparison of Day 1, Day 3 and Day 6 Mx fold change from "4.7.1 Testing knock-down efficiency and responses to transfection at different time points".

	Day 1	Day 3	Day 6
siTLR3	54.89	2.79	7.19
siRIG-I	46	1.50	1.65
siRLR3	"NA"	2.1	5.3
siMAVS	37.06	0.96	2.99
siLMAVS	215.37	20.86	76.58

Table K6. Comparison of siTLR3, siRIG-I, siRLR3, siMAVS and L-siMAVS RLR3 fold-change from "4.7.2 Determine siRNA effectiveness".

	siTLR3	siRIG-I	siRLR3	siMAVS	Transfected control
A. salmon 1	2.28	1.40	0.63	1.80	1.13
A. salmon 2		2	1		0
A. salmon 3	2.60	1.16	0.68	0.86	0.89

Table K7. Comparison of siRNA transfected but poly(I:C)-stimulated, and siRNA transfected but not stimulated Mx fold change from "4.8 siRNA silencing of TLR3, RIG-I, RLR3 and MAVS – test of effects on poly(I:C) stimulation"

	Poly(I:C)			siRNA		
	A.salmon 1	A.salmon 2	A.salmon 3	A.salmon 1	A.salmon 2	A.salmon 3
siTLR3	48.10	18.88	6.19	24.66	10.00	2.81
siRIG-I	41.12		2.08	43.13		1.42
siRLR3	24.81		5.85	35.66		.58
siMAVS	13.05	15.39	6.19	16.75	6.78	4.49

Mean

Mean

Table K8. Comparison of siRNA transfected but poly(I:C)-stimulated, and siRNA transfected but not stimulated ISG15 fold change from "4.8 siRNA silencing of TLR3, RIG-I, RLR3 and MAVS – test of effects on poly(I:C) stimulation"

	Poly(I:C)			siRNA		
	A.salmon 1	A.salmon 2	A.salmon 3	A.salmon 1	A.salmon 2	A.salmon 3
siTLR3	4.58	12.26	0.90	2.49	2.76	1.01
siRIG-I	2.46		0.99	2.05		1.21
siRLR3	1.27		1.14	4.27		23
siMAVS	0.96	2.11	1.66	2.20	0.93	5.85

Mean

Mean

Table K9. Comparison of RBCs transfected with siTLR3 and RBCs transfected with siTLR3, but stimulated with poly(I:C) from "4.8 siRNA silencing of TLR3, RIG-I, RLR3 and MAVS – test of effects on poly(I:C) stimulation" Mx fold change.

	siTLR3	siTLR3 stimulated
A. salmon 1	2.49	4.58
A. salmon 2		
A. salmon 3	1.01	0.90

Mean

Mean

Norges miljø- og biovitenskapelige universitet
Noregs miljø- og biovitskapelege universitet
Norwegian University of Life Sciences

Postboks 5003
NO-1432 Ås
Norway